

337084

**ICBM OVERTEST TECHNOLOGY**

**FINAL REPORT**

**VOL I**

HERCULES INCORPORATED  
SYSTEMS GROUP  
BACCHUS WORKS  
MAGNA, UTAH 84044

AUTHOR: A. S. DANIELS  
S. C. BROWNING  
K. D. SMARTT  
T. D. PAVELKA

OCTOBER 1975

APPROVED FOR PUBLIC RELEASE;  
DISTRIBUTION UNLIMITED

Reproduced by  
NATIONAL TECHNICAL  
INFORMATION SERVICE  
US Department of Commerce  
Springfield, VA. 22151

**PRICES SUBJECT TO CHANGE**

AIR FORCE ROCKET PROPULSION LABORATORY  
DIRECTOR OF SCIENCE AND TECHNOLOGY  
AIR FORCE SYSTEMS COMMAND  
EDWARDS, CALIFORNIA 93523

ADA 017753


250


## FOREWORD

This report was submitted by Hercules Incorporated, Bacchus Works, Magna, Utah 84044 under Contract F04611-73-C-0010, Job Order No. 305910LY with the Air Force Rocket Propulsion Laboratory, Edwards, CA 93523.

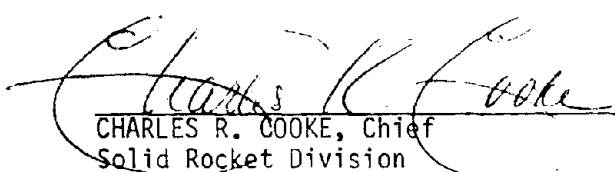
This report has been reviewed by the Information Office/DOZ and is releasable to the National Technical Information Service (NTIS). At NTIS it will be available to the general public, including foreign nations.

This report is unclassified and is suitable for public release.

  
ROBERT A. BIGGERS GS-13  
Project Engineer

  
CHARLES E. PAYNE, Major, USAF  
Chief, Surveillance & Mechanical  
Behavior Section

FOR THE COMMANDER

  
CHARLES R. COOKE, Chief  
Solid Rocket Division

## NOTICES

When U. S. Government drawings, specifications, or other data are used for any purpose than a definitely related government procurement operation, the Government thereby incurs no responsibility nor any obligation whatsoever, and the fact that the Government may have formulated, furnished, or in any way supplied the said drawings, specifications or other data, is not to be regarded by implication or otherwise, or in any manner licensing the holder or any other person or corporation, or conveying any rights or permission to manufacture, use or sell any patented invention that may in any way be related thereto.

## ABSTRACT

This is the final report on the ICBM Overtest Technology Program which was performed by Hercules Incorporated for the Air Force under Contract F04611-73-C-0010. The primary objective of the program was to develop overtest technology for the prediction of ICBM motor service life. The Minuteman II third stage (M57A1) was used as the demonstration vehicle; therefore, an important secondary objective was to make predictions of the M57A1 service life. This report includes the analysis and operations performed in accomplishing the program objectives plus a related history of previous Minuteman work and programs. A manual of recommended practice for incorporating overtest concepts in surveillance programs has been prepared.

A failure mode analysis of the Minuteman motor was prepared, and the most critical failure modes were found to be wing slot cracking and aft centerport debonding in response to the ignition transient. An overtest approach for the full-scale motor tests was selected by comparative structural analyses of the response of the motor to several proposed loadings. High rate hydrotest at a rate of 10,000 psi/sec to 600 psi at 70° F was selected as the overtest approach to be used.

Motor failure criteria and the analysis approach were verified by use of four different configurations of subscale analog vehicles. Wing slot cracking was demonstrated with two model configurations and aft port debonding was demonstrated with a third configuration.

Full-scale motor overtesting was performed on two M57A1 motors; one which was 9 years old and one 6 years old at the time of test. The principal failure mode, wing slot cracking, was demonstrated in both tests. The failure pressure of the 9-year old motor was 475 psi, and the failure pressure of the 6-year old motor was 575 psi. These are substantially above the approximate 275 psi requirement for normal motor pressures at ignition. No debonding of the aft port, the secondary failure mode, occurred in either test.

Event gages were developed for detecting motor failure and successfully employed in full-scale motor high-rate pressure testing. The gages provided valid data on the time of failure and gage response to failure was verified by conventional potentiometer and strain gage responses. The overall demonstrated success ratio for event gages was 71 percent.

The overtested motors were dissected to verify the extent of failure induced by hydrotesting. Physical properties were obtained on propellant, case bond, and boot-flap bond samples obtained from these motors.

Service life predictions were made in two ways:

- (1) An analytical prediction was made from property data and trend data that were adjusted to represent the active motor inventory.
- (2) The overtest results from the overtest program, past programs, and other current programs were extrapolated with age after being adjusted to be representative of the active motor population.

All physical property data and motor firing data from past and current programs were used in the service life predictions. An indefinite service life was projected for the stage III Minuteman II motor. No evidence of aging effects on grain integrity were determined.



VOLUME I  
TABLE OF CONTENTS

<u>Section</u>		<u>Page</u>
	Abstract . . . . .	ii
	List of Figures . . . . .	v
	List of Tables . . . . .	x
I	INTRODUCTION AND SUMMARY	
	A. Introduction . . . . .	1-1
	B. Summary . . . . .	1-5
	C. Technical Approach . . . . .	1-10
	D. Minuteman II Stage III Review . . . . .	1-13
	1. Motor Design and Manufacture Review . . . . .	1-13
	2. Motor Evaluation . . . . .	1-18
	3. Motor Performance Characteristics . . . . .	1-18
	4. Review of Previous M57 Programs . . . . .	1-18
	E. Failure Mode Selection and Overtest Definition . . . . .	1-26
	LIST OF REFERENCES . . . . .	1-30
II	ANALOG TEST PROGRAM	
	A. Introduction . . . . .	2-1
	B. Program Results . . . . .	2-2
	1. Summary . . . . .	2-2
	2. Expanded Analog Test Program . . . . .	2-7
	C. Conclusions from Analog Test Program . . . . .	2-14
	LIST OF REFERENCES . . . . .	2-28
III	FULL-SCALE MOTOR OVERTESTS	
	A. Introduction . . . . .	3-1
	B. Previous Overtest Results . . . . .	3-2
	C. LRSLA Program . . . . .	3-9
	1. Overtest Program Description . . . . .	3-9
	2. Overtest of Motor 32765 . . . . .	3-11
	3. Overtest of Motor 32743 . . . . .	3-11
	4. LRSLA Overtest Summary . . . . .	3-14
	D. Overtest Program . . . . .	3-16
	1. Introduction . . . . .	3-16
	2. Overtest of Six-Year Motor . . . . .	3-17
	3. Overtest of Nine Year Motor . . . . .	3-35
	E. Evaluation of Full-Scale Overtest Results . . . . .	3-41
	LIST OF REFERENCES . . . . .	3-48
IV	PROPELLANT PROPERTIES	
	A. Introduction . . . . .	4-1
	B. CYH Propellant Characterization History . . . . .	4-3
	1. Minuteman Support Program . . . . .	4-3
	2. OOAMA-Hercules Co-Operative Test Program and Propellant Mechanical Property Results from the Second OOAMA-Hercules Co-operative Test Program . . . . .	4-3

## TABLE OF CONTENTS (Cont)

<u>Section</u>		<u>Page</u>
IV (Cont)	3. Third Stage Minuteman Production Support Program . . . . .	4-4
	4. Minuteman Surveillance Program . . . . .	4-4
	5. Minuteman Service Life Study Program . . . . .	4-5
	6. Minuteman II Stage III Motor Categories and Service Life Studies . . . . .	4-6
	7. Investigation of Pressure Oscillations During Firing of the Minuteman II Stage III Motor . . . . .	4-7
	8. LGM-30 Third Stage Dissected Motor Program . . . . .	4-8
	9. Long Range Service Life Analysis Program . . . . .	4-8
	10. Evaluation of Available Data . . . . .	4-9
C.	Interpretation of CYH Propellant Properties . . . . .	4-40
	1. Strain at Maximum Stress . . . . .	4-41
	2. Relaxation Modulus . . . . .	4-52
D.	Propellant Properties for Service Life Predictions . . . . .	4-73
	1. Introduction . . . . .	4-73
	2. Calculation of Strain at Maximum Stress . . . . .	4-74
	3. Calculation of Stress Relaxation Modulus . . . . .	4-74
	4. Conclusions and Recommendations . . . . .	4-77
E.	Acknowledgements . . . . .	4-80
	BIBLIOGRAPHY FOR SECTION IV . . . . .	4-81
V	M57A1 SERVICE LIFE ESTIMATES	
A.	Introduction . . . . .	5-1
B.	Analytical Studies . . . . .	5-1
	1. Method . . . . .	5-1
	2. Loads . . . . .	5-2
	3. Properties . . . . .	5-5
	4. Slot Tip Concentration Effects . . . . .	5-15
	5. Verification of Analysis . . . . .	5-20
	6. Results and Interpretation of Results . . . . .	5-32
C.	Consideration of Full-Scale Overtest Results . . . . .	5-36
D.	Conclusions . . . . .	5-45
	LIST OF REFERENCES . . . . .	5-47

VOLUME I  
LIST OF FIGURES

<u>Number</u>	<u>Title</u>	<u>Page</u>
1-1	Minuteman II Stage III (M57A1) Motor. . . . .	1-15
1-2	Configuration of Design Fix B-1 . . . . .	1-16
2-1	Wing Slot Cracking Failure Mode Model (Circular Centerbore), Case and Grain Subassembly . . . . .	2-3
2-2	Wing Slot Cracking Failure Mode Model (Circular Centerbore), Complete Assembly. . . . .	2-4
2-3	Wing Slot Cracking Failure Mode Model (Slotted Centerbore), Grain Configuration. . . . .	2-5
2-4	Aft-Centerport Bond Failure Mode Model. . . . .	2-6
2-5	Overtest Centerport Cracking Cylinder Hoop Strain E-2500, Centerport Cracking Cylinder 1.0, 10 Rubber Flap. . . . .	2-10
2-6	Overtest Centerport Cracking Cylinder Displacement, Centerport Cracking Cylinder 1.0, 10 Rubber Flap. . . .	2-11
2-7	Overtest Model O/T-012 - Average Pressure, Normalized Centerbore Diameter, Normalized Case Circumference, Normalized Case Strain. . . . .	2-12
2-8	Overtest Model O/T-013 - Average Pressure, Normalized Centerbore Diameter, Normalized Case Circumference. . .	2-13
2-9	Centerport Failure in Propellant, Model O/T-012 . . . .	2-15
2-10	External Propellant Failure, Model O/T-012. . . . .	2-16
2-11	Centerport Failure in Propellant, Model O/T-014 . . . .	2-17
2-12	External Propellant Failure (Case Removed), Model O/T-014 . . . . .	2-18
2-13	Propellant Failure, Model O/T-014 . . . . .	2-19
2-14	Overtest Model O/T-013 - Case Strain (Strain Gage 3). .	2-20
2-15	Overtest Model O/T-012 - Normalized Case Strain (Gage 4). . . . .	2-21

# LIST OF FIGURES (Cont)

<u>Number</u>	<u>Title</u>	<u>Page</u>
2-16	Overtest Model O/T-013 - Normalized Case Strain (Strain Gage 3) . . . . .	2-22
2-17	Overtest Model O/T-015 - Normalized Case Strain (Gages 5 & 6) . . . . .	2-23
2-18	Overtest Model O/T-014 - Normalized Case Strain (Gage 3). . . . .	2-24
2-19	Overtest Model O/T-016 - Normalized Case Strain (Gage 6). . . . .	2-25
2-20	Overtest Model O/T-017 - Normalized Case Strain (Gages 5 & 7) . . . . .	2-26
3-1	Minuteman Third Stage Motor . . . . .	3-3
3-2	Strain Gage Deflectometer . . . . .	3-5
3-3	Propellant Breakwire. . . . .	3-8
3-4	Wing Slot #3 Crack Profile (0032765). . . . .	3-12
3-5	Wing Slot #4 Crack Profile (0032765). . . . .	3-13
3-6	Wing Slot Cracking (Motor 0032743). . . . .	3-15
3-7	Event Gage Locations, 6-Year Motor. . . . .	3-19
3-8	Event Gage Locations, 9-Year Motor. . . . .	3-20
3-9	Event Gage Installed in Wing Slot . . . . .	3-21
3-10	Potentiometer Used in Wing Slots. . . . .	3-22
3-11	Humphrey Rectilinear Potentiometer in Critical Wing Slots . . . . .	3-23
3-12	Linear Potentiometer in Forward End of Center Core. .	3-24
3-13	Linear Potentiometer in Aft Center Port and Stress Relief Groove . . . . .	3-25
3-14	Instrumentation in Aft Center Port. . . . .	3-26
3-15	Special Wing Slot Potentiometer (Hummel Potentiometer)	3-27

# LIST OF FIGURES (Cont)

<u>Number</u>	<u>Title</u>	<u>Page</u>
3-16	High Rate Pressurization Transient. . . . .	3-29
3-17	Aft Face of Section II. . . . .	3-31
3-18	Forward Face of Section III . . . . .	3-32
3-19	Forward Face of Section I . . . . .	3-33
3-20	Aft Face of Section VI. . . . .	3-34
3-21	Extent of Cracking in Forward Dome. . . . .	3-36
3-22	Extent of Cracking Extending from Wing Slots 1 and 3. . . . .	3-37
3-23	Extent of Cracking in Wing Slots 2 and 4. . . . .	3-38
3-24	High-Rate Pressurization Transient for 9 Year Motor . . . . .	3-40
3-25	Cracks in Wing Slot 1 . . . . .	3-42
3-26	Cracks in Wing Slots 2 and 4. . . . .	3-43
3-27	Cracks in Wing Slot 3 . . . . .	3-44
4-1	CYH Propellant Shift Factors. . . . .	4-26
4-2	Short-Time Relaxation Data of Units Obtained from MM History. . . . .	4-30
4-3	High-Rate Strain of Units Obtained from MM History. . . . .	4-31
4-4	Strain at Maximum Stress, Lot 68-62, 2 in./min. . . . .	4-44
4-5	Strain at Maximum Stress, Lot 68-62, 1000 in./in./min . . . . .	4-45
4-6	Strain at Maximum Stress, Lot 1-1-63, 2 in./min . . . . .	4-47
4-7	Strain at Maximum Stress, Lot 1-1-63, 1000 in./in./min . . . . .	4-48
4-8	Strain at Maximum Stress, All Lots Together, 2 in./min . . . . .	4-49
4-9	Strain at Maximum Stress, All Lots Together, 1000 in./in./min. . . . .	4-50

# LIST OF FIGURES (Cont)

<u>Number</u>	<u>Title</u>	<u>Page</u>
4-10	Directly Measured $E_R$ and $E_R$ Calculated from Initial Tangent Modulus - LRSLA Motor 32769 . . . . .	4-56
4-11	Directly Measured $E_R$ and $E_R$ Calculated from Initial Tangent Modulus - LRSLA Motor 33231 . . . . .	4-57
4-12	Initial Tangent Modulus, Lot 68-62, 0.74 in./in./min.	4-62
4-13	Initial Tangent Modulus, Lot 68-62, 1000 in./in./min.	4-63
4-14	Initial Tangent Modulus, All Lots Together, 0.74 in./in./min. . . . .	4-65
4-15	Initial Tangent Modulus, All Lots Together, 1000 in./in./min. . . . .	4-66
4-16	Aging Trend of Relaxation Modulus at $10^{-4}$ Second. . .	4-67
4-17	Relaxation Modulus at 10 Sec, 3 Percent Strain, Five Motor Composite, Dissected Motor Program. . . . .	4-68
4-18	Strain at Maximum Stress for the Operational Motor Population. . . . .	4-76
4-19	Stress Relaxation Modulus for the Operational Motor Population. . . . .	4-79
5-1	M-57 Motor Ignition Pressure as a Function of Motor Age From 169 Firings - Corrected to 70° F . . . . .	5-4
5-2	Comparison of OPRI and Bl Fix Wing Slot Tip Configurations. . . . .	5-16
5-3	Concentration Factor as a Function of Slot Depth for Minuteman Stage III Rocket Motor. . . . .	5-17
5-4	Total Slot Tip Strain as a Function of Slot Tip Radius for Various Propellant Tensile Moduli and Case Stiffness. . . . .	5-21
5-5	Normalized Damage Factors for Overtesting of Motor No. 32765 Based on Strain Dependent and Constant Slot-Tip Strain Concentration Factors . . . . .	5-22
5-6	Stress Relaxation Moduli for Mean CYH Propellant Lot and for Overtested Motors . . . . .	5-26

# LIST OF FIGURES (Cont)

<u>Number</u>	<u>Title</u>	<u>Page</u>
5-7	Allowable Strain Versus Strain Rate for Mean CYH Propellant Lot and for Overtest Motors. . . . .	5-27
5-8	Calculated Maximum Adhesive Bond Shear Stress Per Unit Applied Pressure Versus Propellant Tensile Modulus . . . . .	5-33
5-9	Predicted Cylindrical Hoop Strain at Critical 3.7 Inch Radius per Unit Applied Pressure Versus Propellant Tensile Modulus. . . . .	5-34
5-10	Analytically Calculated Damage Factors at Failure of Overtested Motors Based on Actual Pressurization Transients and Mean Properties for all Motor Lots Compared to Analytically Calculated Required Damage Factors . . . . .	5-39
5-11	Graphical Comparison of Regression Curve of Damage Factor Capability With Required Damage Factor for Motor Serviceability. . . . .	5-41
5-12	Probability of Successful Firing for M-57 Motor (B-1 Fix Configuration) Versus Motor Age-Extrapolated from Overtest Data. . . . .	5-44

# VOLUME I

## LIST OF TABLES

<u>Number</u>	<u>Title</u>	<u>Page</u>
1-1	Summary of High Rate Pressurization Overtests of M57A1 Full-Scale Motors . . . . .	1-9
1-2	List of Overtest Approaches . . . . .	1-28
2-1	Failure Prediction . . . . .	2-9
3-1	Motor Characteristics . . . . .	3-10
4-1	Sources of Data . . . . .	4-10
4-2	Sample Conditions . . . . .	4-15
4-3	Sources of Data for Minuteman Production Powder Lots . . . . .	4-23
4-4	Relaxation Modulus Data Set . . . . .	4-27
4-5	Data Set for Strain at Maximum Stress . . . . .	4-28
4-6	Stress Relaxation Data for Study of Variability . . .	4-33
4-7	Minuteman II Stage III Propellant Acceptance Values . . . . .	4-34
4-8	Trend Data Tensile Test Results . . . . .	4-38
4-9	Biaxial Strain at Maximum Stress Aging Trend Data . .	4-39
4-10	Test for Equality of Means of Strain at High Strain Rates Obtained from FPC's and FSU's . . . . .	4-42
4-11	Test for Equality of Means of Properties Obtained at 2 In./Min CHS . . . . .	4-43
4-12	Rank Test of the Influence of Powder Lot Acceptance Values . . . . .	4-51
4-13	Unit-to-Lot Bias Calculated with Individual Unit Lot Values . . . . .	4-53



VOLUME I  
LIST OF TABLES (Cont)

<u>Number</u>	<u>Title</u>	<u>Page</u>
4-14	Unit-to-Lot Bias of Strain at Maximum Stress Calculated with Weighted Average Lot Values . . . . .	4-54
4-15	Test for Equality of Means of Relaxation Data Obtained with Superimposed Pressure and at Ambient Pressure . . . . .	4-59
4-16	Test of Equality of Means of Relaxation Modulus Obtained from FSU's and Subscale Units . . . . .	4-60
4-17	Rank Test for Influence of Powder Lot Acceptance Values on Relaxation Modulus . . . . .	4-70
4-18	Unit-to-Lot Bias of Stress Relaxation Modulus . . . . .	4-72
4-19	Powder Lots in the Existing Minuteman II Stage III Motor Inventory . . . . .	4-73
4-20	Calculation of Strain at Maximum Stress for the Existing Population of Motors . . . . .	4-75
4-21	Calculation of the Mean and Standard Deviation of the Stress Relaxation Modulus of the Operational Motor Population . . . . .	4-78
5-1	M-57 Motor Ignition Pressures - Corrected to 70 <sup>0</sup> F . . .	5-3
5-2	M-57 Motor Ignition Pressurization Transients (70 <sup>0</sup> F Firings) . . . . .	5-6
5-3	M-57 Material Properties Used in Finite Element Stress Analyses . . . . .	5-9
5-4	Experimental Case Deflection at 300 Psig from Hydroproofing of M-57 Motor Chambers . . . . .	5-10
5-5	M-57 Motor Chamber Experimental Burst Pressures . . .	5-13
5-6	M-57 Mean and Plus 3-Sigma Chamber Deflections for 300 Psig Internal Pressure Obtained from Finite Element Analysis . . . . .	5-14

VOLUME I  
LIST OF TABLES (Cont)

<u>Number</u>	<u>Title</u>	<u>Page</u>
5-7	Computed Radial Case Deflections and Percent of Internal Pressure Load Carried by the Propellant at the Critical Slot Tip Cross Section of the FSU . . . .	5-19
5-8	Propellant Stress Relaxation Moduli (70 <sup>0</sup> F) Input to Viscoelastic Response Analysis . . . . .	5-23
5-9	Allowable Strain Versus Strain Rate (70 <sup>0</sup> F) Input to Viscoelastic Response Analysis . . . . .	5-24
5-10	Pressurization Transient Applied During Overtesting . . . . .	5-28
5-11	Analytically Predicted Overtest Failure Levels of Full-Scale Motors, Constant $K_{\epsilon}$ . . . . .	5-30
5-12	Error of Mean Case Configuration Predicted Pressures from Actual Failure Pressures . . . . .	5-31
5-13	Cylindrical Hoop Strain at Critical 3.7 Inch Slot Tip Radius Per Unit Applied Pressure as a Function of Propellant Modulus . . . . .	5-35
5-14	Capability Statistics at Advanced M-57 Motor Ages . .	5-43

## SECTION I

### INTRODUCTION AND SUMMARY

#### A. INTRODUCTION

The prediction of service life of ICBM solid propellant rocket motors has been and continues to be of major concern. Reliable service life estimates are required to identify the point in time at which a particular motor must be removed from the active inventory or a category of motors no longer meets reliability requirements. Moreover, the prediction must be made far enough in advance to define a suitable motor replacement policy. An advance notice is particularly critical for motors which are no longer in production, and startup time for new production would be critical if a decision is made to replace them with similar motors.

Current ICBM aging and surveillance programs are not sufficient to adequately predict motor service life. Such programs normally involve testing of a limited number of aged motors and certain materials and components which have been stored under simulated operational conditions. Motor firings serve primarily to verify motor performance at a given age, and materials and component tests are usually limited to identification of aging trends.

Motor firings alone cannot be used to define ultimate motor capabilities. Firings can only verify that some motors will perform at a given age, but they provide only meager data to predict failure probabilities. Hence, it is not possible to extrapolate a few successful aged motor firings and identify a time when an unacceptable number of motor failures will begin to occur without making a number of unproven statistical assumptions.

Materials aging trends, theoretically, should be useful for predicting service life. However, many of the aging programs were planned several years ago when the state-of-the-art for structural analysis was not as fully developed as it is now, and the samples being stored and the properties being monitored often were not compatible with analysis requirements. Also, questions have arisen as to the applicability of much of the aging data because storage methods and environments do not adequately recreate motor conditions. Data from propellant aging and surveillance programs have been used to predict service life; however, there is not sufficient confidence in such analyses to allow decisions on phasing motors out of the missile force. Results of one theoretical study using data from aged uniaxial propellant samples of the M57A1<sup>1</sup> predicted that the motor reliability should show an appreciable decrease after 8-1/2 years due to an

---

<sup>1</sup>

References are listed at the end of each section.

increased probability of propellant grain cracking. Subsequent firings of motors of this age have not verified these results; however, there was concern at the start of the project reported herein that the general trends which were predicted may be true.

Accelerated aging has been tried as a means of obtaining early answers regarding propellant grain structural integrity. Generally, this approach has met with disfavor because of a lack of understanding of fundamental aging mechanisms and/or difficulty in defining an appropriate accelerated aging environment. Although accelerated aging was not addressed in this project, it is recognized as vital to a meaningful predictive surveillance program.

The general concept of overtest involves testing of motors or motor components to levels greater than those normally seen in actual operation. If the test is carried to failure, the capability of the motor or component can be experimentally defined for the particular resulting failure mode.

In principle, the overtest concept provides several advantages as a method for estimating motor service life. In applying this approach, full-scale and/or subscale motor analogs of various ages are subjected to simulated environmental and operational loadings to experimentally determine or confirm the critical failure modes of the motor. The margins of safety (or reserve strength) for the critical failure modes relative to the required loading environments are determined by subjecting the test vehicles to load levels sufficient to cause failure. By using experimental means to measure the reserve strength, analysis inaccuracies are largely circumvented. Testing of actual aged units insures proper aging boundary conditions. By thus defining the capability of motors of varying ages to withstand the most critical environments, it should be possible to extrapolate capability-versus-age data to a time when the motor is shown to no longer have sufficient capability to withstand the expected loads.

Overtests need not necessarily be restricted to full-scale motors. For statistical significance relative to a particular failure mode, small analog devices appropriately designed to provide failure data may be more economically desirable.

This report is the final technical report of work performed as a part of the ICBM Overtest Technology Program, Contract No. F04611-73-C-0010, which was conducted by Hercules under contract from AFRPL. The primary objective of the overtest program was to establish and demonstrate the applicability of overtest technology to the general problem of service life predictions. Emphasis was directed to propellant grain structural integrity. A secondary, but extremely important, objective was to make service life estimates for the Minuteman II, stage III motor (M57A1)

which is used in the LGM-30B and F missiles. The M57A1 rocket motor, Minuteman II stage III was selected as the test vehicle to be used in developing ICBM overtest technology. The structural behavior of the M57A1 was fairly well understood; however, an accurate age-life prediction was needed for this motor. Also, surplus units were available from the Air Force strategic inventory thus providing a source for the test vehicles.

Structural overtest procedures had been previously demonstrated for the most significant types of loads with subscale and full-scale M57A1 motors. Specifically, the motor had been overtested to failure by high-rate pressurization. Subscale test vehicles and partial motor analogs had been designed to represent critical failure regions of motors. These were tested to failure to experimentally determine motor integrity.

It is desirable that the technology evolving from the ICBM overtest program be applicable to new motors as well as those already deployed. An overtest program which is planned during development or early production would likely differ considerably from one directed to operational motors. Therefore, the use of the M57A1 motor as a test vehicle does introduce special problems that would not arise in many programs. Thus it does have some disadvantages as a general technology demonstration vehicle.

Several studies have been performed to evaluate aging effects on the M57A1 motor. Some of the results from these programs were used in the planning and interpretation of the overtest program results.

The most likely failure modes for the M57A1 motor were understood from the development program and subsequent studies. A special task was performed under the SAMSO sustaining engineering program (F04701-71-C-003)<sup>1</sup> to identify and screen potential failure modes for the motor. A comprehensive list of postulated failure modes was reduced to five which were studied in detail. Of the five, two potential failure modes were related to the propellant grain. The most likely failure mode was considered to be wing slot cracking under ignition pressure loading. The second mode, aft center port bond breakage, was potentially service life limiting only in a select category of motors manufactured prior to February 1966.

A special investigation was performed for OOAMA\* for categorization of motors in the inventory according to characteristic design and performance features.<sup>2</sup> These motors, except for a block having a different design (manufactured after February 1966), were categorized according to the base grain lots used to cast the CMDB propellant (CYH) used in the motors.\*\* This study

---

\* OOAMA was changed to OOALC during the course of this investigation and may be used interchangeably in this report.

\*\* The M57A1 motor contains two different CMDB propellants, CYH and DDP; however, the CYH propellant is used in the critical stress location.

reinforced the original selection of the two principal failure modes. Consideration of these same two failure modes was extended into LRSLA program tasks related to the M57A1 motor.<sup>3</sup>

Full-scale motor overtest technology applicable to the M57A1 motor originated in the motor development program. Experimental methods were devised and used to determine the behavior of the M57A1 motor in response to the ignition transient. Various overtest approaches were evaluated, and the high-rate hydrotest was chosen as the best for evaluation of the particular failure modes in question. High-rate pressurization test equipment and procedures were developed in the earlier programs and were available for this program. Refinements in the basic approach were made in the overtest and LRSLA programs.

Subscale or motor analog overtests are essential to the total concept of overtest. Much background information on the design and conduct of subscale tests was available to the overtest program. Studies performed under other programs also contributed to the motor analog overtest task.

The most difficult task of the overtest technology program as it relates specifically to the M57A1 motor was created by the availability of vast amounts of laboratory data which were to be interpreted for use in the prediction of M57A1 service life. Data were available from several lots of propellant base grain, full-scale motors, and subscale charges. Varying degrees of characterization were performed over a period of several years to study humidity, temperature, and rate. Programs specifically concerned with propellant aging were conducted. The major problem in interpretation was in finding commonality in the data and in relating the results to the particular motors used in the overtest program and to those M57A1 motors which remain in the Minuteman force. In many cases it was not possible to identify specific base grain lots, and many of the studies were conducted with lots that are no longer represented in the active inventory.

Over 50 sources of data were reviewed. Propellant properties from these earlier studies were used in conjunction with overtest and LRSLA properties to determine a baseline set of analysis properties, aging trends, lot-to-lot variability, within-grain variability, and subscale to full-scale motor differences.

Service life predictions for the M57A1 motor prior to the recent overtest technology and LRSLA programs were based primarily on trends detected in the Minuteman surveillance program. The results of that study, which were based on a select data population, were presented as a function of motor reliability-versus-motor age. It was estimated in that study that reliability of the M57A1 motor would begin to be affected after about 8-1/2 years of aging.

The overtest program basically followed a linear series of tasks, the result of each task being used to better define the subsequent tasks. Thus, the first step was the identification of the critical motor failure modes. Having defined the failure modes that were to be overtested, various test methods that could be used to produce these failure modes were identified, and the most effective approach was identified. Subscale units, one type of which modeled each of the two critical failure modes, were subjected to the overtest procedure previously identified. Having proved that the selected overtest procedure would cause the critical failure modes, two full-scale units were subjected to the overtest procedure. Propellant failure theory was also checked, using the subscale units. An inspection procedure (motor dissection) was then used to confirm that one of the critical failure modes had been induced by the overtest procedure. Physical property testing was performed on materials obtained from the motor dissection operations, and the data thus obtained were used to check the accuracy of the service life analysis procedure. An estimate of motor service life was obtained, using the motor failure pressurities obtained from the motor overtest. An analytical estimate of motor service life was also obtained using an analysis program that had been checked against the actual overtest results. Physical properties of the existing population of operational motors were obtained for the analysis from a study of all of the published Minuteman II, stage III physical property results.

The objective of this report is to present the tasks, procedures, and results related to application of the overtest concept to service life predictions for the Minuteman II, stage III rocket motor. Further details of the ICBM overtest program are reported in monthly progress reports and interim technical reports. The topics covered by the interim reports are treated briefly in the main body of this report.

Neither the analysis of critical physical properties of the Minuteman II, stage III motor nor the prediction of motor service life have been previously reported. Hence, these topics are presented in detail in this final technical report. Finally, the experience gained in the overtest program and in previous or related efforts, is presented as a general manual of overtest technology. The overtest technology presentation is in a separate volume (Volume II) to provide a ready reference for future planning of overtest and predictive surveillance programs.

## B. SUMMARY

A methodology for motor service life prediction through overtesting was developed and demonstrated in this program. The experience gained in the ICBM Overtest Technology Program has been organized into a set of recommended practices for overtesting.

The critical failure modes of the Minuteman II, stage III rocket motor were proved to be wing slot cracking and failure of the aft centerport boot-to-flap bond. Failure modes were examined in light of new data and experience that had been accumulated since 1971 when the first failure mode list was formulated. An updated failure mode list was prepared which consisted of nine failure modes. The two critical failure modes\* are wing slot cracking and aft centerport debonding. The remaining seven failure modes are all of low criticality.

Overtest approaches were listed and evaluated for their applicability for inducing failure by the two most critical failure modes in the M57A1 motor. The applicability of each test approach analyzed was ranked by considering the ratio of the safety factors at the two critical locations of failure. Each overtest approach was also ranked in order of ease of accomplishment and in order of increasing cost. The overall rank of each approach was taken as the sum of the three rank orders obtained. High-rate hydrotest at 70° F had the lowest overall ranking and was thus selected as the overtest approach to be used on two full-scale motors.

The stress analysis of the M57A1 wing slot tips was refined by the use of more advanced methods than those available for the previous work on this motor. The slot tip strain concentration factor was found to be pressure dependent, ranging from 2.93 at 0 psi to 2.60 at 600 psi. Previous analyses used a value of 2.95 for all pressure loads. The motor service life predictions made previously were thus proven to be slightly on the conservative side.

Testing of subscale models was performed to demonstrate that the overtest approach selected for full-scale testing would cause the predicted failures. The two critical motor failure modes were tested through the use of different models, and each was designed to fail by the required failure mode. Aged propellant from Minuteman motors was used in the models. The models demonstrated motor aft centerport boot-to-flap and centerport cracking failure, thus establishing the utility of the analog devices for experimental analysis of particular failure modes. Although it was not possible to demonstrate the total concept of subscale overtests in the surveillance program, the basic technology was demonstrated. The analog devices also verified the analytical techniques and failure criteria.

High-rate pressurization overtests were successfully performed on the 9- and 6-year old motors. Wing slot cracking was demonstrated as the principal failure mode on both motors. Cracking initiated in the

---

\* Critical mode in the context of this report means the limiting mode, not necessarily critical from a normal performance point of view.



forward trim area, about 3 inches forward of the expected critical location. Wing slot cracking was detected by event gages at a pressure of 475 psi in the 9-year motor and at 575 psi in the 6-year motor. The aft centerport boot-to-flap adhesive bond did not experience failure during the test of the 9-year motor. The vulcanized boot-flap bond of the 6-year motor which was not considered to be a likely failure mode was confirmed in that the bond did not experience failure during testing. The extent of cracking was confirmed by posttest inspection and dissection of both motors.

The event gage concept was developed in the overtest program for detection of grain failure. Commercial conductive RTV rubber was selected as the event gage material on the basis of performance on JANNAF dogbone specimens. The conductive RTV is applied directly to the primed propellant surface and allowed to cure in place. Failure is detected by a change in gage resistance. For the motor tests, event gages were applied across the tips of the wing slots and across the high strain areas of the aft center port region.

Physical properties necessary for analysis were obtained from propellant, case bond, and boot-flap adhesive or vulcanized bond materials from the overtested motors. These data were combined with data from past and ongoing Minuteman II, stage III programs to obtain a test data set of propellant properties consisting of relaxation modulus and strain at maximum stress for the operational motor force. Statistical tests were performed on the data to ensure that only homogeneous populations were included. The OALC Dissected Motor Program was the primary source of data for the study of aging trends of propellant properties. Some data obtained from previous programs, Overtest and LRSLA, were available to add to the OALC data. The properties of tangent modulus, strain at maximum stress, and relaxation modulus at 10 seconds were tested for aging trend by calculating the linear regression equations of property versus age. Regressions were performed on data from each powder lot and on all data taken together. Not only were the slopes of the regression lines nearly zero, but the correlation coefficients were so low as to indicate that no cause-and-effect relationship could be established for any change in property as a result of age. It was, therefore, concluded that CYH propellant does not degrade in structural capability as it gets older.

Correlations were obtained to relate relaxation modulus and strain at maximum stress to propellant powder lot acceptance mechanical properties for individual powder lots. The correlation factor associated with each strain rate was multiplied by the weighted average of the lot strain at rupture to directly find the average curve of strain at maximum stress-versus-strain rate for the population of operational motors associated with each lot. The standard deviations for strain at maximum stress and relaxation modulus were calculated as limit values at 95-percent probability using the sample standard deviation and the chi-square statistic.

Service life was calculated by two methods:

- (1) Analytical calculations of capability-versus-age based on interpretation of mechanical properties and loads versus age
- (2) Linear extrapolation of overtest results

In addition to the propellant properties previously discussed, the ignition pressure time transient and motor case stiffness were also needed for the analytical service life prediction. Pressure-time data to describe the ignition transient were extracted from static firing reports for 78 motors. Maximum ignition ( $P_{\max}$ ) pressure was obtained for 91 additional motors. Linear regression analysis of  $P_{\max}$  for all 169 motors showed that ignition pressure was not changing with motor age.

The effect of case stiffness was obtained by adjusting the case properties of finite element runs until the calculated deflection matched the deflection obtained from case hydrotest data. The probability of failure versus time was obtained by a statistically-based requirement/capability analysis program. The resulting service life prediction is thus expressed as the age at which the probability of success falls below a level considered necessary to maintain the credibility of the strategic deterrent. In the actual case of the Minuteman III, stage II motor, however, none of the program inputs were found to have a significant aging trend. The probability of motor success is, therefore, constant, so only one requirement/capability calculation was required. The analysis conclusion was that no failures of the wing slot propellant are expected due to the loads imposed by the ignition transient.

Failure results from high-rate overtest of full-scale units were also used to predict the M57A1 service life. Motors tested in programs in addition to ICBM overtests were used in the prediction. Eight full-scale motors have been high-rate pressure tested to failure. Five of those yielded results that are applicable to the ICBM overtest program. (Refer to Table 1-1.) Additionally, one motor was tested to a pressure of 310 psi with no resulting failure.

In addition to age differences, the motors had design differences and normal variations to be expected in propellant and case properties. Since data were not available by which individual motors could be characterized completely and specifically with respect to the mean of the population, some arbitrary but conservative assumptions were made for interpretation.

Each of the motors was analyzed considering its particular loading program and known geometric features. Propellant and case properties were based on mean values for the total motor population. A cumulative damage factor was calculated for each motor based on these mean properties.

TABLE 1-I

SUMMARY OF HIGH RATE PRESSURIZATION  
OVERTESTS OF M57A1 FULL-SCALE MOTORS

Motor	Cracking Pressure (psi)	Pressurization Rate (psi/sec)	Safety Factor*
SD-9	$P_{\max} = 410$ ; crack initiation pressure <u>not</u> detected	4,000	—
SD-10	$P_{\max} > 655$ ; crack initiation pressure <u>not</u> detected	10,000	—
2-10-16	500-530	12,000	1.82-1.93
2-10-38	$P_{\max} = 310$ ; no cracks	15,000	>1.13
33348 (OT)	575	20,000 to 31,000	2.09
32570 (OT)	475	18,000 to 29,000	1.73
32765 (LRSIA)	500	20,000	1.82
32743 (LRSIA)	492-525	17,000	1.80-1.91
*These figures are somewhat optimistic, as the propellant allowable strain is higher at 500 psi than it is at 275 psi.			

The differences between a damage factor of unity and the calculated value, indicate the degree to which the particular motor deviates from an average motor.

Also using average properties, each individual motor was analyzed considering the expected variations in ignition pressure transient. Damage factors corresponding to the expected ignition loads were thus determined. A failure index was defined by the ratio of the damage factor determined from the test to that determined for normal operation.

Based on interpretation of results from the overtests it was difficult to support any trend analysis. However, by taking a conservative interpretation of failure pressures indicated by the test instrumentation, a slightly downward trend results. Based on a probability of success of 0.9987 at the 90-percent confidence level, a service life of 234 months (19 years, 6 months) is predicted by linear regression and extrapolation. A less conservative interpretation of the overtest results would likely be in agreement with the theoretical predictions which showed no limits on service life due to reduced grain structural integrity.

#### C. TECHNICAL APPROACH

The overtest approach was planned to utilize information from a variety of sources to predict the aging structural behavior of operational Minuteman II, stage III motors. The present force is inadequately defined for a comprehensive analysis. If all motors were identical, such that all motors of the same age would have equal capability, a service life prediction could be made in a relatively straightforward fashion. Overtests could be performed on motors of two different ages and a line extrapolated through the two experimental points to generate a realistic plot of failure pressure versus age.

Overtesting of real motors, of course, does not yield information that is so readily converted into a form useful for service life prediction. The failure pressure measured during a motor overtest must be considered to be a random sample obtained from a statistical distribution of motors of various capabilities. Although an estimate of the mean and variance of the failure pressure of the entire motor population at any desired confidence level at selected ages could be obtained by the overtesting of a large number of motors, the cost and complexity of such a task intuitively rules it out. Therefore, it is necessary to utilize other information and analysis methods to determine the relationship of the motor overtest results to the entire motor population. The associated elements are considered an inherent part of the general overtest methodology.

The ICBM overtest program was accomplished according to a general plan consisting of three major phases with eight main subtasks as follows:

- (1) Phase I - Definition
  - (a) Task I - Selection of Principal Failure Modes
  - (b) Task II - Overtest Modeling
  - (c) Task III - Subscale Verification
- (2) Phase II - Overtest and Inspection
  - (a) Task IV - Motor Overtest
  - (b) Task V - Posttest Inspection
  - (c) Task VI - Subscale Tests
- (3) Phase III - Interpretation of Results
  - (a) Task VII - Motor Service Life Prediction
  - (b) Task VIII - Evaluation of Overtest as a Method for Predicting Motor Service Life

Much of the work associated with a general overtest program had already been accomplished in previous programs for the M57A1 motor. This was particularly true for the definition phase (Phase I). However, in order to conform to the general approach, each of the tasks was addressed and earlier conclusions regarding definition of failure modes and overtest approaches were verified in Phase I.

The list of failure modes previously compiled for the M57A1 motor<sup>2</sup> was updated. Flighttest data and motor surveillance firings were reviewed for further understanding of the structural behavior of the motor. Potential failure modes were tabulated in a list according to decreasing criticality. The failure modes were evaluated according to past related problems, critical aging parameters, predicted margins of safety, and known aging trends.

Various overtest approaches were evaluated analytically. Applicability of the tests were judged on the basis of comparisons of results obtained by analysis of the overtest loading plan and the actual ignition pressure transient. The high-rate pressurization hydrotest at 70° F was selected as the experimental approach to be used for the full-scale motor overtests.

Subscale models were designed and tested to demonstrate the overtest approach selected for full-scale tests. Different subscale models were designed to evaluate two critical failure modes. Each type of model was designed to fail according to one of the chosen failure modes. Test specimens were designed and analyzed using the same methods and material properties as were employed in the analysis of overtest approaches.

Two full-scale motors were overtested by high-rate pressurization. One motor was 6-years old and one approximately 9-years old. The extent of cracking and verification of failure modes were accomplished by post-test inspection and motor dissection.

Overtest results from other programs in addition to the ICBM overtest program were also used in evaluating the M57A1 motor service life. Particular programs of interest were the Minuteman Product Support Program and the current LRSLA program.

Subscale motor analogs were developed and demonstrated for the M57A1 critical failure modes. A design was accomplished in which failures were achieved as centerport cracking during high rate pressure testing. Also, boot-to-flap debonding and stress relief groove failures were demonstrated in aft centerport failure mode analog models. Although these tests were not directly applicable to the Minuteman service life analysis, they do illustrate the utility of analog devices in a general predictive surveillance program.

Motor service life estimates were made by two principal techniques. First, theoretical analyses were performed using materials properties representative of various aging times. Properties were projected to longer aging times for analyses corresponding to future dates by extrapolation of available data and aging trends. Secondly, experimental overtest results from full-scale unit tests of motors of different ages were extrapolated to advanced ages.

The analysis method was verified by results from the full-scale and analog test results. Ignition pressure data were evaluated statistically using results from actual motor firings.

The lot acceptance data and results from subsequent characterization programs were used to derive the necessary properties for the analyses. This was accomplished by establishing correlations between values obtained from various test sample conditions, and applying these correlations to other tests involving specific propellant data sets to obtain a general set of properties. The main sources of data for the theoretical service life analyses were the following programs: ICBM Overtest Technology, Long Range Service Life Analysis, and Dissected Motor Program. These are current programs in which CYH propellant data are being obtained. Other programs and special investigations dating back to 1963 were also required and contributed to the interpretation of propellant data. Available test data were utilized directly where applicable.

Case properties were derived from deflection data taken from 67 case hydroproof tests. Means and standard deviations were calculated.

Geometric changes made during production of the remaining M57A1 motors in the field were accounted for in the analyses.

A requirement/capability analysis was performed for the pre-OPRI motor configuration since these motors possess the lowest margin of integrity initially. Monte Carlo selection of applicable motor parameters was used to produce 105 statistical motor samples.

Failure results from high-rate overtest of full-scale units were also used to predict the M57A1 service life. Motors tests in other programs were used, in addition to ICBM overttests, in the prediction.

Each of the motors was analyzed considering its particular overtest loading program and known geometric features. Each individual motor was also analyzed for a normal firing considering the expected variations in ignition pressure transient. Damage factors corresponding to the expected ignition loads were thus determined. A failure index was defined by the ratio of the damage factor determined from the test to that determined for normal operation. The estimated service life was derived by extrapolation of the failure index-versus-age results from the overtest motors.

Specific recommendations for general application of overtest technology to the prediction of ICBM solid-propellant service life, as it is determined by grain structural integrity, were made based on results from this program. The recommended overtest and analysis approach was defined for motors currently in service or for those in early stages of design and development.

#### D. MINUTEMAN II STAGE III REVIEW

The intent of this paragraph is to review the M57A1 design and programs as they relate to the overtest program. Particular programs and the pertinent results are normally presented in appropriate portions of this report. Therefore, only brief summaries along with the types of significant information obtained are given here.

##### 1. Motor Design and Manufacture Review

A very general description of the M57A1 motor is given in this report. The reader is referred to the Minuteman Data Book and Assembly and Subassembly Drawings for detailed design information.

The Present M57A1 design is different from the design employed in earlier motors. Of particular significance are changes made under the Operational Reliability Improvement Program (OPRI)<sup>4</sup> which resulted in

the final motor configuration. Corrective action taken prior to incorporation of the OPRI modifications consisted of machining an obturating groove in the propellant at the aft centerport. The groove was designed to relieve stresses on the flap-to-insulator (boot). This fix, termed the "B-1 Fix" was incorporated on a number of motors which were built prior to the OPRI motors.

The M57A1 motor design is shown in Figure 1-1 and the B-1 fix in Figure 1-2. The motor case is glass filament-wound reinforced epoxy with special glass reinforcements at the case opening and skirt attach regions. Metal adapters are wound into the case to provide means of attachment for the nozzles, igniter, forward and aft port closures, and thrust-termination hardware. The case is protected from the combustion gases by an internal insulator which covers the internal surface of the case. To provide added protection in the aft end of the motor, an additional thickness of insulation (boot) is bonded to the regular insulation. A shrinkage liner (flap) is employed to allow freedom of motion at the ends of the propellant grain. The shrinkage liner is vulcanized (or bonded, depending on the family of motors) to the boot near the aft tangent line and around nozzle and aft centerport openings.

The M57A1 grain design is a dual-propellant, trilevel configuration. The main propellant, comprising approximately 85 percent of the grain, is CYH. A layer of DDP-77 propellant approximately 9.5 inches thick extends from approximately 1.5 inches aft of the forward tangent line to 8 inches forward of the forward tangent line of the motor. The grain is essentially a slotted-tube type in which the centercore extends only part way through the chamber; thus the motor operates as an end-burner for a large portion of its burning. Slots connect the center tube with four hollow cones that extend into the nozzles. The slots are also in line with four thrust termination (TT) ports which are located near the aft end of the motor.

The motor has four pivoted nozzles. The nozzle design consists of a ball-and-socket joint pivoted about a single axis and sealed by two rubber O-rings. A wiper ring is utilized to scrape the spherical section of the pivoting exit cone to prevent a buildup of slag in the split-line. Each nozzle is movable only in a plane perpendicular to a radial line passing through the longitudinal center of the motor and the center of the nozzle.

#### a. Casting Powder

The casting powder for the M57A1 motor was designated as HDDRA at Radford Army Ammunition Plant (RAAP). All ingredients were supplied to military specifications, and records certifying compliance were kept.



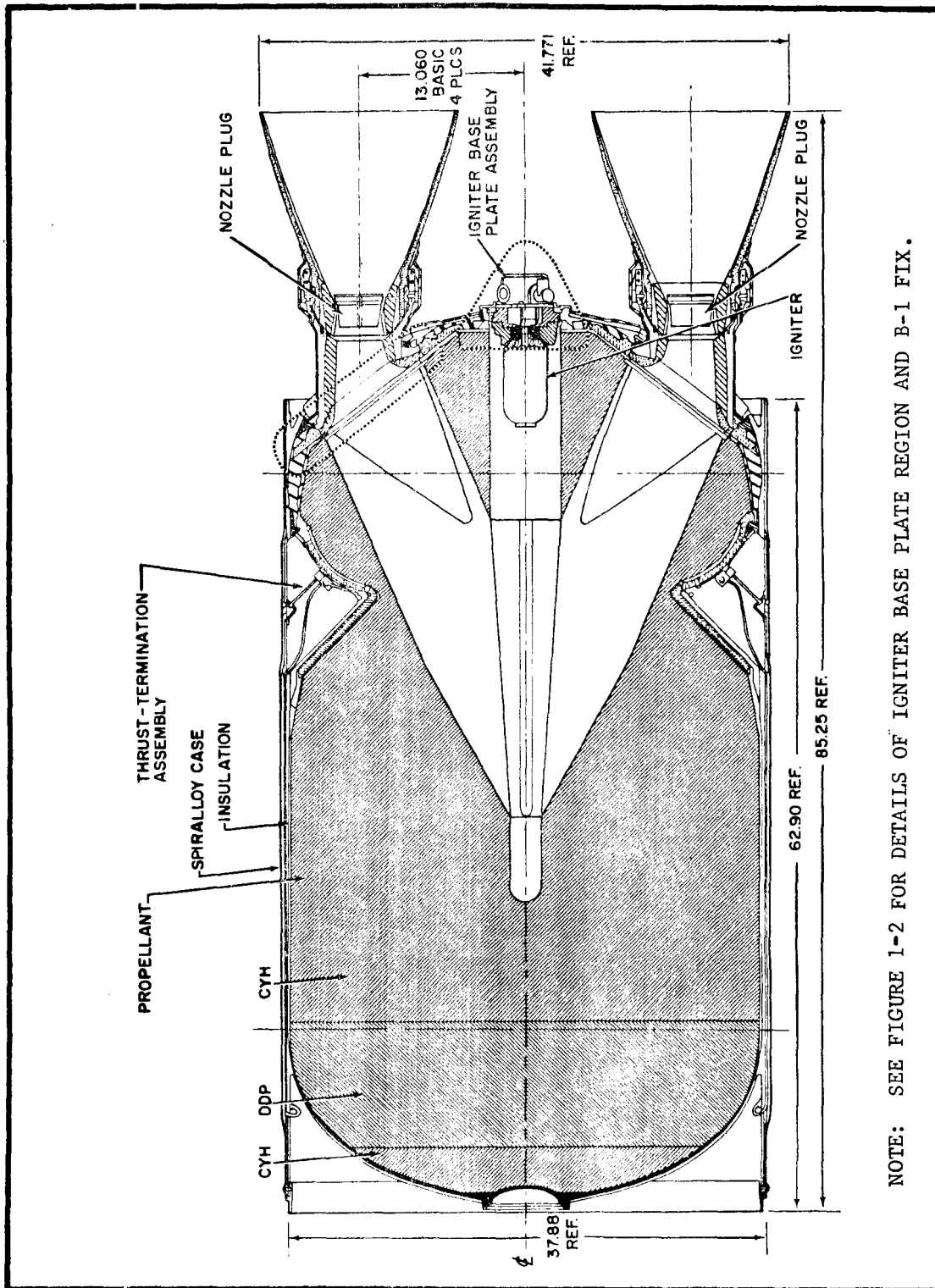


Figure 1-1. Minuteman II Stage III (M-57A1) Motor

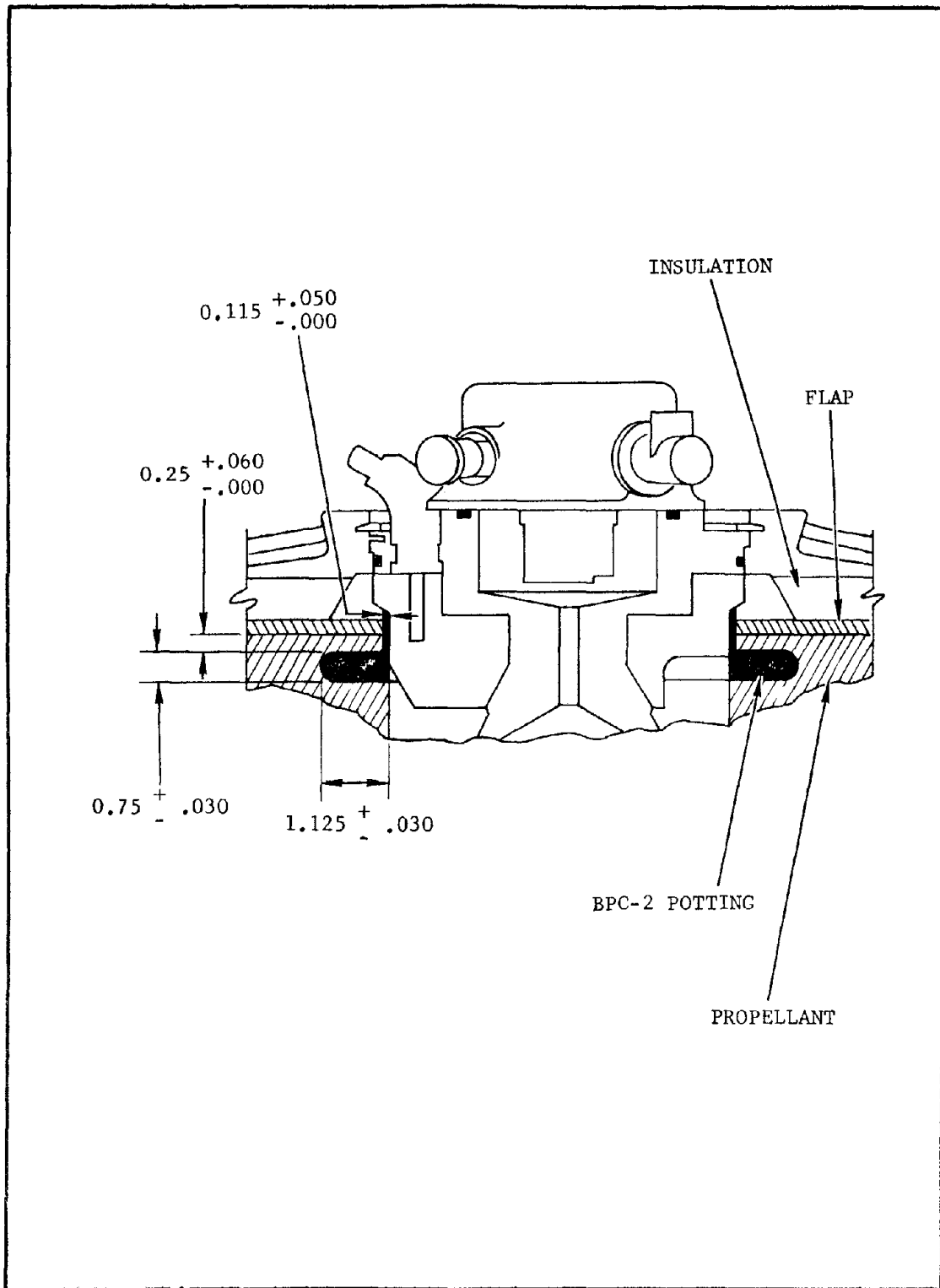


Figure 1-2. Configuration of Design Fix B-1

Ballistics tests using forty pound charge\* (FPC) motors are performed at RAAP and Bacchus Works to determine ballistic performance of each lot of casting powder. Physical properties of propellant manufactured from the powder also are determined at both facilities; therefore, two sets of physical properties data pertaining to the powder were available for review in the oscillations program.

b. Case

Cases for the M57A1 motor were wound at Hercules Rocky Hill and Clearfield plants. There was an eventual changeover to Clearfield as the sole supplier. Differences were observed in manufacturing at the two plants and changes were implemented, principally at Clearfield, to increase burst pressures.

All motor cases were hydrotested to a pressure of 420 psi (approximately 70 percent of design) prior to use. In addition, one out of each production lot of cases was pressurized to failure. Instrumentation during hydrotests consisted of strain gages and linear potentiometers so that changes in case strength and stiffness characteristics could be monitored. Not all data from the hydroproof tests were reduced, however.

c. Motor

The assembly of all essential materials and casting of the propellant grain was accomplished at the Bacchus Works. The propellant grain was manufactured by the cast double-base process. In this process, the empty case is first filled with casting powder. The procedure by which casting powder is loaded into a case in the correct quantity and with uniform distribution and packing density is called mold loading. Casting is the process of introducing the solvent to the casting powder and allowing the mixture to cure to a solid propellant. During this time casting solvent is absorbed by the casting powder, which as it swells, in turn pushes into the interstices formerly occupied by the absorbed liquid. Pressure is maintained on the solvent while the solvent is being added. Mechanical displacements are applied to the propellant by rams to aid in propellant grain consolidation. Many of the changes which were implemented in the OPRI program had to do with motor manufacturing. Detailed descriptions of the individual manufacturing operations can be obtained by referring to Hercules, Bacchus Works Operating Procedures. For individual motors the manufacturing records provide specific information.

---

\* FPC's are routinely used by Hercules to determine burn rate (at different pressures), discharge coefficient, and specific impulse.

## 2. Motor Evaluation

One motor from each production lot of motors was statically fired for lot acceptance. A production lot consisted of twenty motors and did not necessarily represent any particular lot of casting powder. For example, Lot 1-11-66 casting powder was not fired in motor lot evaluations.

Stage III QA static test motors were instrumented with two pressure transducers, an operational pressure transducer (OPT), and a Taber gage.

The static tests were also instrumented with strain gages on the aft dome and linear potentiometers on the aft dome and cylindrical sections.

Accelerometers were used on only a limited number of motors early in the development program.

## 3. Motor Performance Characteristics

The M57A1 motor burns for approximately 55 to 60 seconds at an average chamber pressure of approximately 270 psia, depending upon motor conditioning temperature.

## 4. Review of Previous M57 Programs

The major programs relating to grain structural integrity and aging surveillance are presented in the report with a listing of results applicable to the overtest program.

### a. Minuteman Support Program

Task 9 of the Minuteman Support Program was the first extensive experimental and analytical program aimed at predicting the structural integrity of the Minuteman stage III motor. The objectives of Task 9 were to determine the structural capability of the current grain design and define potential improvements through a better understanding of the structural requirements of the propellant grain. Finite-element analysis techniques were applied to the Minuteman stage III motor for the first time during this program. During the program, the stress concentration factors for the wing slots of the motor were determined experimentally using photoelastic methods and also analytically using a computerized, conformal-mapping, complex-variable technique. A full-scale Minuteman stage III motor was high-rate hydrotested to failure. Wing slot failure was demonstrated at a pressure of 525 psi. The propellant grain of a Minuteman stage III motor was machined to the configuration of the grain at a burn time of 5 seconds and hydrotested. Subscale units (1/3 scale) were pressure tested during the program.

Tests were also conducted to characterize the viscoelastic behavior of CYH propellant.

b. OOAMA-Hercules Co-operative Test Program and Propellant Mechanical Property Results from the Second OOAMA-Hercules Co-operative Test Program

Two cooperative test programs were performed by Hercules and the Ogden Air Materiel Area (OOAMA) now the Ogden Air Logistics Center. The objective of the test programs was to compare mechanical properties obtained by Hercules and Ogden ALC for the Minuteman stage III surveillance program.

In the first OOAMA-Hercules cooperative test program, Hercules and OOAMA performed stress relaxation, constant crosshead speed tensile, and vibrating disc tests. The samples tested were machined by both facilities and a portion of the samples were traded. No differences were detectable between the OOAMA and Hercules low strain rate tensile failure data but there was approximately a 10 percent difference in the high rate tensile failure data. There was also a 10 percent difference in the tensile relaxation modulus data obtained by the two facilities. Not enough samples were tested in the first OOAMA-Hercules cooperative test program to evaluate the reasons for the differences in the test data.

Uniaxial tensile and stress relaxation tests were conducted under the second OOAMA-Hercules cooperative test program and more machined test samples were traded by the two facilities. Hercules normally machines round, necked-down, samples using a spray of water for their tensile tests. OOAMA normally machines JANNAF samples dry for their tensile tests. The tensile relaxation modulus data obtained by Hercules and OOAMA were again statistically similar while the failure data obtained at constant crosshead speeds of 200 and 2000 in./min were statistically different. The failure data obtained from round, necked-down and JANNAF tensile samples were statistically different. The method used to machine tensile samples, wet or dry, did not affect the failure data obtained from the samples.

c. Stage III Minuteman Production Support Program

Task 2 of the stage III Minuteman Production Support Program was an experimental and analytical program to study problems judged to be of the most immediate importance in evaluating the structural integrity of the solid propellant grains.

Improvements were made in the analytical procedures for structural analysis of slotted propellant grain designs. Computer methods for stress analysis were improved by extending the range of application to the approximate solution of three-dimensional problems. A practical approximate solution to structural problems involving large deformations was demonstrated. The Hercules finite-element approach to grain stress

analysis was modified so that the approach could be applied to the approximate large strain analysis of complex geometric configurations. Methods were also added for considering directional variations in material properties.

The feasibility of using the Moire' fringe method to measure strain concentrations and make overall strain field observations was demonstrated on live propellant samples. The experimental data on photoelastic determinations of concentration factors in propellant grains were surveyed, and the pertinent data were consolidated into a single source of reference and method of presentation.

A structural modeling analysis technique was developed for use in experimental stress analysis of complex three-dimensional geometries. The method was applied in an analysis of two different geometric configurations representative of two different burn times of the Minuteman stage III motor.

A mathematical analysis procedure for determining the stresses and strains induced in a solid-propellant rocket motor by nonsymmetrical axial and transverse loadings was developed and demonstrated. Application of the method was made in the analysis of the Minuteman motor for non-symmetrical flight loading.

A combined theoretical and experimental program was conducted to study buckling of solid-propellant rocket motors. A nonlinear theory for buckling due to axial loading of filled cylinders (which allows for large deformations and case orthotropy) was developed. A motor design procedure based on experimental buckling data was suggested and demonstrated using three different motors. Experimental tests were performed on cylinders filled with a propellant-type material and representative of a cross-section of the Minuteman motor. Stiffening effects of the filler material were determined and correlated using the analytical methods of this program.

Specific analyses were performed to determine the effects of axial acceleration on the stresses and strains of the Minuteman stage III motor. Results indicated that the specified axial acceleration had little effect on the case or propellant grain.

Test methods representative of actual motor loading conditions were developed and used to obtain CYH propellant failure data under multiaxial loadings. A multiaxial failure criterion was developed for these propellants.

d. Minuteman Surveillance Program

The Minuteman Stage III Surveillance Program was composed of the following tasks:

- (1) Physical property testing
- (2) Grain failure criteria study
- (3) Case bond failure criteria study
- (4) Service life predictions

Four Minuteman stage III motors, 336, 216, 131, and 67, were sectioned for the physical property testing phase of the Minuteman Surveillance Program. The objective was to determine the effect of age on the mechanical properties of CYH propellant. When the motors were first sectioned, a set of mechanical property tests consisting of stress relaxation, constant crosshead speed tensile, and vibrating disc tests was conducted on the propellant. The sectioned propellant was wrapped in plastic and stored in a 77° F environment. Six months later, another set of mechanical property tests, consisting of stress relaxation, constant crosshead speed tensile, and vibrating disc was conducted on propellant samples cut from the sectioned segment. The samples were machined from the segment just prior to testing. Ultimately, three series of these tests were conducted on the propellant from each motor. Regression analyses were performed on the tensile relaxation modulus and strain at maximum stress data to determine the effect of age on these two propellant mechanical property parameters. Long-term constant strain, creep, and fatigue tests were also conducted on the sectioned propellant.

The grain failure criteria phase of the program was a study to develop a theory of failure for the Minuteman stage III motor propellant grain. Pressure tests of subscale analogs were performed to verify analysis techniques and failure criteria. The basic centerport cracking unit and test procedures currently in use by Hercules were developed as a part of this subscale verification program. A multiaxial stress, variable strain rate, cumulative damage failure theory was verified using the Minuteman stage III propellant, CYH.

There were three objectives in the case bond failure criteria study. These were to: (1) Determine modes of case bond failure, (2) evaluate the various case bond test sample configurations, and (3) establish a failure criterion for the Minuteman stage III case bond system. A number of case bond sample configurations were evaluated for determining the failure properties of a powder embedment case bond system like that used in the Minuteman stage III motor. A modification of the classical Mohr theory was selected as the failure criterion for the Minuteman stage III case bond system.

The final part of the Minuteman Surveillance Program was to use all of the information from the physical property testing phase and the failure criteria studies in the structural service life prediction of the Minuteman stage III motor propellant grain. A mathematical model was made of the most likely grain failure mode which was failure in the longitudinal slot tips during motor ignition. A Monte Carlo simulation technique was incorporated into the stress analyses. With this approach, the parameters were randomly selected from their respective theoretical distributions and inserted in the analyses. The result was a probability distribution of the damage factor at motor age intervals. The damage factor was obtained for motor ages from 2-1/2 to 5-1/2 years and extrapolated to 10 years. The margin of safety was computed from the extrapolated damage factor data. Using this method, the point at which the lower 3-sigma limit of the margin of safety crossed zero was 8-1/2 years.

e. Minuteman Service Life Study Program

The objective of the Minuteman Service Life Study Program was to update the service life prediction for the Minuteman stage III motor. A list of the potential failure modes was made for the motor. The list was then reduced to the five most probable failure modes and these were studied in detail. The failure modes selected for further study were:

- (1) Wing slot tip cracking during ignition transient
- (2) Centerport bond breakage during ignition pressurization
- (3) External insulation bond failure
- (4) Raceway pad bond failure
- (5) Case interlaminar shear failure around the nozzle ports

Propellant tensile relaxation modulus, maximum stress, and strain at maximum stress data obtained during the Minuteman Surveillance Program were reanalyzed to separate the effects of secondary aging and to define the primary aging trends for each propellant mechanical property parameter. The reanalyzed propellant mechanical properties and the adhesive bond strength data were then used in a statistical procedure known as a requirement/capability (R/C) analysis. An R/C analysis was performed for each of the failure modes. It was predicted that cracks could initiate in the wing slots of two out of every 100 firings of 10-year old Minuteman motors. But, whether these cracks would produce motor failures was not known.



f. Minuteman II Stage III Motor Categories and Service Life Studies

The Minuteman II Stage III Motor Categories and Service Life Studies Program was divided into two phases: (1) Categorization of Minuteman II stage III static test motor performance characteristics, and (2) service life studies.

Minuteman II stage III motors were divided into four motor performance categories. Category one covered QA static tests II-QA-01 through V-QA-32. These motors contained randomly-occurring high aft dome internal insulation erosion. To lessen the degree of aft dome erosion, Minuteman motors were retrofit with an interim fix, referred to as the B-1 Fix. Motors having the B-1 Fix had similar motor performance characteristics and form Category Two. Category Three motors were of the configuration qualified during the 18-motor Operational Reliability Improvement Program (OPRI). All of the OPRI motors exhibited similar performance characteristics. The Category Four motors exhibited increased oscillatory combustion.

The service life studies were a continuation of the service life studies begun under the Minuteman Service Life Study Program.

Stress intensity factor data were obtained on CYH propellant 10, 54, and 99 months old. The data did not appear to be affected by the age of the propellant. Additional tensile relaxation modulus data were also obtained on CYH propellant taken from the 10-month old FPC castings and the three Minuteman stage III motors 54, 99, and 102 months old. The tensile relaxation modulus data obtained during the Minuteman Surveillance Program and reanalyzed during the Minuteman Service Life Study for secondary aging were time-temperature shifted to 77° F to correspond in temperature with the new tensile relaxation modulus data obtained during this test program at a temperature of 77° F. Primary aging regression lines were fit to the two sets of tensile relaxation modulus data, and new data and the old time-temperature shifted data.

The fracture mechanics analysis of the wing slot failure mode in Minuteman stage III motors indicated that a crack 0.05 inch deep or deeper in the slot tip of a zero age motor would propagate rapidly upon motor ignition, and a crack 0.07 inch deep or deeper in a 15 year old motor would also propagate. Therefore, the critical crack depth in the wing slots was almost zero for all motor ages.

The analyses of the principal failure modes in the Minuteman stage III motor showed that Categories Two, Three, and Four motors have estimated service lives which are equal to or longer than Category One motors, for all of the failure modes.

Fifteen recommendations were made to improve the propellant and adhesive properties needed for motor service life predictions, and a number of recommendations were made for improved instrumentation for full-scale static test firings.

g. Investigation of Pressure Oscillations During Firing of the Minuteman II Stage III Motor

There was a significant increase in the amplitude of acoustic pressure oscillations in the Minuteman II stage III motor starting with QA Motor 59 and casting powder lot RAD 1-10-66 which resulted in an extensive review of the M57A1 motor and history. In the course of this study, uniaxial tensile and dynamic torsional shear tests were conducted on propellant manufactured from 7 lots of CYH powder. Samples were removed from the original acceptance castings which had been stored at OALC.

The importance of the new uniaxial tensile data was that they were a better measure of the powder lot mechanical property variations than the old powder lot acceptance data. All of the new test samples were tested on one occasion using the same operator and testing machine while maintaining constant humidity and temperature control. The original QA lot acceptance data were obtained over a period of four years which could lead to erroneous conclusions about the mechanical properties of the various powder lots. Slight variations in the test conditions and operator could lead to marked variations in the mechanical properties.

The maximum stress values obtained from the new powder lot tensile tests were all lower than the old QA powder lot acceptance data. Strain at rupture data were about equivalent. The tangent modulus from the powder lot acceptance data were consistently lower than the new powder lot data.

h. LGM-30 Third Stage Dissected Motor Program

The objective of the LGM-30 Stage III Dissected Motor Program was to determine the effective aging on the materials in the Minuteman stage III motor (the program is currently underway at Ogden Air Logistics center). Eighteen Minuteman stage III motors have been dissected and the sectioned materials, propellant, and case bond system, used in various types of physical property and chemical tests. All the tests are being conducted on CYH propellant except two sets of case bond tests. The motors have been dissected. Samples are machined from the sectioned materials as required for testing. The test data in general cover the age range of 4 to 13 years. Linear regression lines have been fit to the data sets, and three sigma bands and 90-90 tolerance bands have been established.

The stress relaxation data obtained during the Dissected Motor Program from CYH propellant show an increase in tensile relaxation modulus with age which is statistically significant. The uniaxial, biaxial, and triaxial tensile strain at maximum stress data obtained during the Dissected Motor Program increased at a statistically significant rate with age.

i. Long Range Service Life Analysis Program

Six Minuteman stage III motors have been dissected and mechanical property tests conducted on materials and bonds in the motors.

Two Minuteman stage III motors have been hydrotested to overtest the critical failure modes associated with ignition loads.

Data from the dissected motor task and the high rate pressure tests have been supplied to TRW for analysis.

j. Investigation of Anomalous Aft Dome Insulator Erosion in the M57A1 Motor

The aft dome insulator investigation was a multithrust program to solve the problem of excessive aft dome erosion as exhibited in the firing of QA motors QA-31 and QA-32. The problem was caused by failure of a boot-to-flap bond at the aft centerport which permitted anomalous gas flame between centerports and one or more of the nozzle ports. Structural problems were investigated in detail and design improvements were recommended.

The principal improvement for the short term and for retrofitting was a stress relief groove at the aft centerport. This was known as the "B-1 Fix." The B-1 Fix, along with vulcanized bonds, was made a permanent design fix in the OPRI program.

k. Operational Reliability Improvement Program (OPRI)

The main element of the OPRI program was that it was an 18 motor program which qualified design and manufacturing changes primarily for the solution of the anomalous aft dome erosion problems. The significance of these changes is discussed in appropriate sections of this report.

#### E. FAILURE MODE SELECTION AND OVERTEST DEFINITION

Identification of critical motor failure modes and selection of the overtest approach were basic tasks. The specific direction for the remainder of the program was determined by the results of these tasks.

An extensive failure mode identification and evaluation study was performed for the M57A1 motor in November 1971.<sup>1</sup> Several different sets of data were examined in the study to identify the critical components, including, (1) previous analysis results, (2) aging results from current surveillance programs, (3) past problems in static and flight testing, and (4) Class I Engineering Change Proposals.

The list of failure modes previously compiled was updated in this program. Flighttest data and motor surveillance firings were reviewed for further understanding of the structural behavior of the motor. Potential failure modes were tabulated in a list according to decreasing criticality. The failure modes were evaluated according to past related problems, critical aging parameters, predicted margins of safety, and known aging trends. The revised list of failure modes is reported in the technical report for Phase I of the overtest program.<sup>5</sup>

Two propellant grain failure modes were selected for further study and for development and demonstration of the overtest concept. Wing slot cracking and failure of the aft centerport flap-to-boot bond were determined to be the most likely failure modes limiting the motor service life. No previously unanticipated failure modes were identified.

The results of the service life study program reported in Reference 1, showed cracking in the slot tip to be the most critical mode. This conclusion was confirmed in the overtest program Phase I studies. Wing slot failure is most likely to occur near the intersection of the slots with the centerbore and may appear in any of the four slot tips. The critical time is during and just following the ignition transient. The results of such a crack occurring could range from abnormal ballistics to a catastrophic chamber rupture. These cracks should be expected during firing only. If cracks are observed prior to firing, it is fairly certain that the motor has been subjected to out-of-specification environments and should not be fired. Propagation of a known preexisting crack during firing is an academic question with CMDB propellant grains.

The analysis given in Reference 1 shows that for normal conditions, wing slot failure would occur after 12 to 13 years of age. However, for a set of adverse condition, lower 3 values, it was predicted that failure could occur as early as 8 to 9 years. These results have been shown to be conservative by high-rate hydrotest results. These showed failure due to cracking at a pressure of 525 psi which is nearly double the critical pressure at ignition.

Another problem area which has caused problems in the past is aft centerport bond failures. The breakdown of either the aft centerport bond or one or more of the nozzle port bonds early in motor operation (0 to 3 seconds) could allow the flow of high velocity gas between the aft dome boot and flap. This, in turn, would lead to heavy erosion of the aft centerport area and/or "dimple" or "eyebrow" erosion such as resulted in failures of motors IV-QA-31, V-QA-32, and V-QA-42. Though this problem was not considered to be as serious, it was given attention in the high-rate hydrotest planning. This failure mode is of concern only in motors retained in the force which were built prior to incorporation of vulcanized bonds in the design.

Drafts of updated tables of potential failure modes were presented for review to OALC and Hercules surveillance personnel and other engineers with experience in various phases of the Minuteman program. A consensus was reached on two points: (1) The new data referred to in the updated tables represents all the relevant surveillance and performance data that have been obtained in the time period under consideration, and (2) judgments as to whether or not the new data changes the previous judgement on criticality are correct.

Various overtest approaches were evaluated for general application and with regard to the M57A1 motor specifically. Applicability of the tests was judged on the basis of comparisons of results obtained by analysis of the overtest loading plan and an actual ignition pressure transient. The high rate pressurization hydrotest at 70° F was selected as the experimental approach to be used for the full-scale motor overtests. It was concluded that thermal cooling is a satisfactory overtest for the failure mode of wing slot tip cracking, but it is not applicable to the aft centerport failure mode.

Details of the study of possible overtesting approaches are reported in Reference 6.

The list of overtest approaches is presented in Table 1-2 which is a condensation of Table 2-1 of Reference 6. Because all motor failure modes previously identified for the M57A1 motor were associated with the ignition transient, only those overtest approaches applicable to the zero-burn motor geometry were included. Otherwise, all loading schemes capable of causing stress or strain on the wing slots or aft centerport bond were included to ensure that all valid approaches were considered in planning the motor overtest.

The high pressurization rate hydrotest was recommended for subscale verification and for use on the full-scale motor tests.

TABLE 1-2

## LIST OF OVERTEST APPROACHES

Test	Comments
<u>Hydrotest Pressures</u>	
Simulate ignition transient	Will not fail grain
Simulate ignition transient rate to higher than normal pressure	Promising
Low-rate pressurization to high pressure	Promising
Condition grain to high temperature, rate to be determined	Promising, if temperature not very high
Condition grain to low temperature, rate to be determined	Promising, if temperature not very low
Artificially weaken grain, simulate ignition transient	Technology not available
Artificially crack grain, simulate ignition transient	Applicability questionable, does not test aft centerport bond
<u>Motor Firing</u>	
	External instrumentation only
Standard motor assembly and firing	Will not fail grain
Artificially crack grain	1) Applicability questionable 2) Partial burn necessary, timing very critical 3) Some data available from OOAMA firings 4) Does not test aft centerport bond
Artificially weaken propellant	Technology not available
Oversized igniter, simulate pressure transient to higher than normal pressure	Promising
High burn rate plugs of propellant inserted into grain to raise pressure	High pressure will occur after initial pressure transient

TABLE 1-2 (Cont)

## LIST OF OVERTEST APPROACHES

Test	Comments
<u>Motor Firing</u> (Cont)	
Small diameter nozzles	Promising
Forward end down	1) Requires partial burn if aft end debonds as planned 2) Does not overtest wing slots
Conditioned to low temperature	Ignition transient lower than normal
Conditioned to high temperature	1) Safety a problem 2) Ignition transient higher than normal 3) Promising
Mechanical loading of grain or bond	1) Technology not available 2) Interpretation difficult
Acceleration test (sled or centrifuge)	Loading does not duplicate the critical load
Thermal loading	Promising. Cold soak tests have cracked wing slots and failed aft centerport bond

#### LIST OF REFERENCES

1. Minuteman Service Life Study Program, MTO-1124-49-3, for SAMSO, Norton Air Force Base, by Hercules Incorporated, Systems Group, Bacchus Works, 1 November 1971.
2. G. H. Bergman and H. L. Holt, Minuteman II Stage III Motor Categories and Service Life Studies; Report No. MTO-1124-60, Hercules Incorporated, Magna, Utah, 31 December 1971.
3. G. F. Lowell, MTO 1124-70, Summary Final Report for the Wing Slot Cracking and Aft Center Port Debonding Failure Mode During High Rate Pressurization Testing of Full Scale Minuteman II, Stage III Rocket Motor LRSLA, May 1975.
4. Summary Final Report, Operational Reliability Improvement Program, MTO-164-242, 8 February 1966.
5. A. S. Daniels, ICBM, Overtest Technology, Task I, Failure Mode Selection, AFRPL-TR-72-123, Hercules Incorporated, Bacchus Works, Magna, Utah, November 1972.
6. A. S. Daniels and J. J. Rotter, ICBM Overtest Technology, Overtest Modeling and Subscale Verification of the Model, AFRPL-TR-74-25, Hercules Incorporated, Bacchus Works, Magna, Utah, February 1974.



## SECTION II

### ANALOG TEST PROGRAM

#### A. INTRODUCTION

There were two major objectives of the analog test program. The first objective was to demonstrate, by subscale testing, that the overttest procedure selected for the program was valid. This objective was to be accomplished by design and testing to failure motor or partial motor analogs representative of the critical failure modes and failure conditions. The second objective was to demonstrate the use of analog devices for obtaining statistical failure data in a more economical way than from full-scale overttests. Essentially the same devices were used for both purposes.

Other objectives associated with the two principal objectives were as follows:

- (1) Design and test subscale models which represent realistic failure modes in ICBM motors
- (2) Verify centerbore cracking detection method
- (3) Demonstrate centerbore strain measuring method
- (4) Demonstrate instrumentation and test operations planned for the full-scale motor tests

An interim report was issued (Reference 1) which covers the subscale verification of the aft centerport debonding failure mode and reports progress on efforts to develop a centerbore-cracking analog device. Subsequent to the issuance of Reference 1, further work was accomplished in which a suitable centerbore cracking analog was demonstrated. The work on centerbore cracking covered in Reference 1 is reevaluated in this report with respect to subsequent subscale testing performed in the program.

Details of the analog test program which were previously reported will not be repeated herein. Emphasis will be given to developments following the preparation of the first interim report on the analog test program. An overview or summary of the task is shown here so as to present the essentials of the analog test program without the aid of the earlier report. Following the summary, the results from the extended effort on analog devices are reported. The general use of analog devices in a predictive surveillance program is discussed in Section VI (Volume II) of the final report.

---

<sup>1</sup>References are presented at the end of this section

## B. PROGRAM RESULTS

### 1. Summary

Motor analog tests were performed in which M57A1 failure modes were verified and analog devices were demonstrated. The demonstration of analog devices representative of critical failure modes provides assurance that they can be applied in a predictive surveillance program to economically obtain statistical data for predicting motor reliability. As far as the M57A1 motor predictions are concerned, the analog tests were beneficial for confirmation of failure modes, analysis, techniques, and overtest approaches. Since the analog test vehicles were manufactured from propellant removed from full-scale motors, the tests did not provide additional data for service life prediction beyond that obtained from the full-scale results.

Various overtest approaches were evaluated analytically. Applicability of the tests was judged on the basis of comparisons of results obtained by analysis of the overtest loading plan and the actual ignition pressure transient. Subscale models were designed and tested to demonstrate the overtest approach selected for full-scale tests. Different subscale models were designed to evaluate the two critical failure modes of aft centerport bond failure and centerbore cracking. Each type of model was designed to fail according to one of the chosen failure modes.

Motor analogs were designed and analyzed using the same methods and materials properties employed in the analysis of overtest approaches. The models were then tested to failure. The model failure mode and pressure at which failure occurred were determined from the test data and posttest inspections of the failed models. These results were compared to the design predictions. Close correspondence between predictions and results for the analog was interpreted as confirmation of the failure modes and the overtest approach selected for the M57A1 motor.

The basic subscale analog design is shown in Figure 2-1. The units incorporated a cartridge-loaded propellant grain in failment-wound cases. Heavy metal end plates were bonded to the ends of the assemblies and were held together with tie bolts. Three design variations were used to evaluate the two principle M57A1 failure modes. Two variations of the basic configuration were used to test the wing slot cracking failure mode. One type had a circular centerbore (Figure 2-2) and the other type a four-slot centerport (Figure 2-3).

Models used to demonstrate aft centerport boot-to-flap failure (Figure 2-4) were of the basic circular bore configuration but, in addition, incorporated elements of the motor aft end. A stress relief groove and flap, bonded to the propellant were employed. The boot was bonded to the end plate and an adhesive bond of controlled radial width was used to connect the flap to the boot.

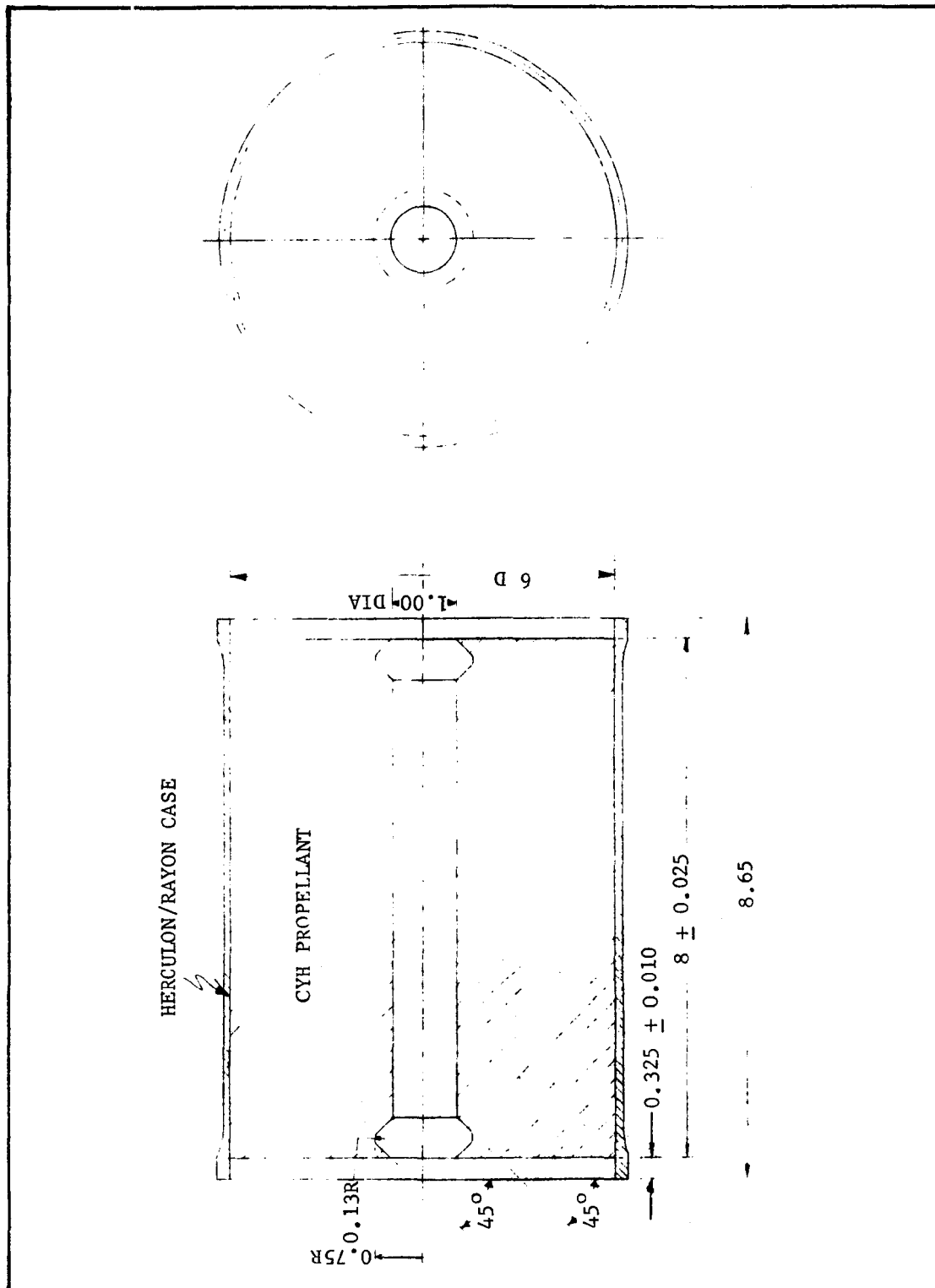


Figure 2-1. Wing Slot Cracking Failure Mode Model (Circular Centerbore),  
Case and Grain Subassembly

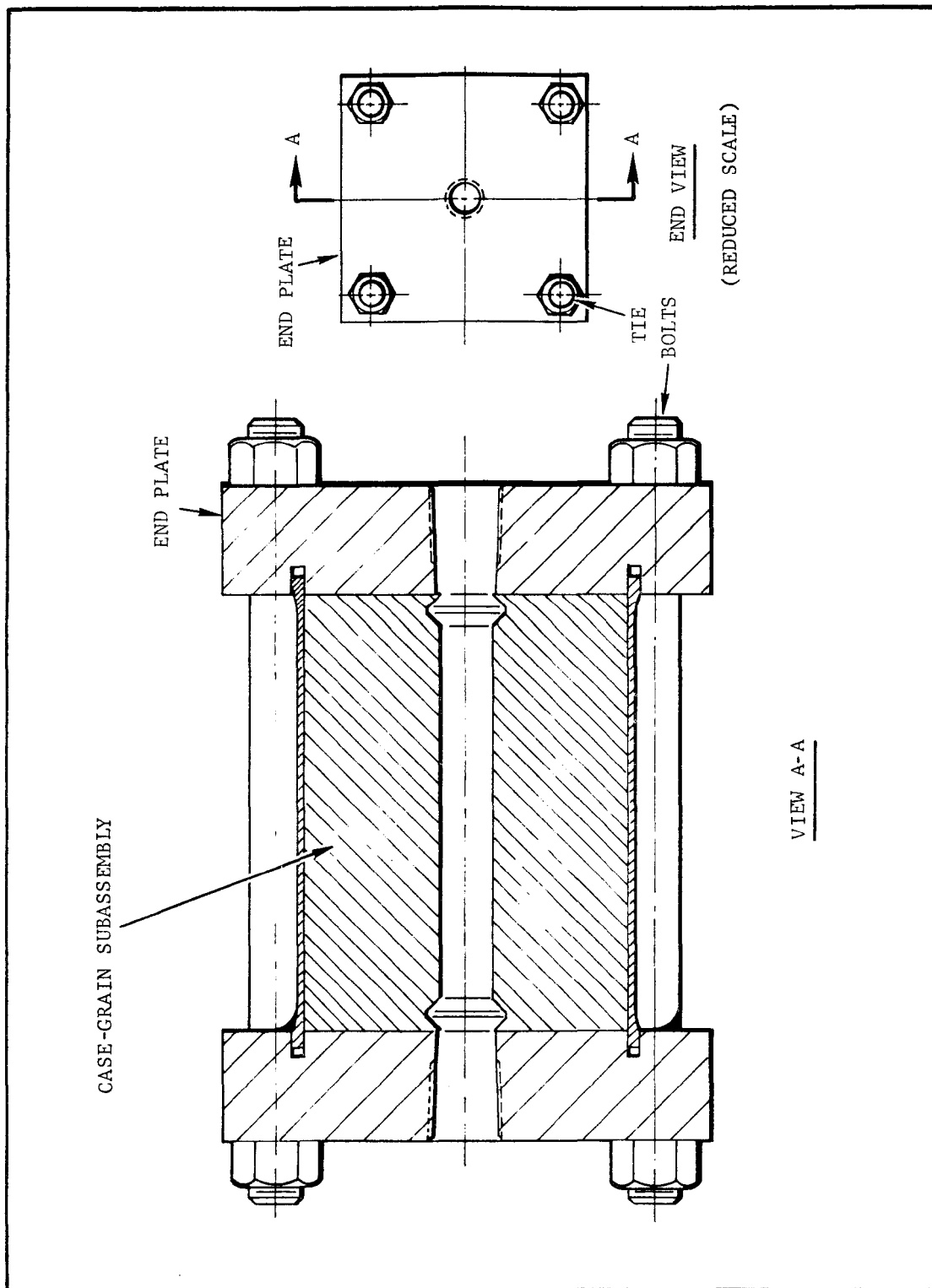


Figure 2-2. Wing Slot Cracking Failure Mode Model (Circular Center Bore), Complete Assembly

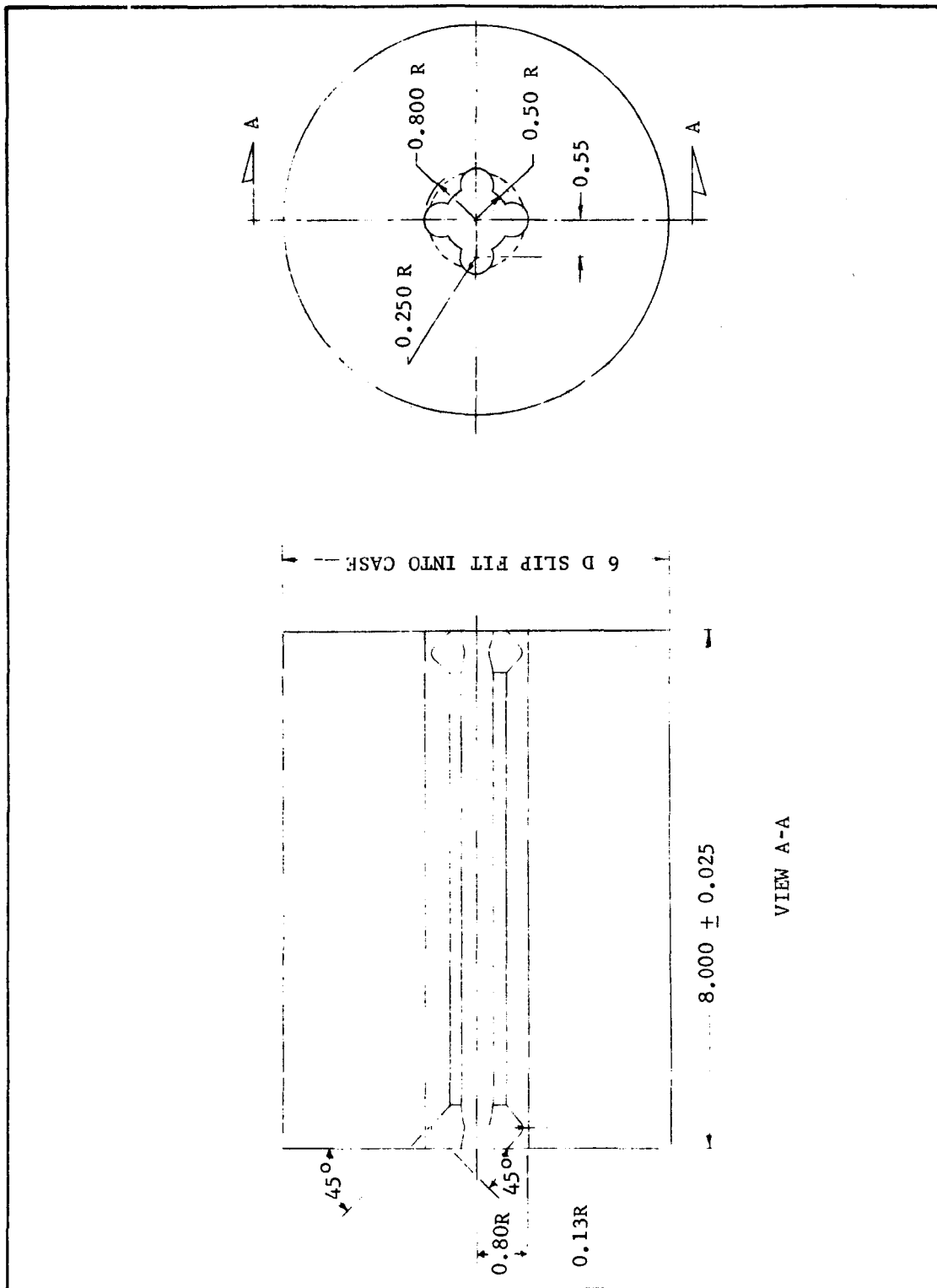


Figure 2-3. Wing Slot Cracking Failure Mode Model (Slotted Centerbore),  
Grain Configuration

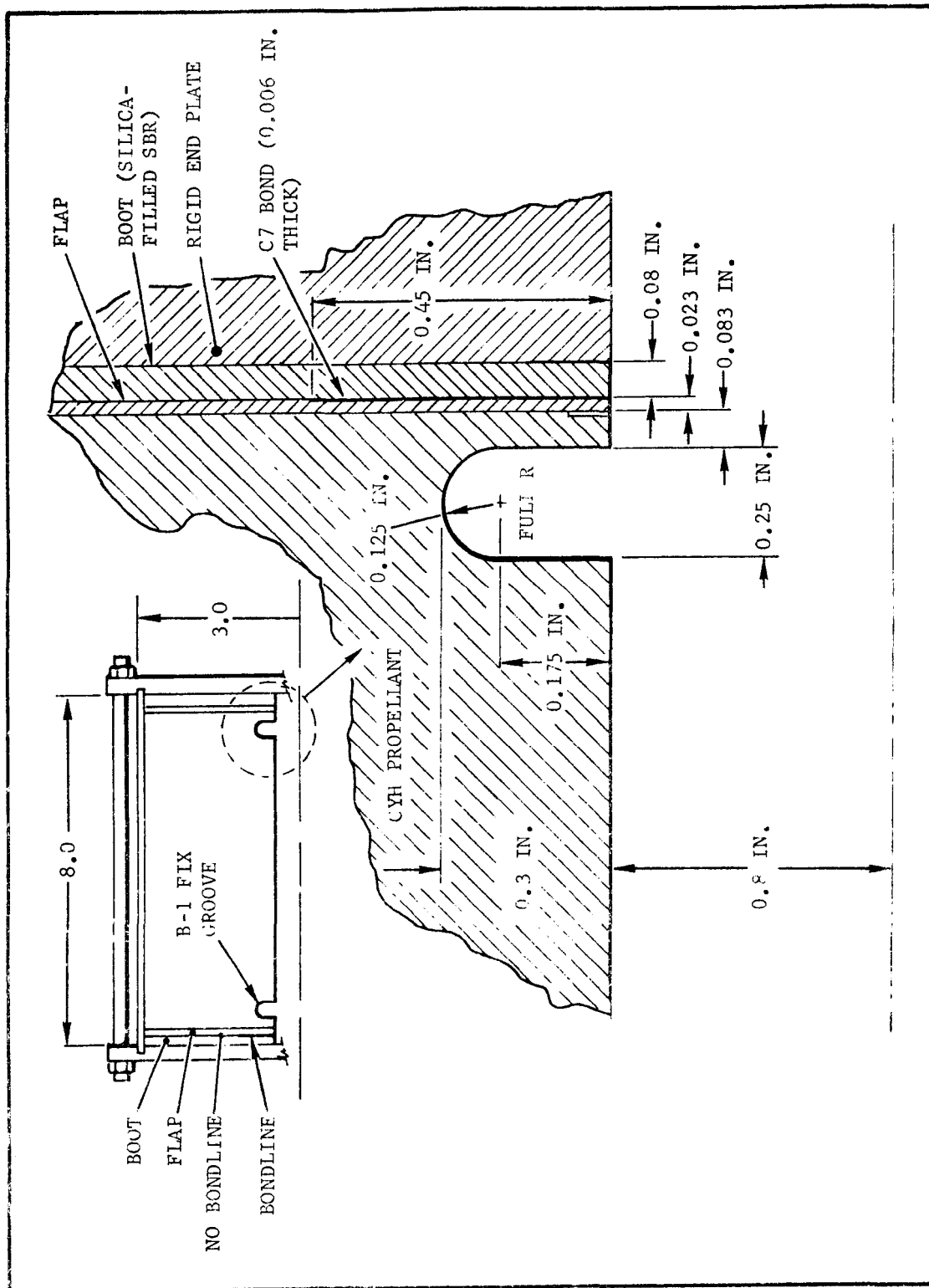


Figure 2-4. Aft-Centerport Bond Failure Mode Model

High rate pressurization, at approximately the M57A1 ignition transient rate (~10,000 psi/sec) was used to load the analogs to failure. The models were instrumented with strain gages on the case and with event gages for detecting propellant cracking on the grain interior surface. After testing, the models were inspected and dissected to determine the nature and extent of the failures. Finally, the measured pressures at which the analog models failed were compared to the analytical prediction. A favorable comparison of the two was interpreted to mean that analytical methods and failure theories used for design of the models were also adequate for the selection of the overtest approach to be used on full-scale M57A1 motors.

Subscale motor analogs were demonstrated for the M57A1 critical failure modes. A design was accomplished in which failures were achieved as centerport cracking during high rate pressure testing. Boot-to-flap debonding and stress relief groove failures were also demonstrated in aft centerport failure mode analog models.

The wing slot cracking mode of failure was demonstrated by the analog test program as most critical for the M57A1 motor. The analytical procedures, including failure criteria, were also verified, thus providing confidence in their use for the full-scale analyses.

The externally-mounted instrumentation was verified for use on the full-scale tests. Event gages<sup>2</sup> detected failures of slotted-bore models, but were unsuccessful on the circular-bore models. The lack of success was not considered a fault of the event gage but more a result of inability to install a sufficient number in the small one-inch centerbore.

## 2. Expanded Analog Test Program

The first circular centerbore (CCC) design reported in Reference 1 had stress relief grooves machined into the propellant to relieve the stresses at the centerport grain-to-end plate bond. Two of these CCC's were tested and both failed by end plate debonding at low pressures. The analog task was then expanded to develop a new CCC design. The new design used rubber stress relief flaps bonded between the grain and the end plates. The new design was shown by analysis to have an adequate margin of safety. Subsequent tests proved the new design to be 100 percent successful.

The slotted centerbore model was not redesigned or tested with the rubber stress relief flaps.

In the original design (stress-relief groove) the end plates were bonded directly to the grain with EA 913.1 adhesive. With the improved design (stress-relief flap) the rubber flaps were bonded to the grain and to the end plates using EA 946 adhesive. In both cases, during assembly the tie rods and nuts were installed and lightly tightened until adhesive was observed squeezing out. The whole assembly was then cured for a minimum of 48 hours at ambient temperature.

Event gages were installed during CCC fabrication. In addition, each case was instrumented with hoop strain gages. For the relief-groove design, twelve strain gages were bonded to the case. For the improved relief flap design, a girth band was assembled around the case in addition to eight strain gages on the case.

The first model tests developed lower test pressure rates than desired due to results from checkout tests which were performed with steel pipe having a volume equivalent to the centerport volume. For the subsequent tests with the stress-relief flap design, the checkout runs using the pipe were discarded and the throttle valve opening was determined from previous CCC test experience. The pressurization rate was closer to the ignition rate of the full-scale motor than had been previously achieved.

Stress analyses were performed on the six CCC's with the improved stress relief design which were tested in the expanded program. These analogs were analyzed after the tests using the actual pressure-time data for each unit. The maximum centerbore strain for each grain tested and the allowable propellant strain were input into the viscoelastic response computer program. The results compared favorably with the test results. The comparative results for each CCC are shown in Table 2-1. Figure 2-5 shows the isostrain plot for the new design, and Figure 2-6 shows the displacement for the grain and rubber flaps at 900 psi.

Six subscale motors of the new rubber stress relief flap design (O/T-012 through O/T-017) were tested. An average pressurization rate of 8115 psi/sec was achieved based on time to maximum pressure. The maximum pressurization rate during pressurization varied from 11,913 psi/sec to 20,434 psi/sec. The desired pressurization rate was 10,000 psi/sec. Typical pressure curves are shown in Figures 2-7 and 2-8.

Each of the six subscale analogs cracked in the centerbore and the failure propagated to the case. The cases ruptured after grain cracking in each test. These tests confirmed the adequacy of the new centerbore cracking cylinder design. The event gages and the leaf deflector failed to provide meaningful data. The data from these two methods of instrumentation did not correlate with any of the possible failure pressures as predicted by analyses and confirmed by case strain gage data. The case strain gage data was used to identify the failure times.

The leaf deflectometers did not remain in contact with the propellant centerbore during pressurization. Results of this program show that, when CCC tests are to be performed at high pressurization rates, the leaf deflectometers are inaccurate and a new device for measuring centerbore deformation is needed.



TABLE 2-1  
FAILURE PREDICTION

Model	Viscoelastic Response Program			Case Strain Gage Data	
	Time (sec)	Pressure (psi)	Centerbore Strain (%)	Time (sec)	Pressure (psi)
O/T-012	0.077	969	33.1	0.077	970
O/T-013	0.115	906	34.7	0.100	970
O/T-014	0.137	885	34.8	0.135	865
O/T-015	0.142	888	34.4	0.145	920
O/T-016	0.081	916	33.8	0.087	995
O/T-017	0.083	933	33.1	0.080	895
O/T-002	0.064	669	28.24	0.063	650

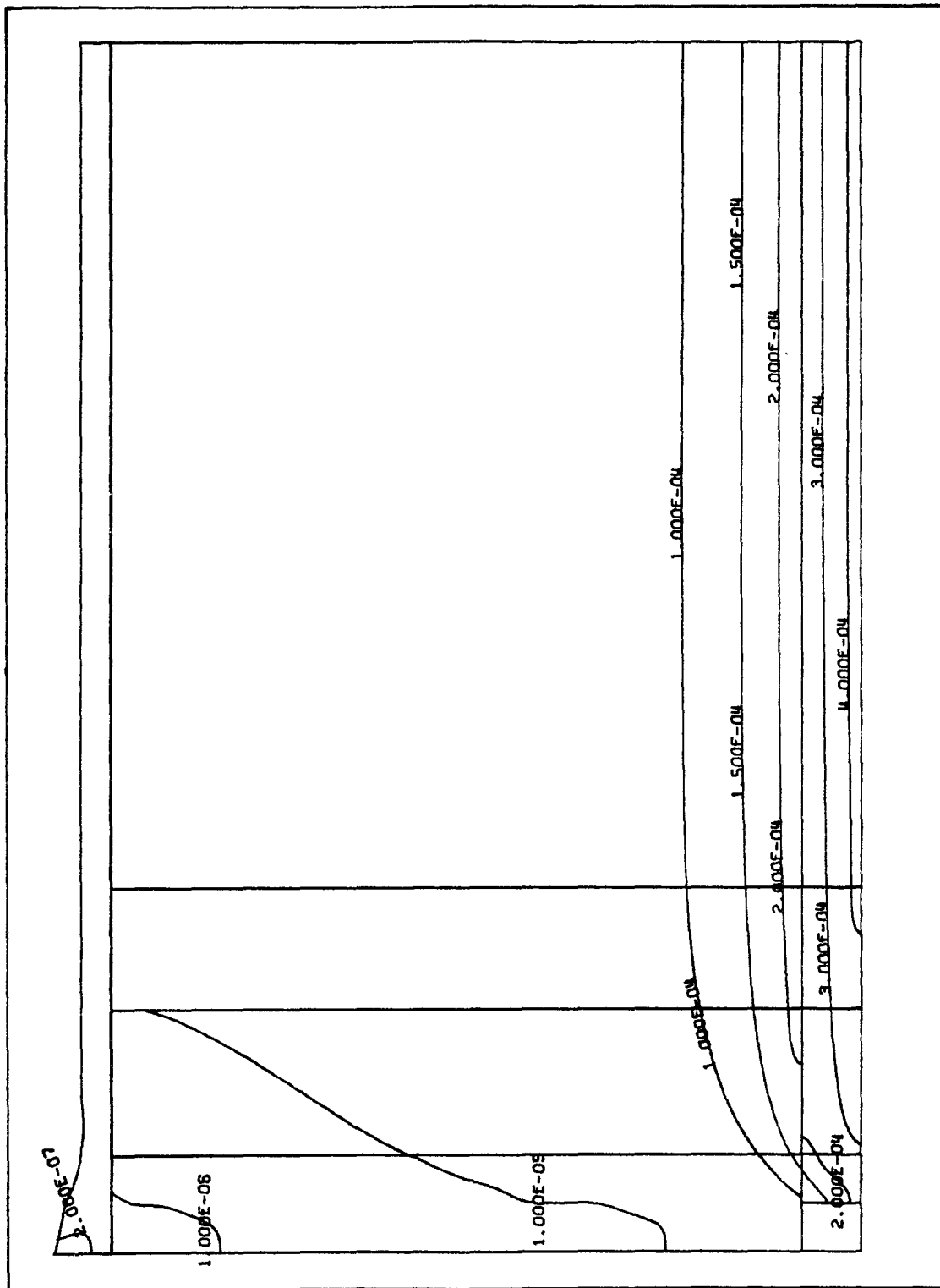


Figure 2-5. Overtest Centerport Cracking Cylinder Hoop Strain E-2500  
Centerport Cracking Cylinder 1.0, 10 Rubber Flap

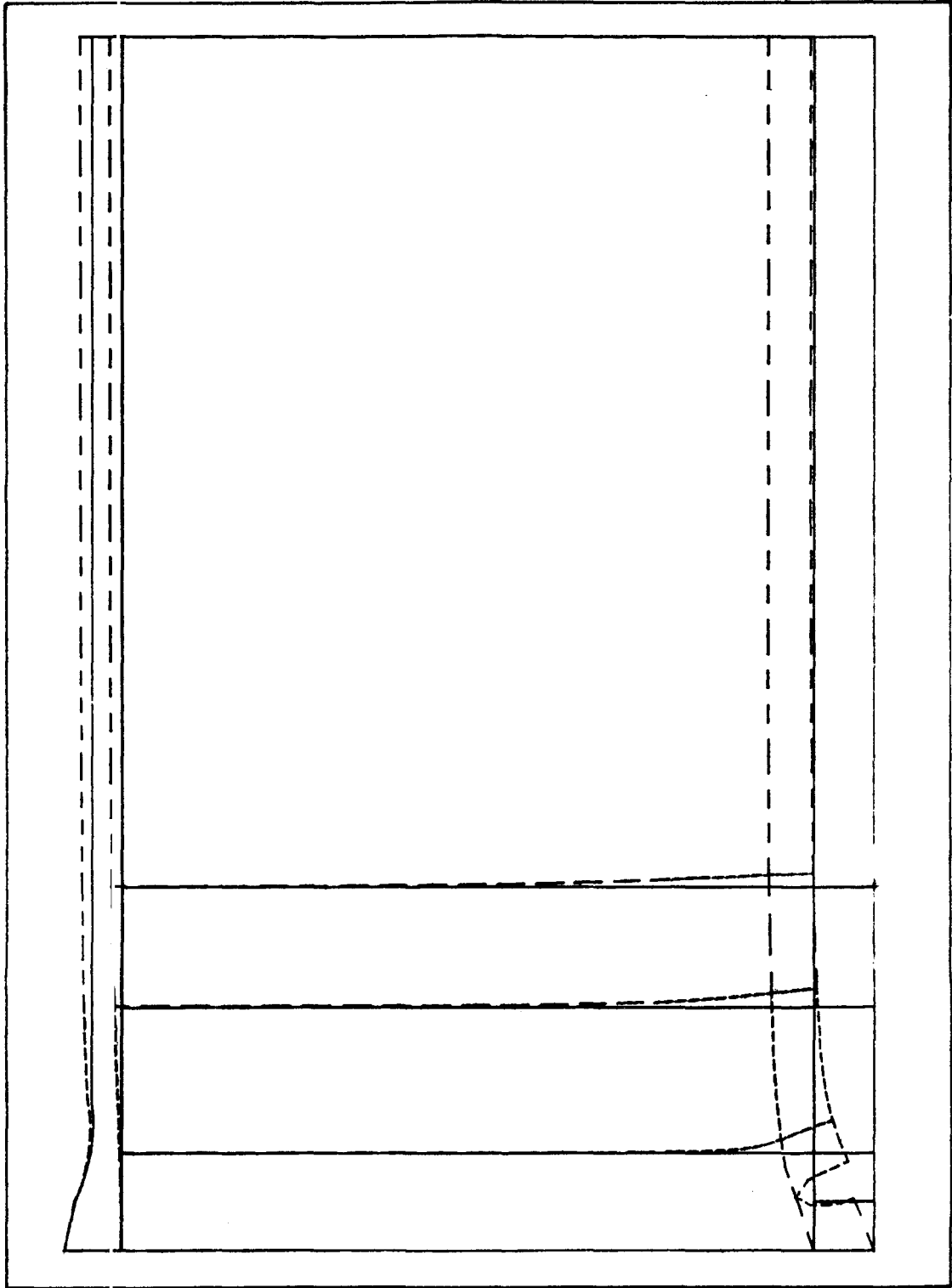


Figure 2-6. Overtest Centerport Cracking Cylinder Displacement  
Centerport Cracking Cylinder 1.0, 10 Rubber Flap

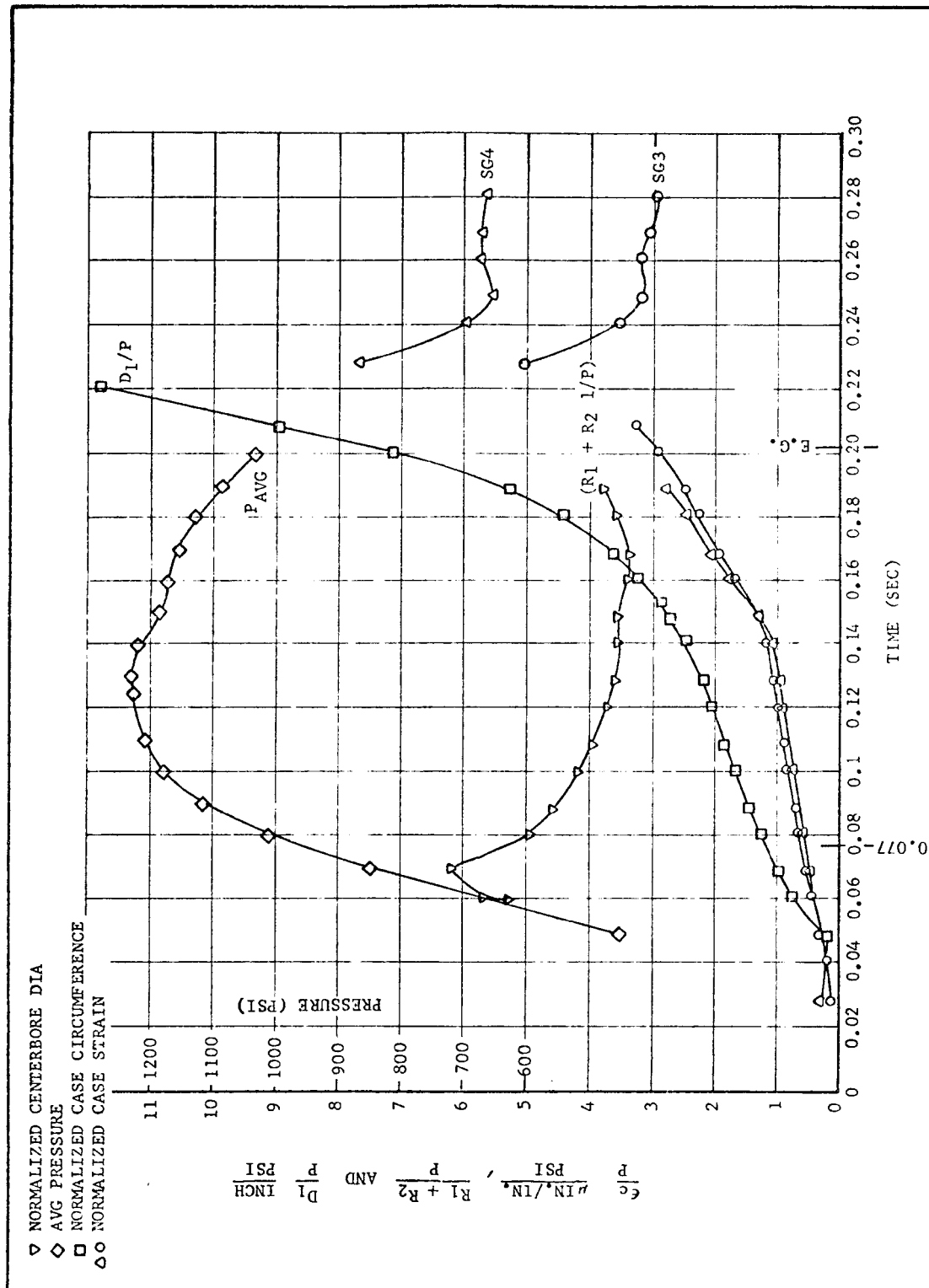


Figure 2-7. Overtest Model O/T-012 - Average Pressure, Normalized Centerbore Diameter, Normalized Case Circumference, Normalized Case Strain

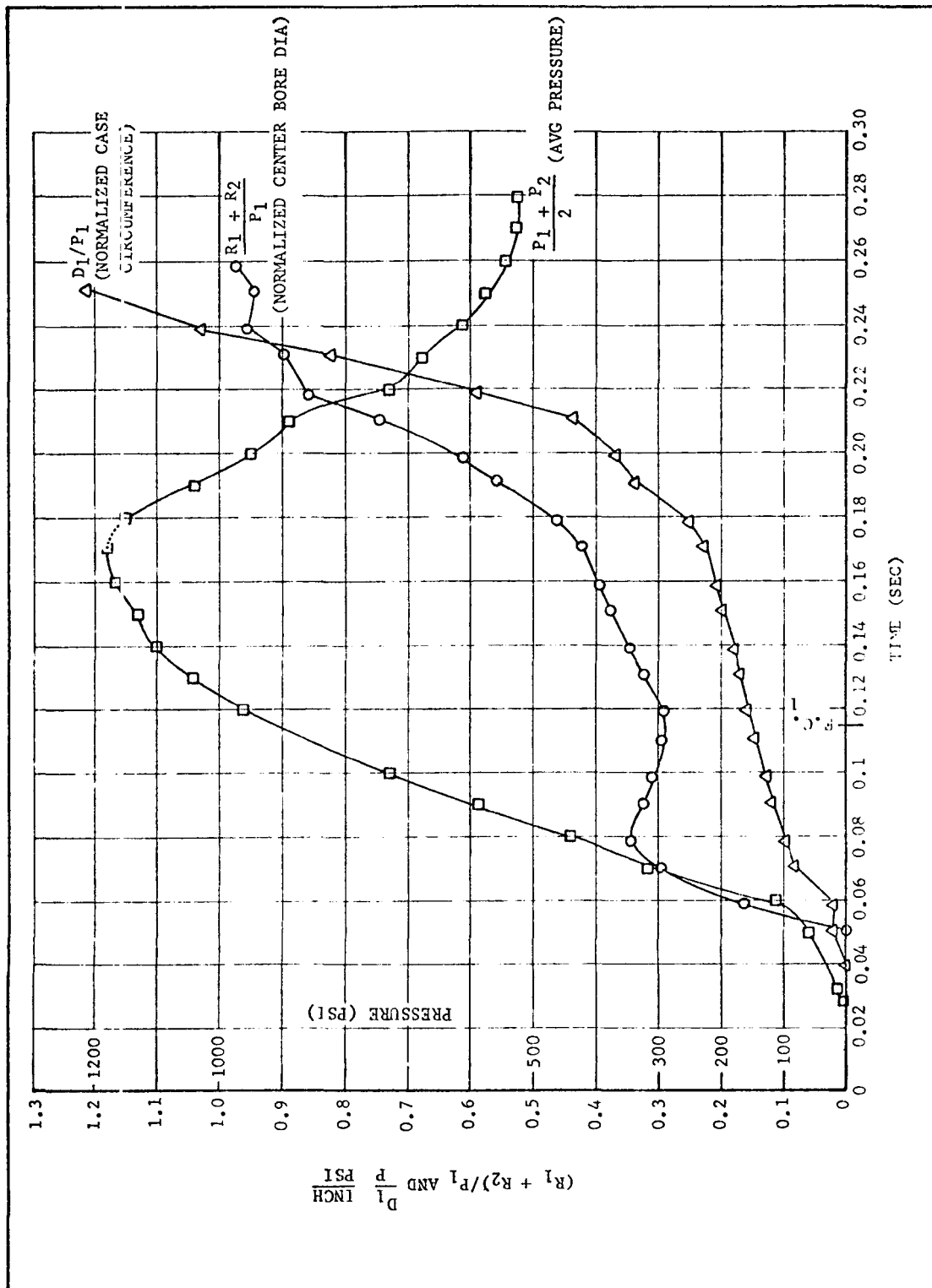


Figure 2-8. Overtest Model O/T-013 - Average Pressure, Normalized Centerbore Diameter, Normalized Case Circumference

The event gages did not perform as expected in these tests. With a 1-inch diameter centerbore, the event gage could only be installed on the ends of the cylinder. The usefulness of event gages depends on where the cracks originate and propagate. In this series of tests, it appears that in four of the six tests, cracks originated on the opposite end of the CCC from the event gage. The cracks appeared to propagate to the event gage but not always through it. Only on the test of O/T-017 does the event gage give data close to the strain gage and analysis results. This event gage opened at 0.0706 seconds while time of failures from strain gage data and analysis was 0.083 second. The main centerbore crack in O/T-017 was through the gage. Why it appears to have opened early is not fully understood. All but two of the gages opened early. Four gages closed again before failure and they also opened again following failure. The event gage on O/T-013 never did open or give any indication of cracking.

Figures 2-9 to 2-13 show the sectioned grains with the event gages and the centerbore cracks. It is not possible to have an event gage which covers the complete centerbore, and therefore, since the failure cracks did not occur in the same place each test and do not propagate the full length of the grain, spot location of event gages is insufficient for consistently determining time of failure.

The case strain gage data appear to show time of failure of the centerbore. The case strains were normalized with respect to pressure and first plotted as a function of time. As shown in Figure 2-14 there is no slope change until the time corresponding with that of maximum pressure which is when the case fails. The normalized case strains were then replotted as a function of pressure (Figures 2-15 through 2-20). Two fairly distinct slope changes are seen from these plots prior to the maximum pressure. The analyses failure pressures based on the cumulative damage theory corresponded very closely to the first slope change on the case strain-pressure plots. The comparative results for each motor are reported in Table 2-1. The difference in the two postulated failure pressures is +8 percent to -4 percent for the motors tested. Failure was predicted at an average pressure of 916 psi by analyses. Strain data indicates failure at 936 psi. This is only a 2 percent difference for the average of the six analogs tested.

#### C. CONCLUSIONS FROM ANALOG TEST PROGRAM

The rubber stress relief flap design for subscale models proved to be an adequate design for high rate pressure hydrotests to study the center-port failure mode. All failures in the six CCC's tested of this design occurred as cracks in the centerbore of the grains.

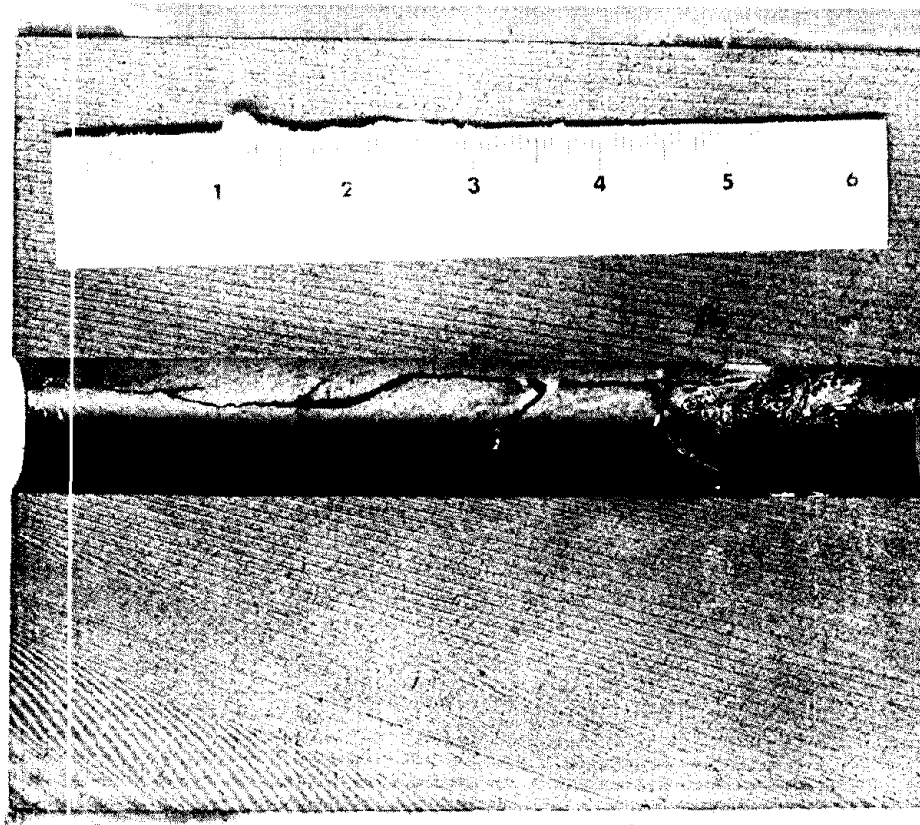


Figure 2-9. Centerport Failure in Propellant, Model O/T-012

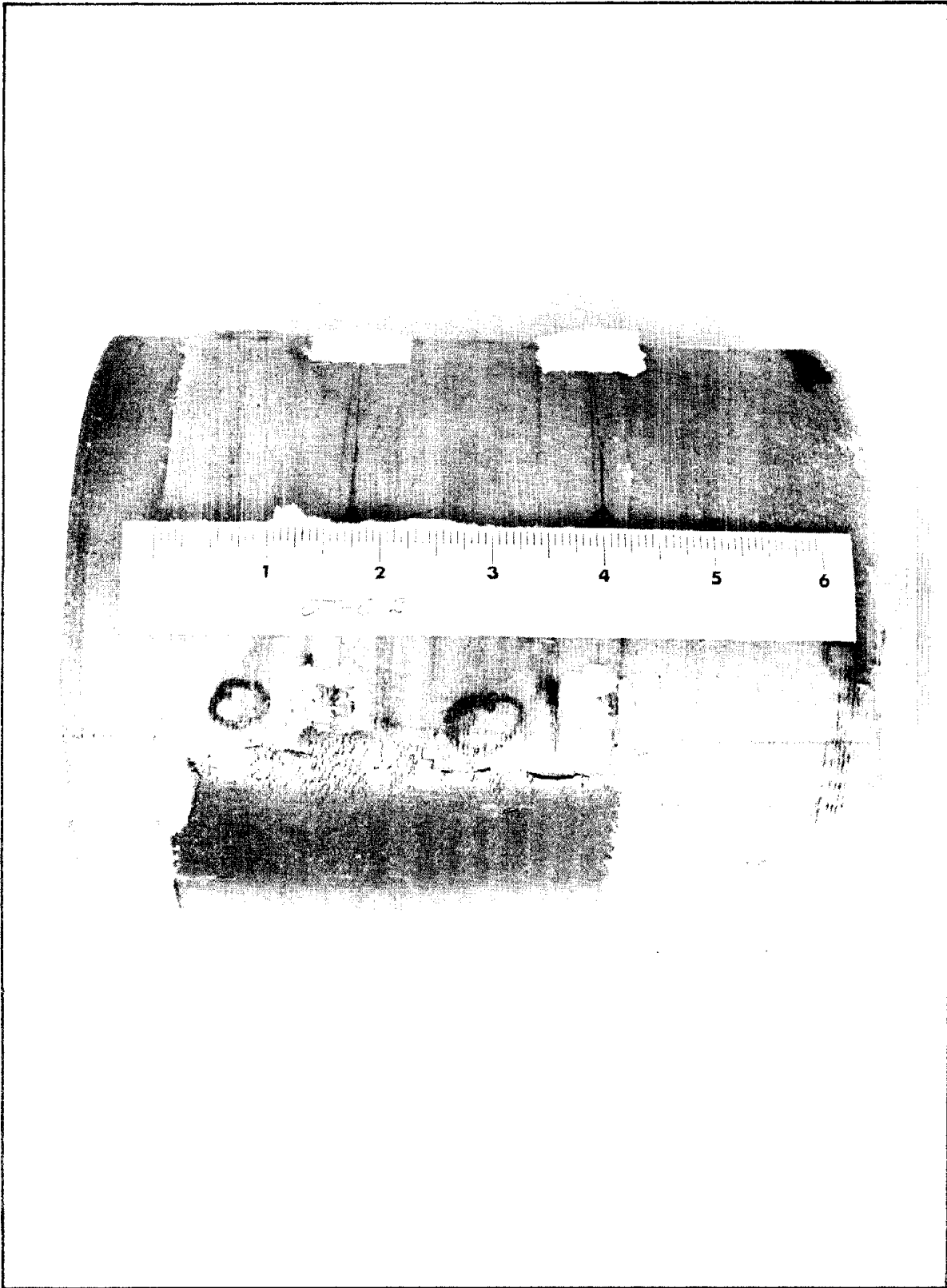


Figure 2-10. External Propellant Failure, Model O/T-012



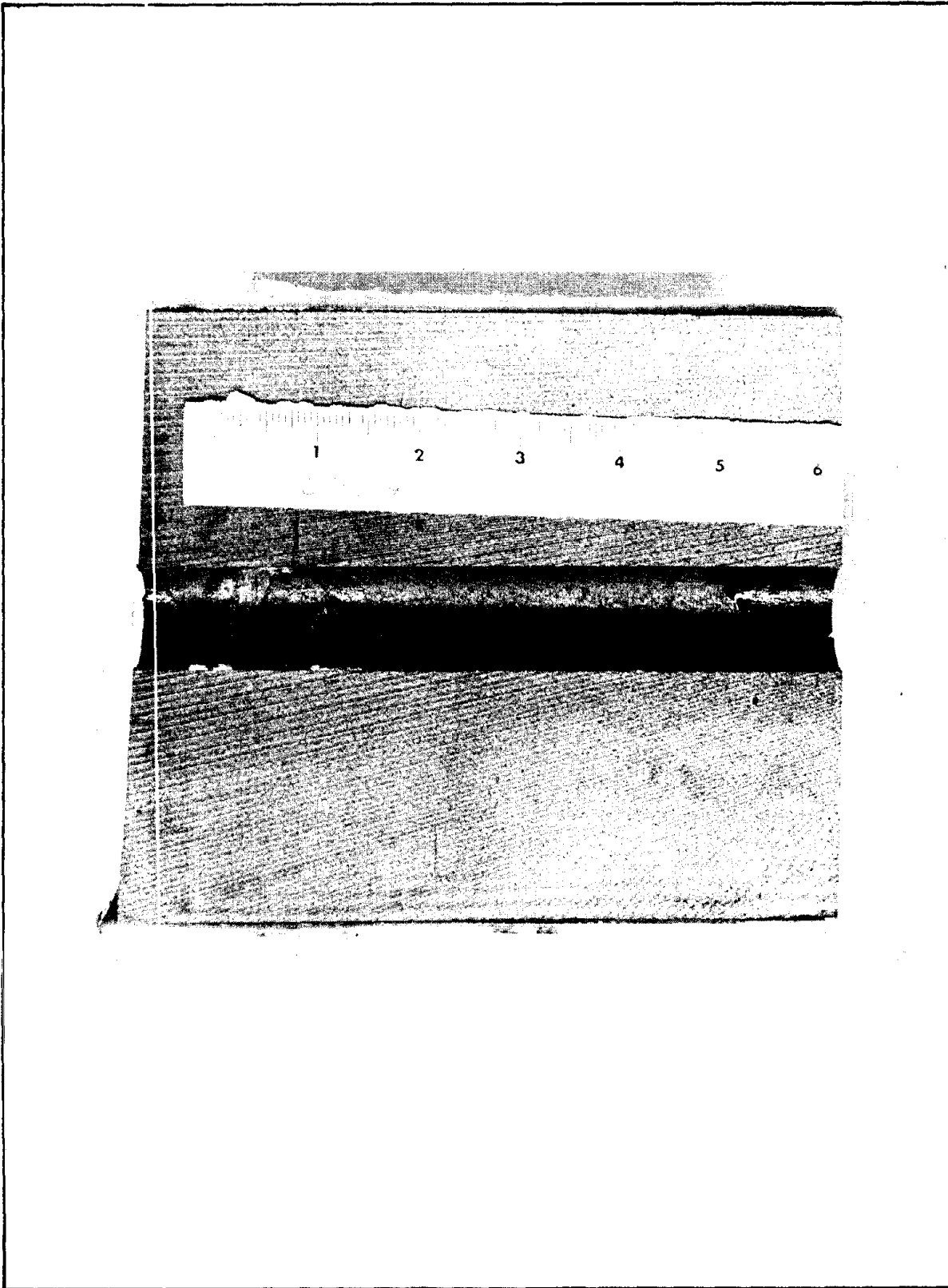


Figure 2-11. Centerport Failure in Propellant, Model O/T-014

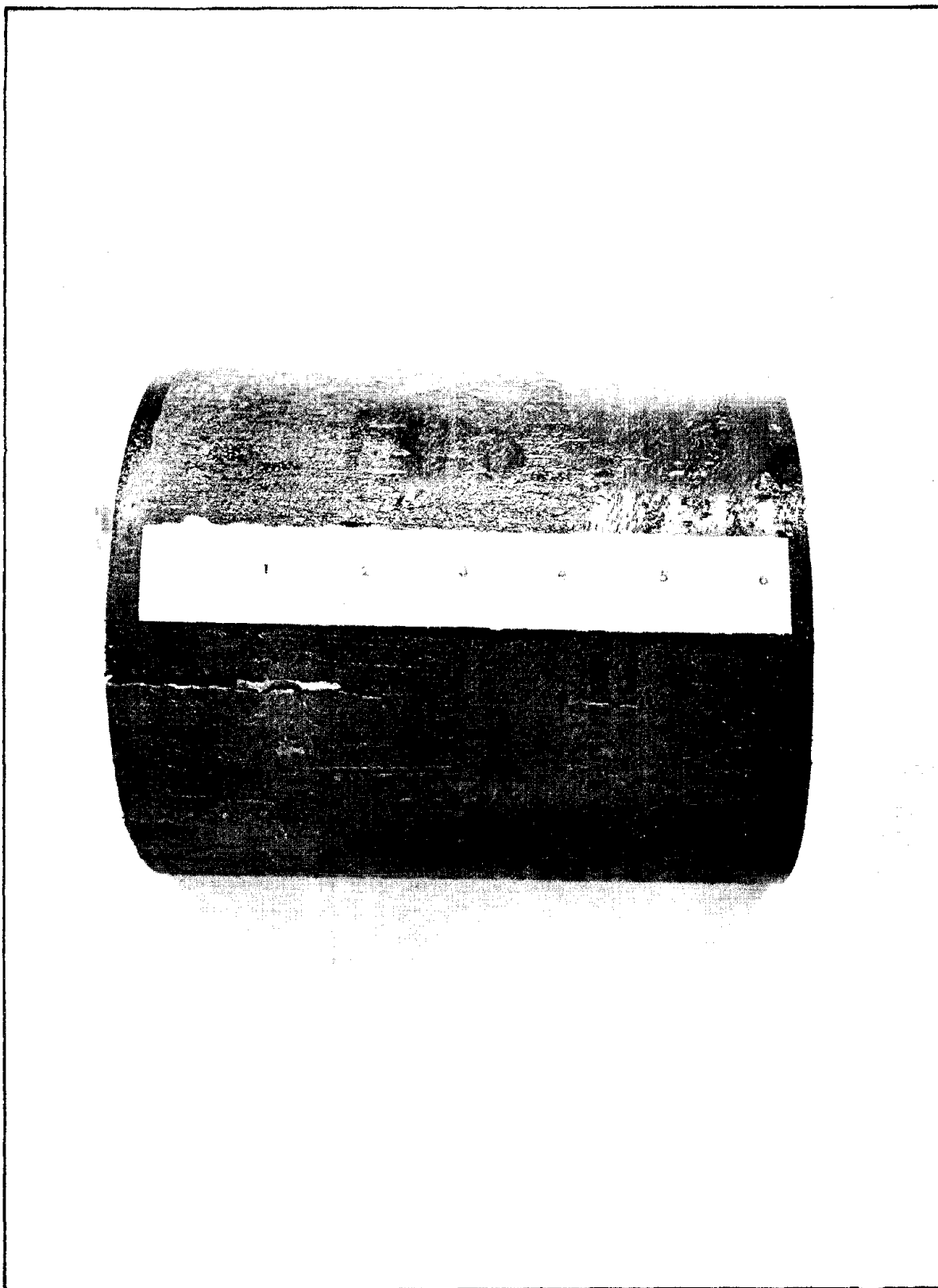


Figure 2-12. External Propellant Failure (Case Removed), Model O/T-014

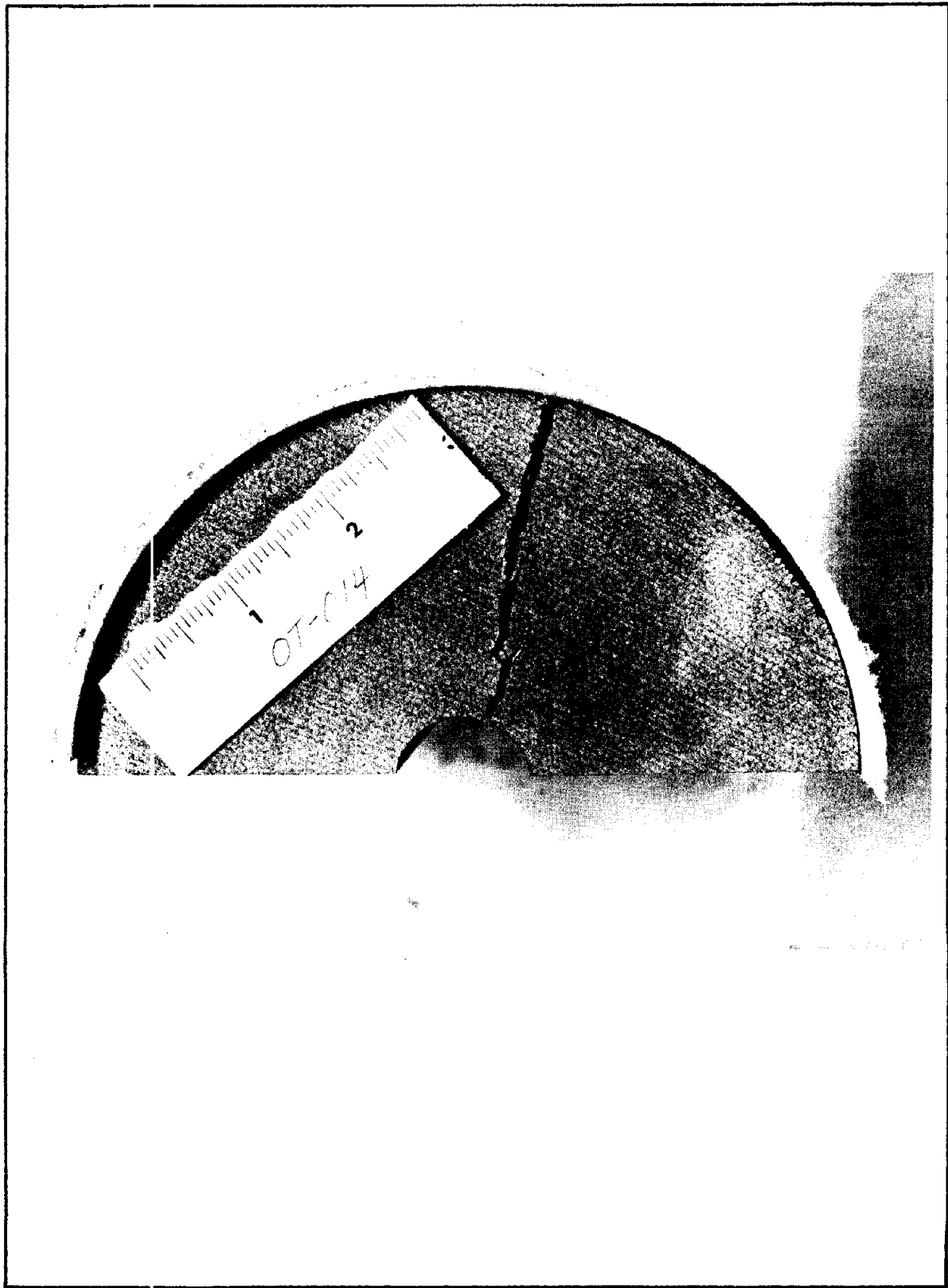


Figure 2-13. Propellant Failure, Model O/T-014

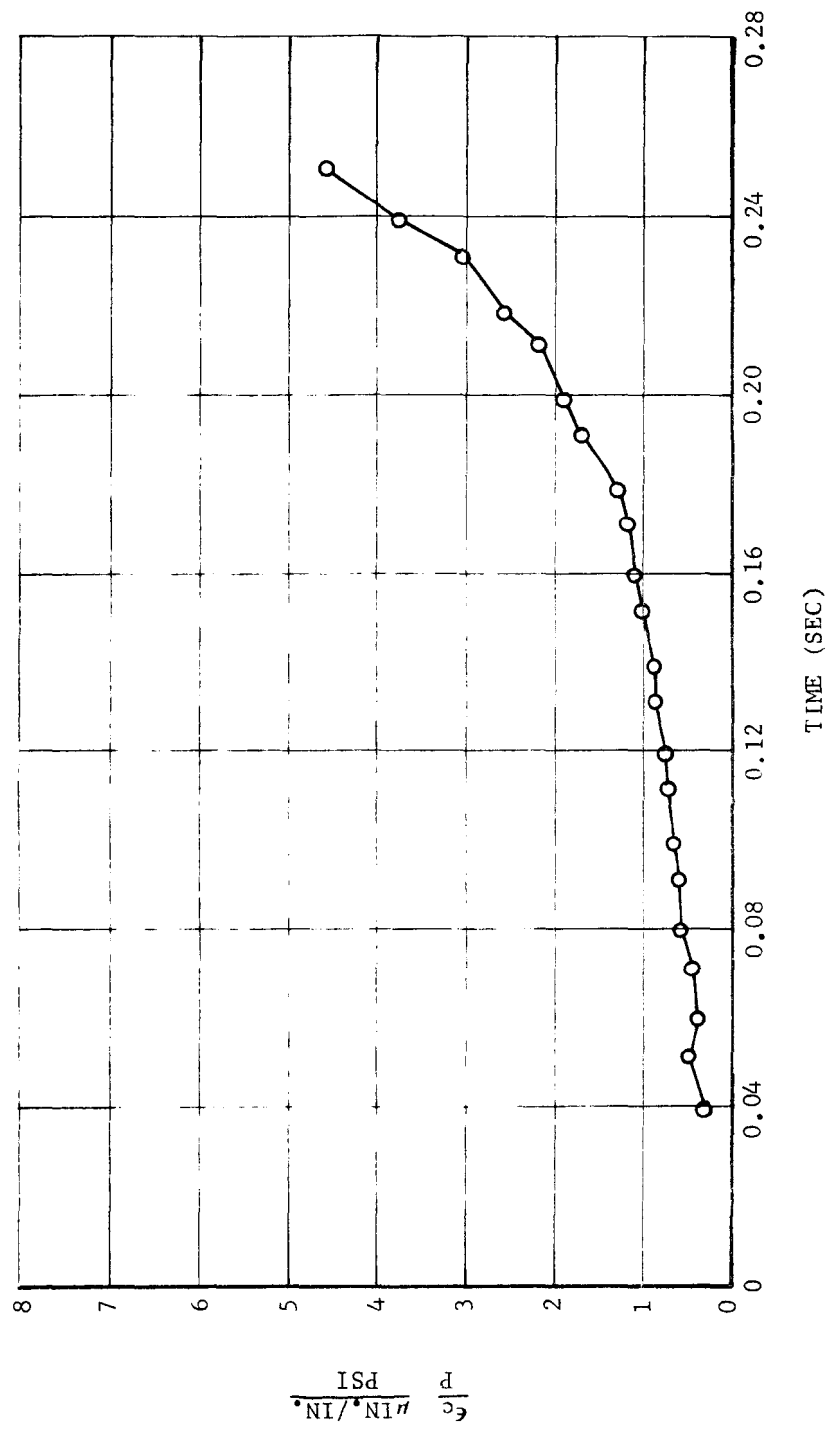


Figure 2-14. Overtest Model O/T-013 - Case Strain (Strain Gage 3)

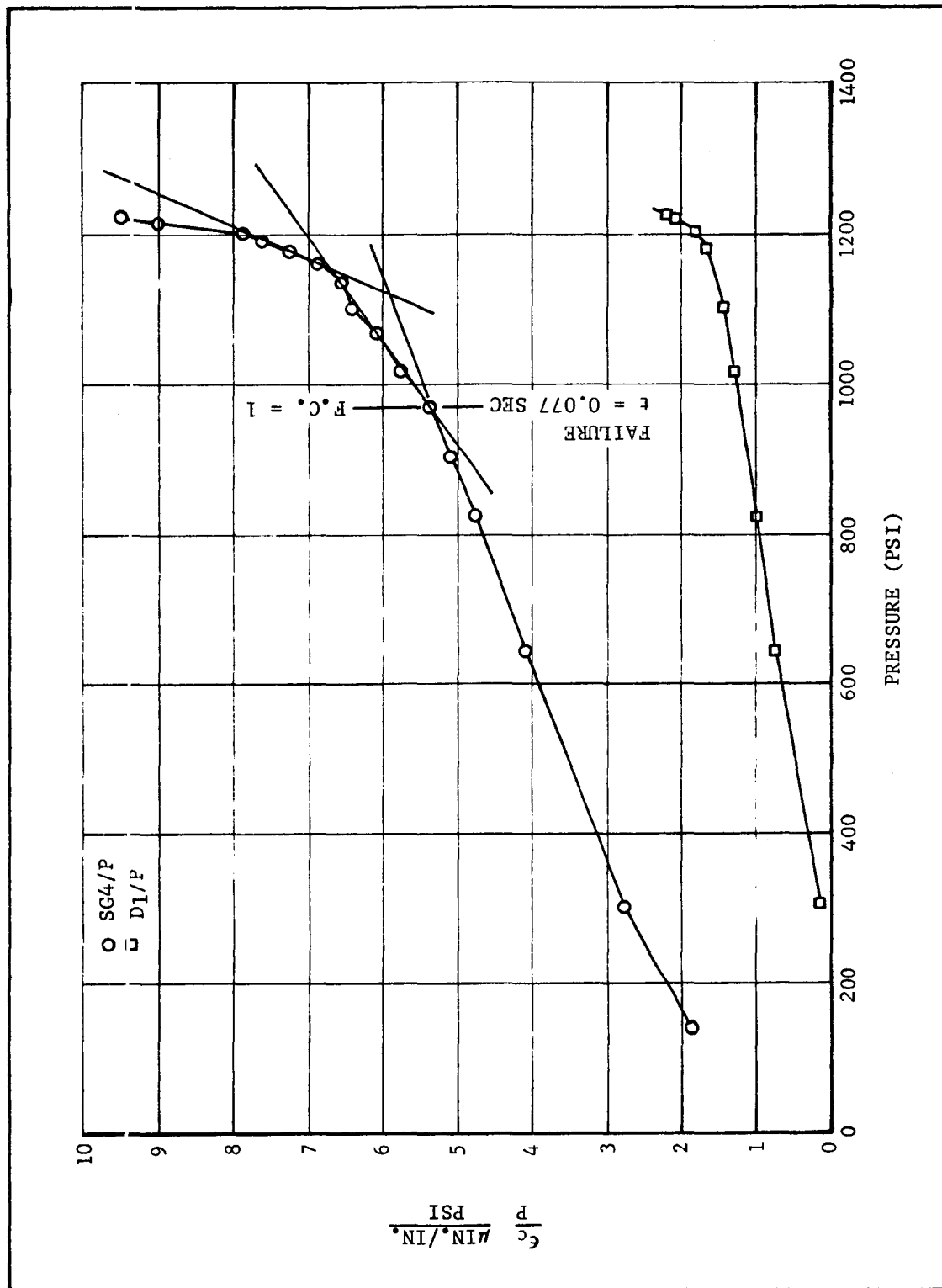


Figure 2-15. Overtest Model O/T-012 - Normalized Case Strain (Gage 4)

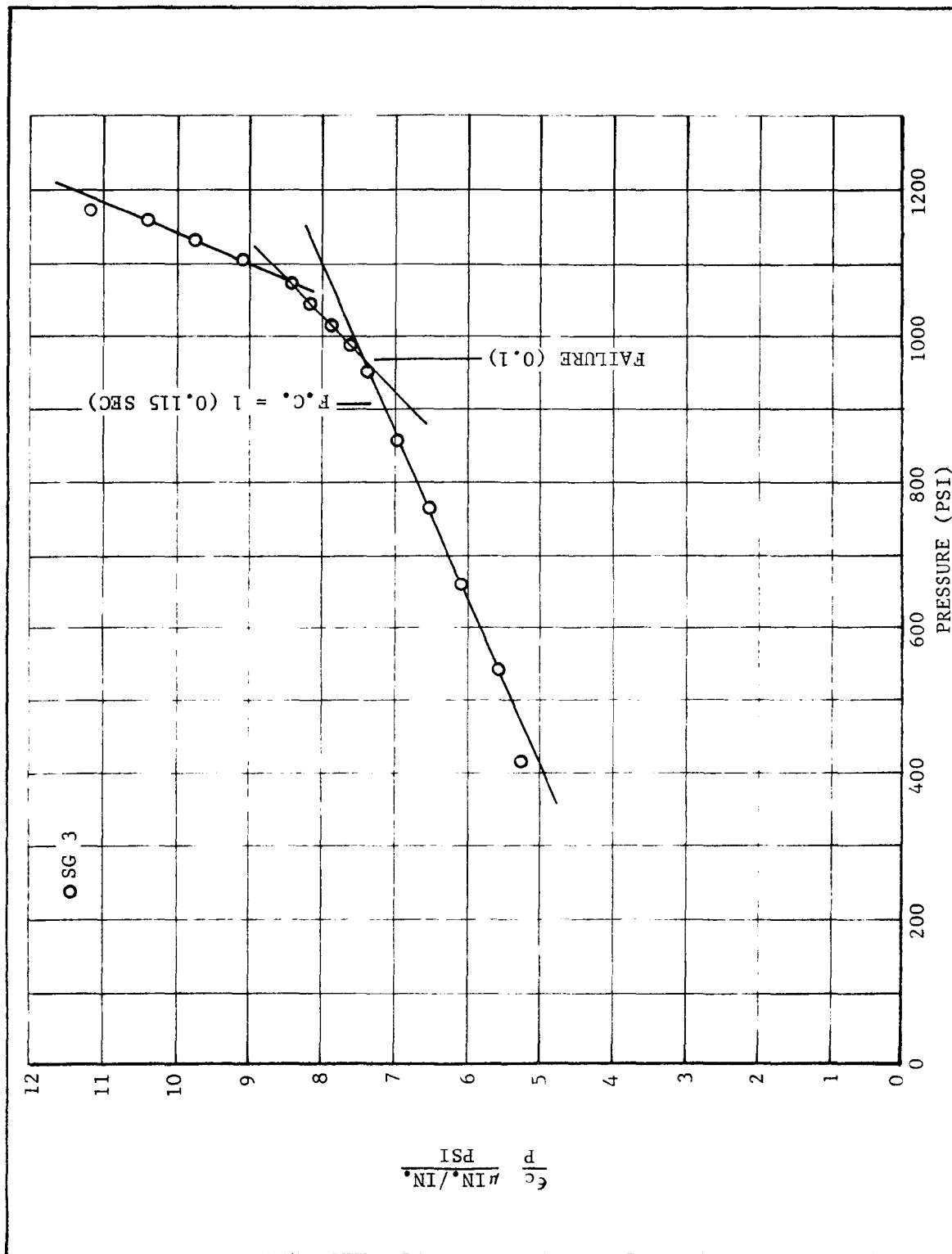


Figure 2-16. Overtest Model O/T-013 - Normalized Case Strain (Strain Gage 3)

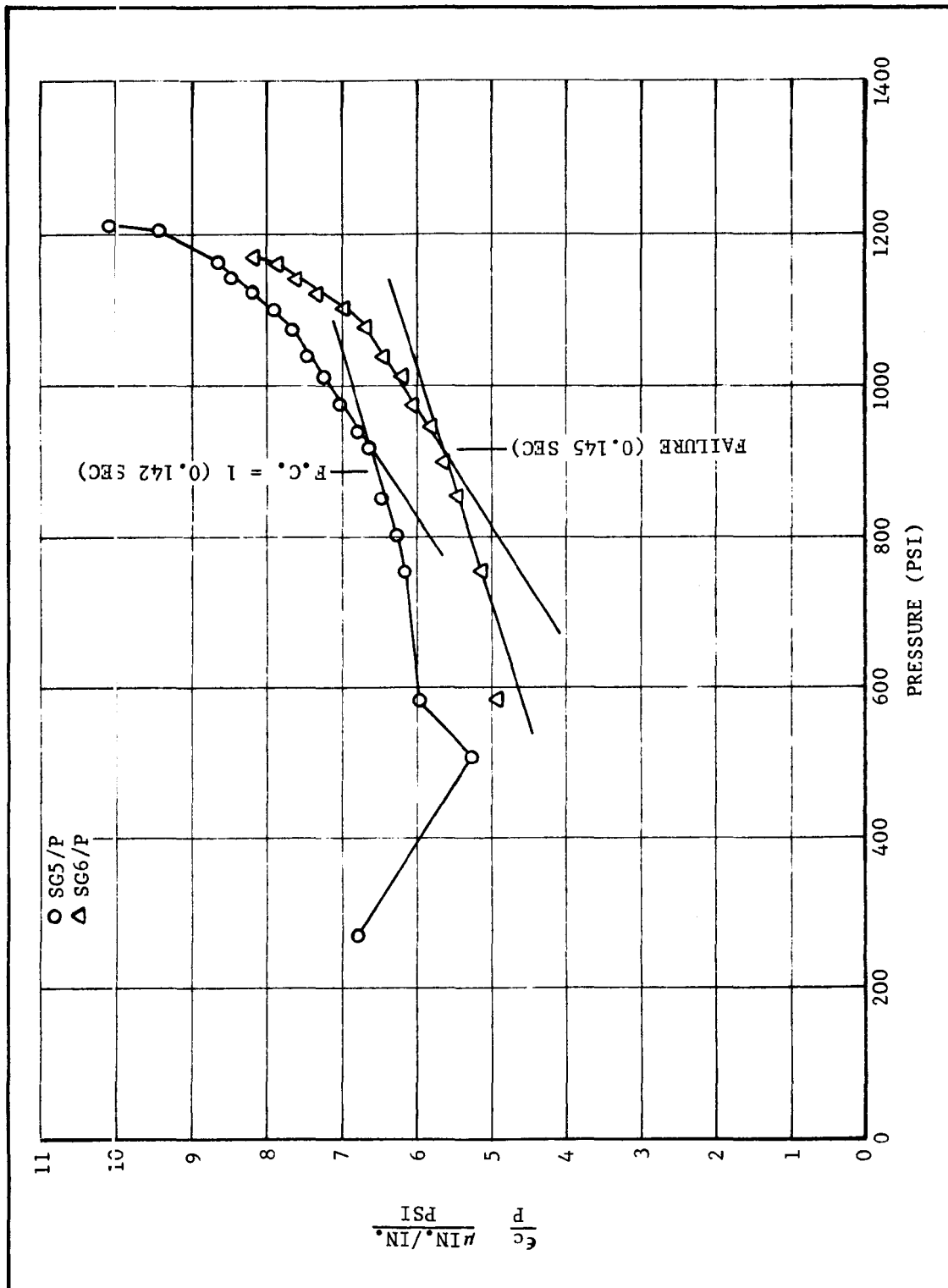


Figure 2-17. Overtest Model O/T-015 - Normalized Case Strain (Gages 5 & 6)

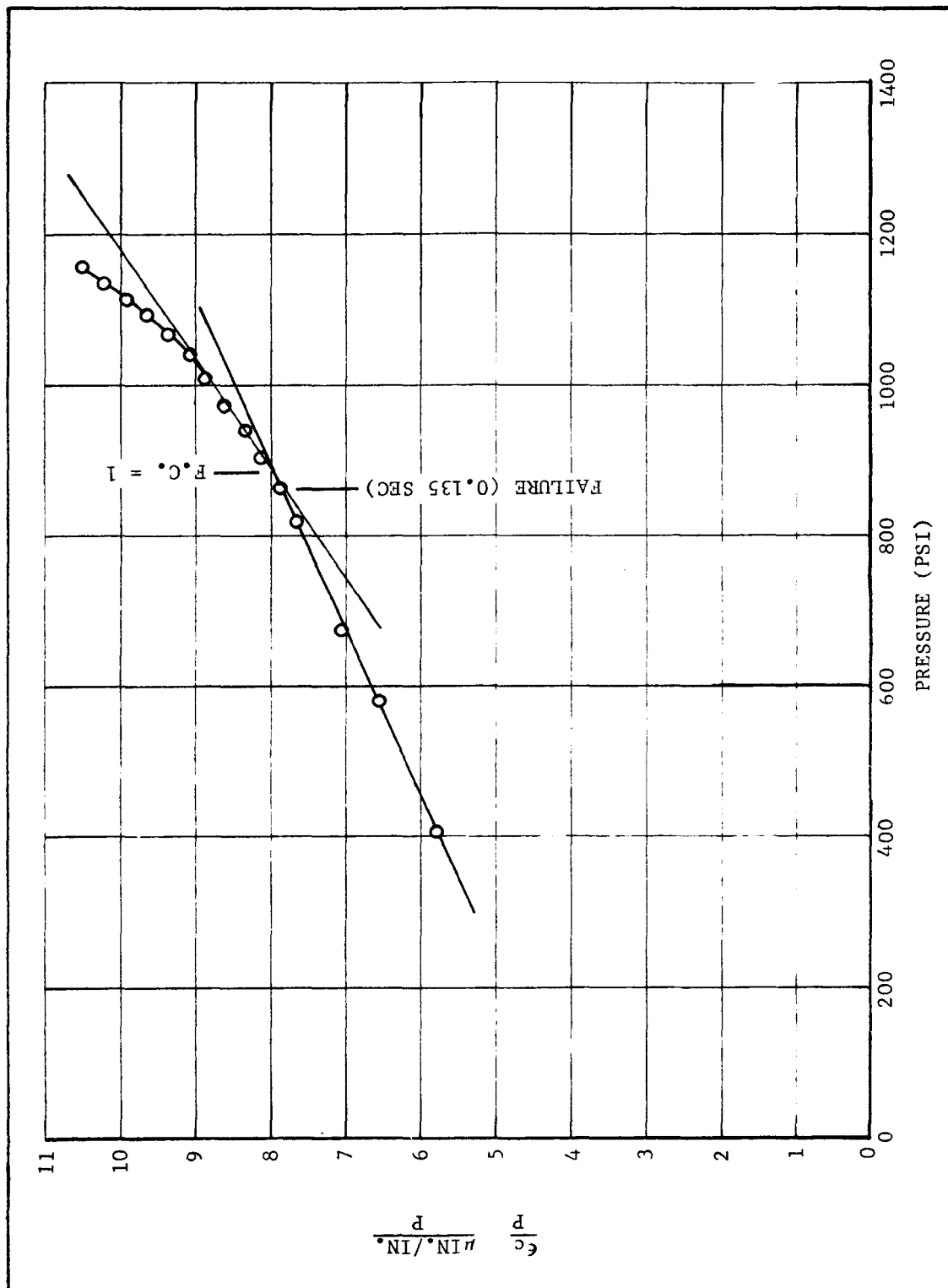


Figure 2-18. Overtest Model O/T-014 - Normalized Case Strain (Gage 3)



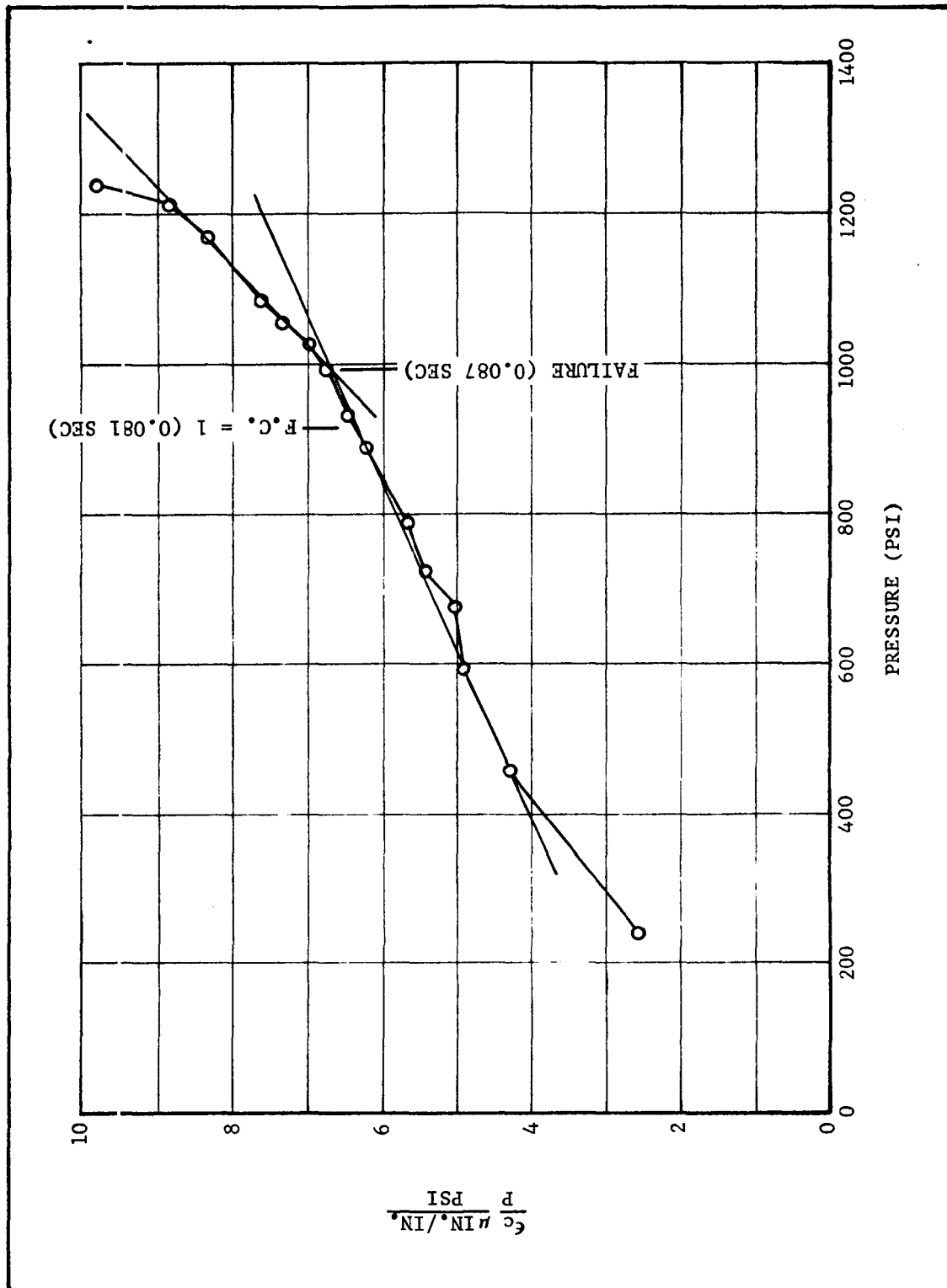


Figure 2-19. Overtest Model O/T-016 - Normalized Case Strain (Gage 6)

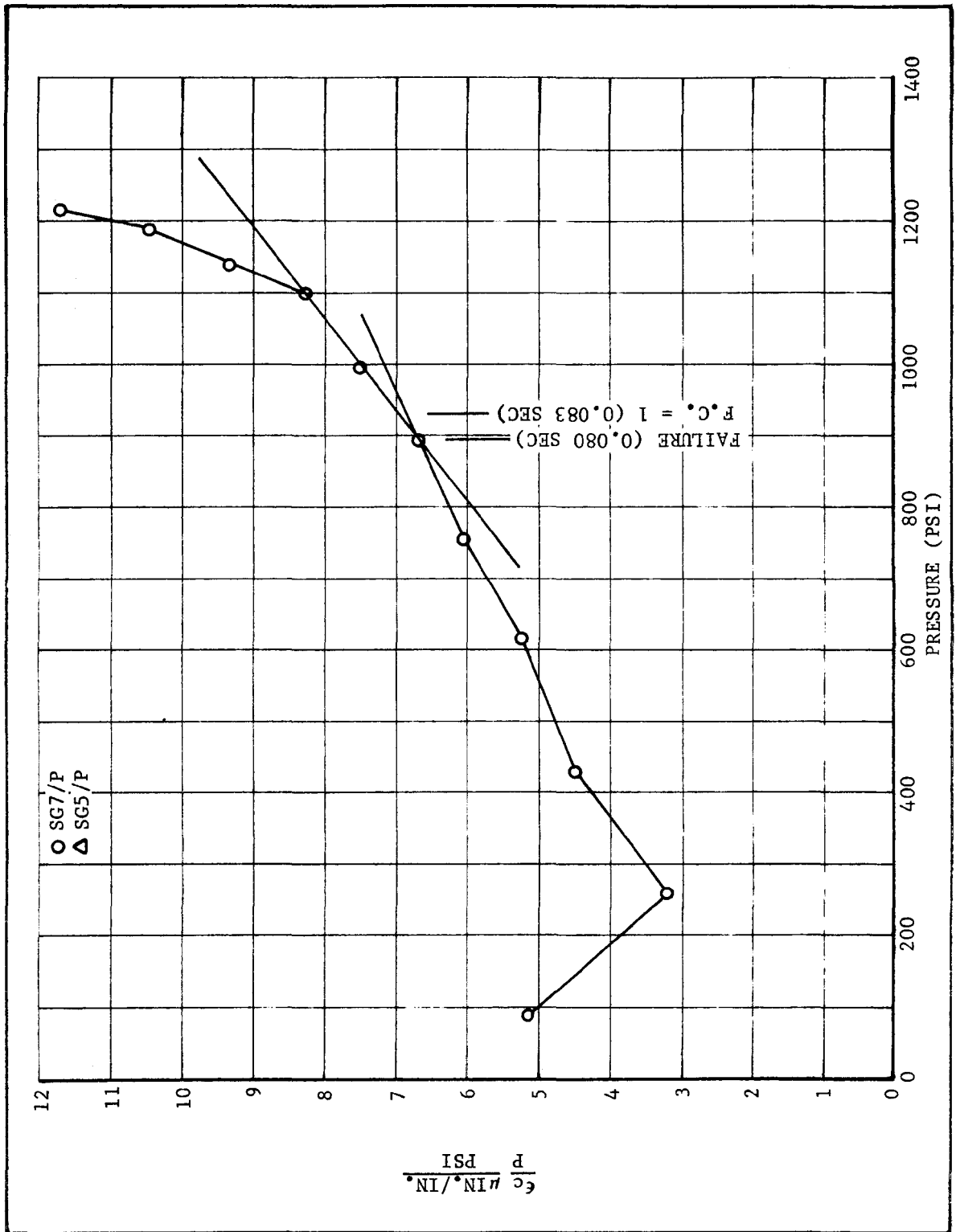


Figure 2-20. Overtest Model O/T-017 - Normalized Case Strain (Gages 5 & 7)

Prediction of analog motor failure was based on cumulative damage failure theory including stress concentration factors for slotted models. The failure theory agreed very closely with CCC failures as indicated by the normalized case strain data (first slope change of strain-pressure plots). The failure theory also agreed closely with the failure of the slotted models as detected by the event gages. The event gages proved unsuccessful in the circular centerbore failure modes due to an inability to install an adequate number in the small, 1 inch, diameter centerbore.

Leaf deflectometers did not function properly in the small centerport designs under high rate hydrotest conditions. There appears to be no adequate way at present to measure the centerbore diameter and the subsequent strain in subscale models under high-rate pressure hydrotest conditions. This is an area which needs future study.

The major objective of the program was accomplished. The wing slot failure is the primary failure mode as demonstrated in the slotted subscale test and the circular centerbore tests with the flap-relieved design. The cumulative damage failure theory used in the analyses of the full-scale M57A1 motor does predict failure. This was borne out by the subscale analyses and high rate hydrotests.

Since only one aged motor was used in each of the subscale tests, the test results could not be used in the service life prediction of the Minute-man motor.

Subscale testing is a valuable tool in the service life assessment. It is recommended that subscale models as well as full-scale motors, be constructed during motor production, stored, aged, and tested. This would provide the data necessary to calculate statistical limits for the motor margin of safety as well as to establish aging trends.

For motor programs no longer in production, the subscale overtest models need to be fabricated from various aged full-scale motors being removed from the force. There is limited flexibility in this program because selection of a particular age or class of motor or propellant is usually prohibited. Moreover, the history of a particular motor removed from the force may not be sufficiently well known to permit confidence in controlled experimentation. It is essential, therefore, that motors made available to a program are applicable. They must be representative of the population of motors being evaluated.

#### LIST OF REFERENCES

1. Daniels, A. S., Rotter, J. J.; ICBM Overtest Technology, Overtest Modeling (Task II) and Subscale Verification of Model (Task III), AFRPL-TR-74-25, Hercules Incorporated, Magna, Utah, February 1975.
2. A. S. Daniels, An Event Gage for the Detection of Propellant Crack Initiation, Presented at the Annual Meeting of the JANNAF Structures and Mechanical Behavior Working Group and the Operational Serviceability Working Group, 26 February 1974.

## SECTION III

### FULL-SCALE MOTOR OVERTESTS

#### A. INTRODUCTION

The primary objectives of Task IV were to demonstrate the concept of overtest in a full-scale ICBM motor, and to provide information for establishing the applicability of such tests in a predictive surveillance program.

Other objectives were to: (1) Determine present structural capabilities of the M57A1 grain and to apply the results (with other related information) to predict the age-out date of the motors, and (2) to identify any potential failure modes of the M57A1 motor grain which have heretofore been unidentified. By determining the capability of motors of various ages to withstand such critical environments, it should be possible to extrapolate motor capability versus age to a time when the motor no longer has sufficient capability to withstand the expected loads. To do this economically, other technologies must be applied in combination with the full-scale overtests.

The first three tasks (I-III) of the ICBM Overtest Program are relevant to the full-scale overtest task. They are reported in References 1 and 2 and are briefly reviewed in the respective sections of this report. Task IV, full-scale motor overtest program, is described in detail in Reference 3. This section will review the motor overtest program conducted under Task IV and other full-scale overtest programs performed on the M57A1 motor. The particular programs of interest are the Minuteman Product Support Program (PSP) and the current LRSLA Program.

It was expected that confirmation of the critical failure mode plus identification of any unexpected failure modes would result from the overtests. The basic information desired from motor overtesting was the pressure at which failure began. Both failure mode and failure pressure are relevant to the prediction of motor service life, whether predictions are by extrapolation of overtest results or by analytical methods. Accordingly, the test operations, instrumentation, and motor inspections were structured to yield the maximum amount of data relative to motor failure; acquisition of data used to validate the mathematical model was considered to be of secondary priority.

This section of the report will evaluate the various programs in terms of the overtest philosophy. Prediction of the motor service life will be reported under Section VI.

---

<sup>1,2,3</sup>References are presented at end of each section.

The full-scale motor configuration studied in the overtest program is shown in Figure 3-1. Selection of motors for the ICBM Overtest Program was made by AFRPL, OOAMA, and Hercules personnel, using the following criteria: (1) The motors were to be structurally sound, with no propellant cracking or debonding evident, (2) the motors were to have been made using powder (base grain) for which lot performance data were available, and (3) the motors were available. It was also requested that propellant grain X-rays made during motor manufacturing be made available. One each from six-year and nine-year old motors were chosen as full-scale test vehicles.

Ideally, the two motors to be selected should be paired with respect to all features so that any differences in the failure pressure could be attributed to age. However, several changes were introduced in the design after several motors were deployed which prevented the study of age alone as the principal variable. A nine-year old motor is the pre-OPRI\* configuration and a six-year old motor is an OPRI motor. The OPRI changes affected the core geometry, case bond, powder loading, casting, cure, and aft center port bond. The prediction of age-out by extrapolating full-scale motor overtest results may be compromised because of difficulties in assessing the effects of these processing changes; however, the task objective of demonstrating the validity of the overtest concept was achieved.

Two types of event gages were evaluated for application in this program, a modular gage which is intended to be bonded across the centerport, and nozzle port insulator-boot-shrinkage liner-propellant interface, and a conductive film gage which was painted and wired into the wing slots. Verification of these methods was accomplished with the subscale tests and applied to the full-scale motor.

The event gages used in the program and their development are reported in detail in References 2 through 4. Further discussion of the event gage work will not be made here.

#### B. PREVIOUS OVERTEST RESULTS

During the Minuteman Support Program, several full-scale motor overtests were performed on the M57A1 motor using high-rate pressurization as the overtest method. The most notable, and applicable, overtests were conducted on full-scale motors SD-9, SD-10, 2-10-16, and 2-10-38 during the period from 1963 to 1965 as reported in References 5 through 7.

Motor SD-9 was the first such unit to be high-rate pressurized and was subjected to two test phases. Phase I subjected the motor to high-rate pressurization to failure. Phase II induced cracks under similar conditions.

---

\*OPRI - Operational Reliability Improvement

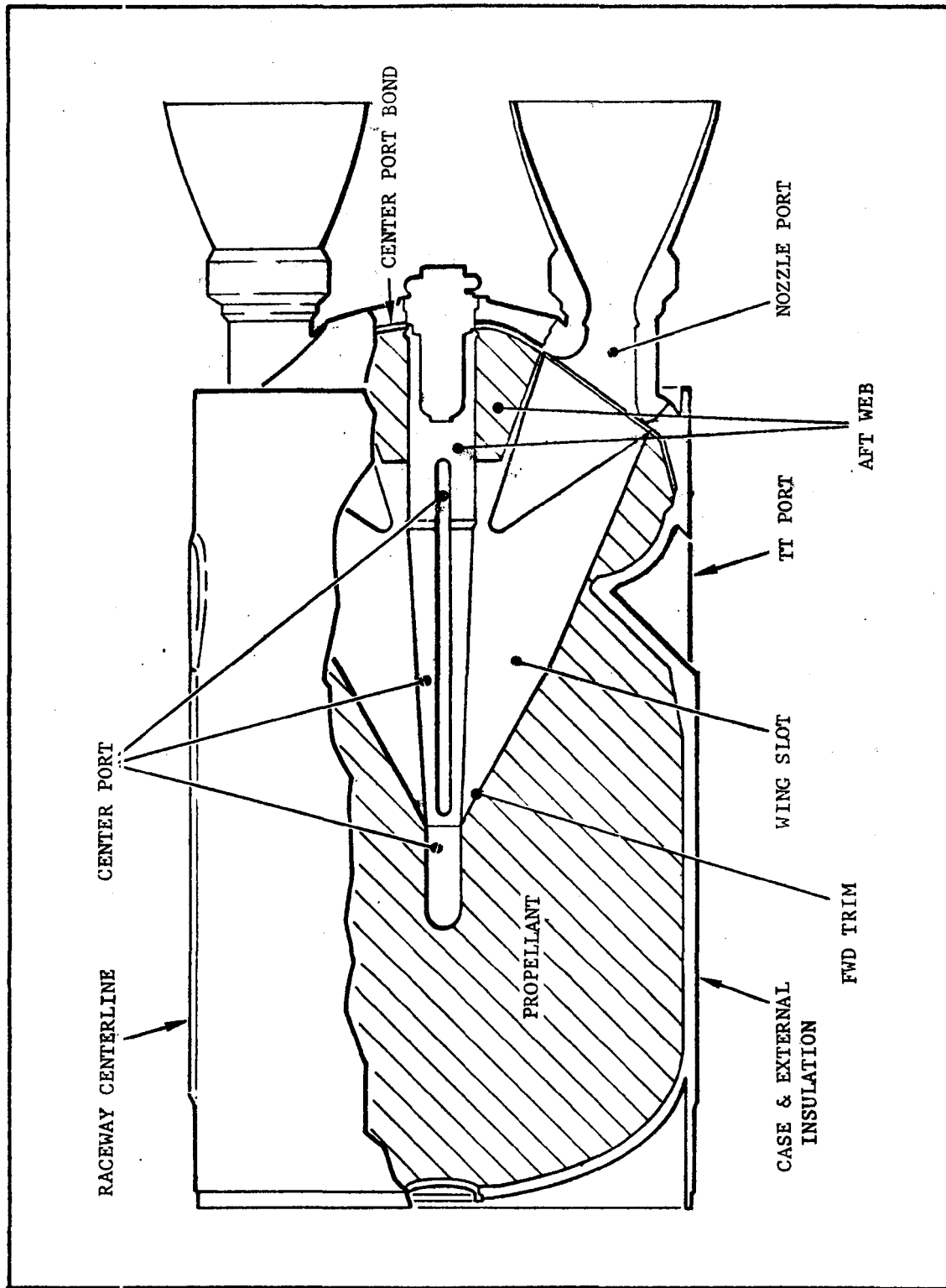


Figure 3-1. Minuteman Third Stage Motor

The first high-rate pressurization of a full-scale motor (SD-9, Phase I) was conducted in February 1963. The pressure in the motor rose at a maximum rate of 4000 psi/sec to an initial peak pressure of 410 psia. This peak pressure was 90 psi higher than the steady state pressure of 320 psia which was reached 0.9 second after opening of the high-rate valve. The "overshoot" in pressure was caused by the conversion of the kinetic energy of the mineral oil flowing into the case into a pressure force as stagnation occurred. Case strain data and internal grain deflectometer data substantiate the occurrence of the recorded pressure peak and pressure fluctuations.

Internal grain deflectometers indicated an average growth in the nozzle wing slot width and centerport diameter of 0.5 inch. This growth corresponds to an increase in grain void volume of 560 cubic inches and to an increase of initial propellant surface area of 130 square inches.

Visual inspection of the motor and propellant after the hydrotest indicated that there were four cracks in the propellant grain. These extended completely through the area between each of the nozzle wing slots and the centercore for a distance of about three to four inches toward the aft end of the motor from the intersection of the nozzle slots with the centercore.

Radiographic inspections of the motor after hydrotest confirmed the presence of the four cracks in the propellant grain in the described areas. The radiographs also indicated no propellant-to-insulator or propellant-to-flap separations in any area. No propellant-to-thrust terminations port boot bond separations occurred.

The second high-rate pressurization of motor SD-9 was conducted in March 1963. The pressure in the motor rose at a maximum rate of 4280 psi/sec to an initial peak of 442 psia. This peak pressure was 80 psi higher than the steady-state pressure of 362 psia, which was obtained 0.9 second after pening of the high-rate valve. The Phase II test exhibited damped pressure oscillations identical to those in the Phase I test.

Post-hydrotest inspection of the motor indicated that the propellant cracks formed during the Phase I test were propagated an additional two to three inches toward the aft end of the motor. No other cracks were formed in the propellant grain. Radiographs indicated only one possible small separation between the propellant and shrinkage liner near the aft centerport, and no propellant-to-boot separations at the thrust termination ports.

The test series on SD-9 utilized a limited number of deflection and strain gage measurements of the motor case during pressurization. Deflection of the wing slots was monitored by using a strain gage deflectometer as shown in Figure 3-2.



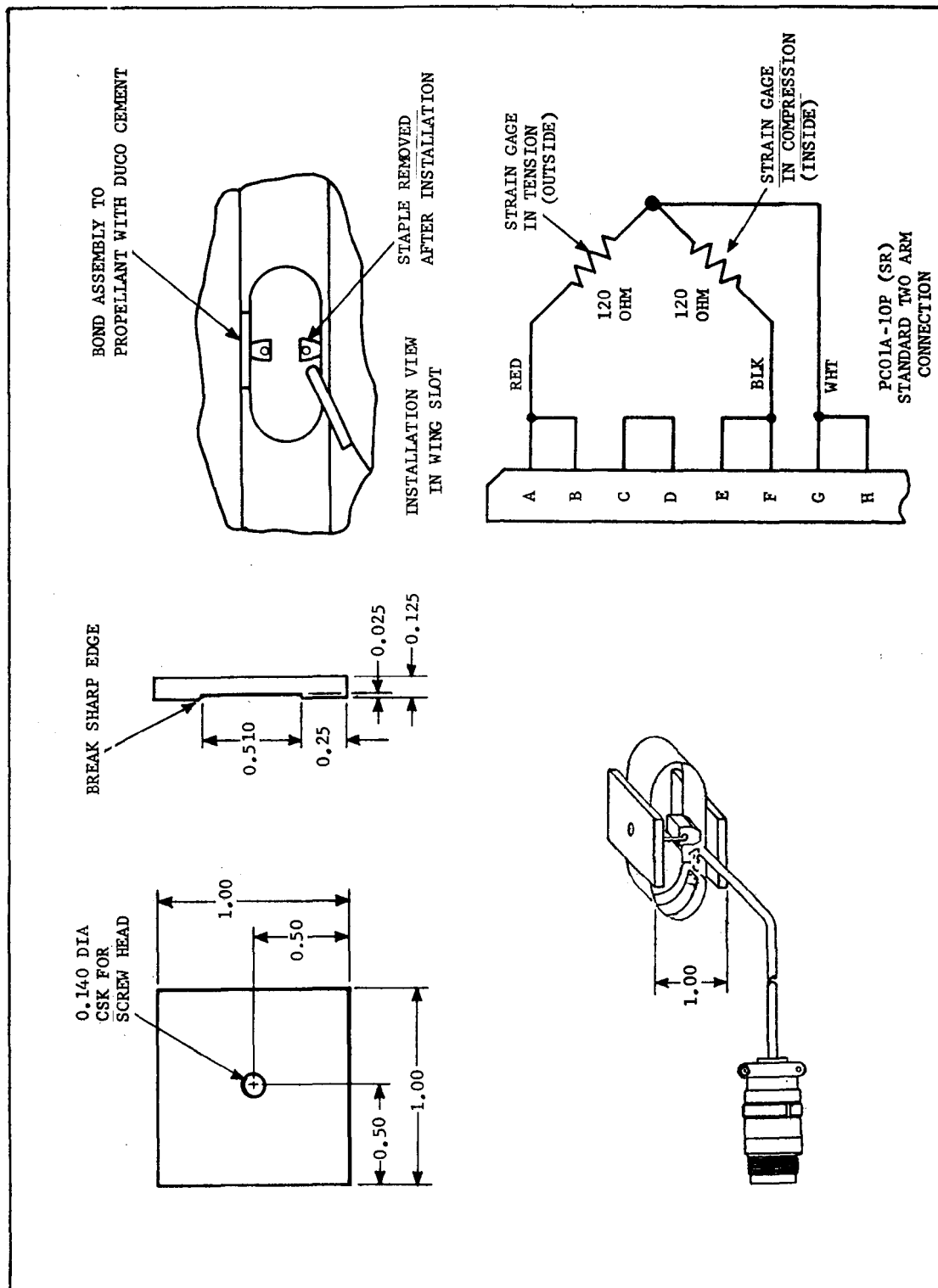


Figure 3-2. Strain Gage Deflectometer

Full-scale motor SD-10, with a case design slightly different from SD-9, was high-rate pressurized in July 1963. Prior to opening the high-rate valve, the high-pressure vessel was charged with nitrogen gas to a pressure of 860 psia. Upon opening the valve, the pressure began to rise in the motor at a rate which averaged 10,000 psi/sec between 50 and 600 psig. The maximum pressure obtained could not be determined because of amplifier saturation on all pressure measurements. Saturation occurred at a pressure of 655 psia. Based upon deflections of the motor case, it is estimated that a maximum pressure in excess of 750 psia was developed. Inspection of the grain and case deflectometers revealed that only one initial pressure hump resulted from this test, in contrast to the damped pressure oscillations formed in Tests I and II on Motor SD-9.

An equilibrium pressure of about 520 psia was held for 13 seconds which was 8 seconds longer than required by the test plan. The system exhaust valve was actuated after five seconds as planned. However, eight seconds were required to bleed the pressure vessel down to the internal motor pressure level, and, as the result, a rapid drop in motor pressure did not begin until 13 seconds after initiation of the test.

A posttest visual examination of the propellant grain core revealed that cracking had occurred in the following areas:

- (1) Number 1 Nozzle Wing Slot - Propellant cracks were formed in both radii of the outboard area of the slot running from the centercore junction to the inflection point in the slot.
- (2) Number 2 Nozzle Wing Slot - The propellant surface was masked by the instrumentation and it was impossible to visually determine if cracks were present.
- (3) Number 3 Nozzle Wing Slot - Propellant cracks were formed in both radii of the outboard slot area. Viewed from the aft end of the motor with the No. 1 nozzle down, the right side crack extended from a point about four inches aft of the wing slot inflection point down into the forwardmost area of the centercore where it necks down to the 2.6 inch diameter. The crack on the left side extended from the centercore junction aft to the inflection point of the slot.
- (4) Number 4 Nozzle Wing Slot - A crack was noted in the outboard area of the slot near the centercore, but the crack extent was masked by the instrumentation.
- (5) Aft Centercore Area - Cracks were formed between each of the four wing slots and the centercore. These cracks were from 8 to 10 inches long and extended aft from the junction of the wing slots and the centercore. They were propagated completely through the grain between the centercore and the wing slots.

All of the cracks noted were less than 0.10 inch in width when initially examined about 10 hours after the test.

Radiographic inspection of the motor under 50 psig internal pressure confirmed the presence of the cracks noted by visual inspection and indicated cracking had also occurred in nozzle wing slots No.'s 2 and 4. The pressure or time at which the cracking began during the test could not be determined from the deflectometer traces.

Possibly one of the earliest event gage devices known was planned for use in the test of SD-10. The propellant breakwire device shown in Figure 3-3 consisted of a conductive silicone rubber material which was bonded in place to the wing slots using a silicone adhesive (General Electric RTV 102). Unfortunately, all of the propellant breakwires were inoperative prior to the initiation of the test. A prefiring check showed that they all exhibited open circuits. From what is now known about this type of event gage, it could be assumed that the problem was the loss of electrical conductivity due to oil penetration of the conductive silicone rubber.

Motor 2-10-16 was subjected to a thermal test cycle and a high-rate pressurization. The thermal cycle test consisted of taking the motor from an equilibrium temperature of 70° F to an equilibrium temperature of 110° F then back to 70° F. The final grain configuration, and movement of the TT liner, indicated that a slight permanent set in the grain results when a motor is subjected to a large temperature gradient for long periods of time.

A pressurization rate comparable to that of an actual firing was obtained on motor 2-10-16, but the desired chamber pressure was exceeded. Wing slot deflections indicated that cracking apparently occurred between 0.06 and 0.07 seconds after pressurization.

The data from motor 2-10-16 shows that the rapid change in slot deflection occurred at a pressure between 500 and 530 psia. Similar wing slot behavior was noted on motor SD-10. This change in slot deformation was due to cracking, as confirmed by visual inspection. Closer examination of the response of the wing slot measurements indicated that cracking first occurred in the wing slot and propagated toward the forward end. As the maximum pressure (580 psia) was approached, the decreasing grain deflection recorded in the wing slots and the rapid change in deflection of the aft dome indicated aft shrinkage liner-to-grain separation. This was also confirmed by visual inspection and was similar to the aft dome behavior in motor SD-10.

In testing motor 2-10-16, many of the previous difficulties were successfully overcome and the pressurization rate was more closely simulated while greatly reducing the chamber pressure overshoot. From the response of the instrumentation and through visual inspection, the location and time at which cracking of the grain occurred was determined.



Figure 3-3. Propellant Breakwire

The last full-scale motor tested before the Overtest and LRSLA Programs was motor 2-10-38. This unit was pressurized at a rate of about 15,000 psi/sec to a maximum pressure of 310 psi. Very little overshoot and very few oscillations were observed as a result of modifications made to the pressurization system. As a result of the low maximum pressure level, wing slot cracking was not observed. An equilibrium pressure of 250 psi was maintained for 19 seconds which caused the aft end to debond at the boot/liner interface. Although the event gages generally gave a poor response during the pressure transient, they could be interpreted sufficiently to give the times at which the debonding occurred.

In summary, the full-scale motor tests during the Minuteman Product Support Program were successful in developing the high rate pressurization system although the explicit objectives for each test were not always fully realized. However, the wing slot cracking failure mode was verified and methods developed and suggested for detecting the pressure at which the cracking occurred.

It should also be realized that there were several changes in the design of the M57A1 motor since the start of production which resulted in some variation of the cracking pressure levels. These variations (case properties, design changes, etc) created motors of several subpopulations of the total force which must be evaluated on a population basis. This specific point will be more fully addressed in the overall analysis.

## C. LRSLA PROGRAM

### 1. Overtest Program Description

Several full-scale motors have been tested under the LRSLA Program. These motors have been tested under high-rate pressurization and thermal cycling test conditions. All of the motors in the LRSLA Program are also being dissected to determine the propellant and casebond properties. Two motors, 32743 and 32765, were high-rate pressurized while a third motor, 32720, was pressurized after inducing cracks in the wing slots. The functional purpose of the latter test was to attempt to propagate induced cracks in the wing slots of the motor after it was conditioned to  $70^{\circ} \pm 3^{\circ}$  F and then pressurized to approximately 320 psig at a high rate (about 7100 psi/sec). The objective of this test was to validate the analytical model of the motor by determining if a pretest induced crack in each wing slot would propagate.

The tests on motors 32743 and 32765 are more applicable to the Overtest Program and will be discussed in more detail. For a complete discussion of the tests on these two motors please see Reference 8.

The motors selected for testing were Minuteman II, Stage III motors with the characteristics shown in Table 3-1. As part of the pretest inspection, widths of the wing slots and centerbore were taken at various locations. Visual inspections were performed on the interior of the motors

TABLE 3-1

## MOTOR CHARACTERISTICS

Characteristic	Motor 32765	Motor 32743
Hercules production number	6F3	6D2
Powder lot		
CYH	1-7-65	1-6-64
DDP	1-1-64	1-1-64
Cast date	8 Mar 65	27 Jan 65
Age at test (month)	101	107
CYH physical properties		
Tensile strength (psi)	334	336
Elongation (%)	57.4	58.0
Elastic modulus (psi)	819	842
C-7 adhesive weight*		
Aft center port (lb)	5	4
Nozzle port (avg)(lb)	7	7
Case serial number	HP00506	HP00486
Hydroburst lot	15B	14B
Burst pressure (psi)	638	591
Silo location	Warren AFB	Warren AFB
Date removed from service	June 73	July 73
*Characteristic of "controlled bond" processing		

for any grain anomalies. The aft centerport areas were also inspected for any anomalies which might adversely affect the tests. The noted anomalies were not considered to be significant. Motor histories were also reviewed and nothing significant was found. Pretest X-rays were taken and compared with the originals taken at time of manufacture and no significant changes were noted.

Motor 32743 was inadvertently filled with water during the storage period. The motor was drained within three hours, wiped out with towels, and blown dry with an air hose. A visual inspection of the grain was performed and no deleterious effects of the water soaking were noted.

## 2. Overtest of Motor 32765

The test objectives for motor 32765 were achieved as the required pressure time envelope was maintained and wing slot cracking occurred in two of the four slots. The motor was tested in September 1973 at the Bacchus Works Test Range.

The test was performed using gaseous nitrogen in the accumulator tank pressurized to 550 psig. The fill rupture disc was ruptured to pressurize the motor. Maximum pressure of 504 psig was reached in the motor in 0.080 seconds and was immediately released. The pressure blowdown was excellent, reaching 200 psig in the motor within 0.160 seconds and was accomplished by rupturing three vent rupture discs which were triggered at 485 psig. This pressurization sequence was in conformance with the specified test envelope.

Observation of the hardware and equipment immediately after test showed that everything worked satisfactorily except that the center of the fill rupture disc blew into the interior of the motor through wing slot 3. The lead wires of the event gages had been torn loose and some gages were apparently destroyed. Upon motor dissection, the wing slots were cut in slices to determine the extent of wing slot cracking. Figures 3-4 and 3-5 show the extent of cracking in wing slots 3 and 4. No cracks were detected in wing slots 1 and 2. The aft centerport and nozzle port bonds were undamaged.

## 3. Overtest of Motor 32743

Motor 32743 was subjected to high rate pressurization testing in an attempt to verify the aft centerport debonding failure mode. Aft centerport debonding did not occur, thus establishing an adequate safety margin in this failure mode. Massive cracking did occur in the wing slots as anticipated.

The test was performed using gaseous nitrogen in the accumulator tank pressurized to 600 psig. The fill rupture disc was ruptured to pressurize the motor. Maximum pressure of 562 psig was reached in the motor in 0.123 seconds and was held for 118 seconds before rupturing the three vent rupture discs.

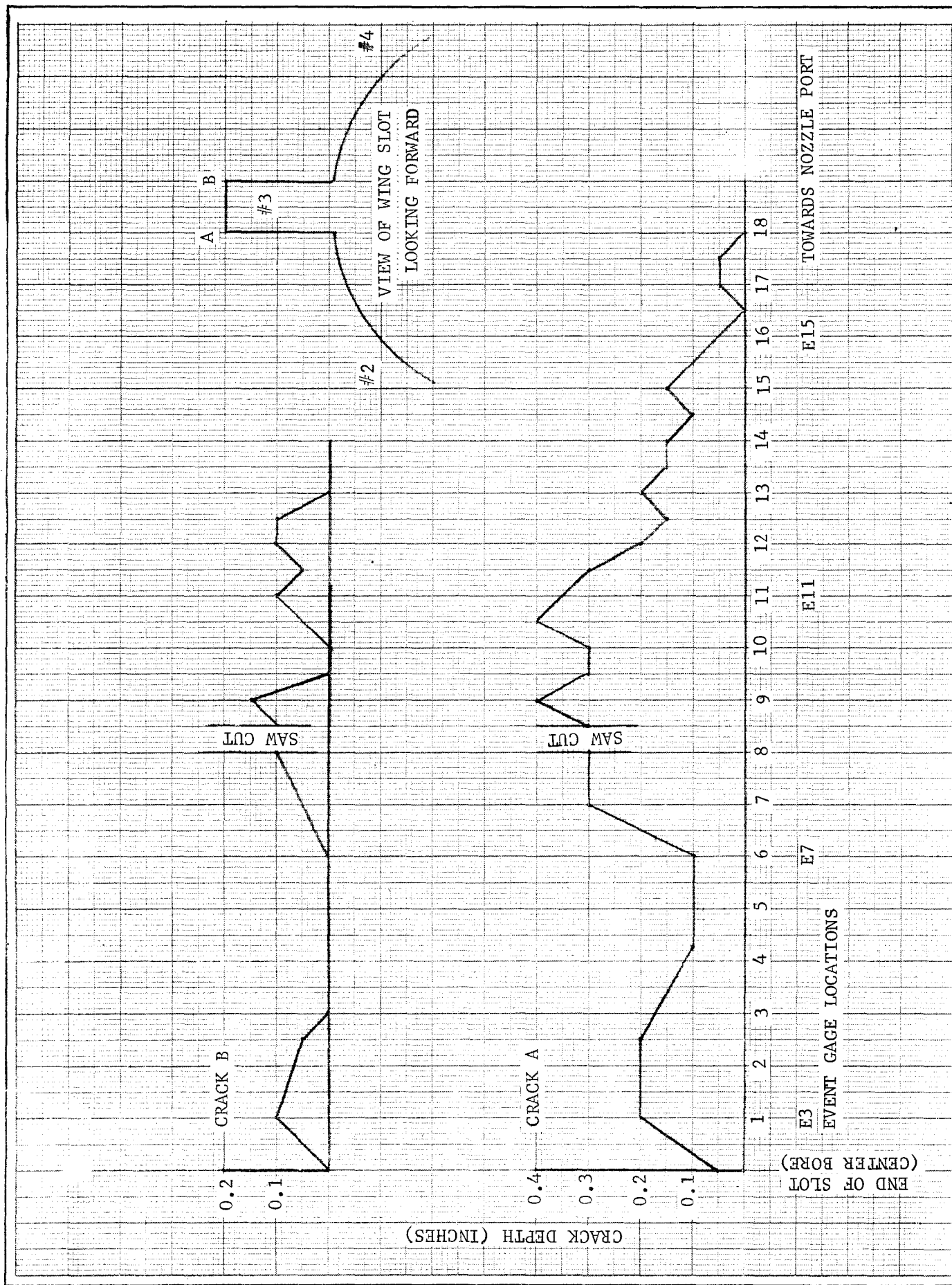


Figure 3-4. Wing Slot #3 Crack Profile (0032765)



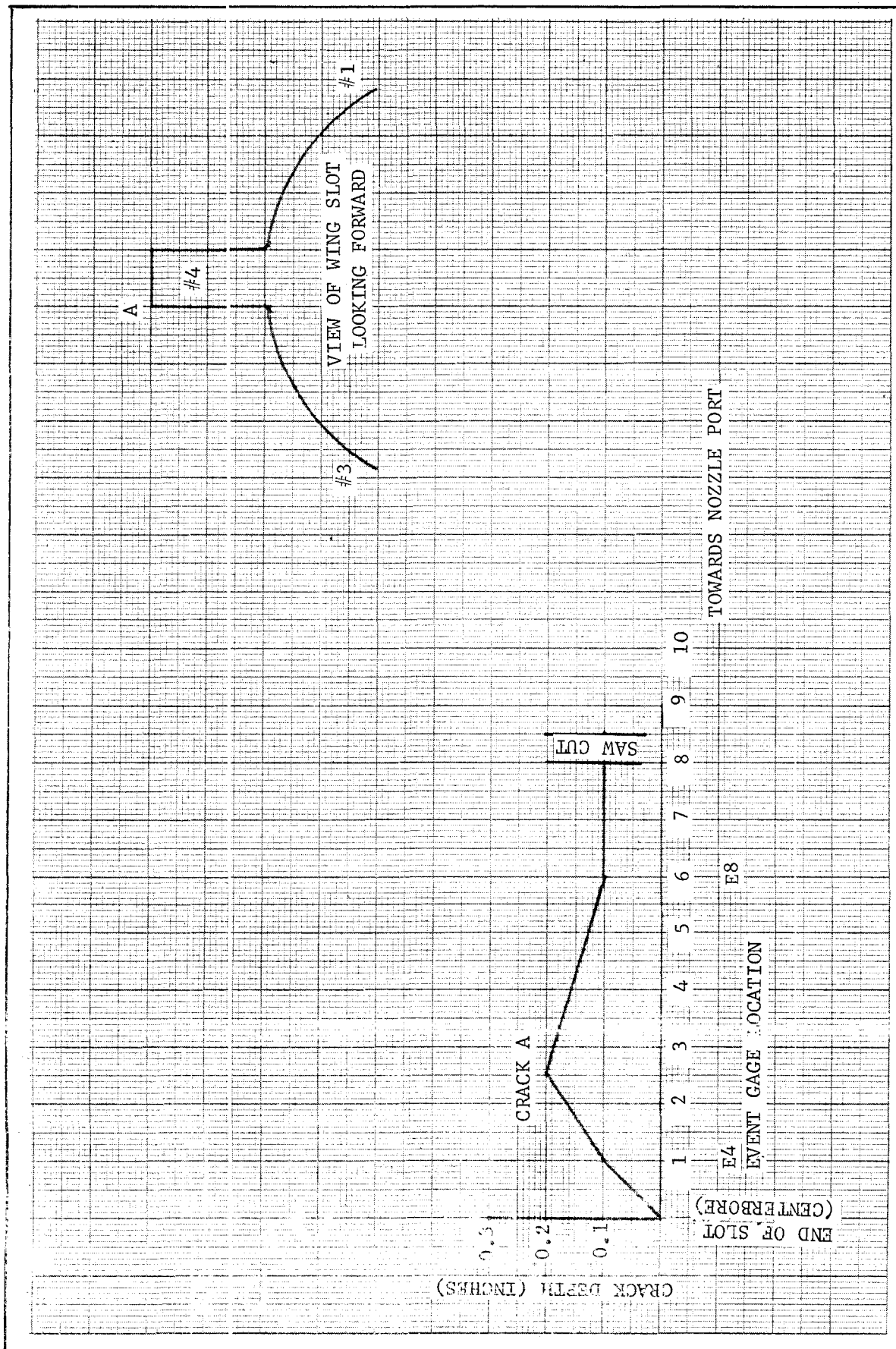


Figure 3-5. Wing Slot #4 Crack Profile (0032765)

Observation of the hardware and equipment immediately after test showed that everything worked satisfactorily except for the accumulator tank vent rupture disc. The blasting cap initiated but did not initiate the linear shaped charge to rupture the disc. The pressure blowdown was accomplished using the two motor vent rupture discs at only a slightly slower rate than would be expected using all three discs.

The problem of the center of the fill rupture disc coming down slot 3 and destroying the event gage lead wires which occurred in Test 1 was solved for the second test by placing the linear shaped charge in a U-shaped pattern instead of a circle. This allowed the center to hinge and thus be retained. Post test visual and dimensional inspection results of the motor cavity were lost and are not available. Figure 3-6 shows a section of the motor with a massive wing slot cracking. The aft center port and nozzle port bonds were found to be undamaged.

#### 4. LRSLA Overtest Summary

The motors were satisfactorily tested to the requirements of the LRSLA Program. Although the instrumentation in the first test (motor 32765) failed to define the precise pressure level at which wing slot cracking occurred, the instrumentation in the second test (motor 32743) showed the first indication of wing slot cracking was between 492-525 psig. This matches well with the physical evidence noted upon dissection of motor 32765. There was only minor cracking in two wing slots which tends to support the hypothesis that cracking had just started at the time of  $P_{max}$  and depressurization of motor 32765.

Deflectometers and event gages were located in wing slots 1 ( $0^\circ$ ) and 2 ( $90^\circ$ ), and event gages were located in the remaining two slots. Thermocouples were located in wing slots 2 and 4. The thermocouples in the wing slots indicate that the change in propellant temperature was negligible during the period of pressurization. The three deflectometers in wing slot 1 all measured wing slot growth of approximately 1/2 inch at the time of maximum pressure. The deflectometer in wing slot 1 failed to produce reliable data.

Cracks were induced in all four wing slots. Nine event gages and one deflectometer all responded to wing slot cracking. The general pattern of gage response was similar in all four slots, as the wing slots cracked at a motor pressure of approximately 520 psi (the range was 492 to 550 psi), and that cracking originated in the forward trim area or between the critical cross-section and the forward trim area. Of particular interest is the sequence of events recorded in wing slot 1: (1) The event gage in the forward trim area began to respond to propellant cracking at a pressure of 522 psi; (2) the plot of deflectometer D1 versus pressure showed an abrupt jump in deflection at 540 psi; and (3) event gage E5 at the critical cross-section responded to propellant cracking at 558 psi. This was also the first test in the LRSLA Program in which the cracking event detected by an event gage was confirmed by response of more conventional instrumentation.

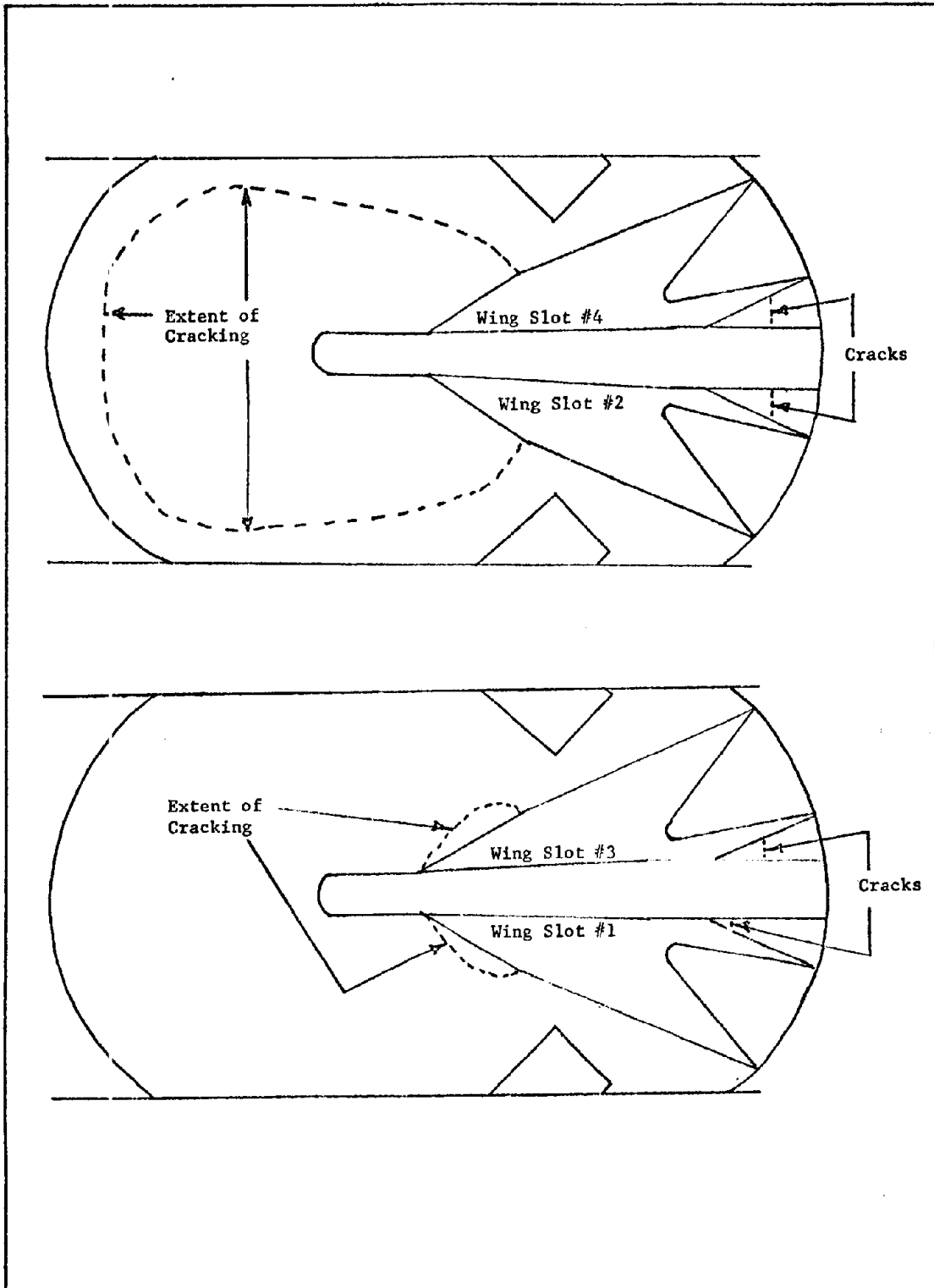


Figure 3-6. Wing Slot Cracking (Motor 0032743)

The Minuteman Stage III rocket motor has a structural capability well above its operating requirements. The failure pressures demonstrated in the high rate tests were 500 and 492 psi (minimum). The critical structural load for motor operation is the average motor ignition pressure, which is approximately 275 psi, at 70° F.

Structural failure initiates in the forward trim area of the wing slots. However, since the actual failure pressures of both motors were close to the predicted value of 500 psi, it is concluded that the forward trim area constitutes only a slight perturbation of the motor structural geometry. This failure mode has been adequately defined.

In neither test was any debonding noted in the aft center or nozzle ports. The aft centerport boot-to-flap bond has a higher structural capability than does the wing slot tips. No boot-flap bond failures were induced in either motor by test pressures that were sufficient to fail the slot tips. The TT port area also has a higher structural capability than does the wing slot tip. Wing slot cracks did not propagate out to the TT ports, and there is no evidence of other structural failure present in the TT ports.

#### D. OVERTEST PROGRAM

##### 1. Introduction

The concept of motor overtest requires application of the load associated with the critical failure mode, to a level sufficient to induce failure. Specifically, for the M57A1 motor (LGM30 B&F common), motor overtest consists of pressurization at a rate in excess of 10,000 psi/second to a maximum of 540 psi. This overtest approximates or exceeds the ignition transient and exceeds the expected ignition pressure maximum of 275 psi. The motor overtest temperature is the same as the missile silo environment (70° F). The critical failure mode is that of wing slot cracking; the initial failure location was predicted to be in the radius of the wing slot tip, located about 4-1/2 inches aft of the intersection of the wing slot and the centerport (3.7 inch radius). The second most critical mode for the M57A1 motor is the debonding of the boot-to-flap bond in the aft centerport; however, this failure was not expected to occur during motor overtesting because of the high margin of safety calculated at the bond.

The overtest procedure to induce the critical failure mode was identified in Task II using analytical methods (Reference 2).

The most important measurement to be obtained from the overtest of the M57A1 motor was the test pressure at which grain failure initiates. In simple terms, the ratio of the measured failure pressure to the expected maximum value of the motor ignition transient may be viewed as the structural safety factor. By overtesting motors of various ages, it should be possible to extrapolate the motor capability (safety factor) versus age data to a time when the motor no longer has sufficient capability to withstand the

expected service loads. In practice, the prediction of the service life of the entire motor population is not as straightforward as the above outline implies. The use of overtest results to predict motor service life is covered in Section VI.

This subsection reviews the overtest program involving 6 and 9 year motors. The test data are discussed and the data applicable to the determination of motor failure pressure are presented. The initial failure sites are identified and the extent of cracking, determined by inspection and motor dissection, is described. The results of the pretest and post-test motor inspections are presented. The equipment, instrumentation, and other details are presented in Reference 3.

## 2. Overtest of Six-Year Motor

The overtesting of the 6 year motor was generally the same as the overtesting of the 9 year motor described in Reference 3. However, the M57A1 motor selected for this second overtest differed from the 9 year motor in more ways than simply being 3 years younger. The 6 year motor was of the configuration designated as LGM-30F\*, while the 9 year motor was an LGM-30B. Seventeen changes in configuration, materials, or processing requirements were made between the B and F versions of the M57A1 (Reference 9). With regards to the performance of the 6 year motor overtest, the important changes were: (1) The slot tip geometry was changed to an elliptical form, which reduced the strain concentration factor to the minimum value possible, and (2) the connection between the aft dome boot and flap (at the centerport and at all four nozzle ports) was changed to a vulcanized joint, which was stronger than the former adhesive bond.

The implications for the overtest of the 6 year motor followed directly from the important OPRI changes. First, a higher test pressure is required to crack the wing slot tips. The deflections in the grain cavity are therefore higher, and the special potentiometers used in the wing slots do not have sufficient stroke capability. Second, aft centerport debonding is not a critical failure mode. Less instrumentation was required in the aft port region, but some instrumentation was necessary to verify that neither boot-flap bond, propellant, or case bond failures occurred during test.

The overtest of the 6 year M57A1 motor (LGM-30F) was a high rate hydrotest at a rate of 10,000 psi/second to a maximum pressure of 640 psi. The motor temperature for the overtest was the same as the missile silo environment, which is 70° F. Wing slot cracking was to be induced by the overtest, other failure modes are of much lower criticality. The overtest

---

\*LGM-30F is also referred to as an OPRI. The first OPRI motor manufactured was designated S/N 32933.

procedure to induce the critical mode was identified in Task II (See Reference 2).

The most important data to be obtained in the overtest of the 6 year motor was the test pressure at which grain failure initiates. However, the use of motors of two configurations, LGM-30B and LGM-30F, introduces an additional complication into the prediction of motor service by the extrapolation of motor failure pressures. The propellant failure pressures must be normalized to a common configuration, using a factor related to the slot tip concentration factors which differed for the two motor designs. The normalized failure pressures of the motors may then be extrapolated versus age to a time when the motor no longer has sufficient capability to withstand the expected loads.

The 6 year M57A1 motor selected for the overtesting was an LGM-30F, S/N 33348, which included the OPRI changes. The motor had been changed to Modified Operational Motor configuration subsequent to Government acceptance.

The motor case was from production lot 44B, which had demonstrated a case hydroburst pressure of 724 psi. The forward skirt had been damaged as the result of a transporter accident.

The motor was cast in April 1968, and was 69 months old when the overtest was performed. The CYH propellant was cast from powder lot RAD-1-16-67, which had the following physical properties at 77° F and a test rate of 2 inches per minute using a JANNAF test specimen:

Tensile strength (psi)	295
Elongation (%)	59
Tangent modulus (psi)	802

The DDP propellant was cast from powder lot RAD-1-5-66.

Instrumentation types and locations were selected with the main objective of detecting either of the two principal failure modes. Instrumentation was therefore concentrated around the critical wing slot section and in the region of the centerport boot-to-flap bond. Instrumentation was provided to measure grain deflection, case and dome strain, and pressure. Event gages were installed to monitor grain cracking. The various installations are shown in Figures 3-7 and 3-8. For details on instrumentation mounted externally on both motors see Reference 3. The event gages installed in the wing slots were of the configuration shown in Figure 3-9. Some of the various instrumentation devices used inside the motor cavity are shown in Figures 3-10 through 3-15.

The high-rate pressure-time curve obtained during the test of the 6 year motor (33348), as indicated by the pressure transducer in the

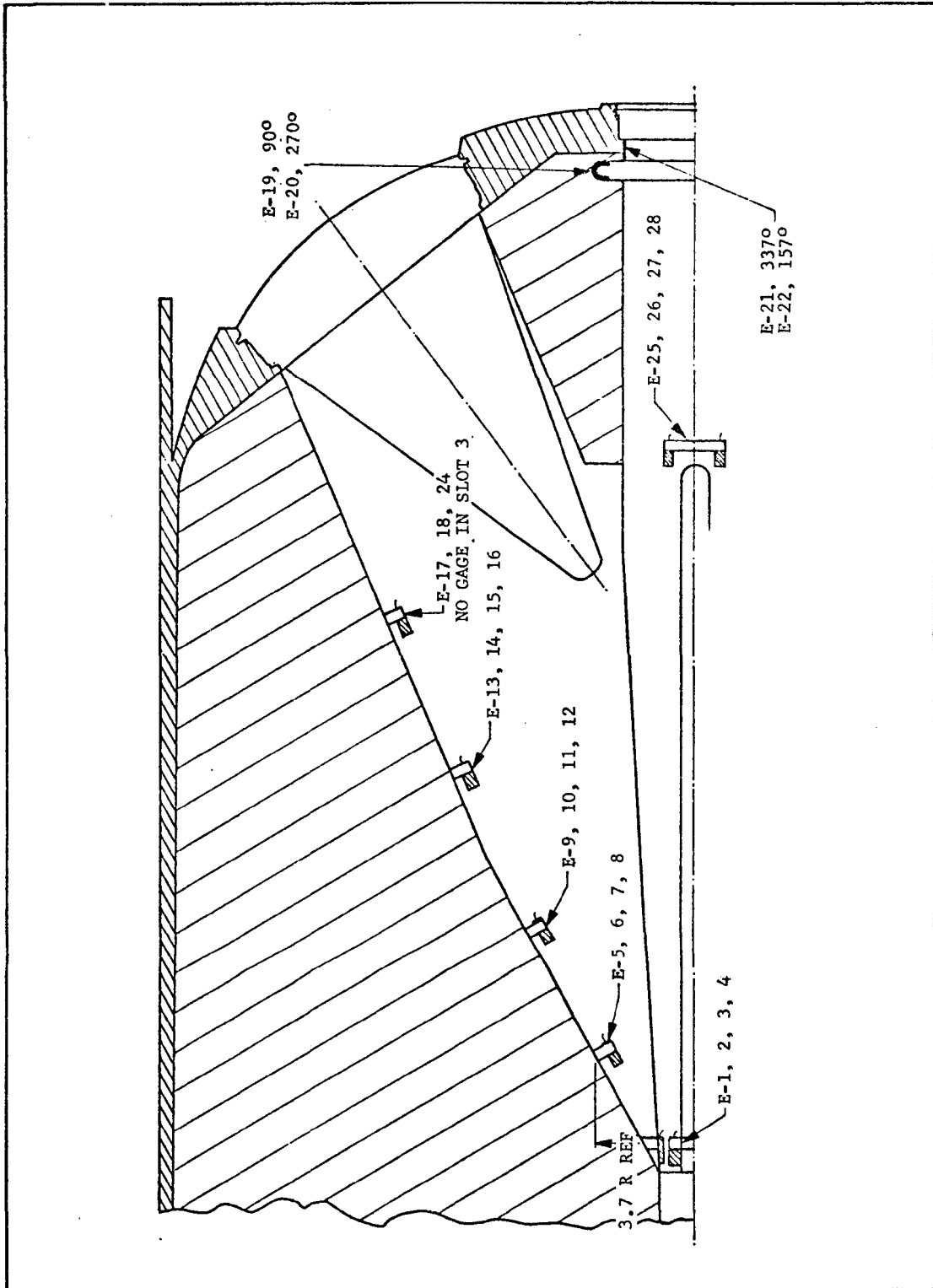


Figure 3-7. Event Gage Locations, 6-Year Motor

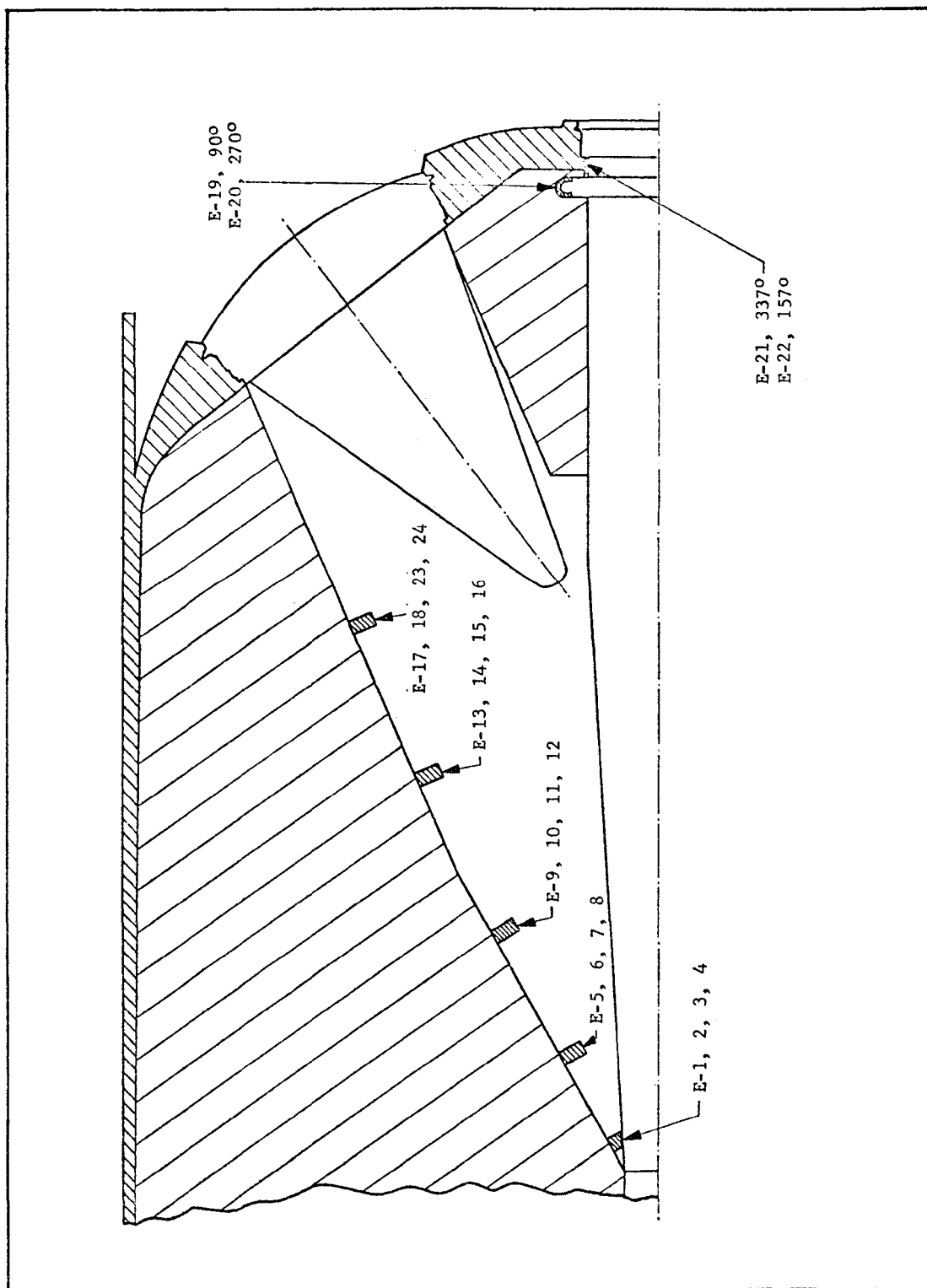


Figure 3-8. Event Gage Locations, 9-Year Motor



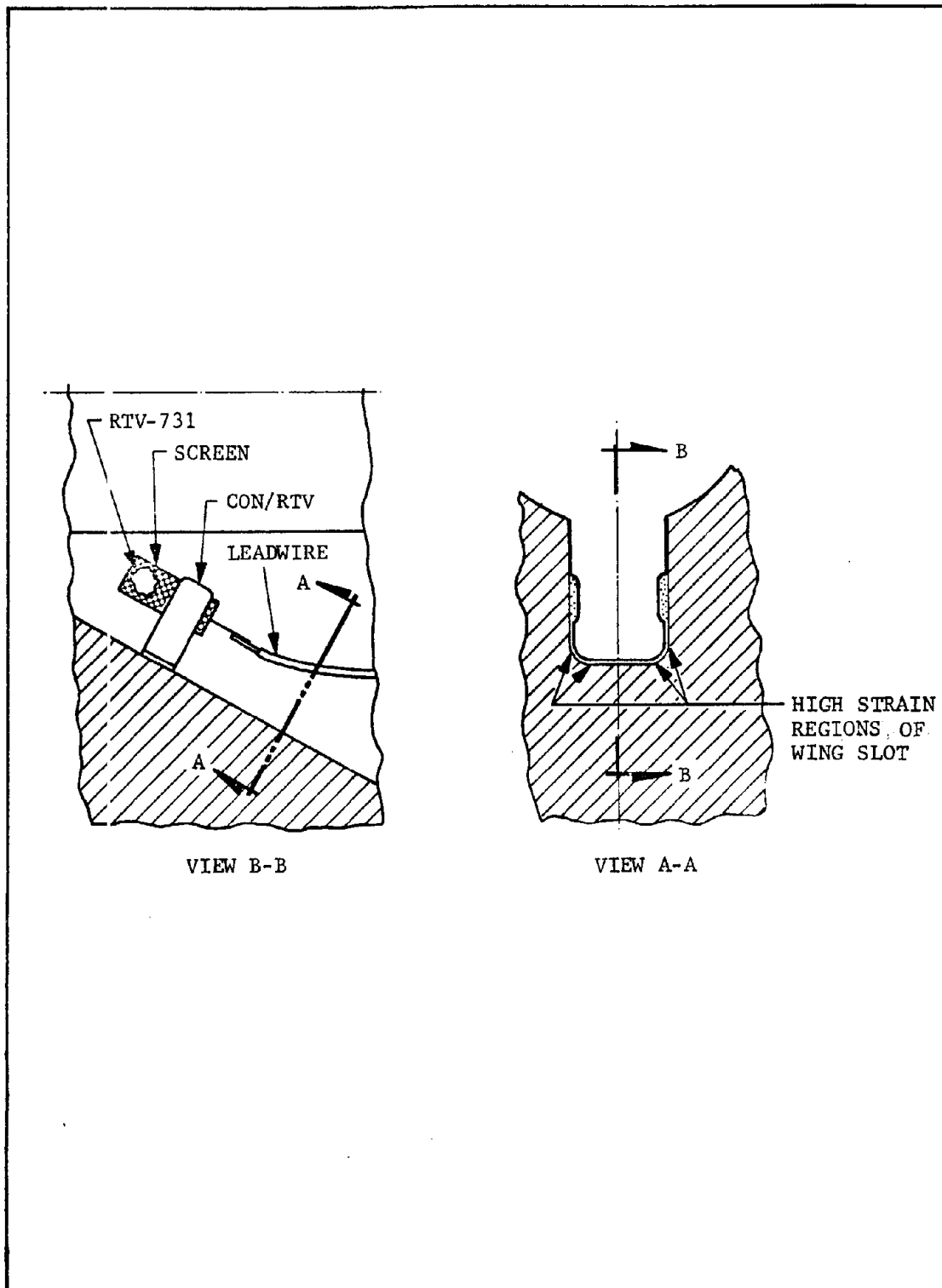


Figure 3-9. Event Gage Installed in Wing Slot

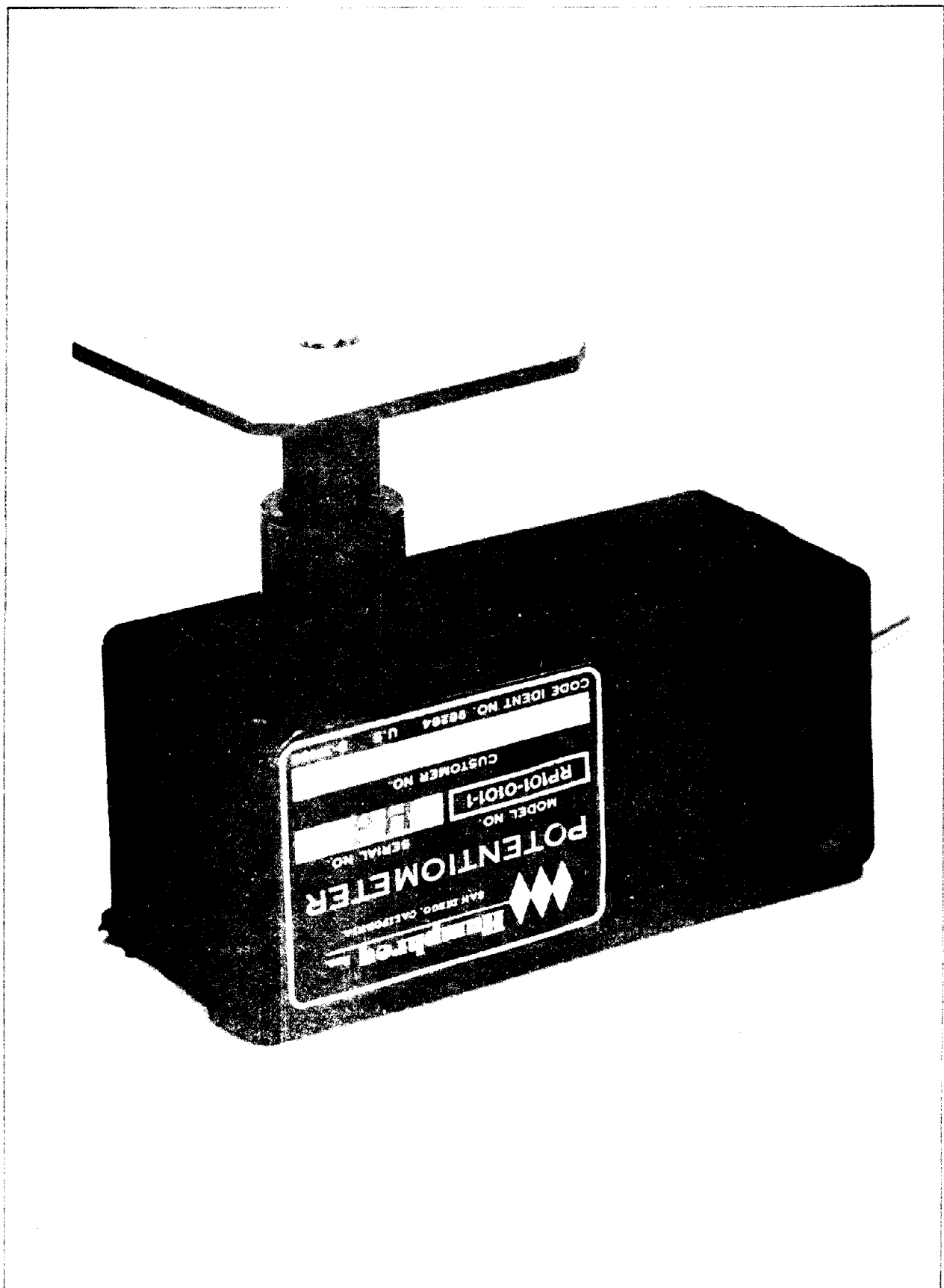


Figure 3-10. Potentiometer Used in Wing Slots

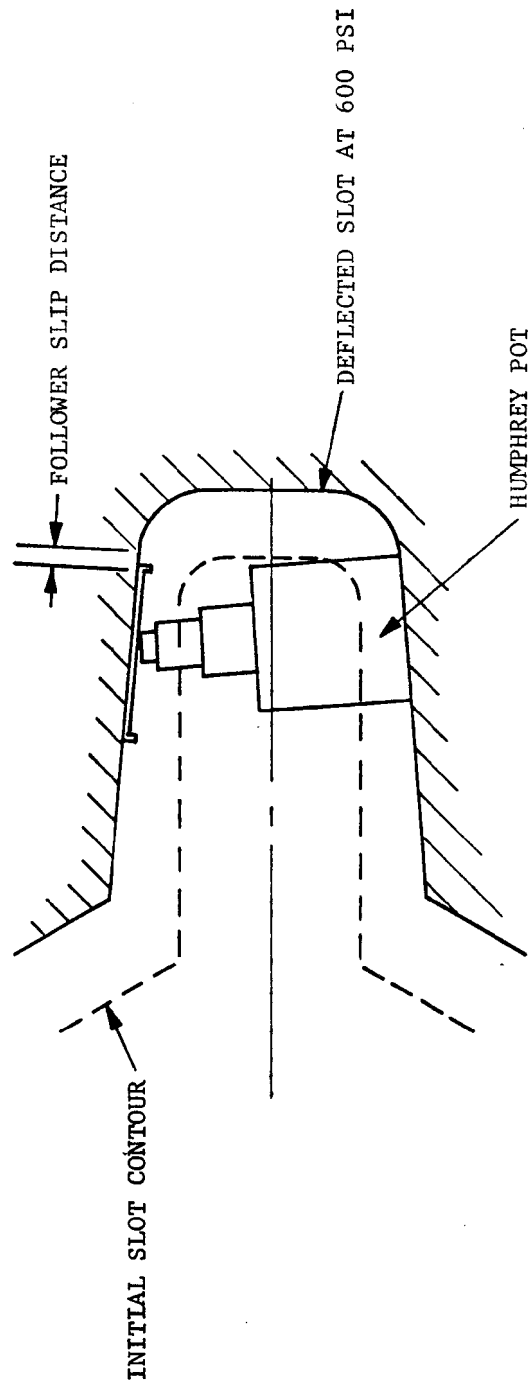


Figure 3-11. Humphrey Rectilinear Potentiometer in Critical Wing Slot

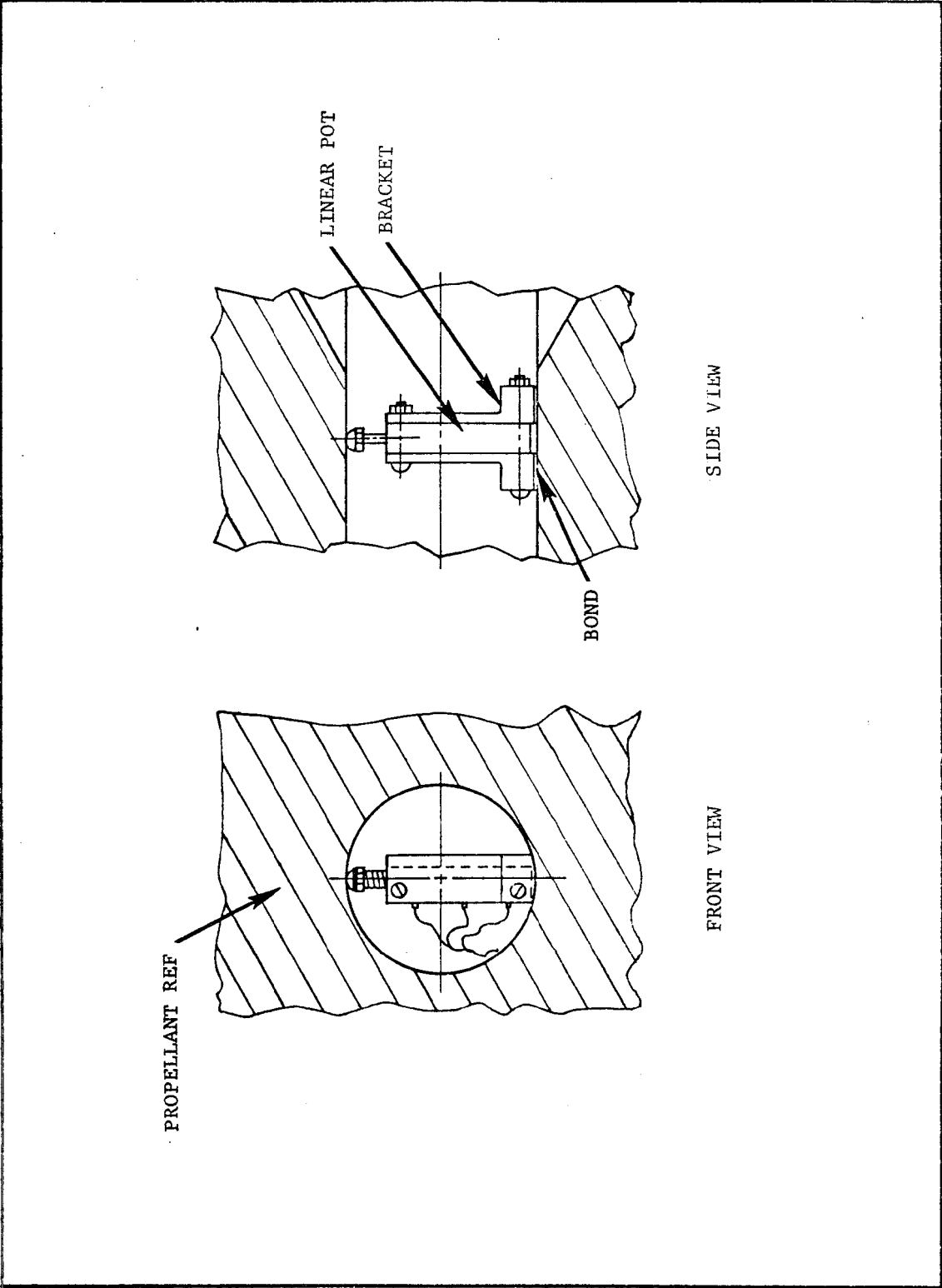


Figure 3-12. Linear Potentiometer in Forward End of Center Core

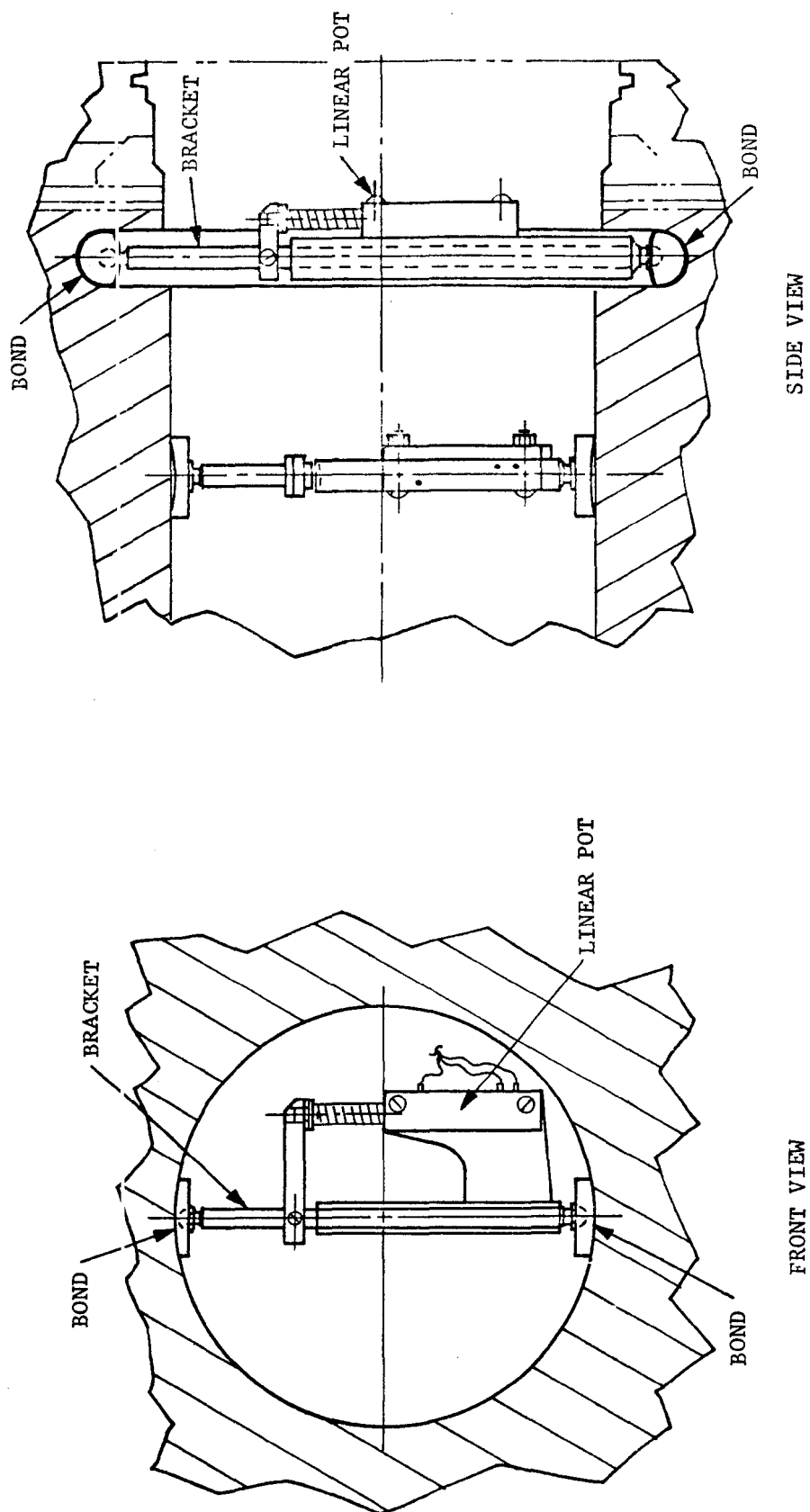


Figure 3-13. Linear Potentiometer in Aft Center Port and Stress Relief Groove

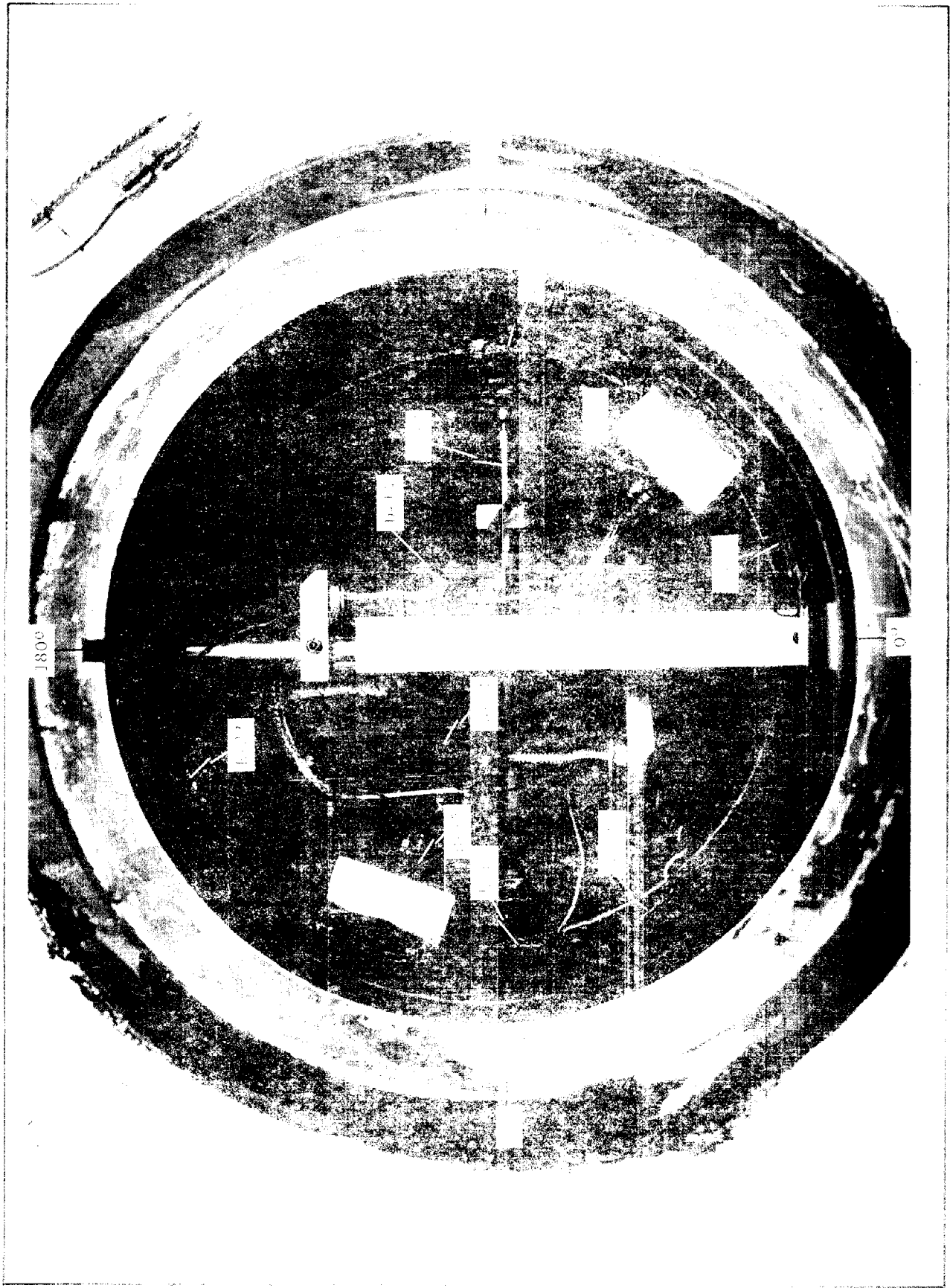


Figure 3-14. Instrumentation in Aft Center Port

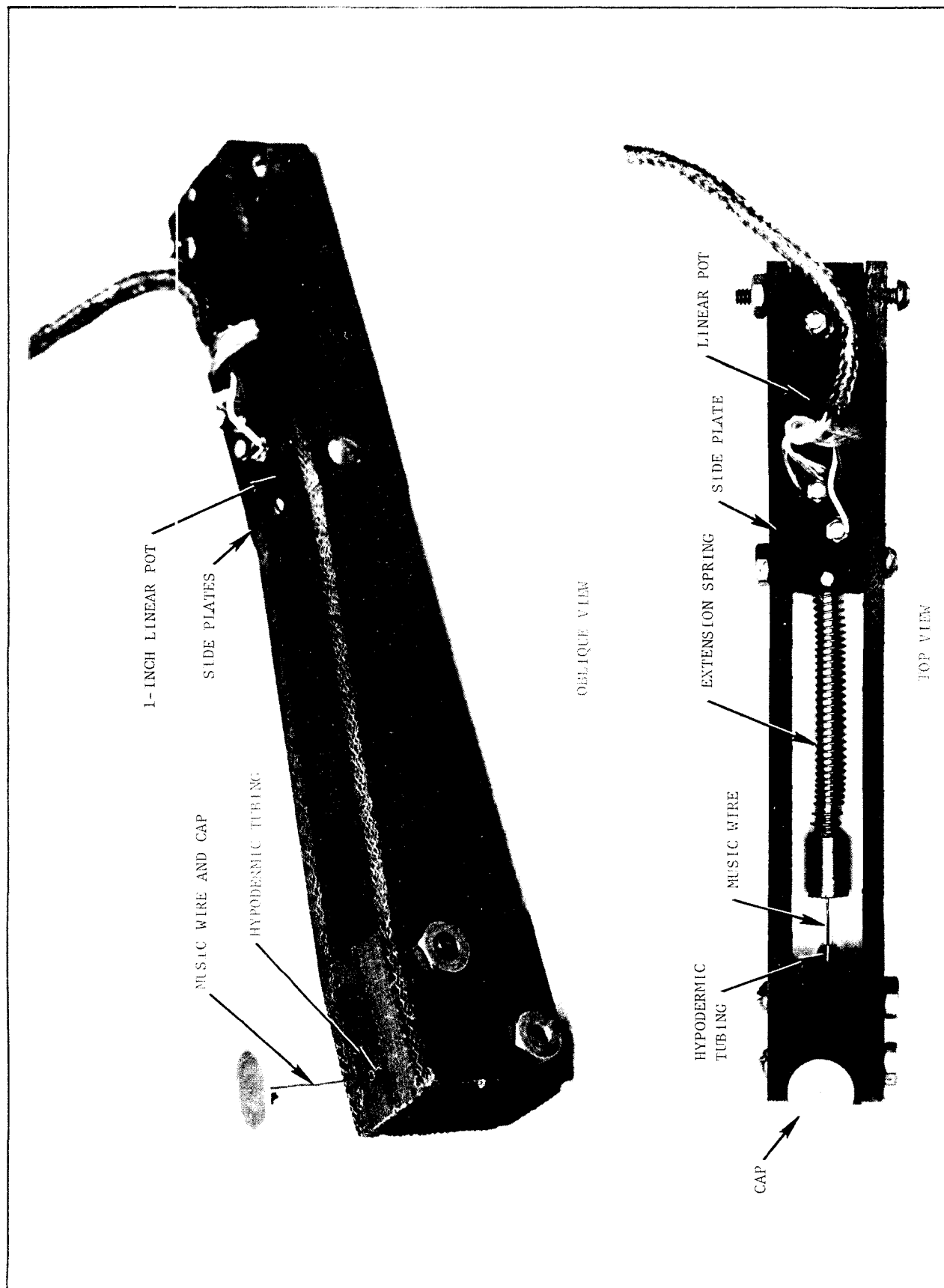


Figure 3-15. Special Wing Slot Potentiometer (Hummel Potentiometer)

aft centerport, is shown in Figure 3-16. The pressurization rate was 20,000 to 30,800 psi/sec (range of measurements at four ports) during the initial part of pressurization which lasted up to 0.03 second. The maximum pressure was 635 psi, at 0.195 second. The degree of overtesting can be judged from the plots of the average ignition transient which has been overlaid on Figure 3-16. The initial test pressure rate is higher than the average ignition rate, and the maximum pressure is greater than twice the maximum ignition pressure, as desired.

Three event gages in the forward trim area of the wing slots responded to cracking events. The pressures at the time of the cracking response were 575 psi, 595 psi, and 585 psi in wing slots 1, 2, and 3, respectively. One event gage in the critical slot tip section of wing slot 1 responded to cracking at a pressure of 585; one gage at the critical section of wing slot 4 may have responded at a pressure 625 psi, but this may be the response of the gage to breaking of leadwires. One event gage in the third row of wing slot 1 responded to cracking at a pressure 620 psi; one gage in the third row of wing slot 2 may have responded at a pressure of 600 psi, but this is more likely the response of the gage to a leadwire breaking. One event gage in the fourth row of wing slot 1 responded to cracking at a pressure of 635 psi.

Wing slot width measured by the Humphrey potentiometers, which were located farthest forward in the wing slots, increased smoothly and fairly linearly with pressure to a maximum value of 0.64 to 0.72 inch. Wing slot deflection measured by the potentiometers in the two rows farther aft in the wing slots (D4 and D9) increased smoothly with pressure to a value of approximately 0.72 inch. None of the potentiometers in the wing slots showed any abrupt changes that could be associated with wing slot cracking on time-history plots nor on crossplots of deflection versus pressure.

Because both potentiometers in the forward end of the centercore debonded from the propellant, no valid data were obtained. Diametrical deflections of approximately 0.5 inch were recorded at two locations in the aft end of the centercore.

Two of the event gages in the aft web responded to cracking events at 465 and 620 psi. Since aft web cracking occurred in a motor that was high-rate tested to 410 psi (Reference 10), the event gage responses were considered to be valid.

The diametrical deflection of the stress relief groove increased smoothly with pressure to about 0.36 inch, except for a hangup of the potentiometer assembly which occurred between 290 and 560 psi.

No debonding of the aft centerport or nozzle ports was recorded by either the axial potentiometer in the aft centerport or by the radially oriented potentiometers in the nozzle ports.



MM 0033348 HYDRO TEST 1-29-74

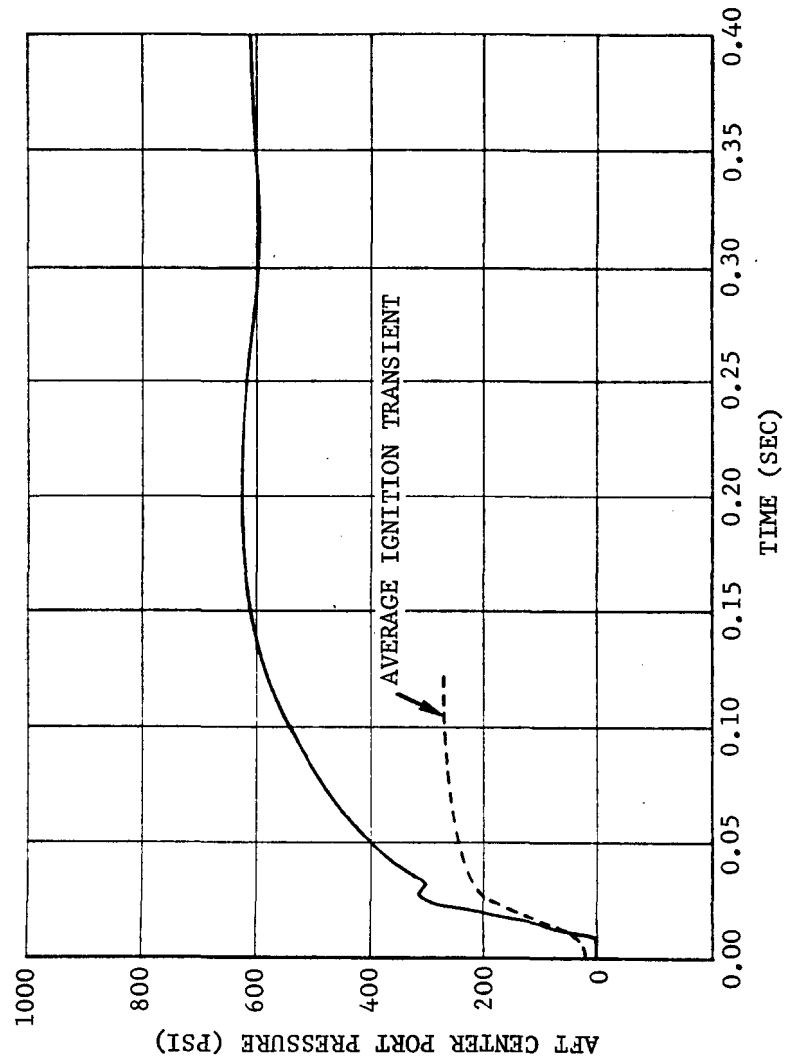


Figure 3-16. High Rate Pressurization Transient

Cracking was induced in all four wing slots. The extent of cracks in wing slots 1 and 3 was roughly equal. The cracks in wing slots 2 and 4 were also roughly equivalent to each other in extent. However, the extent of cracking in wing slots 1 and 3 was much greater than the extent of cracking in wing slots 2 and 4. Generally, there was only one crack in each wing slot, except in the forward trim area. The wing slot tip approximated an ellipse, but was actually formed of tangent circular arcs. The likely location for cracking at the slot tip appears to be the point of tangency between the small and large circular arcs. However, the tendency for cracks to begin at the point of tangency is very weak; in some instances the cracks cross the slot from side to side and at other locations the crack runs down the center of the wing slot. Two cracks are present for about 8 inches in wing slot 3, but they run together on the surface and branch out within the propellant.

The motor instrumentation did not give any information relative to the rate of crack propagation during the motor high rate test. Because of the uncertainties as to the speed of crack growth, the effect of grain cracking on motor performance is not clear. If cracking continued for a large part of the 16 seconds for which pressure was held at 610 psi, the extent of cracking would not be significant for estimates of motor performance because the burning surface could overtake the crack. However, if the crack propagated to its full extent very reapidly, the burning surface would be more than doubled and total motor failure would occur. The test results, therefore, do not give information that definitely defines the criticality of the failure mode of wing slot cracking. The problem of defining motor failure is certainly neither new nor is it confined to the service life analysis of the M57A1 motor (see Reference 10). Using the same rules for evaluation as used in the initial survey of M57A1 failure modes, the extent of cracking is not significant; i.e., a small crack is a failure and a large crack is a failure, so there is no difference between them in this program. To fully evaluate the importance of crack depth would require motor firings.

The extent of cracking was defined through motor dissection. The extent of cracking is illustrated in Figures 3-17 through 3-20, which are photographs of the motor surfaces exposed by the cutting. Each wing slot is identified by its nozzle port number written nearby on the propellant.

The aft face of Section II is shown in Figure 3-17. This section had been marked for further dissection. The first cut had been made before the photograph was made. The double crack at the tip of wing slot 3 extends about 4 inches forward and stops. A third crack starts at the opposite side of the slot and continues forward and outward. The cracks in wing slots 2 and 4 both extend forward from the surface shown, turn to one side of the slot, pass through the sharp cornered section of the forward trim, and stop at the forward end of the wing slots. In both wing slots 2 and 4, the remaining corner of the forward trim area is cracked, but the crack does not extend aft of the trim.

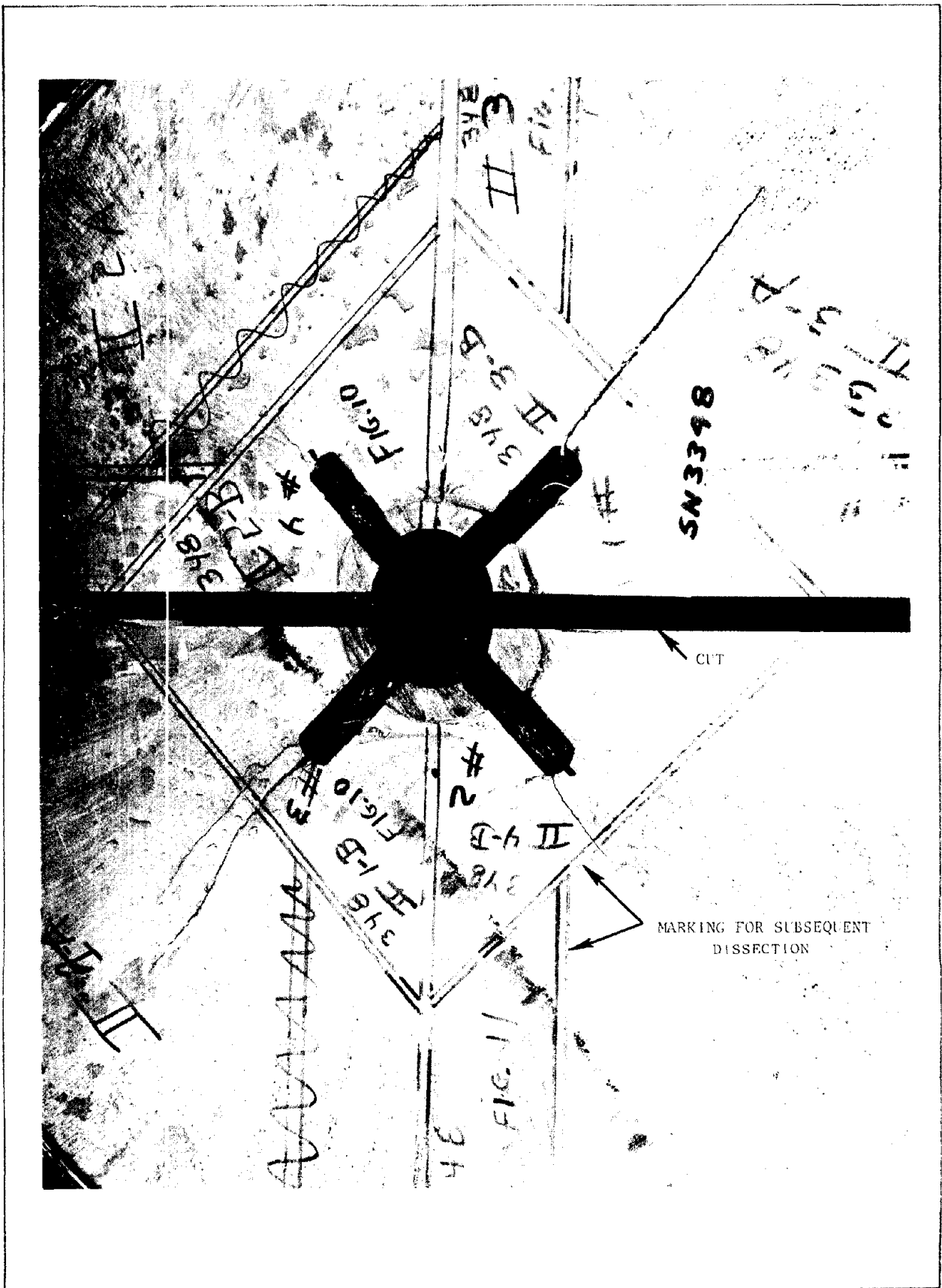


Figure 3-17. Aft Face of Section II

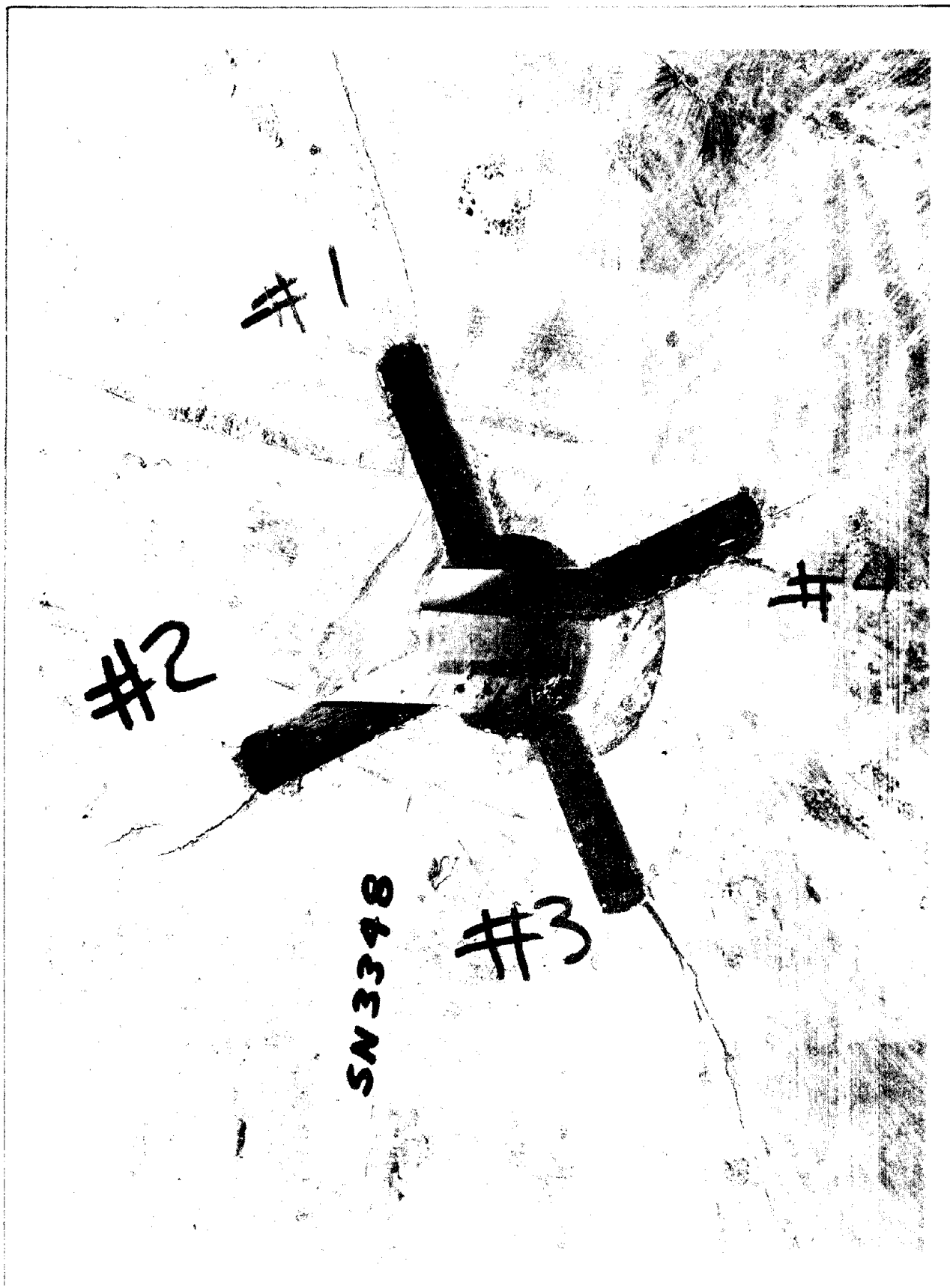


Figure 3-18. Forward Face of Section III

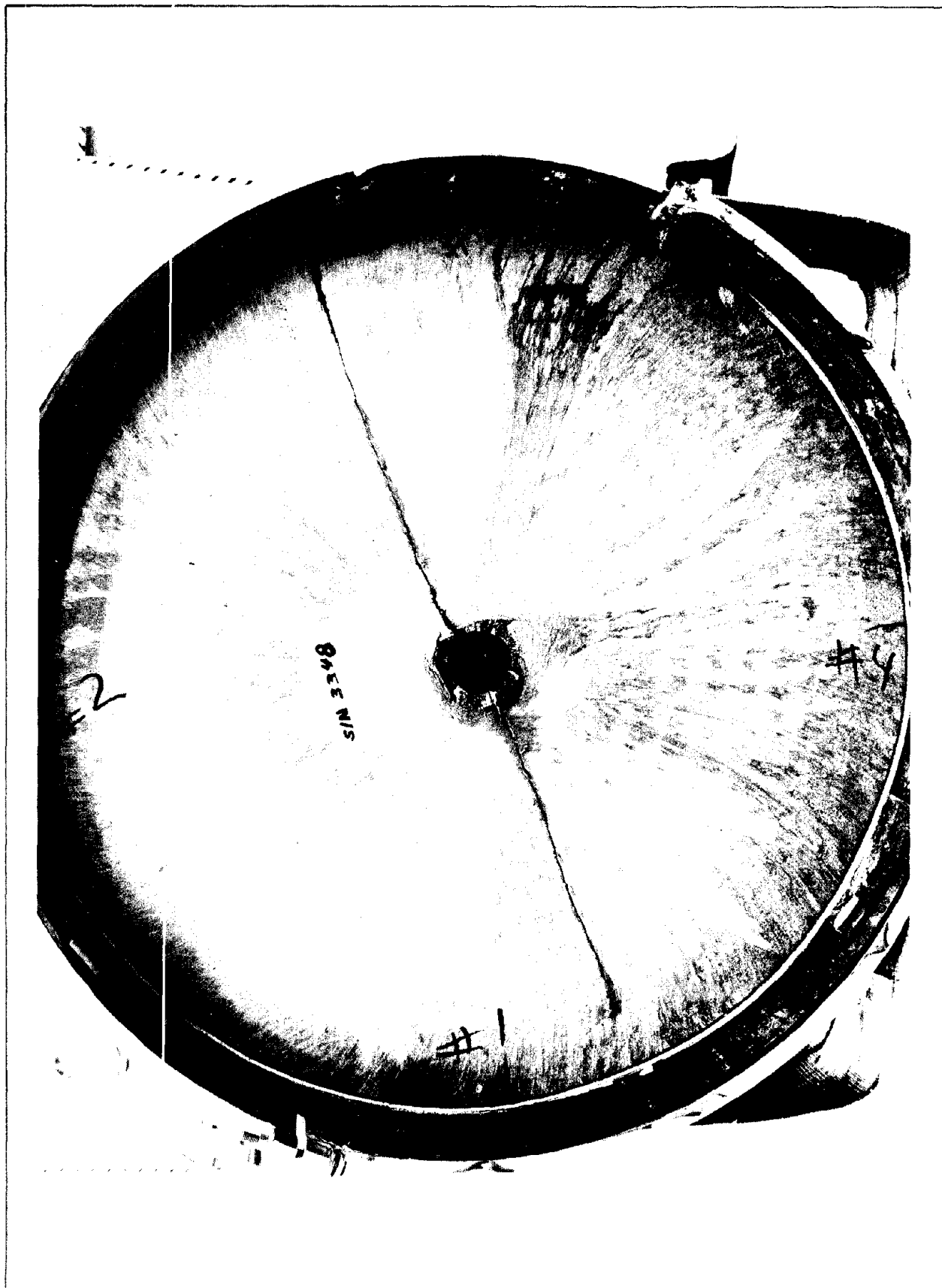


Figure 3-19. Forward Face of Section I

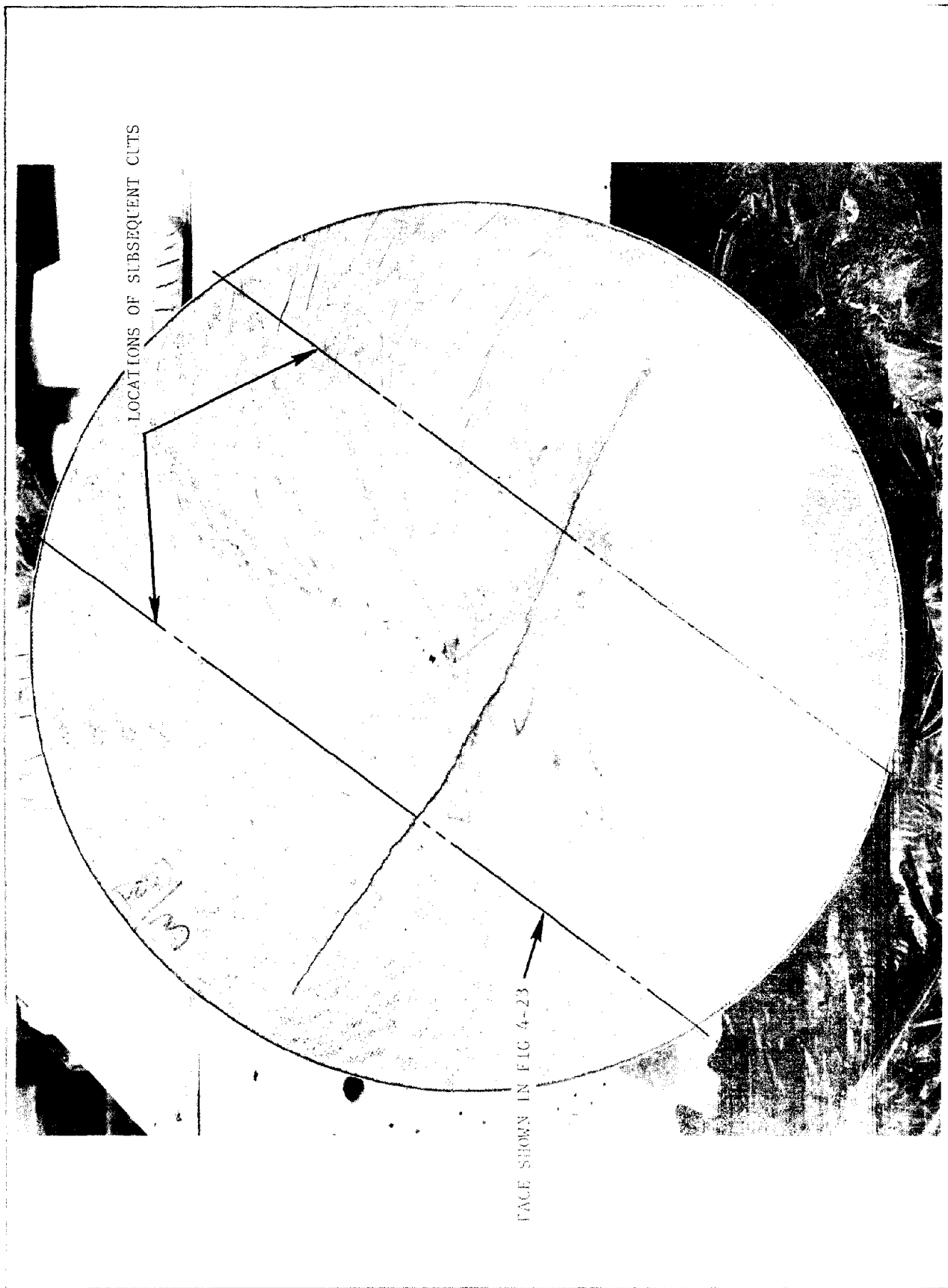


Figure 3-20. Aft Face of Section VI

The forward face of Section III is shown in Figure 3-18. This surface is located, in the uncut motor, 1.2 inches aft of the surface shown in Figure 3-17. The double crack in wing slot 3 (Figure 3-17) has joined and formed one crack at the slot tip surface which branches at about 1.5 inches into the propellant.

The forward face of Section I is shown in Figure 3-19. The forward face of Section II appeared identical to this. The cracks that began in slots 1 and 3 ( $0^{\circ}$  to  $180^{\circ}$ ) have made a slight twist and now lie approximately along the  $160^{\circ}$  to  $340^{\circ}$  diameter. This same crack, still parallel to the  $160^{\circ}$  to  $340^{\circ}$  diameter but shifted 2-1/2 inches from center towards port 4, is shown in Figure 3-20 at the aft face of Section VI, the forward dome. Two more cuts were made on the forward dome piece, revealing the crack in profile as shown in Figure 3-21. The crack extends across this section without entering the region of the forward centerport opening.

The overall extent of wing slot cracking is summarized in Figures 3-22 and 3-23. Although the cracks are in general inclined to the projection planes of the drawings, the cracks are shown at full depth as if rotated into the drawing planes.

The failure of cracks to propagate out to the TT ports is perhaps surprising. One study (Reference 11) included the TT area flap-to-insulation bond as a critical failure mode because of the high stresses predicted for this area. The general appearance of the crack profiles shown in Figure 3-21 leads to the conclusion that the TT ports act as stress relieving features for cracks originating in the wing slots.

### 3. Overtest of the Nine-Year Motor

The 9 year M57A1 motor selected for the overtesting was an LGM-30B S/N 32570 (Hercules Incorporated production number 5H3). The motor configuration has been reworked to incorporate the B-1 fix. The C7/W adhesive weight in the boot-flap bond was 8 gm, which is characteristic of controlled bond processing.

The motor case was from production sublot 3B, which had demonstrated a case hydroburst pressure of 559 psi.

The motor was cast in July 1964 and was 111 months old when the overtest was performed. The CYH propellant was cast from powder lot RAD 1-3-64, which had the following physical properties obtained from a standard JANNAF test sample at  $77^{\circ}$  F and a crosshead speed of 2 inches per minute:

Tensile strength (psi)	299
Elongation (%)	59.2
Tangent modulus (psi)	823

The DDP propellant was cast from powder lot SR 69A-63.

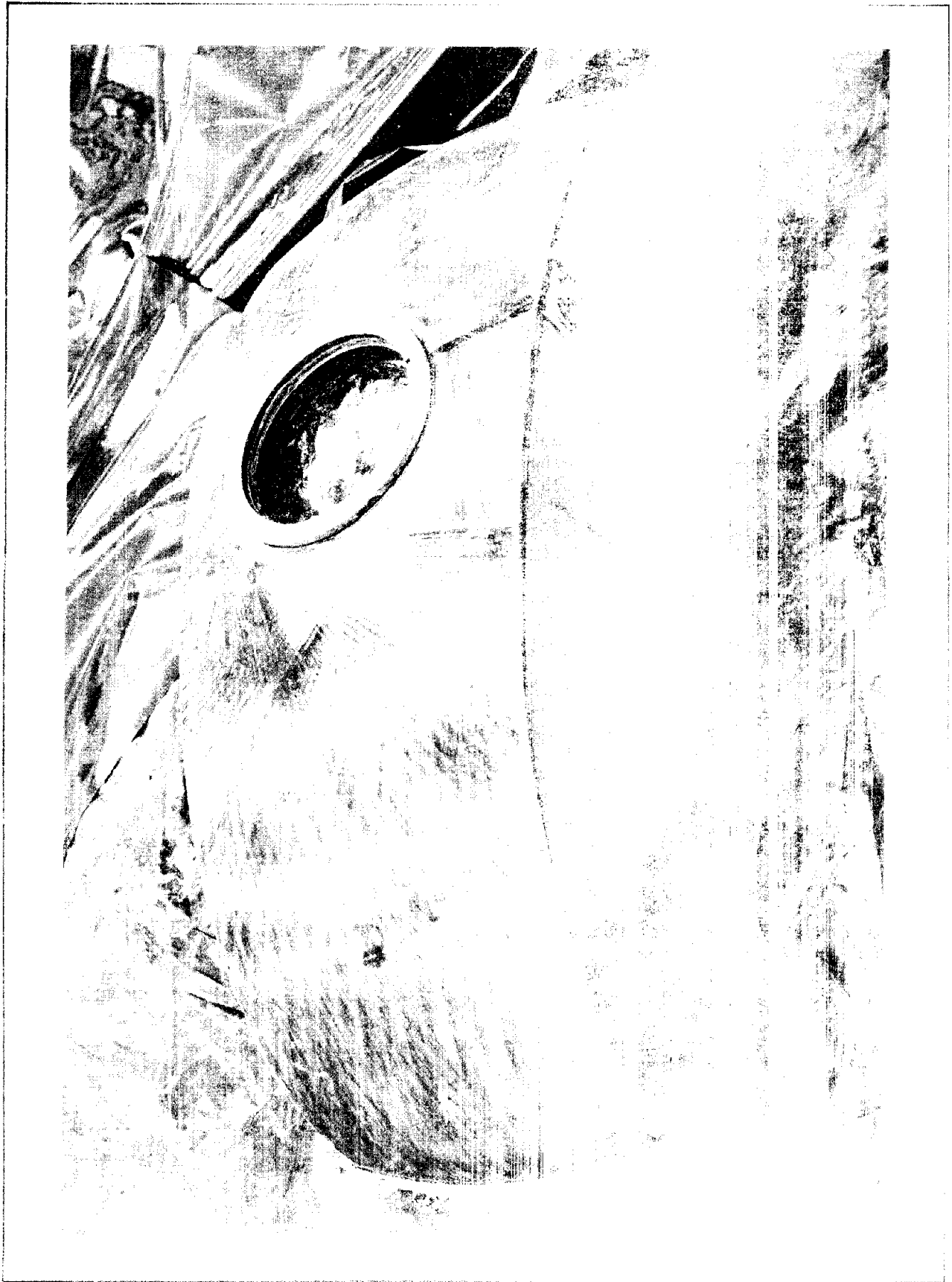


Figure 3-21. Extent of Cracking in Forward Dome



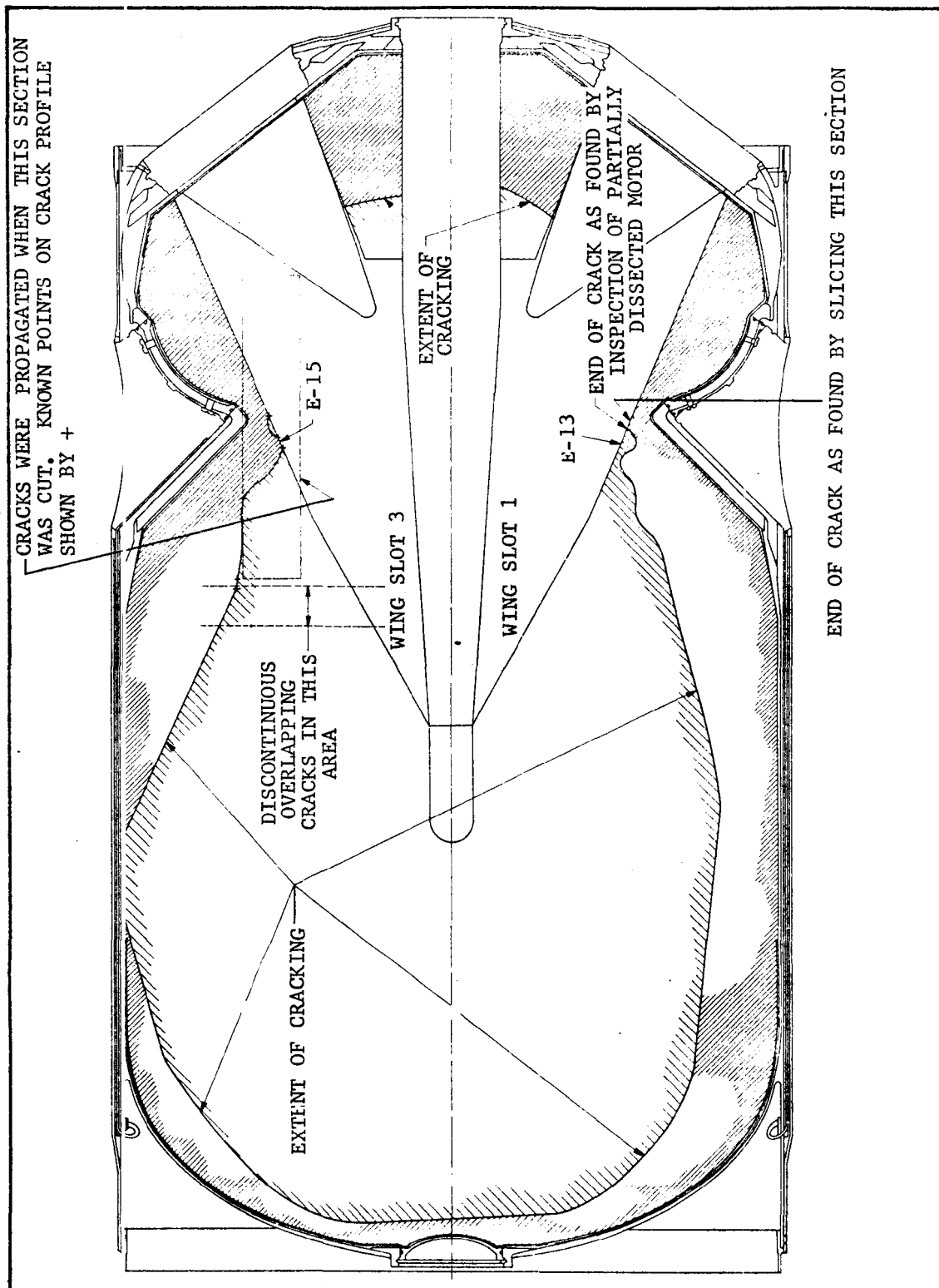


Figure 3-22. Extent of Cracking Extending from Wing Slots 1 and 3

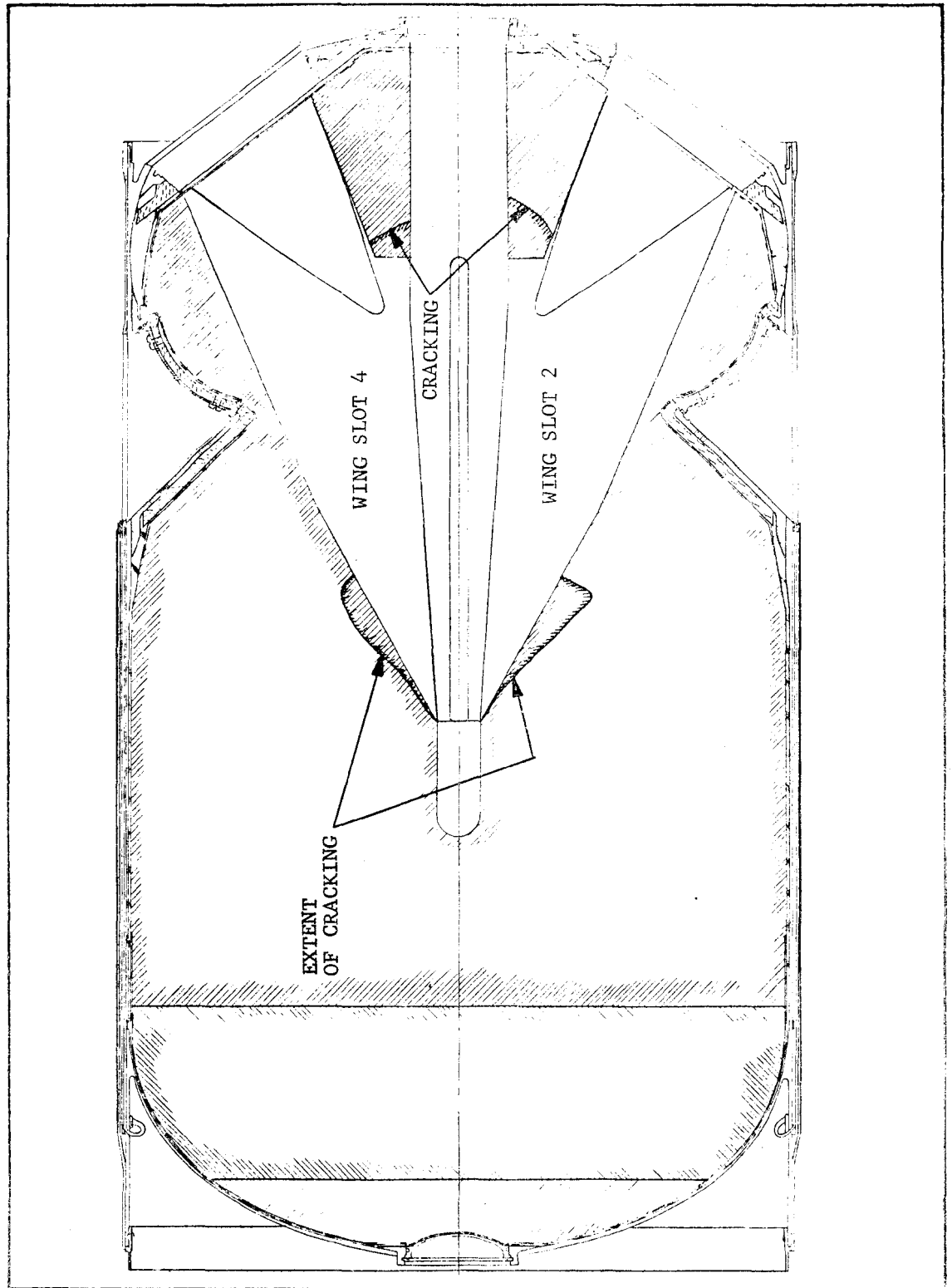


Figure 3-23. Extent of Cracking in Wing Slots 2 and 4

The internal instrumentation for the 9-year motor is given in Figure 3-3. Types of instrumentation are the same as shown for the 6-year motor.

The high-rate pressure-time curve attained during the test of the 9 year motor (motor 32570) is shown in Figure 3-24. The pressurization rate was 17,600 to 28,500 psi/sec (range of measurements at four ports) during the initial part of pressurization, which lasted up to 0.02 second. The maximum pressure was 548 psi at 0.128 second. The degree of overtesting can be judged from the plot of the average ignition transient which has overlaid on Figure 3-24. The initial test pressure rate is higher than the average ignition rate, and the maximum pressure is greater than twice the maximum ignition pressure, as desired.

Three event gages in the forward trim area of the wing slots responded to cracking events. The pressures at the time of the cracking response was 475, 530, and 507 psi in wing slots 1, 2, and 3, respectively. None of the event gages in the critical slot tip section responded to cracking. One event gage (E9) in the third row of gages responded to cracking at 512 psi.\* No other valid event gage responses were obtained.

With slot width increased smoothly and fairly linearly with test pressure to a maximum value of 0.55 inch. The slot width growth was uniform with respect to axial location of the measurement. It was anticipated that cracking in the wing slots would produce an abrupt change in slot width. However, no such indication can be found in the data from any of the potentiometers in the wing slots. Therefore, the attempt made in this test to validate the event gage responses by conventional instrumentation was a failure.

Centerport diameter increased smoothly with pressure. In the aft centerport, the maximum deflection was approximately 0.4 inch. In the forward centerbore, the port growth was larger immediately forward of the slot-centerbore intersection than it was farther forward, as expected. The largest deflection was greater than 0.48 inch, which amounts to only 16 percent strain, which is well within the capability of the propellant. The potentiometer at this location ran out of stroke at 545 psi, but apparently recovered when the grain relaxed during the pressure decay. The diametral growth of the stress relief groove was somewhat smaller, 0.28 inch. No debonding of the aft center port or nozzle ports was recorded by either the axial potentiometers in the aft center centerport or the radially oriented potentiometers in the nozzle ports.

Cracking was induced in all four wing slots. All of the cracks were in the wing slot corners (1/4 inch radius or the sharp edge of the forward trim area), as expected. Cracks were induced in both corners of

---

\*Event gage E10, also in the third row of gages, responded to cracking during the pressure decay period while the motor was at a pressure of 525 psi.

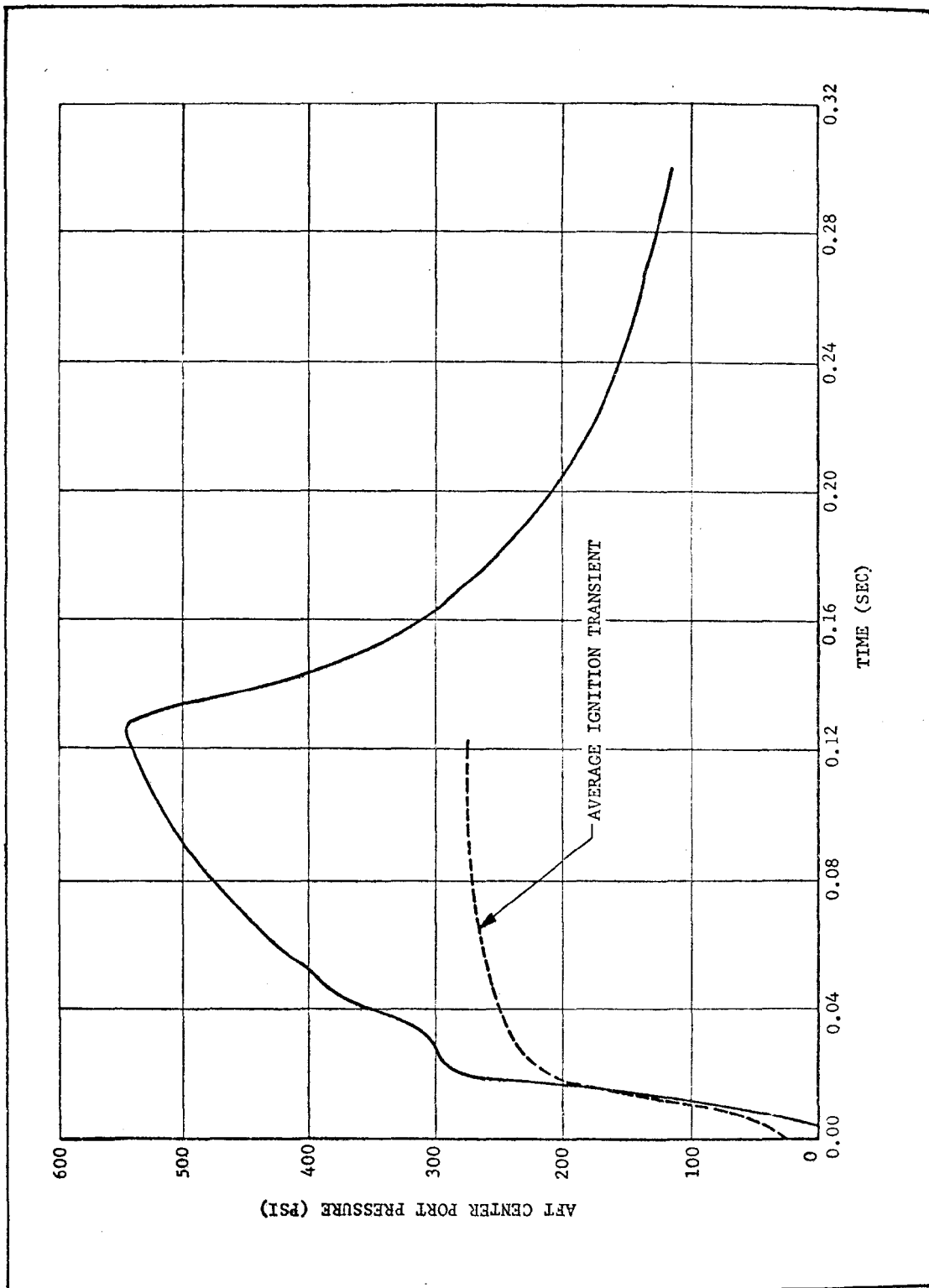


Figure 3-24. High-Rate Pressurization Transient for 9 Year Motor

wing slots 1 and 3 but only in one side of wing slots 2 and 4. The motor conditions prior to and following the tests were determined by visual inspection of the integral motor and of pieces removed from the motor by a carefully planned dissection. Results of the dissections and inspections are considered separately in following paragraphs.

The extent of cracking was exposed by dissecting the motor, using the cutting technique worked out in a previous program (Reference 12). The motor was sawed transversely, and sections containing the wing slots were further transversely cut into slices approximately 1/2 inch thick to expose the slot profile and the cracks. This cutting plan did not provide for removal of the entire length of wing slot in one piece; the first seven inches of the slot was in Section II, and the remainder in Section III.

Figures 3-25 through 3-27 show the extent of wing slot cracking, as measured from the sliced-up wing slot propellant. The end view of the slot profile shown on Figure 3-25 applies to all three of these figures to distinguish which corner of the wing slot is illustrated in the side views of the slots.

In general, the extent of cracking as revealed by dissection is somewhat more extensive than was detected during visual inspection of the integral motor. In particular, the cracks at event gages E12 (Slot 4) and E6 (Slot 2) were found to stop within the event gage location during inspection and gage removal; however, the dissected slices show cracks clearly extended across the grain slices that contained these gages. It is believed that the inspection results at the locations of gages E6 and E12 are more reliable than are the dissection results. The cracks could have been extended through these grain slices during the dissection operation or during the subsequent handling and examination of the slices. The inspection showed no cracks evident at the location of event gage E4, although the gage was found to be broken. The trim area is difficult to visually inspect because the corners of the forward trim area are irregular and sharp, and look very much like a crack even when the propellant is intact. The dissection results from location E4 are believed to show the correct condition induced by the test.

Except for these three locations, inspection and dissection results were the same as far as identifying cracking at event gage locations.

#### E. EVALUATION OF FULL-SCALE OVERTEST RESULTS

In all, there have been eight full-scale M57A1 motors overtested by high rate pressurization, although Motor 2-10-38 was pressurized to a maximum pressure of 310 psi which was not enough to initiate failure. Through the development of event gages and various instrumentation techniques, the state-of-the-art has been advanced to the point where full-scale motor overtests can provide reliable structural integrity data to warrant their use in development programs.

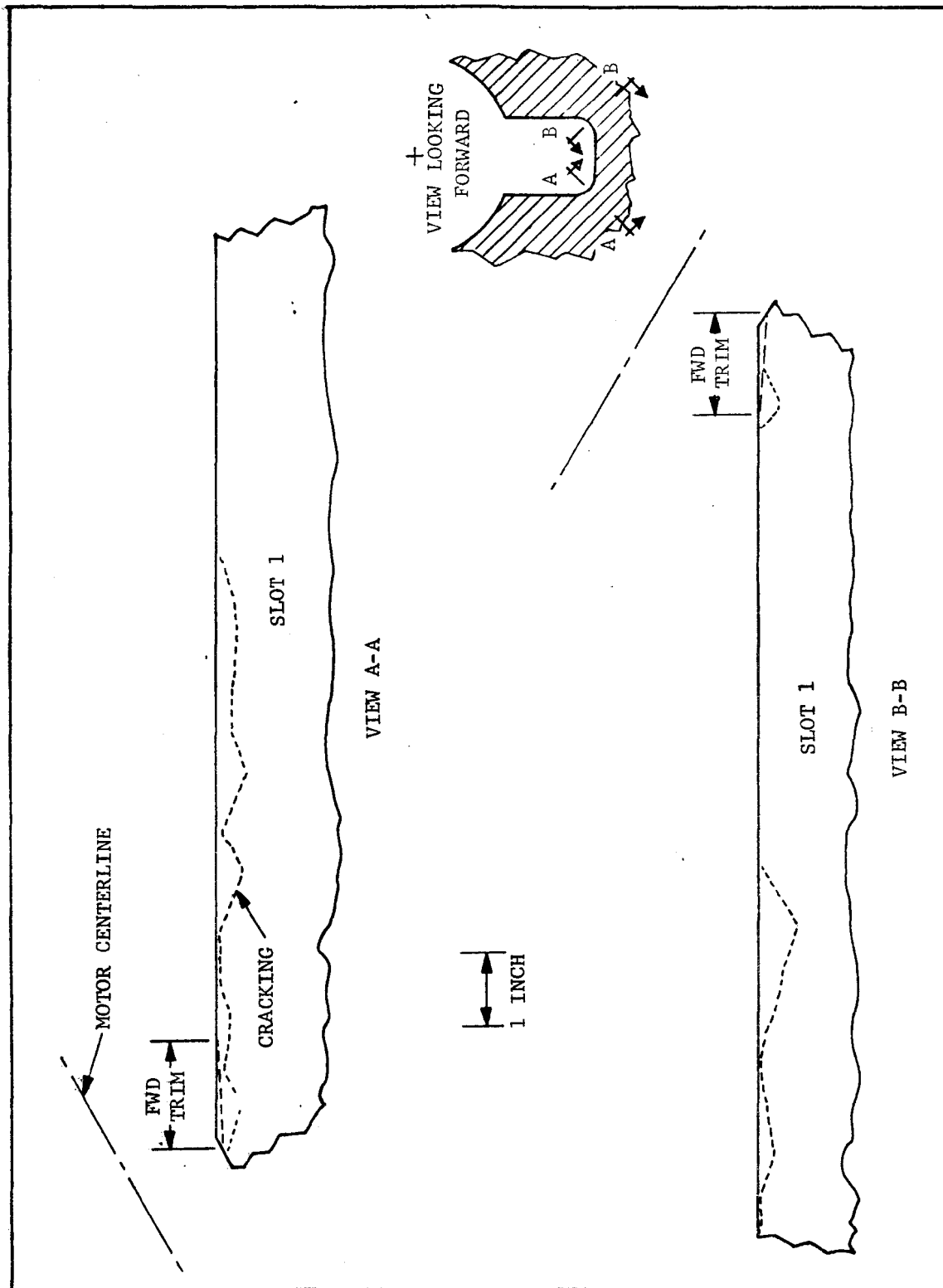


Figure 3-25. Cracks in Wing Slot 1

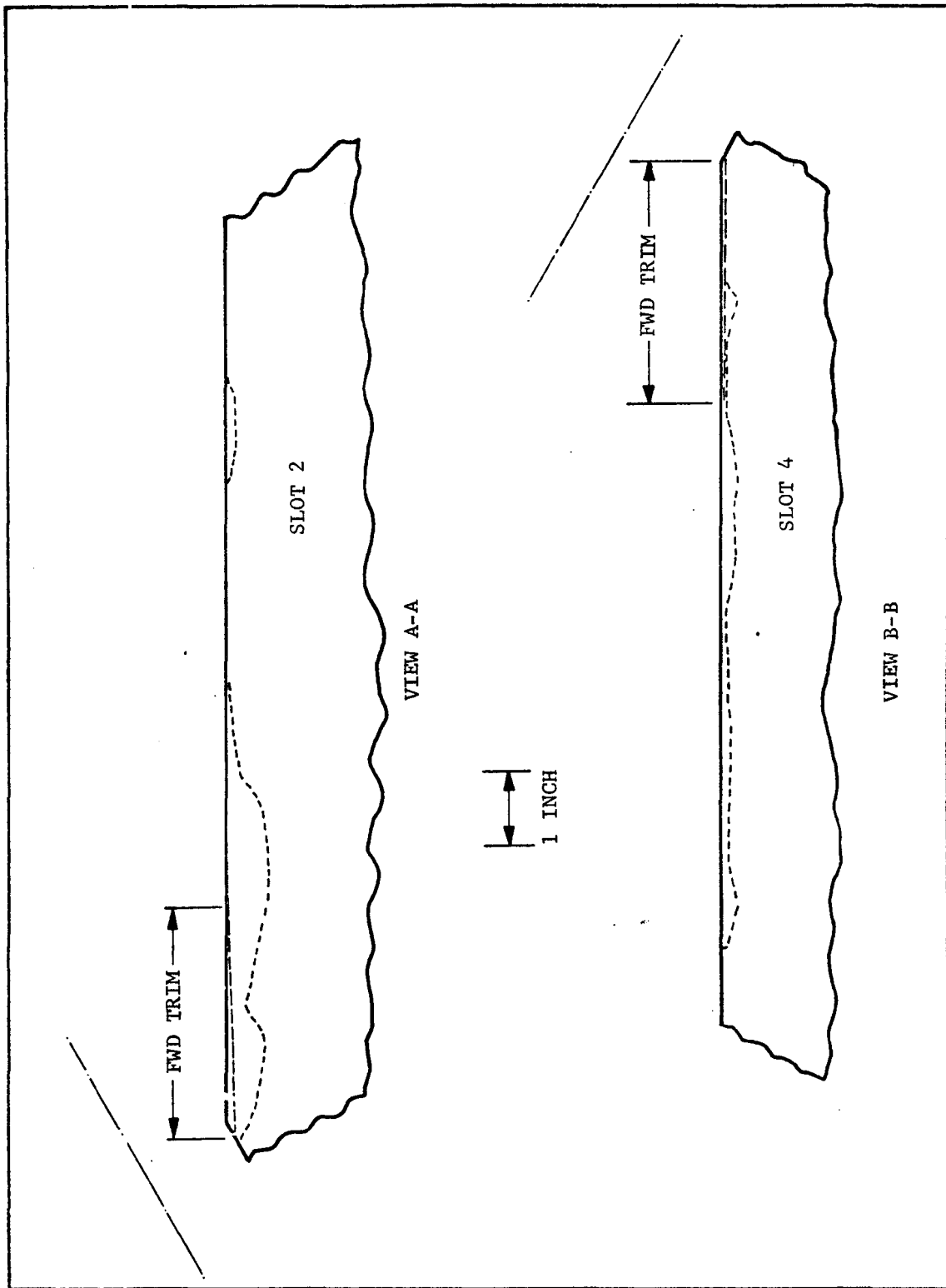


Figure 3-26. Cracks in Wing Slots 2 and 4

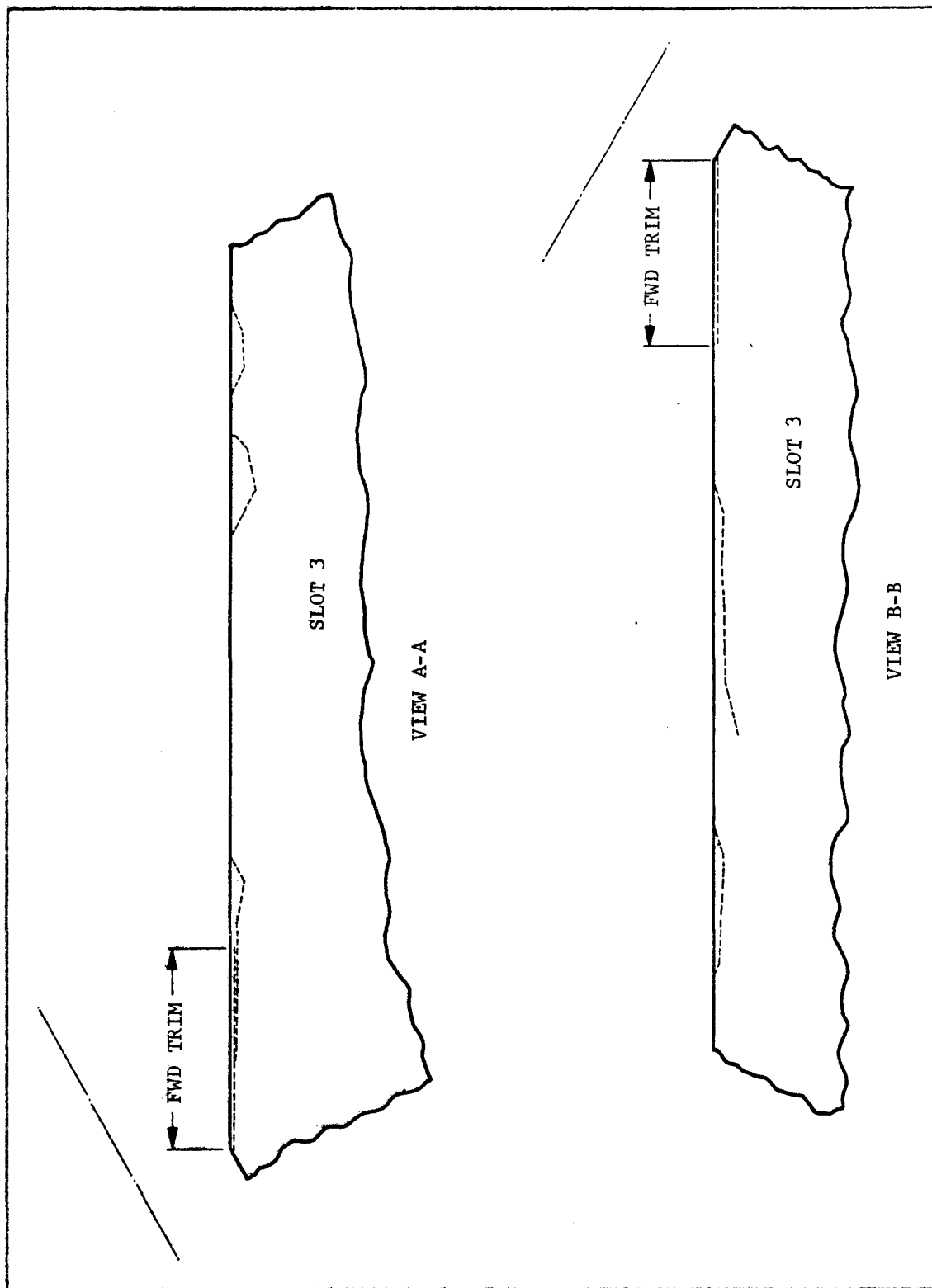


Figure 3-27. Cracks in Wing Slot 3



The Minuteman II Stage III motors used in this program have undergone several design changes since the early development stages. There are basically four categories of motors; pre-B-1 fix motors, B-1 fix motors, OPRI pre-oscillatory motors and the OPRI oscillatory motors. These various subpopulations of the total force require extensive overtesting of full-scale motors for service life predictions. This would be economically unfeasible. However, the overtest results should be evaluated at this point in terms of their usefulness in defining the motor structural capability, failure mode, and failure location under the high rate pressurization conditions.

The M57A1 rocket motor has a structural capability well above operating requirements. The failure pressures demonstrated in the high rate tests were 475 psi and 575 psi for the B-1 fix and OPRI configurations, respectively. The critical structural load for motor operation is the average motor ignition pressure, which is approximately 275 psi at 70° F. The ratios of failure to operating pressure are thus 1.73 and 2.09 for the B-1 fix and OPRI configurations. Corresponding ratios for the other full-scale motors tested to date are shown in Table 3-2.

Structural failure of the motor initiates in the forward trim area of the wing slots. This failure initiation site is about 3-1/2 inches forward of the wing slot section predicted by analysis to be the most critical for slot tip failure. Failure was predicted to occur at 500 psi and 600 psi for B-1 fix and OPRI configurations. This is reasonably close to the observed test failures.

The aft centerport boot-to-flap bond has a higher structural capability than does the wing slot tips. No boot-flap bond failures were induced in either motor by test pressures that were sufficient to fail the slot tips. That the boot-flap bonds were not broken was proven by the fact that bonded areas were removed from the motor, made into shear specimens, and successfully tested.

The TT port area also has a higher structural capability than does the wing slot tip. Wing slot cracks did not propagate out to the TT ports, and there is no evidence of other structural failure present in the TT ports.

Event gages produce better data on propellant failure than do conventional instrumentation installed in the grain cavity or on the motor case. The reliability of an individual event gage in detecting cracking is about 50 percent. The event gage concept is regarded as proven, but development has not yet progressed to the point where satisfactory reliability may be routinely attained.

Motor dissection is not entirely satisfactory in determining the extent of cracking caused by overtesting. Cutting and handling operations are known to have increased the extent of cracking in a few cases. Dimensional inspection of the grain cavity before and after the motor overtest proved to be worthless in determining the extent of cracking.

TABLE 3-2  
SUMMARY OF HIGH RATE PRESSURIZATION  
OVERTESTS OF M57A1 FULL-SCALE MOTORS

Motor	Cracking Pressure (psi)	Pressurization Rate (psi/sec)	Ratio of Failure to Critical Operating Pressure at Ignition ( $P_F/P_i$ )
SD-9	$P_{max} = 410$ ; crack initiation pressure not detected	4,000	---
SD-10	$P_{max} > 655$ ; crack initiation pressure not detected	10,000	---
2-10-16	500 to 530	12,000	1.82 to 1.93
2-10-38	$P_{max} = 310$ ; no cracks	15,000	$> 1.13$
33348 (OT)	575	20,000 to 31,000	2.09
32570 (OT)	475	18,000 to 29,000	1.73
32765 (LRSLA)	500	20,000	1.82
32743 (LRSLA)	492 to 525	17,000	1.80 to 1.91

The overtest program successfully verified the failure mode and location for the ignition pressurization transient in the M57A1 motor. No unusual failure modes were detected and the structural capability of the motor for these conditions was found to be considerably greater than the 275 psi operating pressure level.

#### LIST OF REFERENCES

1. Daniels, A. S., ICBM Overtest Technology; Task I, Failure Mode Selection; Technical Report AFRPL-TR-72-123; Hercules Incorporated, November 1972.
2. Daniels, A. S. and Rotter, J. J., ICBM Overtest Technology; Overtest Modeling (Task II) and Subscale Verification of the Model (Task III); Technical Report AFRPL-TR-74-25; Hercules Incorporated, February 1974.
3. Daniels, A. S., ICBM Overtest Technology; Motor Overtest (Task IV), and Posttest Examination (Task V), Technical Report AFRPL-TR-75- , Hercules Incorporated, February 1975.
4. A. S. Daniels, "An Event Gage for the Detection of Propellant Crack Initiation," JANNAF OSWG/SMBWG Combined Annual Meeting, CPIA Publication 253, July 1974.
5. Evans, R. M., Final Report, High Rate Hydrotests, Phases I and II Test Number SD-9, May 1963.
6. Evans, R. M., Final Report, High Rate Hydrotest, Test Number SD-10, Test I, August 1963.
7. Petek, F., Mechanical Behavior of the Minuteman Stage III Rocket Motor (2-10-16) During a Hydraulically Simulated Ignition Transient, Final Report, Task 9, Minuteman Product Support Program, February 1964.
8. Lowell, G. F., Summary Final Report for the Wing Slot Cracking and Aft Center Port Debonding Failure Mode During High Rate Pressurization Testing of Full-Scale Minuteman II, Stage III Rocket Motors for LRSLA, MTO 1124-70, May 1975.
9. Summary Final Report, Operational Reliability Improvement Program, MTO-164-242, Hercules Incorporated, Bacchus Works, Magna, Utah, February 1966.
10. Evans, R. M.; Final Report, Wing II Continued Development, High Rate Hydrotests, Phases I and II, Test Number SD-9; Reports MTO-164-131 and MTO-164-144; Hercules Incorporated; Magna, Utah; 15 May 1963.
11. Lund, E. F., LRSLA Program Briefing, JANNAF OS and SMBWG Combined Annual Meeting Bulletin, CPIA Publication 253, July 1974.
12. Jensen, F. R., Myers, L. F., Rotter, J. J., and Daniels, A. S.; Minuteman II Stage III Stress Analysis and Dissection, MTO-1124-64, Hercules Incorporated, December 1972.

## SECTION IV

### PROPELLANT PROPERTIES

#### A. INTRODUCTION

An extensive review of previous propellant mechanical characterization programs was accomplished to establish a data set for motor analyses and for determining aging trends. The intent was to make use of all available data in assessing aging effects and not limit the study for a particular set. The propellant properties set must be compatible with state-of-the-art analytical methods which are applied to the analysis of full-scale motors and motor analogs. Properties were measured using propellant from the particular motors of the Overtest Program to minimize uncertainties in analytical predictions for those motors.

The program emphasis on wing-slot cracking failure mode dictated the particular physical properties to be emphasized in this study. Motor behavior in response to ignition loading is primarily determined by case stiffness, propellant relaxation modulus at short times, and propellant strain at maximum stress over the range of strain rates that result from the ignition transient. Case stiffness is covered in Section V of this report. This section is concerned with propellant characterization, specifically the determination of relaxation modulus and allowable strain of CYH propellant in Minuteman II Stage III motors.

In addition to ICBM Overtest Technology, Long Range Service Life Analysis, and Dissected Motor Program, which are current programs in which CYH propellant data are being obtained, other programs and special investigations dating back to 1963 are also sources of data. A bibliography of reports from these completed programs is presented at the end of this section. The major programs of interest are as follows: Minuteman Support Program, Task 9; Minuteman Surveillance Program; Minuteman MACA Program; Pressure Oscillations of Minuteman II Stage III; Service Life Study Program; LRSLA Program; and Motor Categories and Service Life Program. These programs were all performed by Hercules Incorporated. Ogden Air Logistics Command (OALC) and Hercules performed the OOAMA-Hercules Cooperative Test Program. Since these programs often were not specifically directed to obtaining data for service life analysis not all of the data from these programs is applicable to this investigation. On the other hand, most of these programs yielded data which can be used to better understand the service-life-related data.

A general evaluation of the data and data sources is necessary for understanding. First, only propellant lots that were used in the manufacturing of Minuteman II Stage III are considered to provide valid data for this investigation. Propellant used in Minuteman I is therefore not included. This results, for example, in dropping three units out of the six which are presently included in the OALC Dissected Motor Program. Secondly, relaxation modulus data at very short times ( $10^{-6}$  to  $10^{-2}$  seconds)

is practically nonexistent. Current practice is to perform relaxation testing at low temperatures ( $0^{\circ}$  to  $20^{\circ}$  F) and then to time-temperature shift the data to short times at a reference temperature of  $70^{\circ}$  or  $77^{\circ}$  F. Although this technique was demonstrated for CYH propellant in 1965, little low-temperature testing of relaxation modulus has been undertaken until the current programs. Thirdly, not all of the information desired about test conditions can be obtained from the existing reports. Specifically, information on relative humidity levels during sample test and sample conditioning was generally not reported. The effect of relative humidity is known to be sufficient to explain some of the nonconforming data, and is therefore reason to exclude data that does not fit the general pattern.

Finally, statistical analysis demands two contradictory requirements of the data set when compared to the data that are available. Valid predictions require a large sample and at the same time require that the sample be a random selection of a homogenous population. Much of the data was therefore evaluated by a rule that can be stated: 'does this outlying or peculiar data point or set contribute to overall analysis validity by increasing the number of samples or does it decrease validity because it is somehow not representative of the population?' Where appropriate, statistical tests of equality of means were performed but this treatment is only applicable to groups of data, such as determining whether to include data taken from forty-pound charges (FPC's) with data taken from full-scale units (FSU's). A certain degree of judgment was necessary in marginal cases, and some reliance was placed on plotting all the data together. Data that did not fit the pattern were discarded. As often as possible, data from the unit in question were retained; even so, the final set of relaxation modulus data was made up of only 12 units and the set of allowable strain data was made up of 18 units.

The characterization history of CYH propellant is the first topic covered in the body of this section. A digest of each of the major programs which yielded applicable data is presented and the program conclusions are summarized. Information relating to the data, such as unit identification, propellant lot, age, and test conditions are presented in tabular form. The resulting data set is presented, along with discussion of applicability.

The interpretation of the data set is also presented. The determination of the aging trends of propellant properties was a central and critical part of the analyses of propellant data. The various castings from which samples were obtained were of various ages, so a statistically homogeneous population could be formed by correcting all data to a common age. Conversely, if no aging trend existed, all data automatically formed an age-homogeneous population. The effect of propellant casting geometry on physical properties was investigated to see if subscale and full-scale units formed one population. The correlation between individual unit properties and propellant lot properties was investigated; although physical properties are not available for all M57A1 motors, tensile failure data at a rate of 2 in./min at  $77^{\circ}$  F were taken from an FPC for each lot of

propellant powder used in the manufacturing program. Thus, the acceptance data are necessarily the only connective between the few units from which physical properties are available and the large number of Minuteman motors which are still in service.

The final topic of this section presents the statistical manipulations used to calculate the values of the mean and variance of relaxation modulus and strain at maximum stress representative of the operational population of Minuteman motors.

## B. CYH PROPELLANT CHARACTERIZATION HISTORY

The Minuteman II Stage III programs and special investigations which involve the response or characteristics of the propellant grain are presented in digest form together with such published conclusions as relate to propellant physical properties.

### 1. Minuteman Support Program

Task 9 of the Minuteman Support Program was the first extensive experimental and analytical program aimed at predicting the structural integrity of the Minuteman Stage III motor. The objectives of Task 9 were to determine the structural capabilities of the grain design and identify potential improvements through a better understanding of the structural requirements of the propellant grain.

Tests were conducted to characterize the viscoelastic behavior of CYH propellant. The tests included stress relaxation, uniaxial constant crosshead speed tensile, rapid strain rate to high strain levels with hold times, long-term constant strain, and casebond tensile tests.

### 2. OOAMA-Hercules Co-operative Test Program and Propellant Mechanical Property Results from the Second OOAMA-Hercules Co-operative Test Program

Two cooperative test programs were performed by Hercules and the Ogden Air Material Area (OOAMA) now the Ogden Air Logistic Center (OALC). The objective of the test programs was to compare the mechanical properties data obtained by Hercules and OOAMA for the Minuteman Stage III Surveillance Program.

In the first OOAMA-Hercules cooperative test program, Hercules and OOAMA performed stress relaxation, constant-crosshead-speed tensile, and vibrating disc tests. The samples tested were machined by both facilities; some of the samples were traded. No differences were detectable between the OOAMA and Hercules low-strain-rate-tensile failure data, but there was approximately a 10 percent difference in the high rate tensile failure data. There was also a 10 percent difference in the tensile relaxation modulus data obtained by the two facilities. Not enough samples were tested in

the first OOAMA-Hercules Co-operative Test Program to evaluate the reasons for the differences in the test data.

Uniaxial tensile and stress relaxation tests were conducted under the second OOAMA-Hercules Co-operative Test Program. More machined test samples were traded by the two facilities. Hercules normally machines round, necked-down tensile samples using a spray of water. OOAMA normally machines JANNAF samples dry for their tensile tests.

Again, the tensile relaxation modulus data obtained by Hercules and OOAMA were statistically similar while the failure data obtained at constant crosshead speeds of 200 and 2000 in./min were statistically different. The failure data obtained from round, necked-down and JANNAF tensile samples were statistically different. The method used to machine tensile samples, wet or dry, did not affect the failure data obtained from the samples.

### 3. Third Stage Minuteman Production Support Program

Task 2 of Stage III Minuteman Production Support Program was an experimental and analytical program to study those problems judged to be of the most immediate importance in evaluating the structural integrity of solid propellant grains. Test methods representative of actual motor loading conditions were developed and used to obtain CYH propellant failure data under multiaxial loadings. A multiaxial failure criterion was developed for Minuteman type propellants. Maximum principal strain was shown to be the best method of explaining the failure data.

### 4. Minuteman Surveillance Program

The Minuteman Stage III Surveillance Program was composed of the following tasks:

- (a) Physical property testing
- (b) Grain failure criteria study
- (c) Casebond failure criteria study
- (d) Service life predictions

Four Minuteman Stage III motors (336, 216, 131, and 67) were sectioned for the physical property testing phase. The objective was to determine the effect of age on the propellant mechanical properties. When the motors were first sectioned, a set of mechanical property tests consisting of stress relaxation, constant crosshead speed tensile, and vibrating disc tests were conducted on the propellant. The remaining sections of propellant were then wrapped in plastic and stored in a 77° F environment. Six months later, another set of tests, consisting of stress relaxation, constant-crosshead-speed tensile, and vibrating disc tests, was



conducted on propellant samples cut from the sectioned segment. The samples were machined from the segment just prior to testing. Ultimately, three series of these tests were conducted on the propellant from each motor. Regression analyses were performed on the tensile relaxation modulus and strain-at-maximum-stress data to determine the effect of age on these two parameters. The regression analyses of the propellant data show that the tensile relaxation modulus was decreasing with age and the strain at maximum stress capability of the propellant was also decreasing with age. Long-term constant strain, creep, and fatigue tests were also conducted on the sectioned propellant.

The Grain Failure Criteria Study was to develop a theory of failure which could be used to predict failure of a Minuteman Stage III motor propellant grain.

There were three objectives in the Casebond Failure Criteria Study. These were to: (a) Determine potential modes of casebond failure, (b) evaluate the various casebond test sample configurations, and (c) establish a failure criterion for the Minuteman Stage III casebond system.

Several casebond sample configuration were evaluated for determining the failure properties of a powder embedment casebond system like that used in the Minuteman Stage III motor. Four types of casebond failure were obtained during failure tests: (a) Failure in the propellant adjacent to the casebond, (b) cohesive failure in the embedment granules, (c) adhesive failure between the embedment granules and the embedment resin, and (d) adhesive failure between the embedment resin and the barrier coat resin. A modification of the classical Mohr theory was selected as the failure criterion for the Minuteman Stage III casebond system.

The final part of the Minuteman Surveillance Program was to use all of the information from the physical property testing phase and the failure criteria studies in a structural service life prediction of the Minuteman Stage III.

#### 5. Minuteman Service Life Study Program

The objective of the Minuteman Service Life Study Program was to update the service life prediction for the Minuteman Stage III motor.

As part of the Minuteman Service Life Study Program, the propellant tensile relaxation modulus, maximum stress, and strain at maximum stress data obtained during the Minuteman Surveillance Program from Minuteman Stage III motors 336, 131, 216, and 67 were reanalyzed to eliminate the effects of secondary aging.

During the Minuteman Surveillance Program, the sectioned propellant was stored for almost two years before the last series of test samples were machined from the sectioned propellant. Sectioned propellant has a much greater exposed surface-to-mass ratio than the propellant in a

whole or virgin motor grain. Therefore, sectioned propellant would be expected to age more rapidly. Secondary aging is the term used to define the effect of aging on propellant stored as large pieces after a full-scale motor has been sectioned, while primary aging is the term used to define the aging which would occur in the propellant of a whole grain.

Linear regression lines were developed for the secondary aging occurring in the Minuteman Surveillance Program. The regression lines were then extrapolated back to the age of the motors when they were first sectioned to determine the propellant mechanical properties, tensile relaxation modulus, maximum stress, and strain at maximum stress, at the time of motor sectioning. Linear regression lines were then fit to the extrapolated data points for each motor, mechanical property at time of motor cutup, to develop the primary aging trends in each propellant mechanical property parameter.

#### 6. Minuteman II Stage III Motor Categories and Service Life Studies

The Minuteman II Stage III Motor Categories and Service Life Studies Program was divided into two phases: (a) Categorization of Minuteman II Stage III static test motor performance characteristics, and (b) service life studies.

The service life studies were a continuation of the service life studies begun under the Minuteman Service Life Study Program. The objectives of this program were to:

- (a) Determine theoretically if a crack in the slot tip region of a Minuteman Stage III motor grain would propagate during the ignition transient
- (b) Determine the effects of motor categorization on the service life predictions made for the four principal failure modes analyzed during the Minuteman Service Life Study Program
- (c) Define data requirements needed to improve service life predictions
- (d) Identify and recommend instrumentation for full-scale static test firings which would detect motor behavior indicative of aging degradations, in particular, with reference to the four principal failure modes analyzed.

A fracture mechanics analysis was used to determine theoretically if a crack in the slot tip region of a Minuteman motor would propagate during the ignition transient. To support this analysis, critical stress intensity factor data were obtained on CYH propellant 10, 54, and 99 months old. The data did not appear to be affected by the age of the propellant. Additional tensile relaxation modulus data were also obtained on CYH

propellant taken from a 10 month FPC casting and three Minuteman Stage III motors 54, 99, and 102 months old. The tensile relaxation modulus obtained during the Minuteman Surveillance Program and reanalyzed during the Minuteman Service Life Study for secondary aging were time-temperature shifted to 77° F to correspond in temperature with the new tensile relaxation data obtained at 77° F. Primary aging regression lines were fit to the two sets of tensile relaxation data, the new data, and the old time-temperature shifted data. The two sets of data compared very well, lending credence to the original secondary aging analyses of the tensile relaxation.

Fifteen recommendations were made to improve the propellant and adhesive properties needed for motor service life predictions and a number of recommendations were made for improved instrumentation for full-scale static test firings.

7. Investigation of Pressure Oscillations During Firing of the Minuteman II Stage III Motor

There was a significant increase in the amplitude of acoustic pressure oscillations in the Minuteman II Stage III motor starting with QA Motor 59 and casting powder lot RAD 1-10-66. This change in motor behavior initiated a special investigation of acoustic related phenomena in the M57A1 motor and propellant. In the course of this study, uniaxial tensile and dynamic torsional shear tests were conducted on propellant manufactured from 7 lots of CYH powder.

The importance of the new uniaxial tensile data obtained from the seven lots of powder was that the data were a better measure of the powder lot mechanical property variations than the old powder lot acceptance data. The new powder lot mechanical properties were obtained by testing tensile samples cut from the original but aged propellant castings. All of the new test samples were tested on one occasion using the same operator and testing machine while maintaining constant humidity and temperature control. The QA acceptance data were obtained originally over a period of four years. This could lead to erroneous conclusions about the mechanical properties of the various powder lots since slight variations in the test conditions and operator could lead to marked variations in the mechanical properties.

The maximum stress values obtained from the new tensile tests were all lower than the QA powder lot acceptance data. The two sets of strain at rupture data were about equivalent. The tangent moduli obtained from the powder lot acceptance data were consistently lower than the new data.

#### 8. LGM-30 Third Stage Dissected Motor Program

The objective of the LGM-30 Stage III Dissected Motor Program was to determine aging effects on materials in the Minuteman Stage III motor. The program is still underway at Ogden Air Logistics Center. Eighteen Minuteman Stage III motors have been dissected and various types of physical property and chemical tests are now being performed. The following tests are being performed on propellant and casebond samples: (a) Uniaxial tensile, (b) biaxial tensile, (c) triaxial tensile, (d) stress relaxation, (e) constant load creep, (f) Shore A and Shore D hardness, (g) long term constant strain, (h) dynamic shear, (i) casebond peel, (j) casebond tensile, (k) differential thermal analysis, (l) thermogravimetric analysis, (m) burn rate, (n) heat of explosion, (o) thermal coefficient of linear expansion, (p) volumetric expansion, and (q) attenuated total reflectance. The test data in general cover a motor age range from 4 to 13 years. Linear regression lines have been fit to each data parameter along with 3 sigma bands and 90-90 tolerance bands.

The stress relaxation data obtained during the Dissected Motor Program from CYH propellant shows a statistically significant increase in tensile relaxation modulus with age. The uniaxial, biaxial, and triaxial tensile strain at maximum stress data also shows a statistically significant increase with age.

#### 9. Long Range Service Life Analysis Program

There are several objectives in the Minuteman Third Stage Long Range Service Life Analysis (LRSLA) program. These are: (a) Dissect Minuteman Stage III motors and determine the physical properties of the various materials and bonds in the motors, (b) perform high rate pressurization tests on third stage motors (overpressure tests), and (c) supply OALC with physical properties and high rate pressurization data for validation of analytical service life models of the M57A1 motor.

Six Minuteman Stage III motors were dissected and the following mechanical property tests are being conducted:

- (a) Tensile and biaxial tensile tests on CYH propellant
- (b) Fracture toughness tests on CYH propellant
- (c) Stress relaxation tests on CYH propellant
- (d) Tensile and shear tests on CYH/Buna-S bond
- (e) Tensile and shear tests on CYH/Buna-S/C7/Buna-S bond
- (f) Tensile and shear tests on CYH/923.2/Buna-S bond

- (g) Shear tests on Buna-S/962/Buna-S bond
- (h) Shear tests on Buna-S/vulcanized/Buna-S bond
- (i) Stress relaxation tests on Buna-S rubber
- (j) Stress relaxation tests on DDP propellant
- (k) Tensile and shear tests on DDP propellant

The above mechanical property tests have been conducted under superimposed hydrostatic pressures of 0 to 300 psig at test temperatures from -30° to 180° F. The mechanical property data were time-temperature shifted to form master curves for each material and bond. Tests to determine Poisson's ratio, thermal coefficient of linear expansion, and bulk modulus of CYH propellant and the bulk modulus of Buna-S rubber were also performed.

#### 10. Evaluation of Available Data

The programs listed above, plus a few miscellaneous special investigations, plus the LRSIA and Overtest programs are the potential sources of physical property data applicable to the ICBM Overtest Program service life investigation. Reports listed in the bibliography at the end of this section were surveyed to seek out applicable data. The results of the survey are presented in Table 4-1. The table lists individual units considered in each report and outlines the scope of the data presented. Supplementary information on age and propellant lot number is also presented. Table 4-2 is a description of the test conditions for the samples.

Table 4-3 presents data applicable to service life predictions for Minuteman II Stage III motors. The results were extracted from the sources identified in Tables 4-1 and 4-2. Data obtained from Minuteman I units are not presented in Table 4-3. Table 4-3 is further restricted to relaxation modulus, strain at maximum stress, and aging trend data. All CYH powder lots used in the production of Minuteman II Stage III motors are listed in Table 4-3.

The basic data sets for relaxation modulus and strain versus strain rate were developed from the published data listed in Table 4-3. Data were first time-temperature shifted to a reference temperature of 77° F (see Figure 4-1), replotted, and/or averaged where necessary. Finally, data at selected times (relaxation modulus) or rates (strain at maximum stress) were tabulated. Table 4-4 presents the relaxation data and Table 4-5 presents data on strain at maximum stress.

Considering that 47 units are shown in Table 4-3, the presence of only 12 units in Table 4-4 may be confusing. Examination of Table 4-3 indicates that the common range of relaxation times is from 0.04 or 0.07 seconds to 1000 seconds. Table 4-4 presents data applicable to analysis of

TABLE 4-1  
SOURCES OF DATA

Casting No.	Config. and Casting	Cast Date	Lot	Test Date	Age at Test	Program (Report No.)	Comments
1121 1139 1148	FPC FPC FPC	3/13/63 4/24/63 5/9/63	SR-82-60 SR-28-63 SR 78-61	5/15 5/20/63 6/9 6/15/63 6/9 6/15/63	2 mo 2 mo 1 mo	Minuteman Support Program (1)**	E (0.3-0.9% $\epsilon$ ), T, ML, C
1121 1139 1148	FPC FPC FPC	3/13/63 4/24/63 5/9/63	SR-82-60 SR 28-63 SR 28-61	6/25 7/22/63 6/25 7/22/63 6/25 7/22/63	3-4 mo 2-3 mo 1½-2½ mo	Minuteman Support Program (2)	$\epsilon$ , IT, ES, R, ML, TD (SL and ST - only 3 samples per strain rate)
SD-25 No. 6 and 11	FSU Subscale	UK* 9/13/63 10/14/63	UK 28-63	UK UK	UK UK	Minuteman Support Program (4)	R, $\epsilon$ , (E @ 0.04-1000 sec), C, MP, G' R, $\epsilon$ , (E @ 0.04-1000 sec) C, G'
173-1 198-4 201-3 135	TPC TPC TPC TPC	4/60 8/60 8/60 1/60	41-60 Bacchus 1 Bacchus 1 86D-59	5/64 5/64 5/64 5/64	49 mo @ 100°F 45 mo @ 60°F 45 mo @ 100°F 52 mo @ 60°F	Myers (5)	E (0.05-1000 sec) (No time-temp shift used - only curves at 60, 70, 80°F) T, R, $\epsilon$ (0.5- 100 in./in./min), ML (TPC Data), C
1095	FPC	2/18/63	SR 82-60	UK	UK	Myers (6)	E(0.04-1000 sec), G' $\epsilon$ (0.1-100 in./in./min), C, Effect of wet vs dry mach. :
1139 & 1140	FPC	4/24/63	SR 28-63	UK	UK	Time-Temp Superposition, Swanson (7)	(E <sub>R</sub> converted data), C & D, T - gives shift factors (questionable because only one rate tested per temp)
1189	FPC	9/3/63	SR 58-63	UK	UK	Swanson (8)	R, $\epsilon$ , E, ES, C, MPFPC
1732 1754 1772 1770 1768 & 1769	FPC	2/18/66 3/31/66 4/13/66 4/13/66 4/13/66	RAD 1-10-66 RAD 1-10-66 Sublot 53 Sublot 52 Sublot 51	UK	Acceptance Data Only	Jensen & Anderson (9)	E <sub>R</sub> converted data, C, $\epsilon$
1549	UK	2/5/65	1/7/65	UK	UK	Tucker (10)	RH varied, TD
UK	UK	UK	UK	UK	UK	Swanson (11)	C, P, R
1569 1570	FPC	3/16/65 3/16/65	1/7/65 1/7/65	UK	UK	Minuteman Prod. Support, Task 2 (13)	R, T, $\epsilon$ , ES, C (or) D, (MPFPC)
* UK: Unknown      **Numbers refer to report numbers in the Bibliography.							

TABLE 4-1 (Cont)

## SOURCES OF DATA

Casting No.	Config. and Casting	Cast Date	Lot	Test Date	Age at Test	Program (Report No.)	Comments
336-I	FSU	12/62	68-62	6/65	2-1/2 yr	Minuteman	R, E, €
336-II	FSU	12/62	68-62	12/65	3 yr	Surveillance	
216-I	FSU	12/61	82-60	6/65	3-1/2 yr	(17)	Data came from
216-II	FSU	12/61	82-60	12/65	4 yr	Jensen	Reports 35, 41
131-I	FSU	1/61	69A-60	7/65	4-1/2 yr		
131-II	FSU	1/61	69A-60	1/66	5 yr		
67-I	FSU	6/60	41-60	12/65	5-1/2 yr		
UK	UK	UK	UK	UK	UK	MM Surveillance (18) Myers	€ at one rate - UK
UK	UK	UK	UK	UK	UK	MM Surveillance (19)	Case bond data only
UK	PFC	UK	UK	UK (late 65)	UK (~0)	Production Support Task 2 (14)	R, P, €, D
Grain 70	FSU	7/60	SR41-60	UK		OOAMA Dissected	P, D (points are
Grain 131	FSU	1/21/61	SR69A-60	(before 8/73)		Motor Program (30)	not identified as to motor)
31036	FSU	10/3/62	100A 61				Two test cycles about 33 months apart are given..
31057	FSU	10/23/62	68-62				Cannot identify individual motors in list of data and cannot get age of each specimen.
31064	FSU	10/21/62	56-62				One data point can be obtained: allowable strain at rate of 1000 in./in./min w/300 psi, 77° F. Correlation with age not significant
31097	FSU	12/8/62	68-62				
31134	FSU	1/28/63	68-62				
31136	FSU	2/2/63	68-62				
31158	FSU	2/20/63	68-62				
32248	FSU	8/28/63	58-63				
32107	FSU	5/19/63	28-63				
32116	FSU	5/17/63	28-63				
32133	FSU	6/10/63	51-63				
32137	FSU	6/13/63	51-63				
32140	FSU	4/29/63	28-63				
32434	FSU	1/21/64	1-6-63				
32831	FSU	1/29/65	1-8-65				
32174	FSU	1/20/67	1-10-66				
Grain 336	FSU	12/62	SR68-62				
Grain 70	FSU	6/60	41-60	UK (before 6/72)		OOAMA Dissected	R, T
Grain 131	FSU	1/21/61	69A-60			Motor Program (32)	€, D
31036	FSU	10/3/62	100A61	UK (before 6/72)		OOAMA Dissected	P, D (points are identified on curve as to motor)
31057	FSU	10/23/62	68-62			Motor Program (32) (Cont)	35 data points are shown.
31064	FSU	10/21/62	56-62				
31097	FSU	12/8/62	68-62				
31134	FSU	1/28/63	68-62				
31136	FSU	2/2/63	68-62				
31158	FSU	2/20/63	68-62				
32248	FSU	8/28/63	58-63				

TABLE 4-1 (Cont)

## SOURCES OF DATA

Casting No.	Config. and Casting	Cast Date	Lot	Test Date	Age at Test	Program (Report No.)	Comments
32434	FSU	1/21/64	1-1-63			OOAMA Dissected Motor Program 6/72 (32) (Cont)	One data point can be obtained: strain at max stress @ 1000 in./in./min w/300 psi, 77° F. Correlation with age is not significant
32831	FSU	1/29/65	1-8-65				
32107	FSU	5/19/63	28-63				
32116	FSU	5/17/63	28-63				
32133	FSU	6/10/63	51-63				
32137	FSU	6/13/63	51-63				
32140	FSU	4/29/63	28-63				
32174	FSU	1/20/67	1-10-66				
2048	FPC	9/70	1-21-70	6/8/71	10 mo	OOAMA Service Life Study (29)	Tabulated $E_r$ is all at 77° F and no time shorter than 0.07 sec is given
Grain 2158	FSU	7/63	51-63	10/2/71	99 mo		
Grain 2137	FSU	6/63	51-63	5/27/71 & 6/7/71	102 mo		
Grain 3174	FSU	1/67	1-10-66	6/9/71 thru 6/16/71	54 mo		T, E, ST, TD
Grain 336	FSU	12/62	68-62			SAMSO Service Life Study (28)	Strain and modulus data in this report are all taken from reports on properties of grains 336, 131, 216, 67, and 70
Grain 216	FSU	12/61	82-60	7/65 to 6/69	Various		
Grain 131	FSU	1/21/61	69A-60				
Grain 67	FSU	6/60	41-60				
Grain 70	FSU	7/60	41-60				
1273	FPC	1/3/64	1-1-63		67 mo	Pressure Oscillations (27)	2 in./min JANNAF data are compared to same at acceptance test - poor correspondence
1327	FPC	3/27/64	1-3-64		65 mo		
1604	FPC	4/23/65	1-8-65		52 mo		
1779	FPC	5/10/66	1-10-66	8/1/69	39 mo		
1827	FPC	8/24/66	1-14-66		36 mo		
1886	FPC	3/22/67	1-15-67		29 mo		
1912	FPC	7/20/67	1-16-67		25 mo		
UK	UK	UK	UK	UK	UK	Heat Trans. and Stress Analysis Wings II-V (26)	$E_r$ data are from Propellant Manual. Allowable strain curve also is from Propellant Manual. Shows difference of 5 to 7% between UT and BS results
MS 1891	D/L FPC	3/17/67	1-13-66	5/4/67 thru 5/8/67	1-3/4 mo	Second Cooperative Test Program (25)	R, $\epsilon$ , TD & D, ST. Difference between facilities; UT vs JANNAF specimens strain at max stress is different 1 to 1.7%
1571	FPC	3/22/65	RAD 1-7-65	7/65	3 mo	First Cooperative Test Program (12)	HI data only. R, T, $\epsilon$ , E, D



TABLE 4-1 (Cont)

## SOURCES OF DATA

Casting No.	Config. and Casting	Cast Date	Lot	Test Date	Age at Test	Program (Report No.)	Comments
1826 1886	FPC FPC	8/24/66 3/22/67	1-14-66 1-15-67	About 8/67	UK	Special Investigation (24) Mechanical Property Results	R ε, D
336 216 131 67 70	FSU	12/62 12/61 1/61 6/60 7/60	68-62 82-60 69A-60 41-60 41-60	7/65 to 1/69	Various	MM MACA (23)	Same data as in SAMSO Service Life (29). Data are taken from reports of grains 336, 131, 216, 67, and 70
336	FSU	12/62	68-62	8/65, 9/65, 2/66, 9/66, 10/66, 11/66	30 mo 38 mo 46 mo	Phys Prop. Test on Grain 336 (33, 16, 34)	R, T, ε, D, ST for ε. E <sub>R</sub> will not shift to 10 <sup>-4</sup>
Grain 216	FSU	12/24/61	82-60	7/65 2/66 6/66, 7/66	53 mo 62 mo 67 mo	Phys Prop. Test on Grain 216 (35, 36, 37)	R, T, D ε. Bad scatter E <sub>R</sub> will not shift to 10 <sup>-3</sup>
Grain 131	FSU	1/29/61	69A-60	9/65 4/66 9/66, 10/66	56 mo 63 mo 69 mo	Phys Prop. Test on Grain 131 (38, 39, 40)	R, T, D, ε, ST. E <sub>R</sub> will not shift to 10 <sup>-3</sup>
Grain 67	FSU	6/19/60	41-60	1/66 6/66, 7/66 12/66 6/67	65 mo 72 mo 78 mo 84 mo	Phys Prop. Test of Grain 67 (41, 42, 43, 44)	R, T, D, ε, ST. E <sub>R</sub> will not shift to 10 <sup>-3</sup>
Grain 70	FSU	7/2/60	41-60	12/68	91 mo	Phys Prop. Test of Grain 70 (45)	R, T, TD, ε, ST. E <sub>R</sub> will not shift to 10 <sup>-3</sup>
1153 1095	FPC FPC	5/21/63 2/18/63	42B-62 82-60	UK	UK	Task 9 MSP (46)	E <sub>R</sub> to 10 <sup>-5</sup> sec was calculated, not measured beyond 10 <sup>-2</sup> sec. C
UK	T/L FPC	UK	UK	UK	UK	Task 9 MSP (47)	Data are on case bond properties
1121 1139 1148	FPC	3/13/63 4/24/63 5/9/63	82-60 28-63 78-61	6/26/63 thru 7/19/63	2-4 mo	Task 9 MSP (48)	R, D, ε vs ε̇. Data are averaged from all 3 FPC's
1139	FPC	4/24/63	28-63	7/1/63	2 mo	Task 9 MSP (49)	E <sub>R</sub> at 10 <sup>2</sup> and up, long term testing
6 11 SD 25	1/3 scale motors FSU	9/13/63 10/14/63 3/25/63	28-63 28-63 11-63	UK (About 6/64)	UK	Task 9 MSP (50)	ε vs ε̇ from 0.1 to 100. E <sub>R</sub> time 0.04 sec and up. C
UK	CCC	UK	UK	UK (About 2/67)	UK	Subscale Motor Verification (22)	E <sub>R</sub> min time is 0.001 sec
Grain 336 Grain 216 Grain 131 Grain 67	FSU FSU FSU FSU	12/62 12/61 1/61 6/60	68-62 82-60 69A-60 41-60	7/65 to 1/69	Various	Service Life Prediction (20)	Data taken from report on grains 336, 216, 131, & 67

TABLE 4-1 (Cont)

## SOURCES OF DATA

## KEY TO "COMMENTS" COLUMN

## Test Conditions

- R rates varied  
 P superimposed pressure  
 T temperature varied

## What can be obtained from the data

- G' Dynamic shear storage modulus  
 $\epsilon$  Strain at max stress vs strain rate in range 10 to 1000 in./in./min  
 E  $E_R$  from  $10^{-6}$  or  $10^{-4}$  to  $10^0$  sec from stress relax tests  
 IT Initial tangent modulus is presented and can be converted to  $E_R$  from  $10^{-6}$  or  $10^{-3}$  to  $10^0$  sec  
 M Difference in mean between motors can be obtained  
 ML Difference in mean value between lots can be obtained  
 D Data are presented as points on a curve  
 C Data are presented as a curve only  
 TD Data are tabulated  
 ST Standard deviation for variation due to test can be obtained  
 SM Standard deviation due to motor-to-motor differences can be obtained  
 SL Standard deviation due to lot-to-lot differences can be obtained  
 MFPC Difference in mean due to difference between FPC's and motors  
 MP Difference in mean value due to sample position in the motor can be obtained  
 MPFPC Difference in mean value due to sample position in FPC can be obtained

TABLE 4-2

## SAMPLE CONDITIONS

Data Source (Report No.)	Casting No.	Test	Lots	Conditions - Storage and List						Test Date	Age	Comments
				Temp (°F)	RH (%)	P (psi)	Sample and Number	Rates	Test Facility			
Task 9 MSP (Rpt 1) *	1121	Stress Relax.	82-60	60, 70 and 80	Amb	0	Hollow Round Tensile 15/FPC 5/Temp (one test each)	$\dot{\epsilon} = 0.3$ to 0.9%	HI	5/15/63 to 5/20/63	2 mo	No vertical shift used. 0.00025 to 3900 sec at 70° F available
	1139		28-63	70 and 80					HI	6/9/63 to 6/15/63	2 mo	
	1148		78-61						HI	6/9/63 to 6/15/63	1 mo	
	1121	Stress Relax.	82-60	50-110			8 samples		URPC			
Task 9 MSP (Rpt 2)	1121	High-rate Tensile	82-60	77 (Room Temp)	Amb	0	Hollow Round JANNAF Dog- bone (EGL = 2.4 in.) 3 specimen/£	60 - 2500 in./in./min	HAFB	6/25/63 to 7/22/63	3-4 mo 2-3 mo 1½-2½ mo	
	1139		28-63									
	1148		78-61									No new data (all referenced)
Task 9 MSP (Rpt 3)	SD-25	Stress Relax.	11-63	70	Amb	0	Stress relax. 3/each of four motor loca- tions	N/A	HI	N/A	N/A	Data in curve of avg values from 3 samples (0.04-1000 sec)
		Vibrating Disc					Vibrating Disc 3/each from four motor locations. Three tests each					Dynamic shear storage modulus data in curve
		Constant rate tensile					UK sample con- figuration - UK number of samples					$\dot{\epsilon}_{max}$ vs $\dot{\epsilon}$ 1-100 in./in./min $\dot{\epsilon}_{max}$ vs $\dot{\epsilon}$ 1-100 in./in./min curves only. From different motor location
*Report numbers correspond to the numbers in the Bibliography.	No. 6 & 11 subsamples	Stress Relax.	28-63	70	Amb	0	Stress relax 4/subscale (2 from front 2 from aft)	N/A	HI	UK	UK	Curves only
		Vib Disc					Vib Disc 4/subscale (2 from front 2 from aft). Three tests each					Curves only

TABLE 4-2 (Cont)

## SAMPLE CONDITIONS

Conditions - Storage and List												
Data Source (Report No.)	Casting No.	Test	Lots	Temp (°F)	RH (%)	P (psi)	Sample and Number	Rates	Test Facility	Test Date	Age	Comments
(Rpt 4 Cont)	No. 6 & 11 subscales (Cont)	Constant rate tensile		60, 70, and 80			UK config. 45/subscale (all from center section)					Curves only $\sigma_m$ vs $\dot{\epsilon}$ 1-100 in./in./min $\epsilon_m$ vs $\dot{\epsilon}$ 1-100 in./in./min
Aging of CYH & DDP (Rpt 5)	173-1 198-4 201-3	Stress relax.	41-60 Bacchus 1 Bacchus 1	60, 70, and 80	Amb	0	Stress relax. No. UK. UK sample configuration.	$\dot{\epsilon}$ = UK				
	135	Constant rate tensile	86D-59	70 and when samples avail- able 60 and 80			2-6 samples @ each condition	$\dot{\epsilon}$ = 0.5- 100 in./ in./min				
Sample Prepara- tion (Rpt 6)	FPC 1095	Stress relax. constant $\dot{\epsilon}$ tensile. Vib discs	82-60	70	Machined wet/amb RH test	0	3 stress relax 15 const. $\dot{\epsilon}$ tensile 3 vib disc	UK $\dot{\epsilon}$ 0.1-100 cps 50-1000	HJ	UK	UK	To determine effects of wet machining
	FPC1095	Stress relax. constant $\dot{\epsilon}$ tensile. Vib discs		70	Machined dry/amb RH test	0	3 stress relax 15 const. $\dot{\epsilon}$ tensile 3 vib disc	UK $\dot{\epsilon}$ 0.1-100 cps 50-1000	HAFB	UK	UK	To determine effects of dry machining
Time-Tempera- ture Super- position (Rpt 7)	FPC 1139 FPC 1140	Const. $\dot{\epsilon}$ tensile	28-63	-110° to 70	UK	0	Cylindrical Necked-down tensile. UK No./condition	$\dot{\epsilon}$ = 0.85 in./in./min	HI	UK	UK	To verify t - T shift of CYH Also referred to 0.74 in./in./min JANNAF dogbone data at 160 to -60° F (source unknown)
	FPC 1189	Const. $\dot{\epsilon}$ Tensile Stress relax.	58-63	70	UK	0	Tensile 12/ rate from each of 8 layers Stress relax. 4/layer	0.0858, 0.858, 8.58, 858	HI	UK	UK	Demonstration of E calculated from $\dot{\epsilon}$ tests

TABLE 4-2 (Cont)

## SAMPLE CONDITIONS

Conditions - Storage and List													
Data Source (Report No.)	Casting No.	Test	Lots	Temp (°F)	RH (%)	P (psi)	Sample and Number	Rates	Test Facility	Test Date	Age	Comments	
Acceptance Specification (Rpt 9)	FPC 1732	Const. $\dot{\epsilon}$ tensile	RAD 1-10-66 and Sublots 51, 52, and 53	70	UK	0	UK	$\dot{\epsilon} = 74$ in./ in./min	HI	UK	Accept. Data $\approx 0$	Data to justify revision of acceptance tests	
	FPC 1754												
	FPC 1768												
	FPC 1769												
	FPC 1770												
Effect of Humidity (Rpt 10)	FPC 1549	Const. $\dot{\epsilon}$ tensile	1-7-65	77	Varied	0	1/4 in. JANNAP Tensile	UK	HI	UK	UK	Study of RH effects	
Failure Theory (Rpt 11)	UK	Biax rail torsion, uniaxial and JANNAP, diametral compress.	UK	UK	UK	Torsion p = ?	UK	$\dot{\epsilon} = 4, 10,$ 40, 100 in./in./min	HI	UK	UK	Evaluation of Octahedral failure theory	
Time-Tempera- ture Super- position (Rpt 13)	FPC 1569	Uniaxial tensile	1-7-65	-80 to 160	36 - 44% above 32° F	0	Hollow, cyl, necked-down tensile - w/ 60% incl in bonded area	CH rate 0.2, 2, and 20 in./min	HI	UK	UK	Verify time- temp shift applicability. Very hard to extract indi- vidual unit data	
	FPC 1570				No con- trol below 32		6/temp; i.e., 2/rate						
Task 2 PSP (Rpt 15)												CYH data from No. 14 reported previously in Prod. Support Program quar- terly progress report MCS-701- 15, Nov 65	
MM Surveillance (Rpt 17)	336-I	Stress relax. and tensile	68-62	70	UK	0	UK	0.8, 8, 80, and 800 in./in./min	HI	UK	2-1/2 yr 3 yr	Surveillance Program - Series I and II Tests. Data obtained from reports 35 - 41	
	336-II		82-60										
	216-I												
	216-II												
	131-I		69-A-60										
	131-II		41-60										
Failure Properties (Rpt 18)	UK	Const. $\dot{\epsilon}$ tensile	UK	75	UK	0	4 samples, config. UK	200 in./ min CHS	HI	UK	UK	4 samples with no const. strain or vib were obtained for control samples	

TABLE 4-2 (Cont)

## SAMPLE CONDITIONS

Conditions - Storage and List												
Data Source (Report No.)	Casting No.	Test	Lots	Temp (°F)	RH (%)	P (psi)	Sample and Number	Rates	Test Facility	Test Date	Age	Comments
Case-Bond Failure Criteria (Rpt 19)	UK	Case bond strength tests	UK	75	UK				HI	UK	UK	Case bond failure criteria study. Case bond data only
MM Production Support Program Task 2 (Rpt 14)	UK	Tension	UK	70	UK	0-1000	UK-prob JANNAF. One replica	3: 7.8, 78, 780	HIB	UK (late 65)	UK (-0)	£ and effect of pressure on £ vs £
OOAMA Dissected Motor Program Aug 73 (Rpt 30)	Grain 70	BS + Pressure	41-61	Amb (77°) (storage was "Amb")	Amb	300	BS (189 total, cannot tell which sample gave which data)	1000 in./ in./min	OOAMA	UK (before Aug 73)	UK (cannot tell indi- vidual samples)	Allow strain at 1000 in./ in./min (everything is grouped together to get an aging trend) (32 data points are shown on regression plot) (Grain 131 is reported separately, 4 points 8-1/2 to 11-1/2 years
	Grain 131		69A-60									
	31036		100A61									
	31057		68-62									
	31064	56-62	Tension	77	Amb	0	JANNAF 1/4 in. (40 data points)	0.667				
	31097	68-62										
	31134	68-62										
31136	68-62	Tension	77	Amb	0	JANNAF 1/4 in. (40 data points)	0.667					
31158	68-62											
32248	58-63	Tension	77	Amb	0	JANNAF 1/4 in. (38 data points)	0.667 x 10 <sup>-4</sup>					
32107	25-63											
32116		Tension	51-63	Amb (77)	Amb	0	BS (38 data points)	0.1143				
32133	51-63											
32137	51-63											
32140	28-63											
	32434	Stress Relax.	1-1-63	Amb (77)		0	Stress relax. 44 data points	3%				
	32831		1-8-65									
	33174		1-10-66									
	Grain 336		68-62									
OOAMA Dissected Motor Program Jun 72 (Rpt 32)	Grain 70	1/4 in. JANNAF tension	41-61	50, 70, 90	UK	0	1/4 in. JANNAF (No. replicas not given)	0.74, 7.4, 74, 740	OOAMA and HIB	UK (before Jun 72)	UK	£ and effect of £ on £ vs £
	Grain 131		69A-60									
	31036	Tension + pressure	100A61	77				BS (No. replicas not given)	1000 in./ in./min	OOAMA		

TABLE 4-2 (Cont)

## SAMPLE CONDITIONS

Conditions - Storage and List												
Data Source (Report No.)	Casting No.	Test	Lots	Temp (°F)	RH (%)	P (psi)	Sample and Number	Rates	Test Facility	Test Date	Age	Comments
(Rpt 32 Cont)	31057	Tension + pressure	68-62	77 (storage 70 ± 10)	Amb	300	BS	1000 in./ in./min				Strain at max stress at 1000 in./in./min. 35 data points are shown on regression plot; identified by motor No.
	56-62											
	31064	Tension	68-62	77 (storage 70)	Amb	0	JANNAF 1/4 in.	0.667				
	31097											
	31134	Tension	68-62	77	50 ± 10	0	JANNAF 1/4 in.	0.667 x 10 <sup>-4</sup>				
	31136											
	31158	Tension	68-62	77	Amb	0	BS	1000				
	32248											
	32434	Tension	1-1-63	77	Amb	0	Stress relax.	3%				
	32831											
32107	Stress relax.	28-63	77	Amb	0	Stress relax.	3%					
32116												
32133	Stress relax.	51-63	77	Amb	0	Stress relax.	3%					
32137												
32140	Stress relax.	28-63	77	Amb	0	Stress relax.	3%					
Grain 331												
OOAMA Service Life Study (Rpt 29)	FPC 2048	Stress relax.	1-21-70	77	50		Stress relax. 1/2 %, 4 or 5 replicas	HI	HI	6/8/71 10/2/71 5/27/71 and 6/7/71	10 99 102	No Er or ε at reqd times/ rates
	Grain 2158											
	Grain 2137		51-63									
	Grain 3174	Stress relax.	1-10-66	0, 20, 40, 77, 140	UK		Stress relax. 1/2%, 4 or 5 replicas			From 6/9/71 thru 6/16/71	54	Can get Er curve
SAMSO Service Life Study (Rpt 28)	Grain 336	Tension	68-62	50, 70, 90	UK	0	UT (?)	0.83, 8.3, 83, 830	HI	7/65 to 1/69	Varian	Data was taken from reports on grains 333, 131, 216, 67, and 70
	Grain 216	Stress relax.	82-60	50, 70 90	UK	0	Stress relax.	Strain not given				
	Grain 131											
	Grain 67											
	Grain 70											
Pressure Oscillations Report (Rpt 27)	FPC 1273	Tension (repeat acceptance test)	1-1-63	UK (77?)	UK	0	JANNAF 1/4 in.	2 in./min	HI	8/1/69	67 65 52 39 36 29 25	Repeated the acceptance test.
	FPC 1327											
	FPC 1604											
	FPC 1779											
	FPC 1827											
Heat Transfer and Thermal Stress Analysis (Rpt 26)	FPC 1886		1-15-67	70	UK	0	UT and BS	UK		UK	UK	Data taken from Propellant Manual
	FPC 1912											
	UK											
Second HI- OOAMA Coopera- tive Test (Rpt 25)	MS 1891 FPC	Tension, stress relax.	1-13-66	77	46 to 48	0	JANNAF 1/4 in, UT, SR	Tension: CHS 2, 200, 2000. SR: 0.01 and 0.03 in.	HI and OOAMA	5/67	1-3/4	Er at 0.07 sec. ε vs ε curves and data

TABLE 4-2 (Cont)

## SAMPLE CONDITIONS

Conditions - Storage and List												
Data Source (Report No.)	Casting No.	Test	Lots	Temp (°F)	RH (%)	P (psi)	Sample and Number	Rates	Test Facility	Test Date	Age	Comments
First Cooperative Test (Rpt 12)	FPC 1571	Tension, SR	1-7-65	40, 77 100	UK	0	JANNAF 1/4 in., UT, SR	Tension: 0.067, 0.67, 6.67, 1000 SR: 0.05 and 1%	HI data only	7/65	3	Er at 40° will shift to 10 <sup>3</sup> sec. € vs € data plots are only at end points of 10-1000
Mechanical Property Results (Rpt 24)	FPC 1826 FPC 1886 FPC (No SN)	Tension, SR	1-14-66 1-15-67 1-10-67	77	UK	0	UK - JANNAF? SR	0.74, 7.4, 74, 740. ER UK	HI	Abt 8/65	UK	€ vs € @ 77. Er 0.07-1000 sec
MM MACA Program (Rpt 23)	FSU 336 FSU 216 FSU 131 FSU 70 FSU 67	Tension, SR, vibrating disc	68-62 82-60 69A-60 41-60 41-60	Tension 50, 70, 90 SR 70	UK	0	UK-JANNAF ? SR	0.8, 80, 800 Er UK	HI	7/65 to 1/69	Various	Data was taken from reports on grains 336, 216, 131, 70, 67
Tests on Grain 336 (Rpt 33)	336	Tension, SR, vib disc	68-62	50, 70, 90	29 to 38	0	JANNAF ?, 5 replicas SR, 4 replicas	0.74, 7.4, 74, 740 ER 0.015	HI	8/65 and 9/65	30	Er 0.07- 1000 sec
Tests on Grain 336 (Rpt 16)	336	Tension, SR, vib disc	68-62	70	Tension 42, SR 40	0	JANNAF ? 5 replicas SR, 4 replicas	0.74, 7.4, 74, 740 ER 0.005	HI	2/66	38	
Tests on Grain 336 (Rpt 34)	336	Tension, SR, vib disc	68-62	Tension 70 SR 50, 70, 90	Tension and SR 40	0	JANNAF ?, 5 replicas SR 4 replicas	0.74, 7.4, 74, 740 ER 0.5	HI	9/66, 10/66, 11/66	46	Comparison of samples stored 2-1/2 mo vs test after machining
Test on Grain 216 (Rpt 35)	216	Tension, SR, vib disc	82-60	50, 70, 90	29 to 50	0	JANNAF ? 5 replicas SR 4 replicas	0.74, 7.4, 74, 740 ER 0.015	HI	7/65	53	Er 0.7-1000 sec € vs € bad scatter
Test on Grain 216 (Rpt 36)	216	Tension, SR, vib disc	82-60	70	40 to 42	0	JANNAF ? 5 replicas SR 4 replicas	0.74, 7.4, 74, 740 ER 0.005	HI	2-66	62	
Test on Grain 216 (Rpt 37)	216	Tension, SR, vib disc	82-60	50, 70, 90	40	0	JANNAF ? 5 replicas SR 4 replicas	0.74, 7.4, 74, 740 ER 0.5	HI	6/66 and 7/66	67	€ vs € bad data scatter



TABLE 4-2 (Cont)

## SAMPLE CONDITIONS

Data Source (Report No.)	Casting No.	Test	Lots	Conditions - Storage and List							Test Facility	Test Date	Age	Comments
				Temp (°F)	RH (%)	P (psi)	Sample and Number	Rates						
Test on Grain 131 (Rpt 38)	131	Tension, SR, vib disc	69A-60	50,70, 90	29 to 38	0	JANNAF ? 5 replicas SR 4 replicas	0.74, 7.4, 74, 740 ER 0.015			HI	9/65	56	$E_R$ 0.07-1000 sec
Test on Grain 131 (Rpt 39)	131	Tension, SR, vib disc	69A-60	70	42	0	JANNAF ? 5 replicas SR 4 replicas	0.74, 7.4, 74, 740 ER 0.005			HI	4/66	63	
Test on Grain 131 (Rpt 40)	131	Tension, SR, vib disc	69A-60	Tension 70 SR 50, 70,90	40	0	JANNAF ? 5 replicas SR 4 replicas	0.74, 7.4, 74, 740 ER 0.005			HI	9/66, 10/66, 11/66	69	
Test on Grain 67 (Rpt 41)	67	Tension, SR, vib disc	41-60	50,70, 90	40	0	JANNAF ? 5 replicas SR 4 replicas	0.74, 7.4, 74, 740 ER 0.005			HI	1/66	65	$E_R$ 0.07-1000 sec
Test on Grain 67 (Rpt 42)	67	Tension, SR, vib disc	41-60	70	40	0	JANNAF ? 5 replicas SR 4 replicas	0.74, 7.4, 74, 750 ER 0.005			HI	6/66	72	
Test on Grain 67 (Rpt 43)	67	Tension, SR, vib disc	41-60	50, 70, 90	40	0	JANNAF ? 5 replicas SR 4 replicas	0.74, 7.4, 74, 740 ER 0.005			HI	12/66	78	
Test on Grain 67 (Rpt 44)	67	Tension, SR, vib disc	41-60	70	Tension 42 SR 40	0	JANNAF ? 5 replicas SR 4 replicas	0.74, 7.4, 74, 740 ER 0.005			HI	6/67	84	
Test on Grain 70 (Rpt 45)	70	Tension, SR, vib disc	41-60	50,70, 90	45 and 40	0	JANNAF ? 5 replicas SR 4 replicas	0.74, 7.4, 74, 740 ER 0.005			HI	12/68	91	$E_R$ 0.07-1000 sec
Task 9 MSP (Rpt 46)	FPC 1153 FPC 1095	SR	42B-62 82-60	70	UK	0	SR ? UK number	UK			HI (?)	UK Abt 9/63		Data from 10 <sup>-2</sup> to 10 <sup>4</sup> sec, calculated $E_R$ to 10 <sup>-5</sup> sec
Task 9 MSP (Rpt 47)	T/L FPC	Case bond tensile	UK	70	UK	0	UK number CBT	UK			HI (?)	UK Abt 9/63	UK	Case bond tensile sample development

TABLE 4-2 (Cont)

## SAMPLE CONDITIONS

Conditions - Storage and List												
Data Source (Report No.)	Casting No.	Test	Lots	Temp (°F)	RH (%)	P (psi)	Sample and Number	Rates	Test Facility	Test Date	Age	Comments
Task 9 MSP (Rpt 48)	FPC 1121	High rate tensile	82-60 28-63 78-61	80 (OOAMA test at 77)	UK	0	UT UK number	0.04,0.08, 0.4,0.8,4, 8,80,100, 400,1000, 2000	HI and OOAMA		2-4 mo	ER 0.01 sec and up. € vs € is avg of all 3 FPC. ER has no data points and is avg for all 3 FPC
	FPC 1139											
	FPC 1148											
Task 9 MSP (Rpt 49)	FPC 1139	Long term constant strain	28-63	UK 72?	UK	0	UT 3 replicas? SR 6 replicas?	10%,20%, 30%,40%, 44.9%,49.9%, 51.1%	HI	UK Abt 3/64		ER from 10 <sup>2</sup> to 10 <sup>6</sup>
Subscale Verification Program (Rpt 22)	CCC's Casting No. UK	CCC pressure test and tensile	UK	70	UK	N/A	CCC 7. Tensile 2 replicas	8.6 and 86	HI	UK Abt 2/67	UK	€ at 8.6 and 86 for 2 CCC's
Service Life Prediction (Rpt 20)	FSU 336	Tensile, SR, vib disc, constant strain	68-62 82-60 69A-60 41-60	50,70, 90	UK	0	SR 4 replicas, tensile 5 replicas, 7 test cycles	Tensile 0.8,80, 800	HI	7/65 to 1/66	Various	ER 0.04-1000 sec. Data taken from reports on 336,216,131, and 67
	FSU 216											
OOAMA Dissected Motor Program Oct 1974 (Rpt 53)	FSU 131	Biaxial strip + pressure	58-62 68-62 1-1-63 1-10-66 69A-60	77	Amb	300	3 replicas BS	1000 in./ in./min	OALC	74116	Various	€ at 1000 aging trend data
	FSU 67											
	FSU 31064											
	FSU 31134											
	FSU 32434											
	FSU 33174											
	Grain 131											
	Tension	77	Amb	0	JANNAF 1/4 in. 5 replicas	0.667 x 10 <sup>-4</sup>		74350		Aging trend data		
	Tension	77	50 ± 5 20 during break- down	0	JANNAF 1/4 in. 5 replicas	0.667 x 10 <sup>-4</sup>		UK (1974)				
	Biaxial strip	77	Amb	0	BS 1 sample	0.1143		UK (1974)				
	Stress relax.	77	Amb	0	SR 3 replicas	3%		UK (1974)		10,50,100, and 1000 sec aging trend		
	Vib disc	UK	UK	0				UK (1974)				

TABLE 4-3

## SOURCES OF DATA FOR MINUTEMAN PRODUCTION POWDER LOTS

Powder Lot	Available Data
SR 68-62	<ol style="list-style-type: none"> <li>1. FSU 336; <math>\epsilon</math> vs <math>\dot{\epsilon}</math> from 1 to 1000 in./in./min at 70° F; <math>E_R</math> from 0.01 to 1000 sec at 50 and 70° F; Reports 33, 16, 34 - Chappell &amp; Myers</li> <li>2. FSU's 31057, 31097, 31134, 31136, and 31158; <math>\epsilon</math> at 1000 in./in./min, 300 psi, 77° F, BS; Elong; ITM; <math>E_R</math> at 10 sec; OOAMA Dissected Motor Program, Reports 32 and 53</li> </ol>
SR 11-63	<ol style="list-style-type: none"> <li>1. FSU SD 25; <math>\epsilon</math> vs <math>\dot{\epsilon}</math> from 1 to 100 in./in./min at 70° F; <math>E_R</math> from 0.04 to 1000 sec at 70° F; Report 4 - Myers, Task 9</li> </ol>
SR 28-63	<ol style="list-style-type: none"> <li>1. FSU's 32107, 32116, and 32140; <math>\epsilon</math> at 1000 in./in./min, 300 psi, 77° F, BS; Elong; ITM; <math>E_R</math> at 10 sec; OOAMA Dissected Motor Program, Report 32</li> <li>2. 1/3 Scale MM No. 6 and No. 11; <math>\epsilon</math> vs <math>\dot{\epsilon}</math> from 0.74 to 74 in./in./min at 60, 70, and 80° F, curves only and 60 and 80° F curves look bad; <math>E_R</math> from 0.04 to 1000 sec at 70° F, and very different for different locations; Report 4 - Myers, Task 9</li> <li>3. FPC 1139; <math>\epsilon</math> vs <math>\dot{\epsilon}</math> from 60 to 2500 in./in./min at 77° F; <math>E_R</math> from 0.04 to 1000 sec at 60, 70, and 80° F; Task 9, Beavers, Reports 1 and 2</li> <li>4. FPC's 1139 and 1140; <math>E_R</math> from <math>10^{-10}</math> to <math>10^4</math> sec at 70° F; Swanson, Report 7</li> </ol>
SR 9B-63	No data
SR 51-63	<ol style="list-style-type: none"> <li>1. FSU's 32133 and 32137; <math>\epsilon</math> at 1000 in./in./min, 300 psi, 77° F, BS; Elong; ITM; <math>E_R</math> at 10 sec; OOAMA Dissected Motor Program, Report 32</li> <li>2. FSU's Grain 2158 and 2137; <math>E_R</math> from 0.07 to 1000 sec at 77° F; OOAMA Service Life Study, Report 29</li> </ol>
SR 58-63	<ol style="list-style-type: none"> <li>1. FSU 32248; <math>\epsilon</math> at 1000 in./in./min, 300 psi, 77° F, BS; Elong; ITM; <math>E_R</math> at 10 sec; OOAMA Dissected Motor Program, Report 32</li> <li>2. FPC 1189; <math>\epsilon</math> vs <math>\dot{\epsilon}</math> from 0.001 to 1000 in./in./min at 70° F, but strain curve has no points and is plotted beyond test limits of 0.0858 to 858 in./in./min; <math>E_R</math> from 0.01 to 1000 sec at 70° F; Swanson, Report 8</li> </ol>

TABLE 4-3 (Cont)

## SOURCES OF DATA FOR MINUTEMAN PRODUCTION POWDER LOTS

Powder Lot	Available Data
RAD 1-1-63	<ol style="list-style-type: none"> <li>1. FSU 32434; <math>\epsilon</math> at 1000 in./in./min, 300 psi, 77° F, BS; Elong; ITM; <math>E_R</math> at 10 sec; OOAMA Dissected Motor Program, Reports 32 and 53</li> <li>2. FPC 1273; Elong; ITM; Pressure Oscillation, Report 27</li> </ol>
RAD 1-2-64	No data
RAD 1-3-64	<ol style="list-style-type: none"> <li>1. O/T Motor 33348; <math>\epsilon</math> vs <math>\dot{\epsilon}</math> from 10 to 1000 in./in./min + 300 psi at 77° F; <math>E_R</math> from 10<sup>-5</sup> to 1 sec at 70° F</li> <li>2. FPC 1327; Elong; ITM; Pressure Oscillation, Report 27</li> </ol>
RAD 1-4-64	No data
RAD 1-5-65	<ol style="list-style-type: none"> <li>1. LRSLA FSU's 32645 and 32633; <math>\epsilon</math> vs <math>\dot{\epsilon}</math> from 10 to 1000 in./in./min + 300 psi at 77° F; <math>E_R</math> from 10<sup>-6</sup> to 1 sec at 77° F + 300 psi</li> </ol>
RAD 1-6-64	<ol style="list-style-type: none"> <li>1. LRSLA FSU's 32720 and 32743; <math>\epsilon</math> vs <math>\dot{\epsilon}</math> from 10 to 1000 in./in./min + 300 psi at 77° F; <math>E_R</math> from 10<sup>-6</sup> to 1 sec + 300 psi at 77° F</li> <li>2. FPC 1571; <math>\epsilon</math> at 6.7 and 670 at 40, 77, and 100° F; <math>E_R</math> from 10<sup>-3</sup> to 1 sec at 77° F; First Co-Op Program, Report 12</li> </ol>
RAD 1-7-64	<ol style="list-style-type: none"> <li>1. LRSLA FSU's 32765, 32769; <math>\epsilon</math> vs <math>\dot{\epsilon}</math> from 10 to 1000 in./in./min + 300 psi at 77° F; <math>E_R</math> from 10<sup>-6</sup> to 1 sec + 300 psi at 77° F</li> <li>2. FPC 1571; <math>\epsilon</math> at 6.7 and 670 at 40, 77, 100° F; <math>E_R</math> from 10<sup>-3</sup> to 1 sec at 77° F; First Co-Op Program, Report 12</li> </ol>
RAD 1-8-65	<ol style="list-style-type: none"> <li>1. FSU 32831; <math>\epsilon</math> at 1000 in./in./min, 300 psi at 77° F, BS; Elong; ITM; <math>E_R</math> at 10 sec; OOAMA Dissected Motor Program, Report 32</li> <li>2. FPC 1604; Elong; ITM; Pressure Oscillation, Report 27</li> </ol>
RAD 1-9-65	No data

TABLE 4-3 (Cont)

## SOURCES OF DATA FOR MINUTEMAN PRODUCTION POWDER

Powder Lot	Available Data
RAD 1-10-66	<ol style="list-style-type: none"> <li>1. FSU 33174; <math>\epsilon</math> at 1000 in./in./min + 300 psi at 77° F, BS; Elong; ITM; <math>E_R</math> at 10 sec; OOAMA Dissected Motor Program, Report 32</li> <li>2. FSU Grain 3174; <math>E_R</math> from <math>10^{-6}</math> to 1 sec at 77° F; OOAMA Service Life Study, Report 29</li> <li>3. FPC 1779; Elong; ITM; Pressure Oscillation, Report 27</li> <li>4. FPC w/o S/N; <math>E_R</math> from 0.07 to 1000 sec, 77° F, Curve Only; <math>\epsilon</math> vs <math>\dot{\epsilon}</math> from 10 to 1000 in./in./min, Curve Only; Report 24</li> </ol>
RAD 1-11-66	No data
RAD 1-12-66	No data
RAD 1-13-66	<ol style="list-style-type: none"> <li>1. FPC 1891; <math>\epsilon</math> vs <math>\dot{\epsilon}</math> at 86 and 860 in./in./min at 77° F; Second Co-Op Program, Report 25</li> </ol>
RAD 1-14-66	<ol style="list-style-type: none"> <li>1. LRSLA FSU 33231; <math>\epsilon</math> vs <math>\dot{\epsilon}</math> from 10 to 1000 in./in./min + 300 psi at 77° F, BS; <math>E_R</math> from <math>10^{-6}</math> to 1 sec + 300 psi at 77° F</li> <li>2. FPC 1826; <math>\epsilon</math> vs <math>\dot{\epsilon}</math> from 10 to 1000 in./in./min at 77° F, Report 24</li> <li>3. FPC 1827; Elong; ITM; Pressure Oscillation, Report 27</li> </ol>
RAD 1-15-66	<ol style="list-style-type: none"> <li>1. FPC 1886; <math>\epsilon</math> vs <math>\dot{\epsilon}</math> from 10 to 1000 in./in./min at 77° F; Report 24</li> <li>2. FPC 1886; Elong; ITM; Pressure Oscillation, Report 27</li> </ol>
RAD 1-16-67	<ol style="list-style-type: none"> <li>1. O/T FSU 33348; <math>\epsilon</math> vs <math>\dot{\epsilon}</math> from 10 to 1000 in./in./min + 300 psi at 70° F; <math>E_R</math> from <math>10^{-5}</math> to 1000 sec at 70° F</li> <li>2. FPC 1912; Elong; ITM; Pressure Oscillation, Report 27</li> </ol>
RAD 1-17-68	No data
RAD 1-18-68	No data
RAD 1-19-68	No data
RAD 1-20-70	No data
RAD 1-21-70	<ol style="list-style-type: none"> <li>1. FPC 2048; <math>E_R</math> from 0.07 to 1000 sec; Report 29</li> </ol>

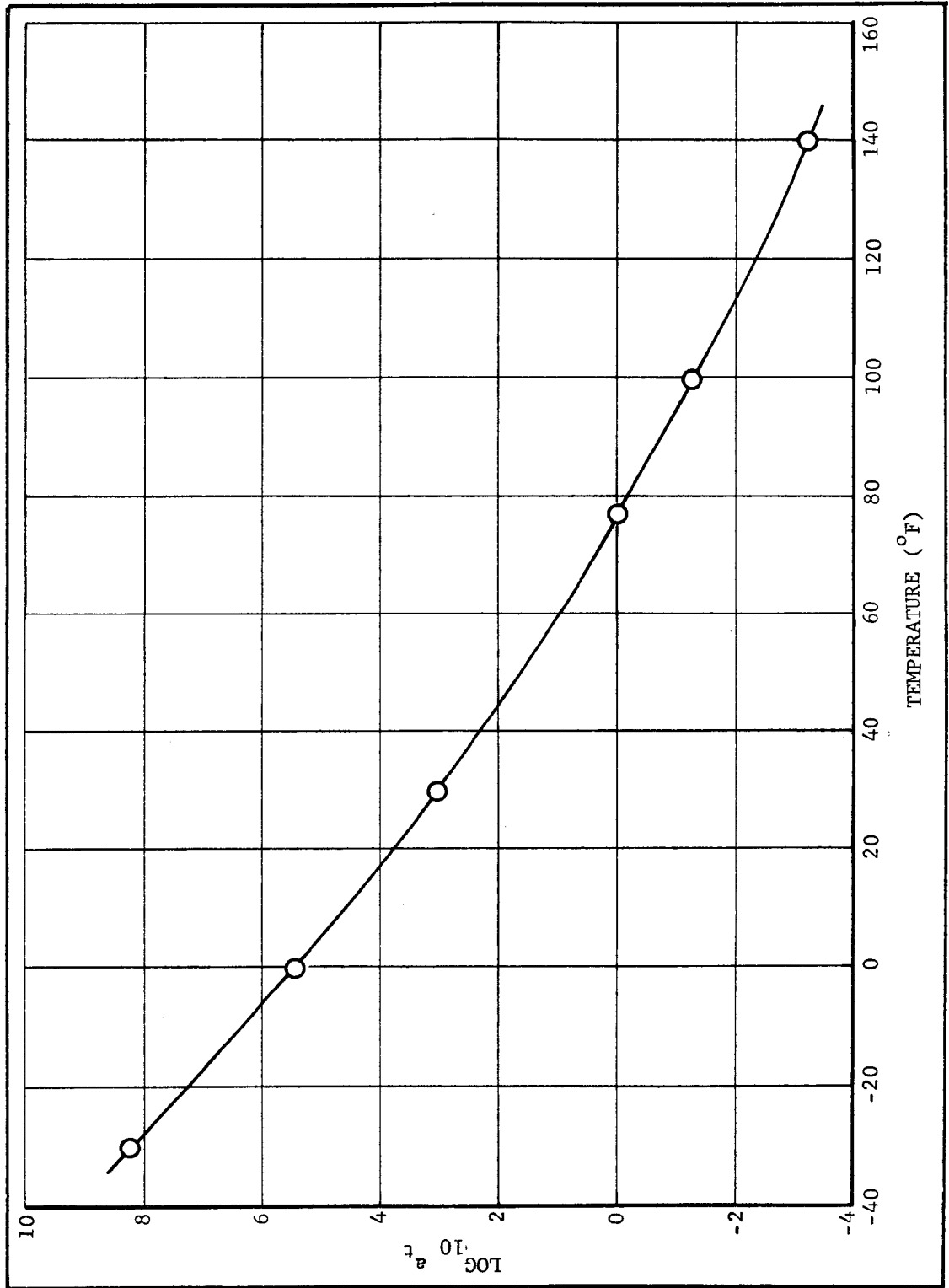


Figure 4-1. CYH Propellant Shift Factors

TABLE 4-4

## RELAXATION MODULUS DATA SET

Unit	Relaxation Modulus - psi									
	Relaxation Time - seconds									
	10 <sup>-6</sup>	10 <sup>-5</sup>	10 <sup>-4</sup>	10 <sup>-3</sup>	10 <sup>-2</sup>	10 <sup>-1</sup>	1	2.45	10	
32765	39,000	21,000	11,333	6,067	3,267	1,783	1,233	1,100	923	
32633	49,333	29,000	15,667	8,567	4,800	2,767	1,733	1,440	1,183	
32769	42,333	23,000	12,333	6,600	3,566	1,817	1,350	1,170	983	
32743	43,333	25,000	13,333	7,367	3,900	2,400	1,883	1,630	1,417	
32645	46,000	25,333	14,000	7,667	4,133	2,266	1,600	1,400	1,200	
32720		24,000	12,333	6,367	3,167	2,317	1,650	1,460	1,233	
33348		23,000	16,000	9,000	4,950	2,750	1,770	1,600	1,380	
33231		23,500	12,000	6,033	3,267	1,833	1,333	1,200	1,050	
FSU 3174	28,100	21,200	14,100	8,200	4,220	2,450	1,600	1,490	1,250	
FPC 1571		29,000	15,500	8,100	4,300	2,400	1,440	1,200	910	
32570		23,100	14,500	7,900	4,150	2,480	1,700	1,500	1,280	
FSU 336			14,000	7,500	4,100	2,590	1,680	1,377	1,190	
Reference Temperature 77°F										

TABLE 4-5  
DATA SET FOR STRAIN AT MAXIMUM STRESS

Unit	Strain at Maximum Stress - %									
	Strain Rate - in/in/min									
	10	20	40	70	100	200	400	700	1000	
FSU 25	45.9	44.2	42.2	40.6	39.4	36.9				
1/3 Scale 11	49.0	48.8	47.9	46.3	45.0	40.9				
FPC 1891				41.8				32.5		
FPC Lot 1-10-66	52.5	51.0	48.0	45.0	43.0	39.5	36.0	33.8	32.0	
FPC 1826	54.5	52.0	48.5	46.0	43.5	39.5	35.8	33.0	31.5	
FPC 1886	55.5	53.5	50.5	48.0	44.8	41.5	37.5	34.5	32.5	
FSU 32633	45.8	43.9	41.6	39.5	37.7	35.4	33.6	32.0	30.9	
FSU 32765	48.5	46.5	44.0	41.9	40.7	39.2	35.9	34.3	33.2	
FSU 32645	46.5	44.7	42.8	40.9	39.5	37.3	34.9	33.0	31.8	
FSU 32743	48.0	46.1	43.9	42.2	40.9	38.6	36.4	34.7	33.6	
FSU 32769	49.1	47.5	45.5	43.6	42.4	41.0	37.6	36.0	34.8	
FSU 32720	48.0	46.1	44.0	42.0	41.0	38.7	36.3	34.6	33.5	
FSU 33231	50.5	48.3	46.1	43.8	42.4	39.2	36.4	34.5	33.4	
FSU 33348	45.0	43.0	41.1	39.8	39.0	37.5	36.0	34.4	33.4	
FSU 32570	46.2	45.5	44.3	43.2	42.5	40.3	38.0	36.0	35.3	
FPC 1189	46.3	43.6	40.8	38.8	37.7	35.3	33.2	31.3	30.2	
FSU 336	49.0	47.0	45.0	44.0	43.0	41.0	38.0	36.0	35.0	
FPC 1139				40.8	38.9	35.2	32.5	30.2	28.9	
Reference Temperature 77°F										



the motor at ignition and therefore includes only units for which short-time relaxation data are available. In addition, the data presented for FPC's 1139 and 1140 in Report No. 7\* were presented after shifting to 700° F and neither shift factors nor the sample data are recoverable from the report: the shift factors are not those in Figure 4-1 and are apparently different for each data point. Because of the errors involved in guessing at the required shift factors, it was judged that these units did not add to the overall validity of the data set.

The relaxation modulus for FSU 336 presented in Table 4-4 also requires some explanation. Relaxation testing was done on propellant from this unit at three different times, specifically at ages of 30, 38, and 45 months. Primary and secondary aging trends were calculated. The data presented herein were taken from the first series of tests for grain 336, which was the time of initial dissection of the motor (Report No. 33). The value of  $10^{-4}$  seconds in Table 4-4 for grain 336 was extrapolated since the shortest time presented in the report at 77° was 0.00023 seconds. All other values are within the shifted time range of the relaxation data.

The LRSLA and Overtest motors provided most of the relaxation modulus data presented in Table 4-4. The LRSLA motors are serial numbers 32633, 32755, 32769, 32743, 32645, 32720, and 33231. The first six of these are model LGM 30B motors and the last one is an LGM 30F motor. The six-year Overtest motor is S/N 33348, and it is an LGM 30F motor. The nine-year Overtest motor is S/N 32570, and it is an LGM 30B motor. Relaxation testing was performed on LRSLA samples at a constant strain at 2 percent with superimposed pressure of 300 psi. Relaxation testing was performed on the Overtest motors and on motors FPC1571, FSU3174, and FSU336 at ambient pressure at strains from 1/2 to 1 percent. Samples were taken from two motor locations in the LRSLA motors and three motor locations in the Overtest motors. Test data from the several locations in each motor were averaged together to give the single relaxation curve which is tabulated for each motor in Table 4-4. Data from all twelve units of Table 4-4 are presented in graphic form in Figure 4-2. Although the data are closely grouped, it should be noted that the two LGM 30F motors (S/N's 33348 and 33231) are on the high and low sides, respectively, of the range of data.

Twenty units listed in Table 4-3 have been tested in uniaxial or biaxial tension at strain rates between 10 and 1000 in./in./min, but only 18 of these units are represented in Table 4-5. The two units that were not used are 1/3 scale Minuteman No. 6 and FPC 1571. Figure 4-3, which is a plot of data from 20 units, indicates that these two units are markedly different than the rest of the population. Data at only two rates, 10 and 1000 in./in./min could be extracted from the report on FPC 1571. Other data on units made from powder lot RAD 1-7-65 were available from the LRSLA program, so it was judged that the inclusion of FPC 1571 into the data set would only increase the variance of the data without improving its validity. The shape of the curve of strain versus strain rate of 1/3 scale Minuteman No. 11 was so different from the shapes of the curves from all other units that the data were not included in Table 4-5.

\*Report numbers given in the text of this section correspond to the report numbers listed in the Bibliography at the end of this section.

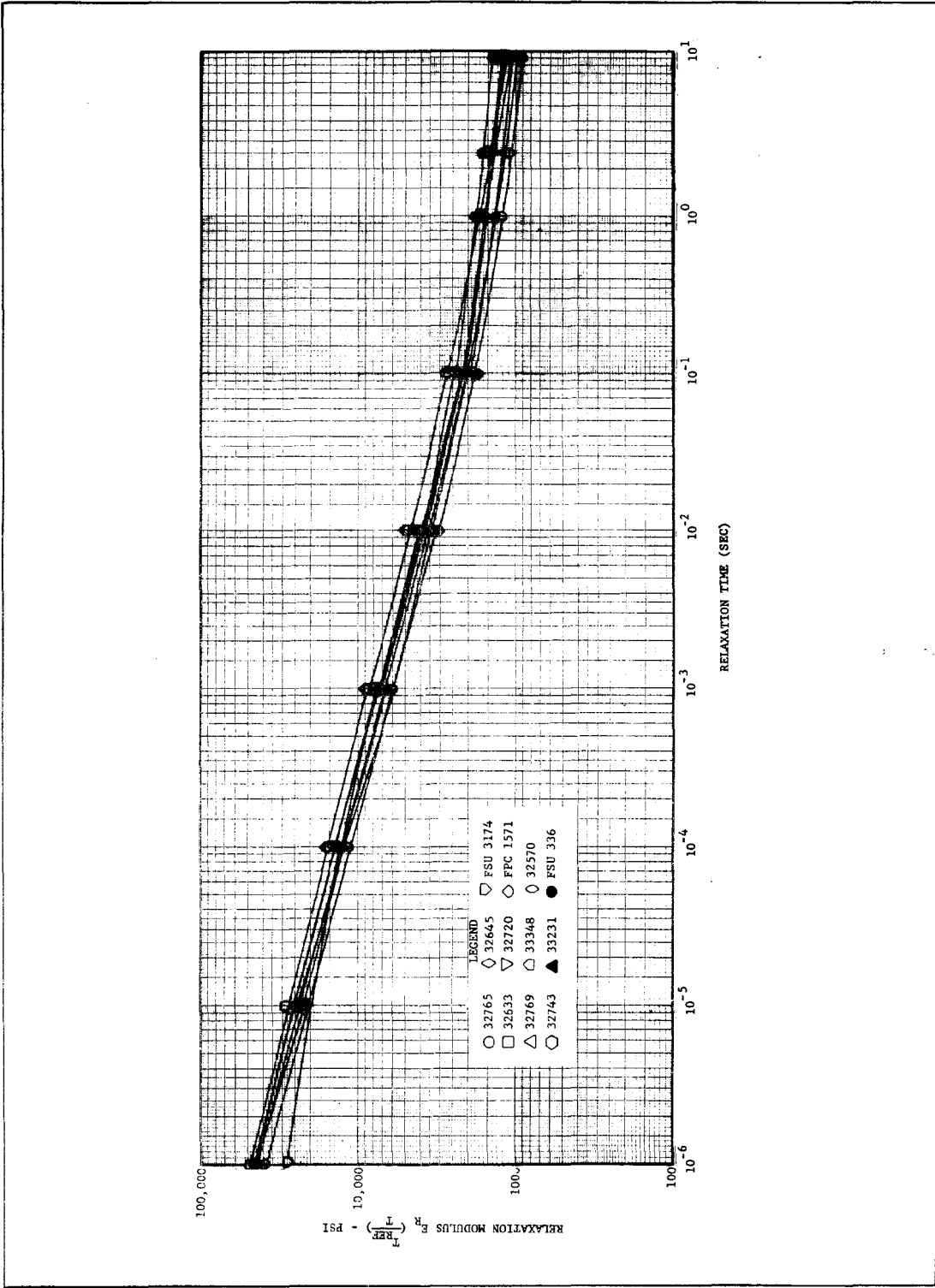


Figure 4-2. Short-Time Relaxation Data of Units Obtained from MM History

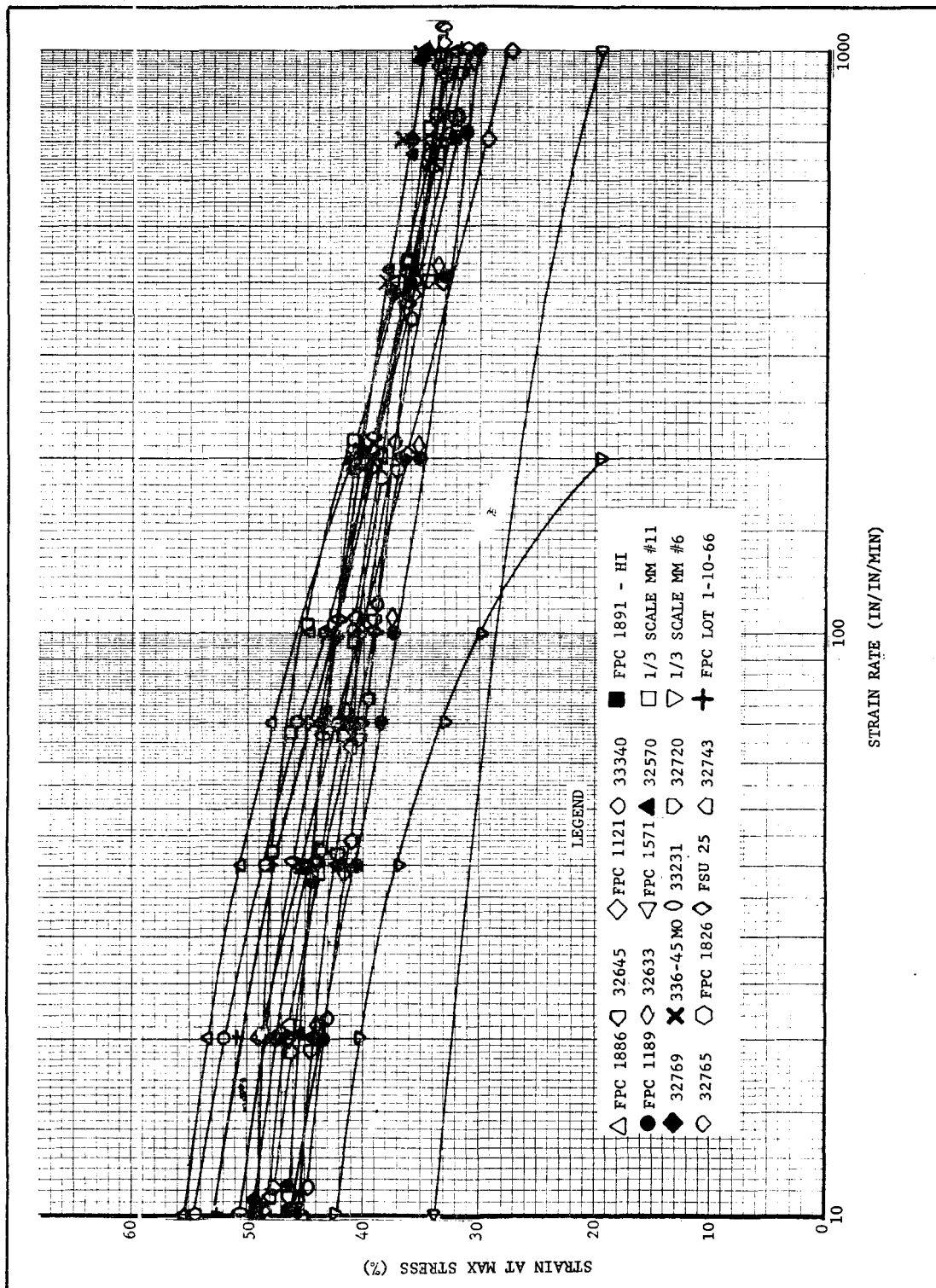


Figure 4-3. High-Rate Strain of Units Obtained from MM History

The data from the LRSLA and Overtest motors were taken in both uniaxial tension and biaxial tension with superimposed pressure of 300 psi. Samples from the Overtest motors and from LRSLA motor S/N 32633 were tensile tested at a variety of rates over the range of interest. The testing of propellant from the remaining LRSLA motors was performed only at three (temperature shifted) rates which were 0.86, 860 and  $10^6$  in./in./min at 77° F. The data taken from unit 32633 was presumed to establish the shape of the strain versus strain rate curve for each sample location for all LRSLA motors, and the individual LRSLA motor data were used to position the strain curves for the individual units. To extract the data presented in Table 4-5 for these six LRSLA motors, at each sample location the shifted individual unit data were plotted together with the curve obtained from S/N 32633, a curve was drawn through the data points parallel to that of 32633, and strain at maximum stress was read from the curve at each rate listed in Table 4-5. This process was repeated for each of the sample locations for both uniaxial tension specimens and biaxial strip specimens. Strains at each rate were averaged to give the data presented for each motor.

The strain data reported for FSU 25 was taken from four different locations. Testing was performed at ambient pressure. The strain at each rate was read from the curves presented in the report for each of the four locations. The average strain at each rate was calculated and is presented in Table 4-5. In the report for FPC 1891, data were presented only at rates of 86 and 860 in./in./min. Curves were drawn through these points and strain was read at rates of 70 and 700 in./in./min, but there was not enough confidence in the validity of the curves to interpolate strain values any farther away from the published data points. The data presented in Table 4-5 for FPC 1891 is the average of results of three test groups of uniaxial tension samples and two test groups of JANNAF samples made and tested by Hercules Incorporated.

Because the relaxation modulus data (Table 4-4) sample is small, the validity of the variation in relaxation modulus calculated from this population was questionable. Additional data are available (see Table 4-3) for relaxation times of 0.07 second and larger. The variance of modulus at short times can be equated with the variance obtained in the range of 0.1 to 10 seconds by time-temperature shifting of test data measured at low temperatures and relaxation times of 0.07 second and larger. Twelve units, in addition to the twelve already presented in Table 4-4, could be added to the data set, and this resulting sample of 24 units is shown in Table 4-6. The propellant lots from which these units were made, and the age of the unit at the time of sample testing are also shown in the table.

Propellant lot acceptance data are presented in Table 4-7. These data are given here because Report No. 31 has never been published in entirety.

The majority of the data pertaining to aging trends was obtained by OALC in the Dissected Motor Program. Three sections of the Dissected

TABLE 4-6  
STRESS RELAXATION DATA FOR STUDY OF VARIABILITY

Unit	Propellant Lot	Age @ Test Months	Relaxation Modulus - psi			
			Relaxation Time - sec			
			0.1	1.0	2.45	10
32633	RAD 1-5-64	107	2767	1733	1440	1183
33231	RAD 1-14-66	91	1833	1333	1200	1050
32720	RAD 1-6-64	115	2317	1650	1460	1233
32645	RAD 1-5-64	112	2266	1600	1400	1200
32743	RAD 1-6-64	110	2400	1883	1630	1417
32769	RAD 1-7-65	108	1817	1350	1170	983
32765	RAD 1-7-65	105	1783	1233	1100	923
33348	RAD 1-16-66	71	2750	1770	1600	1380
32570	RAD 1-3-64	113	2480	1700	1500	1280
FSU 3174	RAD 1-10-66	54	2450	1660	1490	1250
FPC 1189	SR 58-63	6*	2380	1580	1438	1071
FSU 336	SR 68-62	30	2590	1680	1377	1190
SD 25	SR 11-63	6*	2721	1822	1595	1293
1/3 Scale 6	SR 28-63	0*	2230	1420	1210	934
1/3 Scale 11	SR 28-63	0*	2500	1691	1490	1093
FPC 2048	RAD 1-20-70	10	2589	1775	1550	1255
FSU 2158	SR 51-63	99	2354	1660	1470	1202
FSU 2137	SR 51-63	102	2174	1552	1370	1139
FPC 1891	RAD 1-13-66	2	1978	1283	1129	907
FPC Lot 1-10-66	RAD 1-10-66	Unknown	1950	1250	1070	850
FPC 1826	RAD 1-14-66	6*	1900	1300	1120	925
FPC 1886	RAD 1-15-67	0*	1780	1190	1020	850
FPC 1571	RAD 1-7-65	3	2150	1410	1200	950
FPC 1139	SR 28-63	6*	2180	1420	1210	1015
* Test date is not given in the report. If the report date is more than 1 year after the unit cast date, the age is assumed as 6 months. If the report date is less than 1 year after the cast date, the age is assumed as zero.						

TABLE 4-7

## MINUTEMAN II STAGE III PROPELLANT ACCEPTANCE VALUES

Powder Lot No.	Maximum Stress (psi)	Strain at Rupture (%)	Initial Tangent Modulus (psi)
<u>CYH Propellant</u>			
SR-68-62	394.3	64.8	768.2
SR-11-63	320	66.6	634
SR-28-63	284	68.0	602
SR-9B-63	312	59.5	721
SR-51-63	326	66.1	683
SR-58-63	366	61.7	791
RAD 1-7-64	334	57.4	819
RAD 1-8-65	341	55.8	918
RAD 1-9-65	295	55.8	869
RAD 1-10-66	299	59.7	736
RAD 1-11-66	329	60.6	792
RAD 1-12-66	343	60.4	801
RAD 1-13-66	284	60.3	726
RAD 1-14-66	300	60.7	743
RAD 1-15-67	295	61.2	752

TABLE 4-7 (Cont)

## MINUTEMAN II STAGE III PROPELLANT ACCEPTANCE VALUES

Powder Lot No.	Maximum Stress (psi)	Strain at Rupture (%)	Initial Tangent Modulus (psi)
RAD 1-16-67	295	59.0	802
RAD 1-17-68	336	58.8	836
RAD 1-18-68	312	60.2	880
RAD 1-19-68	350	61.1	811
RAD 1-20-70	296	60.3	850
RAD 1-21-70	335	60.8	759
<u>DDP Propellant</u>			
SR-67-62	298	66.1	630
SR-8-63	311	60.5	755
SR-27-63	308	59.8	710
SR-70-63	320	49.9	881
SR-69A-63	301	57.6	839
RAD 1-1-64	300	58.0	849
RAD 1-2-65	323	54.7	952
RAD 1-3-65	337	52.4	978
RAD 1-4-66	260	57.3	741

TABLE 4-7 (Cont)

## MINUTEMAN II STAGE III PROPELLANT ACCEPTANCE VALUES

Powder Lot No.	Maximum Stress (psi)	Strain at Rupture (%)	Initial Tangent Modulus (psi)
RAD 1-5-66	278	56.8	848
RAD 1-7-67	278	55.9	908



Motor Program are utilized in this study: low rate tensile, high rate triaxial, and stress relaxation. The Dissected Motor Program data are available from Reports 30, 32, and 53, and are therefore not tabulated here. However, applicable trend data obtained by Hercules in the Overtest, LRS LA, and the various Minuteman programs are to be added to the Dissected Motor Program trend data in interpreting the program results. Therefore, the Hercules data are presented here.

The conditions of the low rate tensile test performed by OALC are: 1/4 inch JANNAF sample, crosshead speed 2 in./min (strain rate of 0.74 in./in./min), 77° F, and ambient pressure. The reduced data obtained from each test are maximum stress, stress at rupture, strain at maximum stress, strain at rupture, and initial tangent modulus. Table 4-8 presents the applicable Hercules data obtained at the same test conditions, together with propellant lot and age. The OOAMA-Hercules Cooperative Test Program (report No. 25) revealed a difference in the data reduction method for maximum stress which resulted in a statistically significant difference in data. Furthermore, propellant stress is not a necessary property for the calculation of motor failure. For these reasons and because the trends in strain and in modulus are emphasized in this aging trend study, values of propellant stress are not shown in Table 4-8. Report No. 25 did further prove that strain at maximum stress obtained from JANNAF samples and uniaxial tension samples at crosshead speeds of 2 in./min was not statistically different, so these data are included in Table 4-8 along with an indication of sample type.

The tension testing performed on samples from motors SD-25, 1/3 scale MM 6, and 1/3 scale MM 11 was conducted at 70° F. The lowest rate tested was 2 in./min (which could be 0.86 or 0.74 in./in./min - the sample type is not identified in Report 4). The equivalent rate for shifting to 77° F is 0.3 or 0.25 in./in./min. It does not appear advisable to extrapolate these data outside the rate range presented; therefore, no data from these units are given in Table 4-8.

Data from an FPC cast from Lot RAD 1-10-66 are presented in Report 24, but insufficient information is given in the report to identify the unit and the casting date. Since the purpose of Table 4-8 is to define aging trends, this unit was excluded from Table 4-8.

The values presented for FPC 1891 are the averages from samples tested by Hercules and OALC. Data presented for the LRS LA and Overtest motors are the averages of all samples tested from these units. Data from FSU 336 are omitted from Table 4-8 because testing was performed at 70° F at 0.86 in./in./min; extrapolation of these data to 0.3 in./in./min to perform temperature shifting was not justifiable.

The values presented for LRS LA motor 32633 were obtained from specimens machined about 1 year after initial motor dissection. The LRS LA requirements did not include testing of tension samples at 2 in./min, 77° F,

TABLE 4-8

TREND DATA  
TENSILE TEST RESULTS

Unit	Propellant Lot	Age (mo.)	Sample Type	Strain at Max Stress (psi)	Strain at Rupture (%)	Initial Tangent Modulus (psi)
32769	RAD 1-7-65	108	UT	44.1	51.7	1938
32765	RAD 1-7-65	105	UT	44.7	53.5	1559
32645	RAD 1-5-64	112	UT	42.1	49.4	1829
32743	RAD 1-6-64	110	UT	44.1	51.1	1550
32720	RAD 1-6-64	115	UT	44.5	49.6	1554
32633	RAD 1-5-64	107	UT	42.1	48.8	1818
32570	RAD 1-3-64	113	UT	40.1	47.4	1576
33348	RAD 1-16-66	71	UT	42.7	49.1	2084
FPC 1273	RAD 1-1-64	67	J	40.1	47.4	998
FPC 1327	RAD 1-3-64	65	J		47.1	946
FPC 1604	RAD 1-8-65	52	J		47.8	918
FPC 1779	RAD 1-10-65	39	J		60.	840
FPC 1827	RAD 1-14-66	36	J		61.5	882
FPC 1886	RAD 1-15-67	29	J		61.5	864
FPC 1886	RAD 1-15-66	0*	UT	49		
FPC 1912	RAD 1-16-67	25	J		59.6	869
33231	RAD 1-14-66	91	UT	48.5	55.2	1546
FPC 1891	RAD 1-13-66	2	J	48.8	57.6	
FPC 1189	SR 58-63	6*	UT	38.7		
FPC 1571	RAD 1-7-65	3	J	50.	58.	
FPC 1826	RAD 1-14-66	6*	UT	49		
*Test date is not given in the report. If the report data is more than 1 year after the unit cast date, the age is assumed as 6 months. If the report data is less than 1 year after the cast date, the age is assumed as zero.						
Test Conditions: 2 in/min CHS 77°F ambient pressure						

and ambient pressure, so the sample testing was carried out in the Overtest program. NPC 1886 was subjected to testing at two different times and thus appears twice in Table 4-8. The first test was performed as part of a special investigation performed in 1967 (Report No. 24), in which strain at maximum stress was determined at 4 rates from 0.8 to 860 in./in./min. Propellant from FPC 1886 was also used in the Pressure Oscillation Investigation (Report 27); the acceptance testing was repeated in August 1969.

The high rate triaxial test performed by OALC is as follows: biaxial strip sample, 1750 in./min (1000 in./in./min) test rate at 77° F temperature and superimposed pressure of 300 psi. The only additional data applicable to aging trend analysis were obtained from the LRSLA program and are presented in Table 4-9. These values from biaxial strip tests were obtained in the same manner as for Table 4-3, and are not significantly different from the average values presented at a rate of 1000 in./in./min for the LRSLA motors.

TABLE 4-9

BIAXIAL STRAIN AT MAXIMUM STRESS AGING TREND DATA

Unit	Age (months)	Strain at Maximum Stress (%)		
		Cylindrical Section	Aft Dome	Average
32633	107	31.5	31.5	31.5
32765	105	33.5	31.0	32.3
32645	112	32.0	32.7	32.4
32743	110	32.9	33.2	32.6
32769	108	36.0	32.0	34.0
32720	115	34.8	34.0	34.4
33231	91	35.0	33.5	34.3
Sample: Biaxial strip Reference temperature: 77° F Strain rate: 1000 in./in./min Superimposed pressure: 300 psi				

Results of stress relaxation testing from the Dissected Motor Program are reported as values of relaxation modulus at 10, 50, 100, and 1000 seconds. These times are large compared to the time range that is used in motor failure calculations. The shortest of these times was therefore chosen for trend analysis. The test conditions were 77° F and 3 percent constant strain. Data in addition to that from the Dissected Motor Program are presented in Table 4-6.

#### C. INTERPRETATION OF CYH PROPELLANT PROPERTIES

The objective of this section is to refine and correlate the raw data set previously discussed and to transform these data to a form suitable for the prediction of motor service life.

The ideal way to characterize the entire motor population at a given time would be to obtain data at regular intervals on relaxation modulus and strain at maximum stress from every motor in the existing inventory. The mean and variance calculated from such ideal data would then obviously be the exact mean and variance of the population at each time. The next best way to characterize the population would be to obtain relaxation modulus and strain at maximum stress from a random sample of motors of the entire population at various times. The statistics calculated from this sample data set would then be technically considered to be estimates of the mean and variance of the entire population. Statistical techniques would be used to calculate upper and lower limits within which lie the true mean and variance of the entire population as a function of time. Necessarily, the higher the probability that the true mean and variance lie within the upper and lower limits, the wider these limits are.

The problem at hand, however, bears only a faint resemblance to the ideal situation outlined above. Propellant properties are not available from the individual motors still in the inventory. Available data were taken for a variety of purposes and at a variety of times. Unit age then becomes the only possible time base, which will be difficult to interpret if strong age-dependency exists, as the motor inventory consists of units of various ages.

The propellant lot acceptance data approximate the desired random sample of all motors at zero unit age. The lot data, however, have a number of deficiencies which hinder establishing the values of properties for service life calculations. The lot acceptance test was performed on samples cut from an FPC cast from the powder from each propellant lot. The acceptance uniaxial tension tests were as follows: 1/4 inch JANNAF specimen, 2 in./min crosshead speed (0.74 in./in./min strain rate), 77° F temperature, and ambient pressure. The propellant properties needed for service life calculations are: relaxation modulus from  $10^{-6}$  to 1 second, and strain at maximum stress at strain rates from 10 to 1000 in./in./min.

## 1. Strain at Maximum Stress

The data set for strain at maximum stress, Table 4-5, consists of data from 11 full-scale units and 7 subscale units. Since it is possible that the strain capability of propellant depends on the casting configuration, a t-test\* of equality of means was performed on the data at rates of 70 and 700 in./in./min. Table 4-10 presents the data and statistics used in the test. It is concluded that the means are not significantly different, so the data from all units may be grouped and considered together.

The trend data presented in Table 4-8 are also composed of a mixture of FPC and FSU data. Table 4-11 presents the t-test of equality of means for data taken at 2 in./min crosshead speed. FPC's and FSU's are equivalent in regard to strain, but not in regard to initial tangent modulus. In the study of aging trends of tangent modulus, only data taken on propellant from FSU's can be compared to trend data obtained in the Dissected Motor Program.

The method of trend analysis reported herein, and in the Dissected Motor Program, is to plot the value of the physical property versus age for the samples, and to calculate the regression equation as:

$$(\text{Value of Property}) = \text{Constant} + (\text{Aging Trend} \times \text{Age})$$

The standard deviation with respect to the trend line ( $S_y/x$ ) and the correlation coefficient (R) are also calculated. The correlation coefficient is of value in determining the dependence of the property on age. The quantity  $R^2 \times 100$  is equal to the percentage of the variation of the data which is explained by the regression line. A minimum correlation coefficient of 0.8 is required to establish the existence of a valid relationship between the dependent and independent variables; i.e., 64 percent of the variation in the property is accounted for by the linear regression equation.

The trend data relating to strain were first examined on the basis of individual propellant lots. One of the difficulties with this approach is that there are few lots for which many data points have been obtained. More data are available on lot SR 68-62 than any other. Trend data on strain at maximum stress from low rate tensile tests are presented on Figure 4-4, and from high rate triaxial tests on Figure 4-5. The most important result of the regression analyses of these data is that for both strain rates the correlation between strain and age is too low to suggest the existence of a correlation. If only data obtained by OALC are considered, there is excellent agreement between the aging trends (0.015 to 0.018 percent strain per month). However, if all available data

---

\*The statistical treatments used in this report are taken from: Bowker, A. H. and Lieberman, G. J., Engineering Statistics, Prentice-Hall, Inc., Seventh Printing, 1965.

TABLE 4-10

TEST FOR EQUALITY OF MEANS OF STRAIN AT HIGH STRAIN RATES  
OBTAINED FROM FPC'S AND FSU'S

Strain Rate - 70 in./in./min			Strain Rate - 700 in./in./min		
Unit	Strain (%)	Unit	Strain (%)	Unit	Strain (%)
FPC 1891	41.8	SD 25	40.6	FPC 1891	32.5
FPC Lot 1-10-66	45.0	32633	39.5	FPC Lot 1-10-66	33.8
FPC 1826	46.0	32765	41.9	FPC 1826	33.0
FPC 1881	48.0	32645	40.9	FPC 1886	34.5
FPC 1189	38.8	32743	42.2	FPC 1189	31.3
FPC 1139	40.8	32769	43.6	FPC 1139	30.2
1/3 Scale 11	46.3	32720	42.0		
		33231	43.8		
		33348	39.8		
		32720	43.2		
		FSU 336	44.0		
$N_x = 7$ $\bar{x} = 43.81$ $S_x = 3.37$ $t = 1.59$ $t_{0.005, 16} = 2.921$			$N_y = 11$ $\bar{y} = 41.95$ $S_y = 1.60$ $t = 2.18$ $t_{0.005, 14} = 2.977$		
Accept equality of means at 1% significance level (~99% confidence level)			Accept equality of means at 1% significance level (~99% confidence level)		

TABLE 4-11

TEST FOR EQUALITY OF MEANS OF PROPERTIES OBTAINED AT 2 IN./MIN CHS

Strain at Maximum Stress				Strain at Rupture				Initial Tangent Modulus			
Unit	Strain (%)	Unit	Strain (%)	Unit	Strain (%)	Unit	Strain (%)	Unit	Modulus (psi)	Unit	Modulus (psi)
FPC 1273	40.1	32769	44.1	FPC 1273	47.4	32769	51.7	FPC 1273	998	32769	1938
FPC 1886	49.0	32765	44.7	FPC 1327	47.1	32765	53.5	FPC 1327	946	32765	1559
FPC 1891	48.8	32645	42.1	FPC 1604	47.8	32645	49.4	FPC 1604	918	32645	1829
FPC 1189	38.7	32743	44.1	FPC 1779	60.0	32743	51.1	FPC 1779	840	32743	1550
FPC 1571	50.0	32720	44.5	FPC 1827	61.5	32720	49.6	FPC 1827	882	32720	1554
FPC 1826	49.0	32633	42.1	FPC 1886	61.5	32633	48.8	FPC 1886	864	32633	1818
		32570	47.7	FPC 1912	59.6	32570	47.4	FPC 1912	869	32570	1576
		33348	42.7	FPC 1891	57.6	33348	49.1			33348	2084
		33231	48.5	FPC 1571	58	33231	55.2			33231	1546
$N_x = 6$ $\bar{x} = 45.93$ $s_x = 5.10$ $t = 0.75$				$N_x = 9$ $\bar{x} = 55.61$ $s_x = 6.28$ $t = 0.55$				$N_x = 7$ $\bar{x} = 902.4$ $s_x = 55.05$ $t = 117.58$			
$t_{0.005, 13} = 3.012$ Accept equality of means at 1% significance level				$t_{0.005, 16} = 2.921$ Accept equality of means at 1% significance level				$t_{0.005, 14} = 2.977$ Reject equality of means			

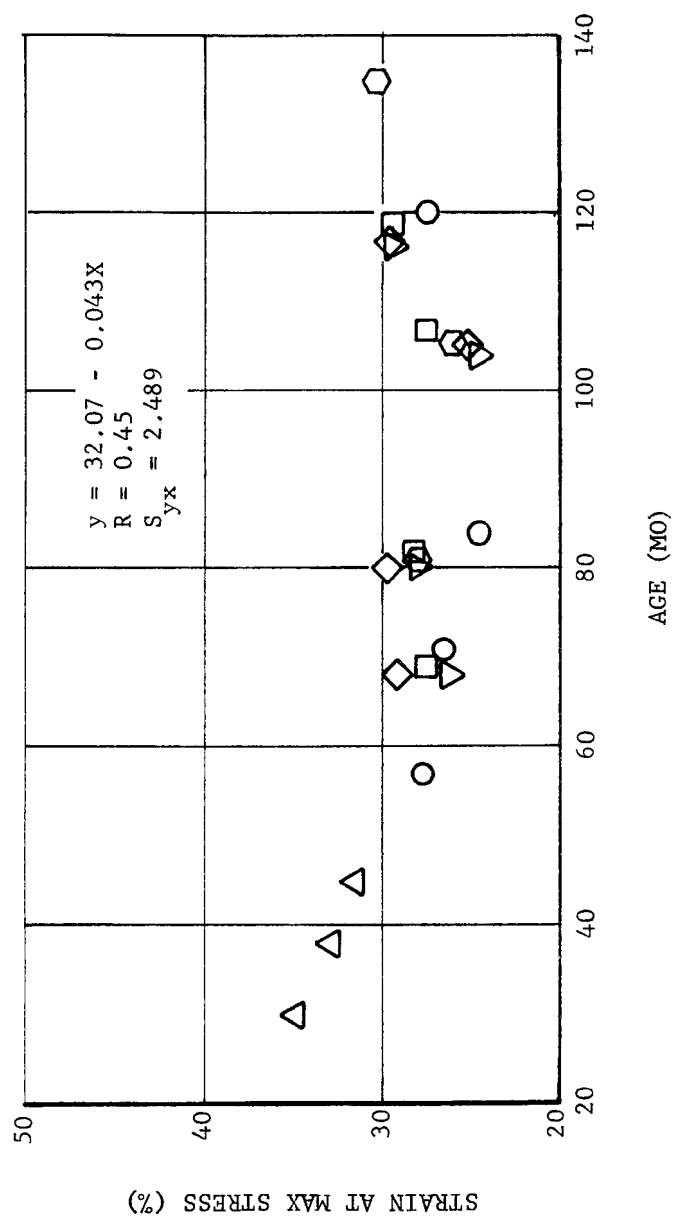


Figure 4-4. Strain at Maximum Stress, Lot 68-62, 2 in./min



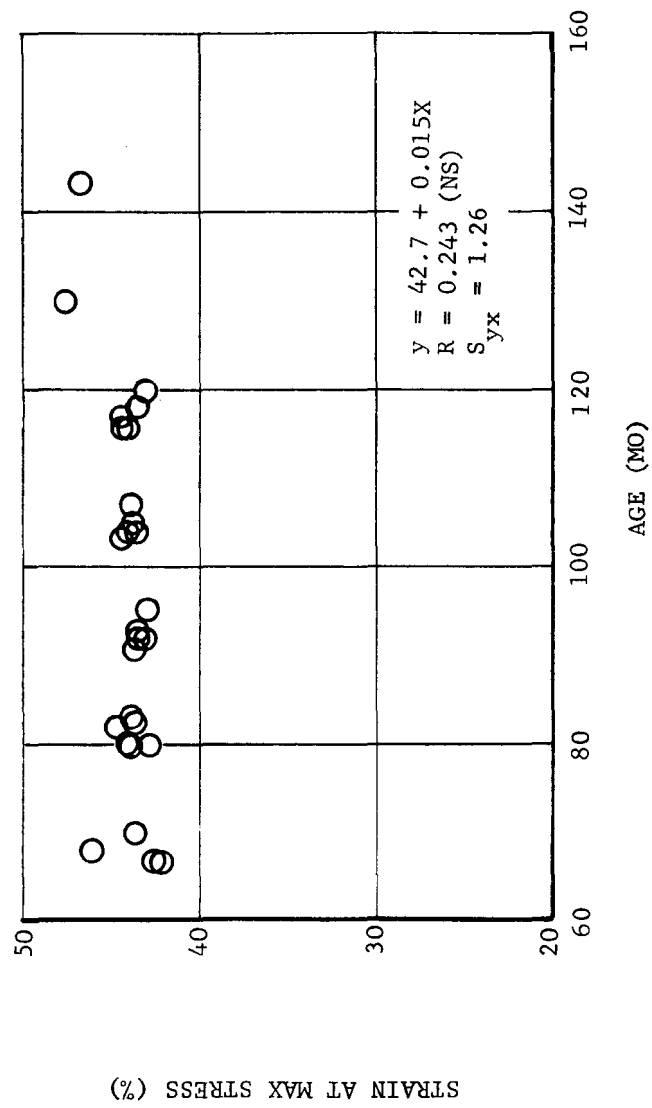


Figure 4-5. Strain at Maximum Stress, Lot 68-62, 1000 in./in./min

applicable to this lot are considered, the high rate triaxial tests are found to indicate a decreasing trend and the low rate tensile tests indicate an increasing trend. It is absurd to consider that propellant aging in bulk depends upon the sample which will be machined from it at some later date. The low correlation coefficient indicates that no relationship exists between strain and age, i.e., there is no aging trend indicated from the data.

Aging trend data from lot RAD 1-1-63 is presented in Figures 4-6 and 4-7. The OALC data comes from only one motor. The conclusions are almost the same as for lot SR 68-62. The low value of the correlation coefficient indicates that there is no cause-and-effect relationship between age and strain. When all data are considered, there are contradictory aging trends indicated by low rate tensile and high rate triaxial testing results. When only OALC data is considered, the agreement between aging trends is poor, being different by a factor of 10. No aging trend is indicated by these data.

This same sort of trend analysis was also performed for all the other propellant lots of Minuteman II powder that are included in the Dissected Motor Program. These lots are: RAD 1-8-65, SR 58-63, SR 28-63, SR 51-63, and RAD 1-10-66. In addition, the aging trend of strain at rupture was examined. For all lots, it was concluded that no aging trend existed.

Data from all powder lots are grouped together for the trend study illustrated in Figures 4-8 and 4-9. The regression equations and descriptive statistics of the regression are also given. Figure 4-8 presents data taken at 2 in./min crosshead speed and Figure 4-9 presents data taken at 1000 in./in./min. Data from both test conditions have a decreasing regression line, although the slope of the high rate triaxial data is 2-1/2 times as great as the slope of the low rate tensile data. As was the case for strain data examined on the basis of individual lots, the correlation coefficient is too low to prove the existence of a cause-and-effect relationship between strain and age. The conclusions that were previously drawn from the analysis of separate lot data are supported by this examination of all data. For propellant property of strain at maximum stress, no age-related changes are occurring.

The next step in the analysis of strain data was to determine if the properties of each propellant powder lot are directly related to the value of properties measured in other units (FPC's or FSU's) made from the same powder lot. There is no standard statistical treatment available to directly treat this problem, but a variant of the rank-sum test is suggested as giving an indication. Table 4-12 shows a comparison of ranking based on individual unit values at 100 in./in./min and 700 in./in./min, versus ranking in order of lot acceptance values of strain at rupture. In case of ties in value, the average rank was assigned. If the value of the lot acceptance test determined absolutely the value of the property in the unit made from the lot, the six highest lots would appear in order

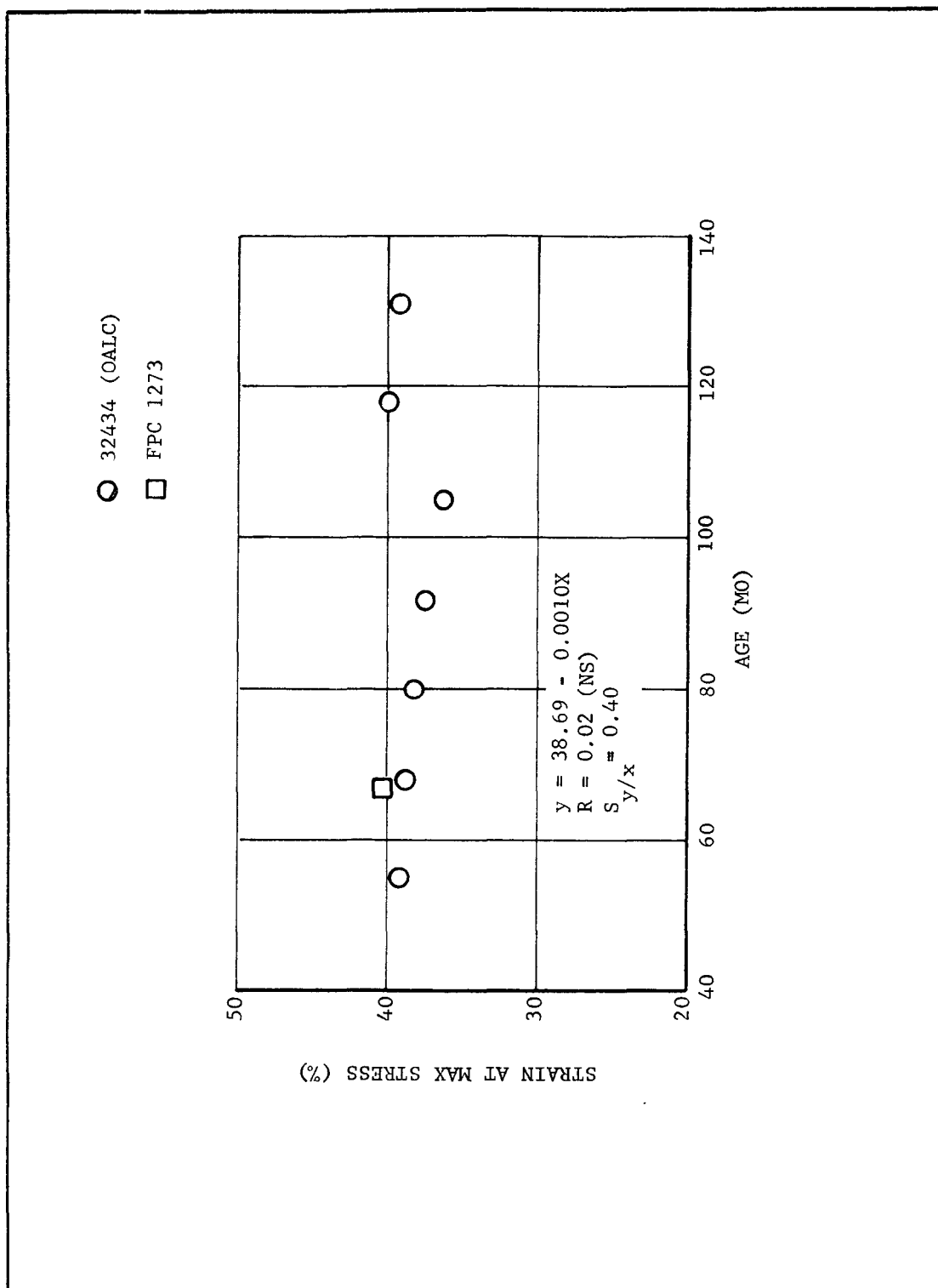


Figure 4-6. Strain at Maximum Stress, Lot 1-1-63, 2 in./min

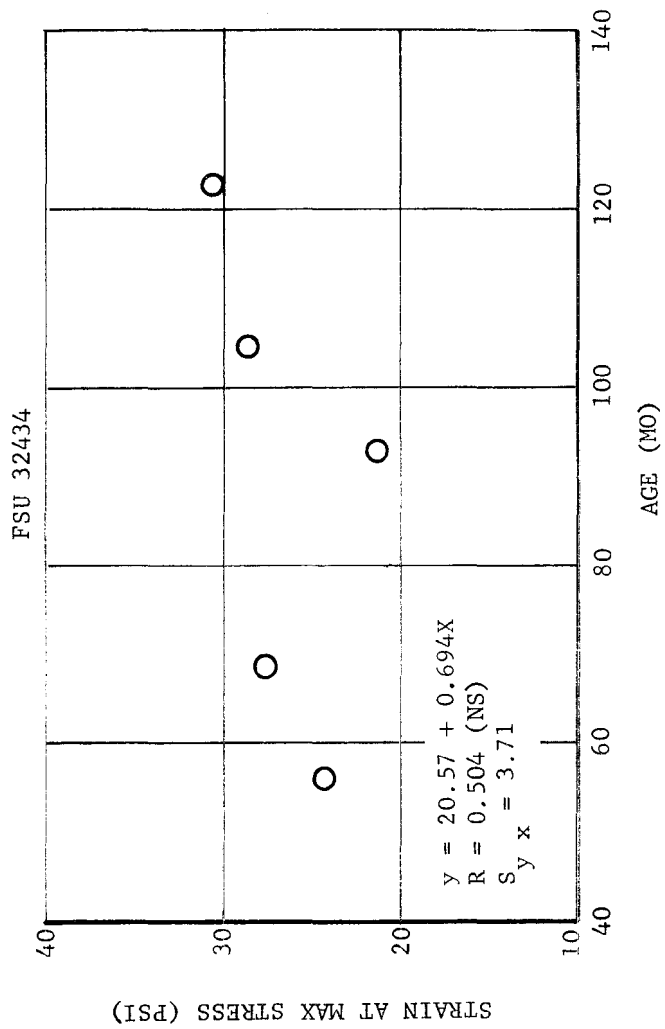


Figure 4-7. Strain at Maximum Stress, Lot 1-1-63, 1000 in./in./min

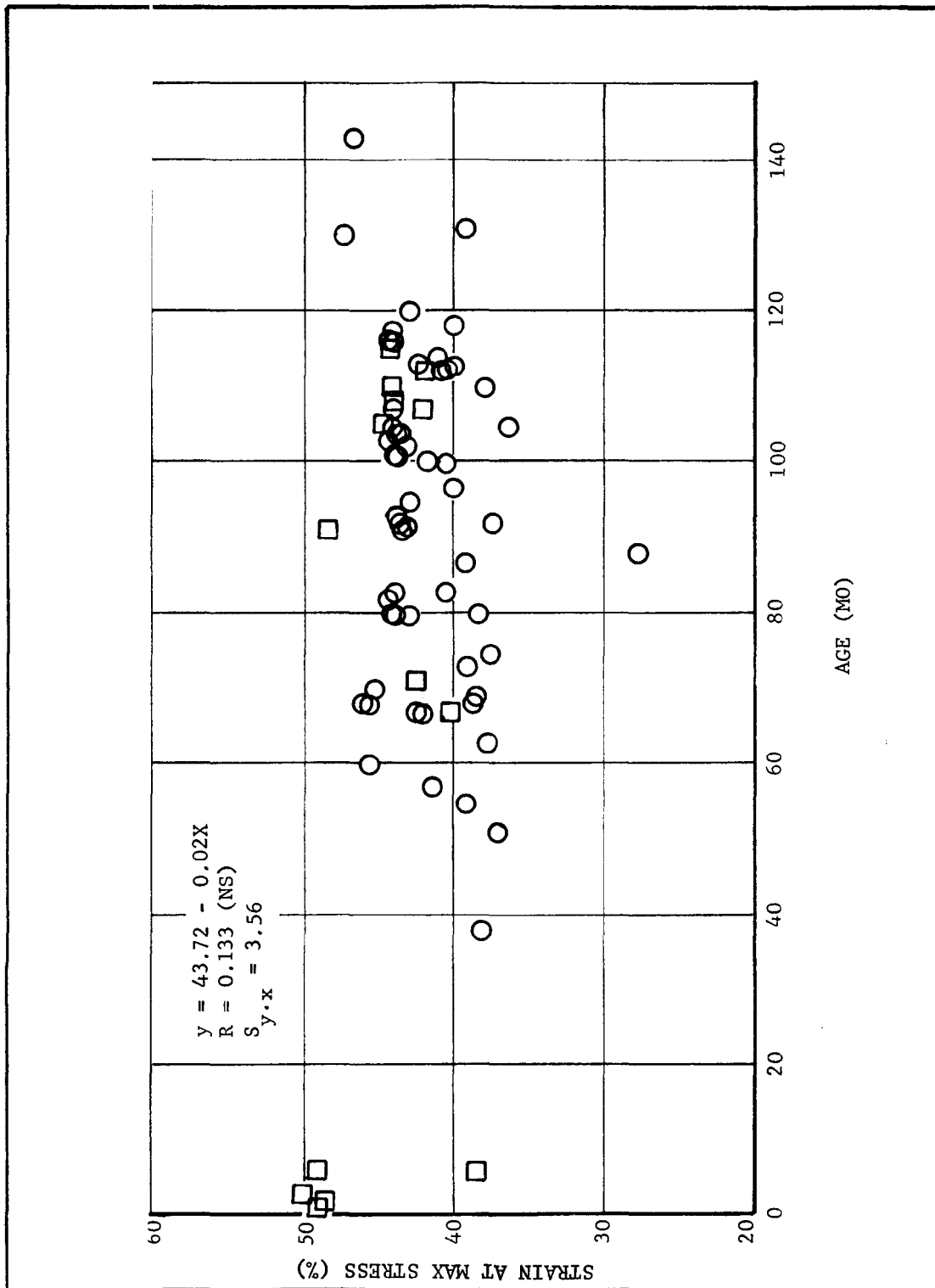


Figure 4-8. Strain at Maximum Stress, All Lots Together, 2 in./min

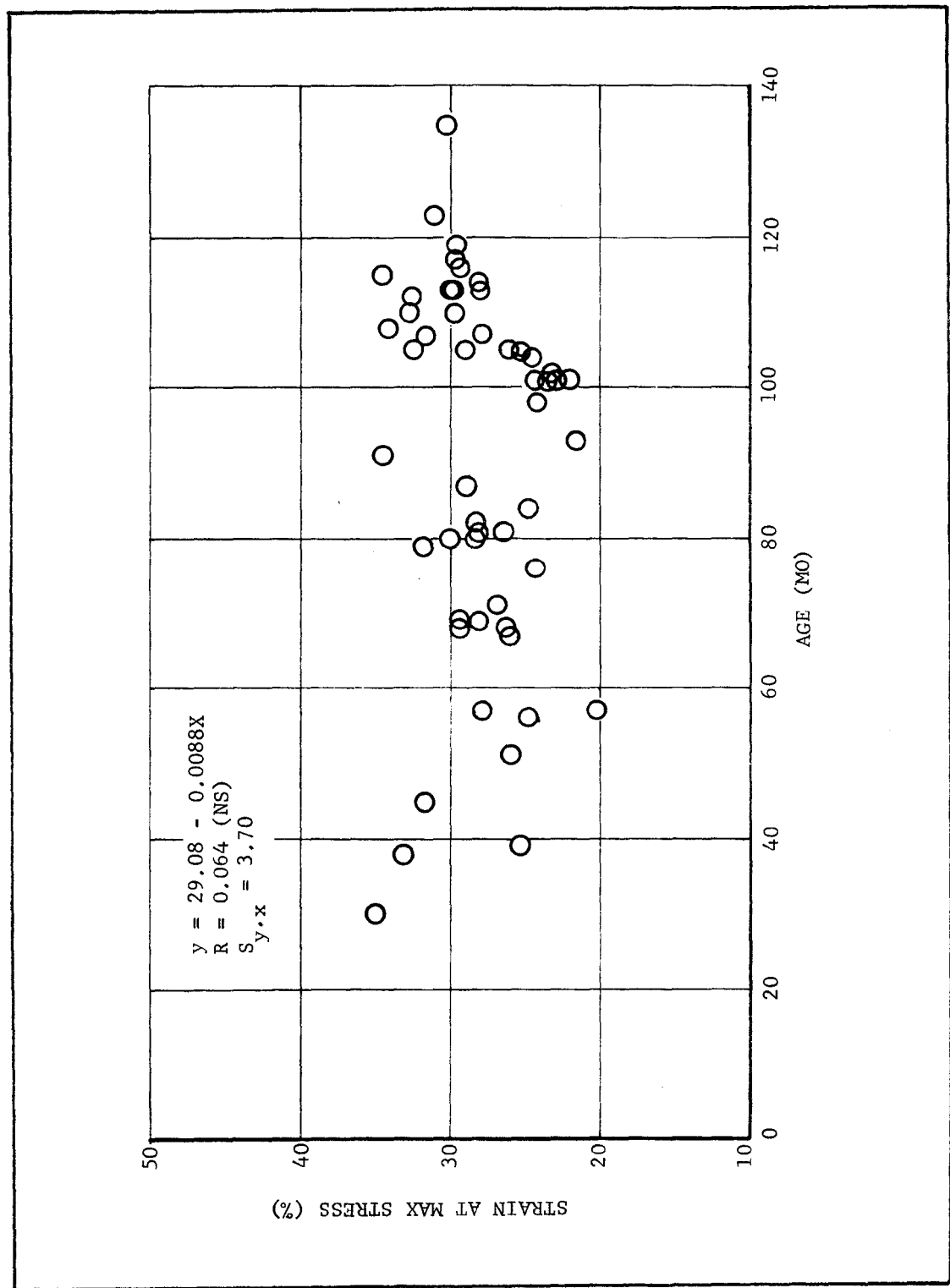


Figure 4-9. Strain at Maximum Stress, All Lots Together, 1000 in./in./min

TABLE 4-12

RANK TEST OF THE INFLUENCE OF POWDER LOT ACCEPTANCE VALUES

Strain at 100 in./in./min				Strain at 700 in./in./min			
Unit	Rank of Strain	Rank of Lot Value	Summary	Unit	Rank of Strain	Rank of Lot Value	Summary
1/3 Scale 11	1	1	There are 12 lots in this sample of units	32769	2	12	There are 12 lots in this sample of units
FPC 1886	2	5		32570	2	8	
FPC 1826	3	6		FSU 336	2	2	
FPC Lot 1-10-66	4	7		32743	4	11	
FSU 336	5	3	5 of 9 Units in top half of sample are lot rank 6 or less	32720	5	11	3 of 8 Units in top half of sample are lot rank 6 or less
32570	6	8		33231	6.5	5	
33231	7.5	6		FPC 1886	6.5	4	
32769	7.5	12		33348	8	9	
32720	9	11	5 of 8 Units in bottom half of sample are lot rank 7 or more	32769	9	12	4 of 8 Units in bottom half of sample are lot rank 7 or more
32743	10	11		FPC Lot 1-10-66	10	7	
32765	11	12		32645	11.5	10	
32645	12	10		FPC 1826	11.5	5	
SD 25	13	2		FPC 1891	13	6	
33348	14	9		32633	14	10	
FPC 1139	15	1		FPC 1189	15	3	
32633	16.5	10		FPC 1139	16	1	
FPC 1189	16.5	4					

associated with the units in the top half of the table, and the six lowest lots would appear in order in the bottom half. Such is not the case in Table 4-12. However, at 100 in./in./min, more than half of the units in the upper half of the table were made with powder lots in the upper half of the lot ranking. Similarly, more than half of the units in the bottom half of the table were made from lots in the bottom half of the lot ranking. Evidently, at 100 in./in./min, the value of strain in individual units is influenced, but not determined, by the powder lot properties. At 700 in./in./min however, the correspondence of lot properties to individual unit properties is no better than expected by chance. It is concluded that the lot acceptance properties do have some bearing on strain values demonstrated for individual units, although they did not bear a direct relationship to one another. Therefore, some function derived from the lot properties may be employed to define the strain values of the population of the motors left in the service inventory.

The preceding discussion in this section established that certain of the subscale data are equivalent to FSU data; that data from units of all ages may be grouped; and that value of strain capability of individual units was weakly related to lot acceptance data. These were all necessary preliminary steps leading to the final step, which is to find a correlation between propellant properties and operational motor properties. The approach taken to obtain the desired correlation was to calculate the bias at each rate for each unit presented in Table 4-5. This bias (a correlation factor) was formed by dividing the individual unit value of strain by a function of the lot value of strain at rupture. At each rate, the biases of all units were averaged and the standard deviation was calculated. This calculation was done twice, using different functions of the lot acceptance values. The first trial was made using the lot properties associated with individual units. The results are presented in Table 4-13. The second trial was made using the weighted average of the lot properties of units in the sample (Table 4-18). The best correlation (the lowest standard deviation of the bias) between lot properties and unit properties was obtained from the use of the weighted average of lot properties of the sample. This is a convenient result because of the straightforward way in which properties of the whole motor population from the lot-to-motor bias may be calculated using the weighted average of the motor population.

## 2. Relaxation Modulus

The data set for relaxation modulus are presented in Table 4-3. Eleven of these units are FSU's, and the remaining one is an FPC. The t-test is not appropriate for testing one sample against a group (see Table 4-10; the variance of each group enters into the calculation). The similarity of the stress relaxation modulus ( $E_R$ ) of FPC 1571 to  $E_R$  of the rest of the sample is shown in Figure 4-2, in which FPC 1571 is found to be somewhat on the high side but well within the limits of the group. The data from FPC 1571 are therefore accepted as part of the homogeneous sample of units for analyses of relaxation modulus.



TABLE 4-13

UNIT-TO-LOT BIAS CALCULATED WITH INDIVIDUAL UNIT LOT VALUES

Unit	Bias									
	Strain Rate - in./in./min									
	10	20	40	70	100	200	400	700	1000	
32743	.828	.795	.757	.728	.705	.666	.628	.598	.579	
32765	.845	.810	.767	.730	.709	.683	.625	.598	.578	
32769	.855	.828	.793	.760	.739	.714	.655	.627	.606	
33231	.832	.769	.759	.722	.699	.646	.600	.568	.550	
32720	.828	.795	.759	.724	.707	.667	.626	.597	.578	
32645	.792	.761	.729	.697	.673	.635	.595	.562	.542	
33348	.763	.729	.702	.675	.661	.636	.610	.583	.566	
32570	.780	.769	.748	.730	.718	.681	.642	.608	.596	
32633	.780	.748	.709	.673	.642	.603	.572	.545	.526	
FSU 336	.742	.715	.688	.665	.647	.610	.566	.562	.515	
SD 25	.689	.664	.634	.610	.592	.554				
1/3 Scale 11	.721	.718	.704	.680	.662	.601				
FPC 1891				.693				.539		
FPC 1139				.600	.572	.518	.478	.444	.425	
FPC Lot 1-10-66	.879	.854	.804	.754	.720	.662	.603	.566	.536	
FPC 1826	.898	.857	.799	.758	.717	.651	.590	.544	.519	
FPC 1886	.907	.874	.825	.784	.732	.678	.613	.564	.531	
FPC 1189	.750	.707	.661	.629	.611	.572	.538	.507	.489	
Average	.806	.776	.740	.701	.677	.634	.596	.563	.542	
Std Deviation	.0638	.0605	.0527	.0524	.0503	.0513	.0445	.0438	.0461	

TABLE 4-14

UNIT-TO-LOT BIAS OF STRAIN AT MAXIMUM STRESS CALCULATED WITH WEIGHTED AVERAGE LOT VALUES

Unit	Bias									
	Strain Rate - in./in./min									
	10	20	40	70	100	200	400	700	1000	
32743	.832	.799	.761	.731	.709	.669	.631	.601	.582	
32765	.841	.806	.763	.726	.705	.679	.622	.594	.575	
32769	.851	.823	.789	.776	.735	.711	.652	.624	.603	
33231	.875	.837	.799	.759	.731	.679	.631	.598	.579	
32720	.832	.799	.763	.728	.711	.671	.629	.600	.581	
32645	.806	.775	.742	.709	.685	.646	.605	.572	.551	
33348	.780	.746	.712	.690	.676	.650	.624	.596	.579	
32570	.801	.789	.768	.749	.737	.698	.659	.624	.612	
32633	.794	.761	.721	.685	.653	.614	.582	.555	.536	
FSU 336	.834	.802	.773	.747	.726	.685	.636	.600	.579	
SD 25	.795	.766	.731	.704	.683	.640				
1/3 Scale 11	.849	.846	.830	.802	.780	.709				
FPC 1891				.724	.674	.610	.563	.523	.501	
FPC 1139				.707	.745	.685	.624	.586	.554	
FPC Lot 1-10-66	.910	.884	.832	.780	.754	.684	.620	.572	.546	
FPC 1826	.945	.901	.841	.797	.776	.719	.650	.580	.563	
FPC 1886	.962	.927	.875	.832	.776	.719	.650	.580	.563	
FPC 1189	.802	.756	.707	.672	.653	.612	.575	.542	.523	
Average	.844	.814	.775	.740	.712	.668	.620	.583	.564	
Std Deviation	.054	.053	.049	.044	.041	.035	.028	.028	.030	

Initial tangent modulus and  $E_R$  are equivalent, as one point on the  $E_R$  curve may be calculated from initial tangent modulus obtained from a constant-strain-rate test. The equivalent was developed in Report No. 8 as,

$$E_R = (M + 1)(ITM)(1 + \epsilon)$$

where:

$E_R$  = Relaxation modulus

$M$  = Slope of  $E_R$  versus time curve on log-log plot

ITM = Initial tangent modulus

$\epsilon$  = Strain (in linear range)

The modulus correspondence is evaluated at a time when the stress-strain curve is linear. CYH propellant remains linear up to about 5 percent strain. Conservatively choosing 3 percent strain as the point at which the transformation is made, for a strain rate of 0.74 in./in./min, the corresponding relaxation time is:

$$t = \frac{0.03}{0.74} \times 60 = 2.45 \text{ seconds}$$

The slope ( $M$ ) of the mid-range of the relaxation time curves given in Figure 4-2 is -0.27 decades/decade. Thus the transformation between initial tangent modulus (ITM) and  $E_R$  is:

$$E_R \text{ at } 2.45 \text{ seconds} = 0.752 \text{ (ITM)}$$

That the correspondence between  $E_R$  and initial tangent modulus is realistic as well as theoretical is illustrated by Figures 4-10 and 4-11, which present  $E_R$  calculated from initial tangent modulus data which were taken at several rates and temperatures using propellant taken from the aged motors. In both Figures 4-10 and 4-11,  $E_R$  calculated from the initial tangent modulus of the propellant lot data is shown to be low relative to measured  $E_R$ . This is consistent with the findings presented in Table 4-11, which show that initial tangent moduli taken from FPC's are lower than those taken from FSU's.

Data from the seven LRSLA motors presented in Table 4-4 are actually a mixture of data taken with superimposed pressure of 300 psi and ambient pressure. The short time data presented in Table 4-4 for times from  $10^{-6}$  to  $10^{-2}$  seconds were actually obtained at a temperature of 30° F and superimposed pressure of 300 psi. When these data were time-temperature shifted, the largest shifted time was 0.04 second. Data for

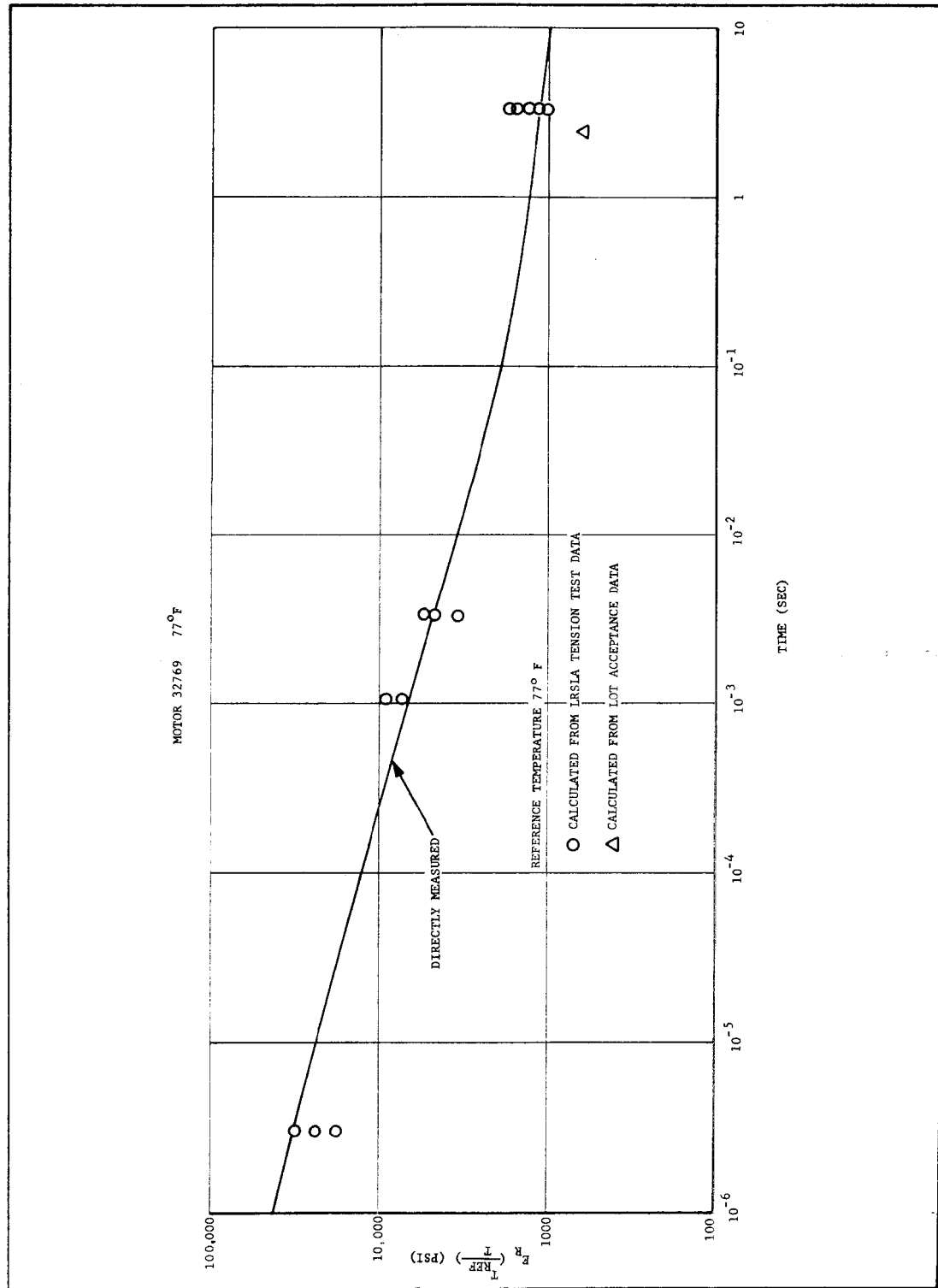


Figure 4-10. Directly Measured  $E_R$  and  $E_R$  Calculated from Initial Tangent Modulus - LRSLA Motor 32769

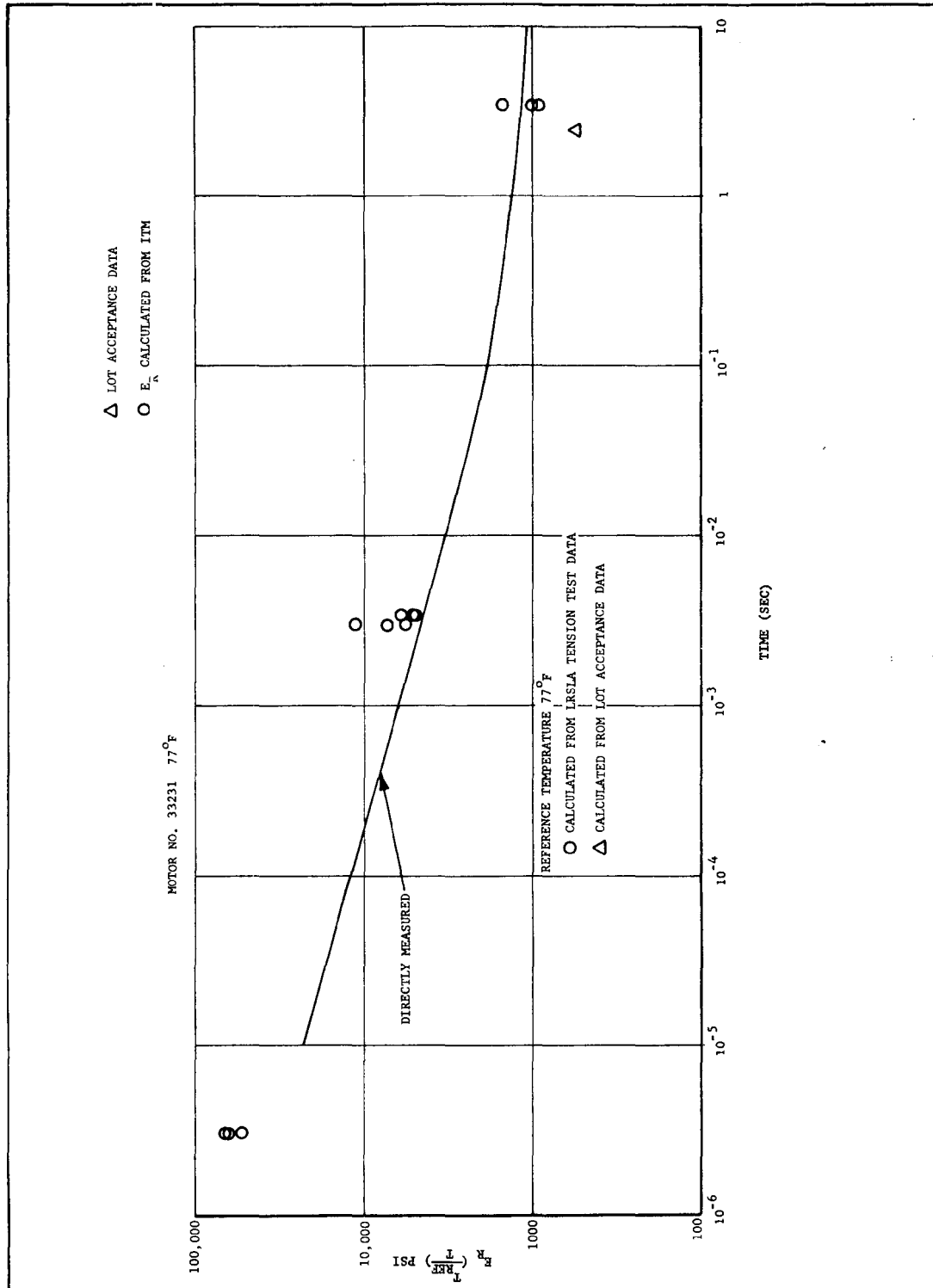


Figure 4-11. Directly Measured  $E_R$  and  $E_R$  Calculated from Initial Tangent Modulus - LRSLA Motor 33231

times from 0.1 second to 10 seconds were obtained from curves of relaxation tests performed at 77° F and ambient pressure. To check the validity of this juxtaposition of pressurized and nonpressurized data, the t-test presented in Table 4-15 was performed. The pressurized relaxation moduli were obtained by extrapolating the shifted modulus curves to 0.1 second. The ambient pressure data were obtained by averaging tabulated data from three motor locations. Thus they are slightly different from the values presented in Table 4-4. The result of the t-test is that there is no difference in pressurized and ambient relaxation modulus data at 0.1 second. This result, combined with the close correspondence of all the motors in this sample, presented in Figure 4-2, is taken to indicate that it is permissible to use both the pressurized and ambient test motors together in the relaxation data sample.

The test of the equivalence of relaxation modulus data obtained from FSU's and FPC's is given in Table 4-16 for the four times presented in Table 4-6. Equality of relaxation modulus is accepted for times of 0.1, 1.0, and 2.45 seconds, but not for 10 seconds. The t-statistic is seen to grow larger for increasing relaxation times, such that the equivalence of relaxation data from FPC's and FSU's is progressively worse for longer relaxation times. The conclusion from this study of the effect of casting configuration is that data from only FSU's are compatible with trend data from the Dissected Motor Program, which reports relaxation data at a minimum time of 10 seconds.

Trend analysis of relaxation modulus may be performed with initial tangent modulus results or directly with relaxation data. Furthermore, the study may be made either on individual propellant lots, or on all lots grouped together. There are thus a total of four permutations for the trend study. The problem with this trend study is that the majority of the available data are not in the correct time range needed for the calculation of motor service life as it is limited by ability to withstand the ignition transient.

The trends in relaxation modulus as indicated by initial tangent modulus data will be presented first. Data from lot SR-68-62 is presented in Figures 4-12 and 4-13. More data points are available from this lot than for any other; this lot was also used in the discussion of propellant strain. Figure 4-12 shows test results from the Dissected Motor Program, only, for initial tangent modulus from tension testing at 0.74 in./in./min. The regression equation and associated statistics for the data are also shown on the figure. The regression slope is positive, but the correlation coefficient indicates that no correlation exists.

High rate triaxial test results of tangent modulus are presented on Figure 4-13 for lot SR-68-62. These data are more applicable to relaxation modulus trends that affect motor service life because, at 3 percent strain, these data correspond to a relaxation time of 0.0018 second. A negative aging trend is indicated, but the correlation coefficient is insufficiently high to prove a correlation.

TABLE 4-15

TEST FOR EQUALITY OF MEANS OF RELAXATION  
 DATA OBTAINED WITH SUPERIMPOSED  
 PRESSURE AND AT AMBIENT PRESSURE

Unit	Relaxation Modulus - Psi	
	With 300 Psi Superimposed Pressure	Ambient Pressure
32765	1933	1774
32633	2767	2207
32769	2066	1959
32645	2333	2337
33231	1933	1836
32720	1800	2330
32745	1933	2406
$\bar{X}$	2109	2121
S	335	260
$N_y = N_x = 7$ $t = 0.075$ $t_{.005, 12} = 3.055$ $t < t_{\frac{\alpha}{2}, N_x + N_y - 2}$ Decision: Accept equality of means at 1% significance level		

TABLE 4-16

TEST OF EQUALITY OF MEANS OF RELAXATION MODULUS  
OBTAINED FROM FSU'S AND SUBSCALE UNITS

Relaxation Modulus at 0.1 Second				Relaxation Modulus at 1.0 Second			
Unit	$E_R$	Unit	$E_R$	Unit	$E_R$	Unit	$E_R$
32769	1817	FPC 1139	2180	32769	1360	FPC 1139	1420
32743	2400	FPC 2048	2589	32743	1883	FPC 2048	1775
32645	2266	FPC 1189	2380	32645	1600	FPC 1189	1580
33348	2750	FPC 1-10-66	1950	33348	1770	FPC 1-10-66	1250
33231	1833	FPC 1826	1900	33231	1333	FPC 1826	1300
FSU 3174	2450	FPC 1886	1780	FSU 3174	1660	FPC 1886	1190
32570	2480	FPC 1571	2150	32570	1700	FPC 1571	1410
FSU 336	2590	FPC 1891	1978	FSU 336	1680	FPC 1891	1283
SD 25	2721	1/3 Scale 6	2230	SD 25	1822	1/3 Scale 6	1420
FSU 2158	2354	1/3 Scale 11	1978	FSU 2158	1660	1/3 Scale 11	1691
FSU 2137	2174			FSU 2137	1552		
32765	1783			32765	1233		
32633	2767			32633	1733		
32720	2317			32720	1650		
$N_x = 14$ $N_y = 10$ $\bar{X} = 2336$ $\bar{y} = 2111.5$ $S_x = 336$ $S_y = 244.2$ $t = 1.80$ $t_{.005, 22} = 2.819$ Decision: Accept equality of means of $E_R$ at 0.1 second				$N_x = 14$ $N_y = 10$ $\bar{X} = 1617$ $\bar{y} = 1431$ $S_x = 189$ $S_y = 194$ $t = 2.35$ $t_{.005, 22} = 2.819$ Decision: Accept equality of means of $E_R = 1.0$ second			



TABLE 4-16 (Cont)

TEST OF EQUALITY OF MEANS OF RELAXATION MODULUS  
OBTAINED FROM FSU'S AND SUBSCALE UNITS

Relaxation Modulus at 2.45 Second				Relaxation Modulus at 10 Second			
Unit	$E_R$	Unit	$E_R$	Unit	$E_R$	Unit	$E_R$
32769	1170	FPC 1139	1210	32769	983	FPC 1139	1015
32743	1530	FPC 2048	1550	32743	1417	FPC 2048	1255
32645	1400	FPC 1189	1438	32645	1200	FPC 1189	1071
33348	1500	FPC 1-10-66	1070	33348	1380	FPC 1-10-66	850
33231	1200	FPC 1826	1120	33231	1050	FPC 1826	925
FSU 3174	1490	FPC 1886	1020	FSU 3174	1250	FPC 1886	850
32570	1500	FPC 1571	1200	32570	1280	FPC 1571	950
FSU 336	1377	FPC 1891	1129	FSU 336	1190	FPC 1891	907
SD 25	1595	1/3 Scale 6	1210	SD 25	1293	1/3 Scale 6	934
FSU 2158	1470	1/3 Scale 11	1490	FSU 2158	1202	1/3 Scale 11	1093
FSU 2137	1370			FSU 2137	2137		
32765	1100			32765	923		
32633	1440			32633	1183		
32720	1460			32720	1233		
$N_x = 14$ $N_y = 10$ $\bar{x} = 1414$ $\bar{y} = 1243$ $s = 162$ $s = 184$ $t = 2.41$ $t_{.005, 22} = 2.819$ Decision: Accept equality of means $E_R$ at 2.45 second.				$N_x = 14$ $N_y = 10$ $\bar{x} = 1194$ $\bar{y} = 985$ $s_x = 138$ $s_y = 126$ $t = 3.79$ $t_{.005, 22} = 2.819$ Decision: Reject equality of means of $E_R$ at 10 second.			

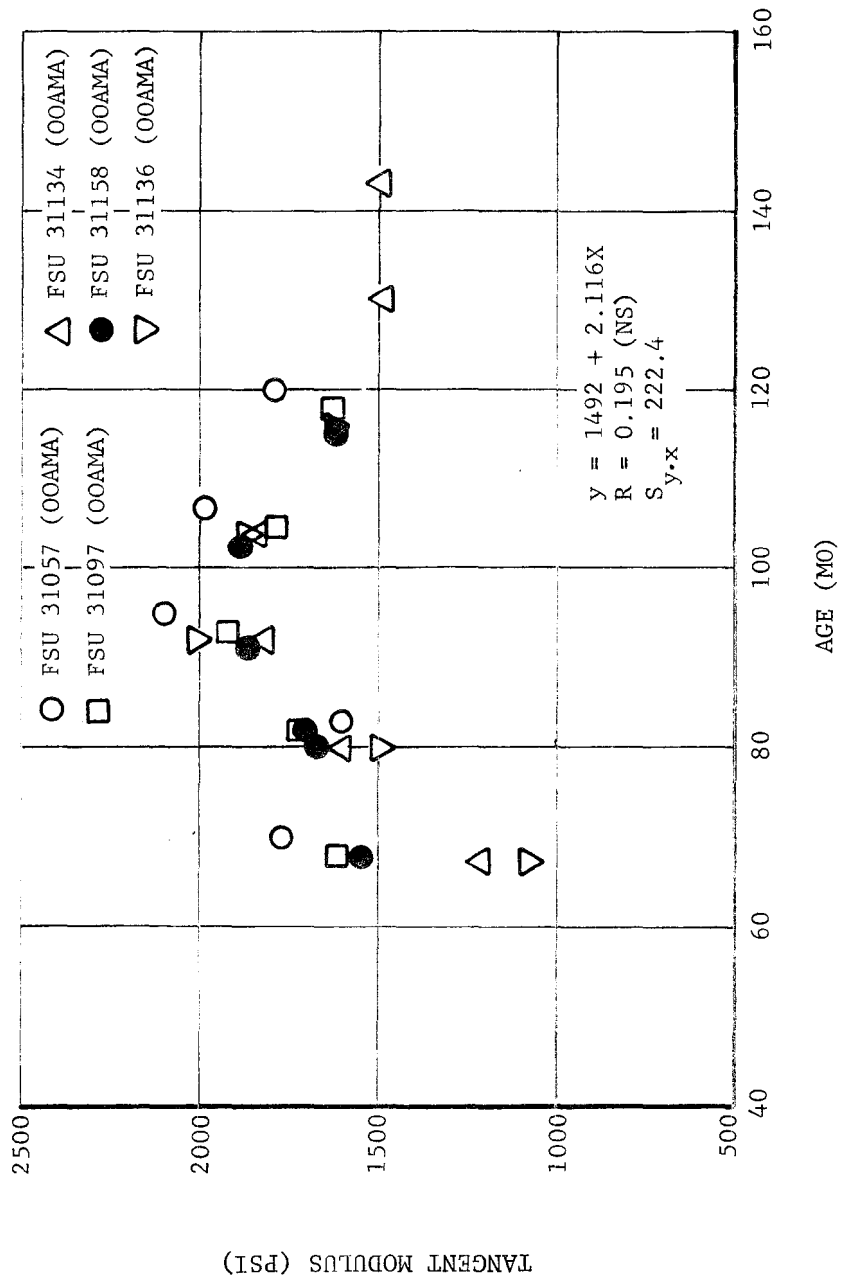


Figure 4-12. Initial Tangent Modulus, Lot 68-62, 0.74 in./in./min

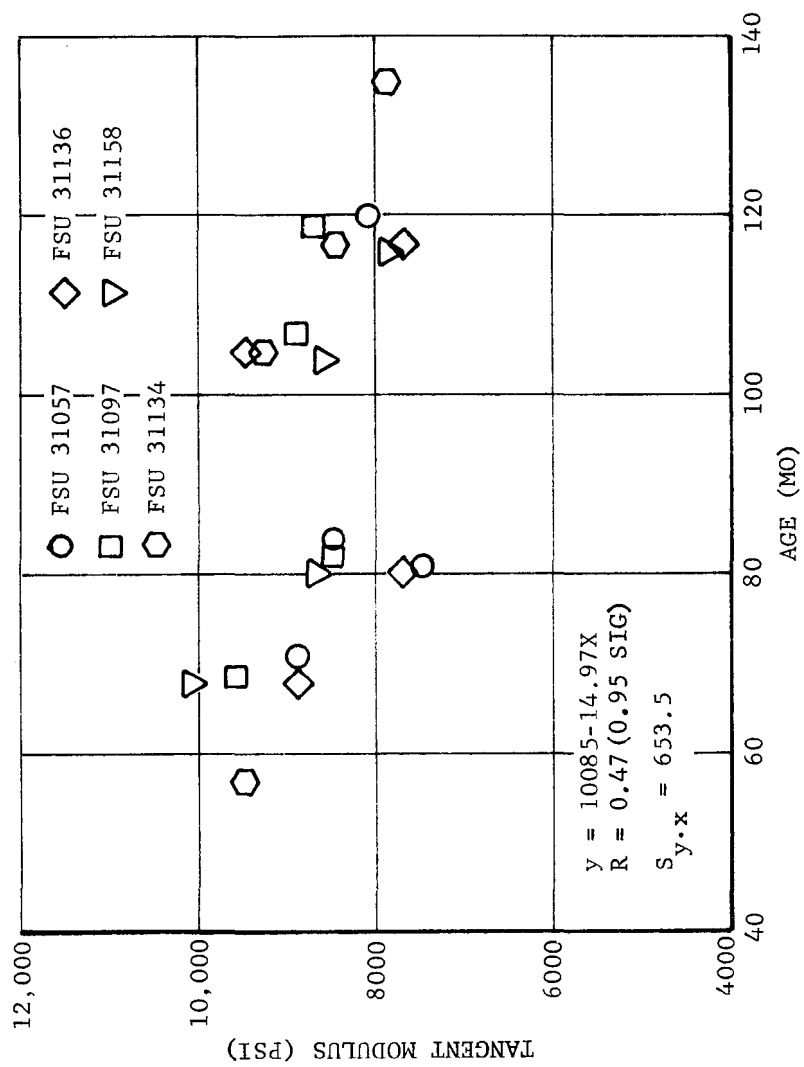


Figure 4-13. Initial Tangent Modulus, Lot 68-62, 1000 in./in./min

Tangent modulus data from the other six Minuteman II powder lots in the Dissected Motor Program were also examined for evidence of an aging trend. In all cases, it was concluded that no aging trend exists.

Data from all powder lots are presented in Figures 4-14 (JANNAF samples at 0.74 in./in./min) and Figure 4-15 (biaxial strip at 1000 in./in./min). Data from Table 4-8 for FSU's only are included in Figure 4-4, along with all data from Minuteman II propellant obtained in the Dissected Motor Program. Figure 4-15 is made up of only data from the Dissected Motor Program. The aging trends are opposite in direction for the two types of samples tested. The low-rate tensile data show a positive aging trend of 1 psi/month and the high-rate triaxial data show a negative aging trend of 10 psi/month. In both cases, the correlation coefficient is low and there is no cause-and-effect relationship indicated.

A direct approach is to use the data presented in Table 4-4 for an aging study. Relaxation modulus at 10 seconds was selected for presentation. There are only 12 data points, which limits the usefulness of this approach. Furthermore, six of these points are from motors of approximately 9 years of age. These data are presented in Figure 4-16. The aging trend is negative; its value is -17.8 psi/month. The correlation coefficient is only 0.44, so no significant relationship with age is indicated.

The lack of an aging trend is also shown by data from the Dissected Motor Program. Ten seconds is the shortest relaxation time reported. The most recent trend curve from the Dissected Motor Program (Report 53) is given herein as Figure 4-17. The trend is positive and the correlation is low. Only two of the five motors included in this regression are from powder lots used for Minuteman II.

A comparison of the aging trends that have been reported in the Dissected Motor Program may be significant. Testing was reported in 1972 (Report 32), 1973 (Report 30), and 1975 (Report 53). The regressions for 10 second relaxation modulus are as follows:

$$1972: y = 962 + 3.5 \times \text{age in years}$$

$$R = 0.452$$

16 motors

$$1973: y = 1034 + 2.6 \times \text{age in years}$$

$$R = 0.376$$

16 motors

$$1974: y = 1096 + 1.5 \times \text{age in years}$$

$$R = 0.263$$

5 motors

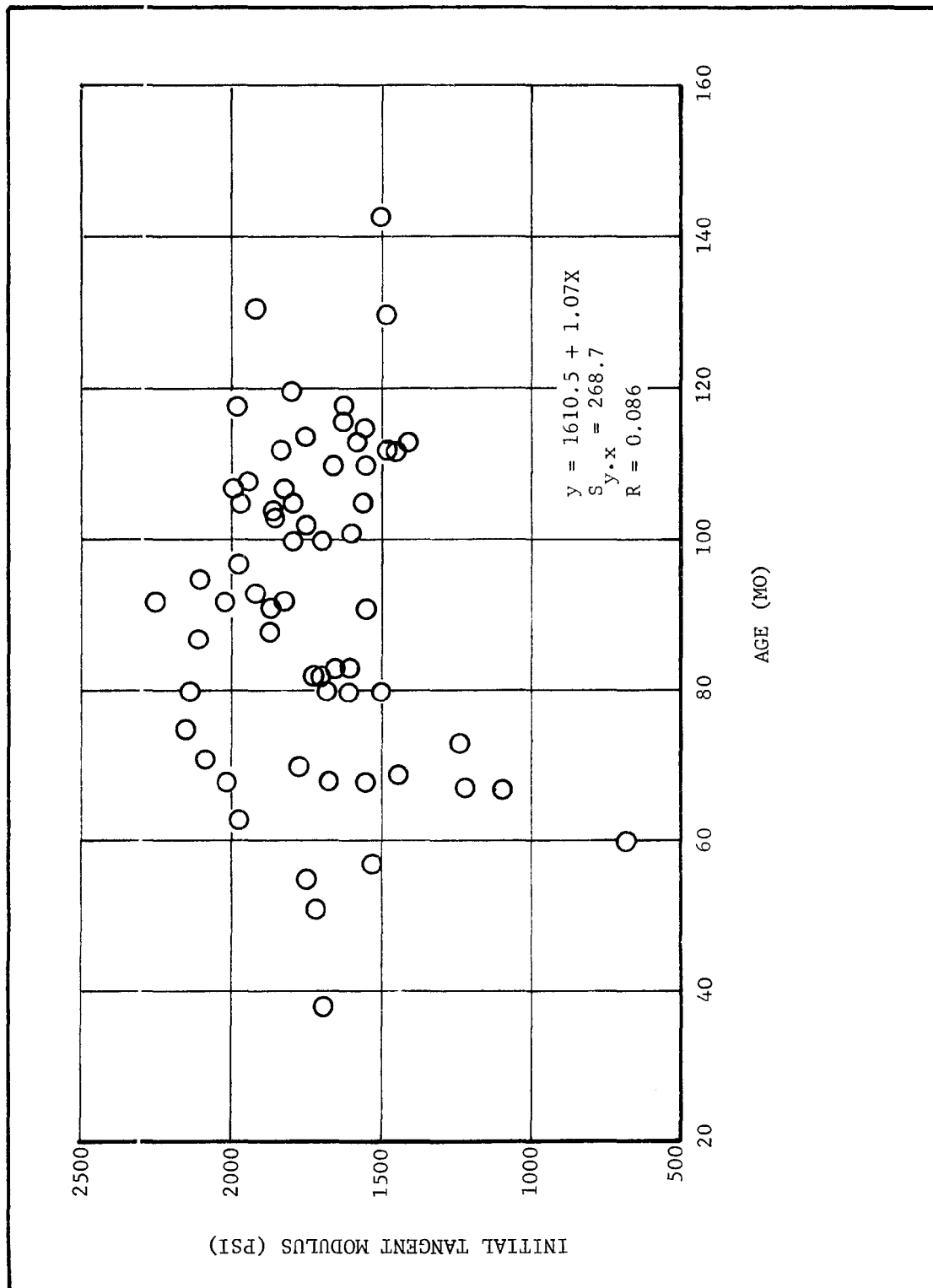


Figure 4-14. Initial Tangent Modulus, All Lots Together, 0.74 in./in./min

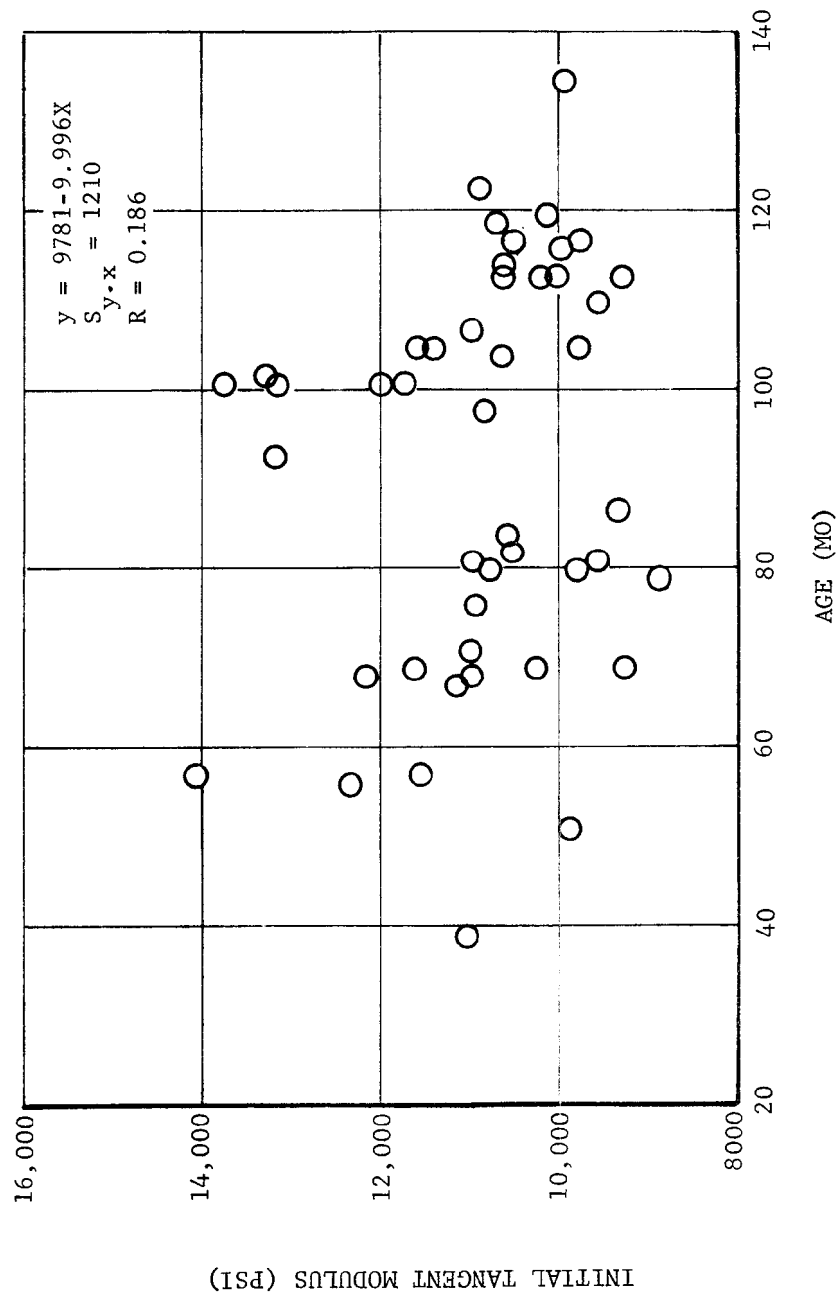


Figure 4-15. Initial Tangent Modulus, All Lots Together, 1000 in./in./min

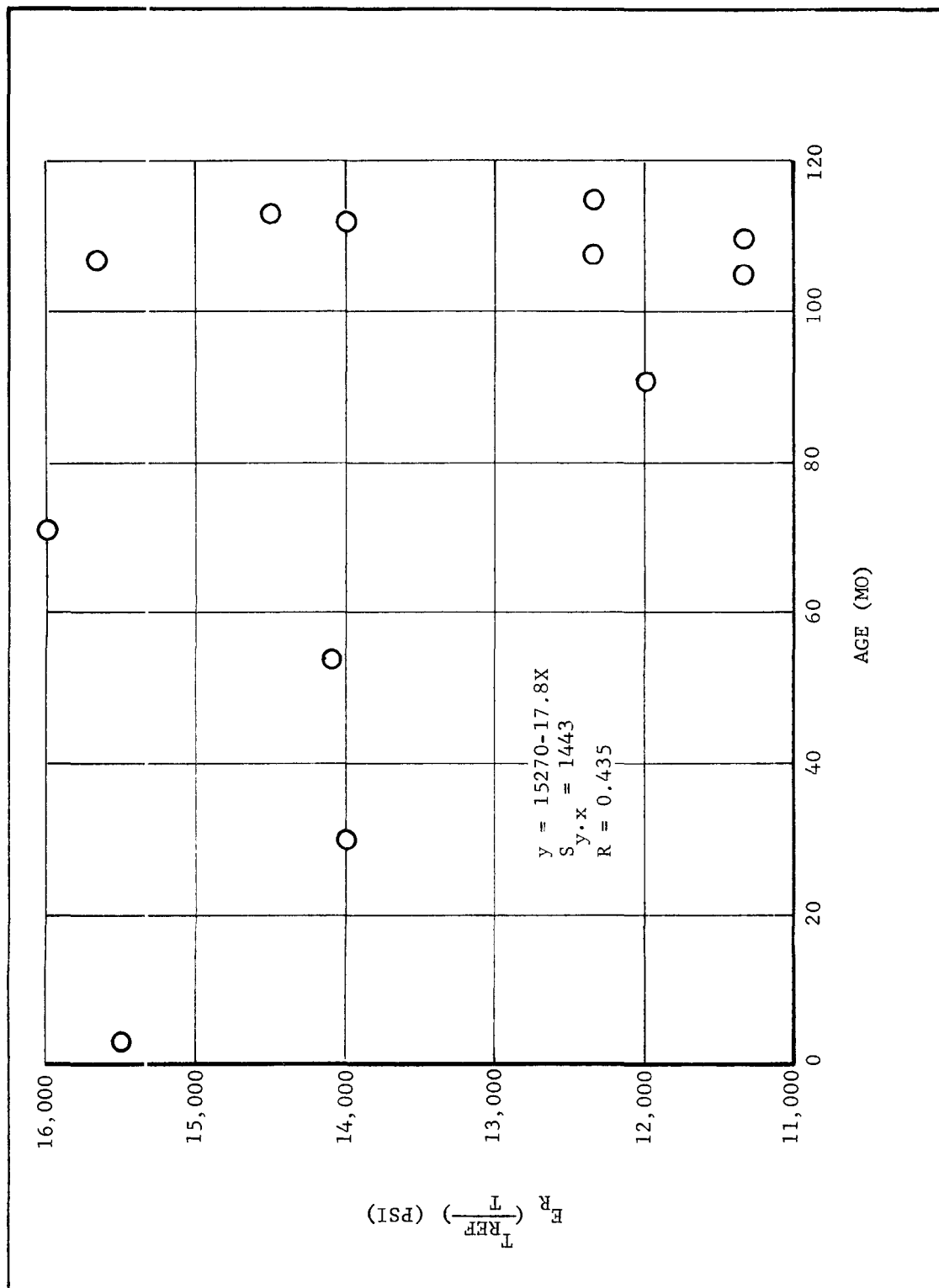


Figure 4-16. Aging Trend of Relaxation Modulus at  $10^{-4}$  Second

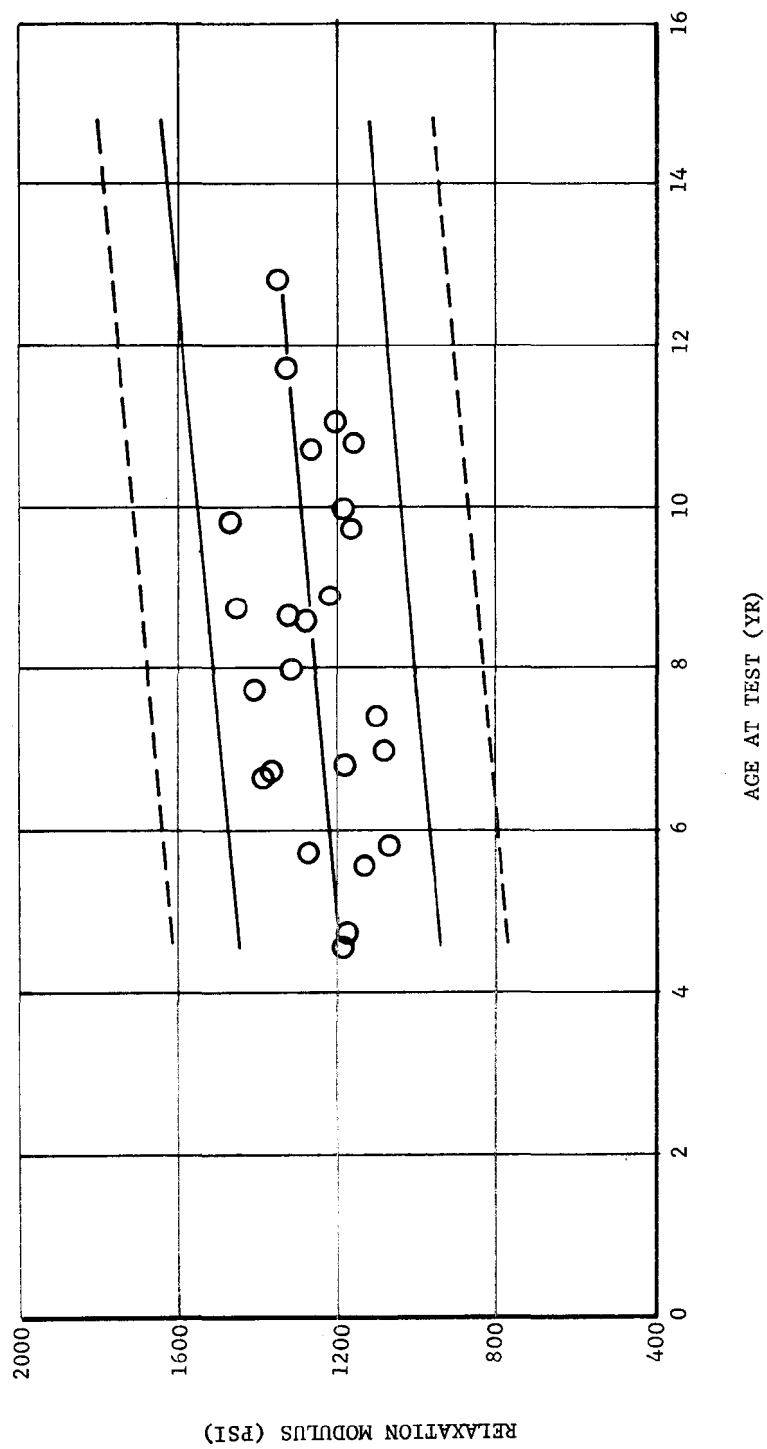


Figure 4-17. Relaxation Modulus at 10 Sec, 3 Percent Strain, Five Motor Composite, Dissected Motor Program



As more data are added for each motor that is reported, the aging trend is more closely approaching zero and the correlation is getting lower (worse).

The overall conclusion from this study of propellant aging trends is that there is no trend at all. Thus, relaxation modulus data may be considered as a homogeneous, constant population.

The next step in the analysis of relaxation modulus data is to determine whether the properties of each propellant powder lot are directly related to the value of properties measured in other units made from the same powder lot. The same approach that was used to evaluate strain is used here. The rank comparison is presented in Table 4-17 for  $E_R$  at 0.1 second and at 1.0 second. These times were chosen to permit the use in the sample of the largest number of units. The progressively poorer equality demonstrated between FPC and FSU data at larger times precluded using all data given in Table 4-6. The relationship between lot value and unit value is very loose, as indicated by the nearly random order in which the rank of the lot appears in Table 4-17. Nevertheless, there are some suggestions that powder lot properties influence individual unit properties, especially in the lower half of the table. Units made from the same powder lot have a tendency to be ranked adjacently or closely grouped if they are in the bottom half. Especially, note that the pairs of units 1/3 scale 6 - FPC 1139 (Lot SR 28-63) and FPC 1826-33231 (Lot RAD 1-14-66) both appear as adjacent unit ranks at both times considered. The triplet 32765-32769-FPC 1571 (Lot RAD 1-7-65) also exhibits a clustering in unit rank, as 32769 is adjacent in unit rank to 32765 at 0.1 second and to FPC 1571 at 1.0 second. One would wish for more and better data on this subject, but the grouping in the bottom half of the table is suggestive. The hypothesis is offered that a minimum property value exists that is characteristic of each propellant lot. Some units, because of fortuitous and unknown circumstances, may develop properties higher than the minimum. The FPC used for propellant acceptance may or may not demonstrate the minimum value for the lot, and hence may not be characteristic of the lot. This is nearly pure speculation, but would help explain why some units for a particular propellant lot tend to demonstrate like physical properties and some do not.

As was shown in the section of this report relative to strain, the data set for propellant relaxation modulus has been proved to be a homogeneous sample of the population of all motors, and the lot acceptance value had little relationship to the value of relaxation modulus demonstrated by individual units. The remaining investigation concerning propellant modulus is to determine if there is a practical correlation between the relaxation modulus of individual units and the propellant lot acceptance data. This correlation will then be used in the following portion of this report to calculate the relaxation modulus values of the Minuteman II Stage III motor inventory.

TABLE 4-17

RANK TEST FOR INFLUENCE OF POWDER LOT  
ACCEPTANCE VALUES ON RELAXATION MODULUS

$E_R$ at 0.1 Second			$E_R$ at 1.0 Second		
Unit	Rank of Modulus	Rank of Lot	Unit	Rank of Modulus	Rank of Lot
32633	1	3	32743	1	2
33348	2	6	SD 25	2	14
SD 25	3	14	FPC 2048	3	1
FSU 336	4	8	33348	4	6
FPC 2048	5	1	32633	5	3
1/3 Scale 11	6	15	32570	6	4
32570	7	4	1/3 Scale 11	7	15
FSU 3174	8	11	FSU 336	8	8
32743	9	2	FSU 2158	9.5	13
FPC 1189	10	7	FSU 3174	9.5	11
FSU 2158	11	13	32720	11	2
32720	12	2	32645	12	3
32645	13	3	FPC 1189	13	7
1/3 Scale 6	14	15	FSU 2137	14	13
FPC 1139	15	15	FPC 1139	15.5	15
FSU 2137	16	13	1/3 Scale 6	15.5	15
FPC 1571	17	5	FPC 1571	17	5
FPC 1891	18	12	32769	18	5
FPC Lot 1-10-66	19	11	33231	19	10
FPC 1826	20	10	FPC 1826	20	10
33231	21	10	FPC 1891	21	12
32769	22	5	FPC Lot 1-10-66	22	11
32765	23	5	32765	23	5
FPC 1886	24	9	FPC 1886	24	9
<p>There are 15 lots in this sample. 3 of 8 units in the top third of the sample are lot rank 1 to 5. 1 of 8 units in middle third are lot rank 6-10. 2 of 8 units in bottom third are lot rank 11-15. 8 of 12 units in top half are of lot rank 1-8. 8 of 12 units in bottom half are lot rank 8-15.</p>			<p>There are 15 lots in this sample. 4 of 8 units in top third are of lot rank 1-5. 1 of 8 units in middle third are lot rank 6-10. 2 of 8 units in bottom third are lot rank 11-15. 8 of 12 units in top half are of lot rank 1-8. 8 of 12 units in bottom half are of lot rank 8-15.</p>		

The approach taken to obtain the mean value of relaxation modulus at each time is similar to that taken for strain, but a different data set was used, as there are not enough samples in the primary data set (Table 4-4) to establish a correlation. A correlation or bias was obtained between a function of propellant lot data and the individual unit values at 2.45 seconds (Table 4-6). A coefficient of variation was also obtained from the values of the large population of relaxation modulus given in Table 4-6. The correlation coefficient so obtained applies only to the value of relaxation modulus at 2.45 seconds and thus can be used to calculate only the mean relaxation modulus of the entire motor inventory at 2.45 seconds. The remainder of the calculation of mean relaxation modulus at other required times, and the calculation of variance at each required time is given in paragraph D of this section.

The calculation of the correlation at 2.45 seconds is given in Table 4-18. The individual units and relaxation modulus values in the first two columns of Table 4-18 are taken from Table 4-6. Initial tangent modulus values for the propellant lot from which each unit was made are given in the third column and are taken from Table 4-7. In the fourth column, the initial tangent modulus of each lot has been transformed into the equivalent relaxation modulus at 2.45 seconds, using the relationship developed earlier. In the fifth column, the bias or correlation has been calculated by dividing the unit relaxation value (column 2) by the lot relaxation value (column 4).

A second approach to the correlation calculation is given in the sixth and final column of Table 4-18. The weighted average of the relaxation moduli of the lots making up the sample (bottom of column 4) is divided into the individual unit relaxation modulus values. The average value and the standard deviation are calculated for each of columns 2, 4, 5, and 6. The coefficient of variation is calculated by dividing the average relaxation modulus of the individual units into the standard deviation. This coefficient will be used in paragraph D to estimate the sample variance of the relaxation modulus of the motor inventory. The best correlation is given by the use of the weighted average of the lot properties, as is shown by the lower value of standard deviation of the two correlation trials.

The interpretation of data on relaxation modulus is now completed. The actual calculations of the average and variation of relaxation modulus is shown in paragraph D. In this section, the limits of homogeneity of the data set given in Table 4-4 and 4-6 were developed, and it was shown that the homogenous portion of the data could be used without further correction for lot effect, age, or casting configuration.

TABLE 4-18

## UNIT-TO-LOT BIAS OF STRESS RELAXATION MODULUS

Unit	E <sub>R</sub> at 2.45, 77°F Psi	Lot Tangent Modulus Psi	E <sub>R</sub> From ITM Psi	Bias on Individual Lot Values	Bias on Weighted Avg/Sample
32633	1440	835	628	2.29	2.55
33231	1200	743	559	2.15	2.13
32720	1460	842	633	2.31	2.59
32645	1400	835	628	2.23	2.48
32743	1630	842	633	2.57	2.89
32769	1170	819	616	1.90	2.07
32765	1100	819	616	1.79	1.95
33348	1600	802	603	2.65	2.84
32570	1500	823	619	2.42	2.66
FSU3174	1490	736	553	2.69	2.64
FPC1189	1438	791	595	2.42	2.55
FSU336	1377	768	578	2.38	2.44
SD25	1595	634	477	3.35	2.83
1/3 Scale 6	1210	602	453	2.67	2.15
1/3 Scale 11	1490	602	453	3.29	2.64
FPC2048	1550	759	571	2.72	2.75
FSU2158	1470	683	514	2.86	2.61
FPC1891	1129	726	546	2.07	2.00
FPC1-10-66	1070	736	553	1.93	1.90
FPC1826	1120	743	559	2.00	1.99
FPC1886	1020	752	566	1.80	1.81
FPC1571	1200	819	616	1.95	2.13
FPC1139	1210	602	453	2.67	2.15
FSU 2137	1370	683	514	2.67	2.43
$\bar{X}$	1343		564*	2.41	2.38
S	188		59.61	.427	.334
Coefficient of variation = $\frac{188}{1343} = .140$					

\*Weighted average of the sample

#### D. PROPELLANT PROPERTIES FOR SERVICE LIFE PREDICTIONS

##### 1. Introduction

In this paragraph, the calculations of strain at maximum stress and the stress relaxation modulus for the service life estimates of the existing motor population are presented. Recommendations for improving the utility of the ongoing aging trend study are also given. The preceding paragraph indicated that the propellant lot acceptance values of the existing motor population would be used to find mean values of the required material properties. Specifically, the weighted averages of initial tangent modulus and of strain at rupture would be multiplied by the correlation factors or biases presented in Tables 4-14 and 4-18. The first step in calculating the weighted averages is to define the existing motor population. The motor inventory was obtained from an ACMS Configuration Index Report dated 2 May 1975 (last updated in January 1975). The motors assigned to operational wings were identified, and the powder lots from which they were manufactured were tabulated. An adjustment was made for motor changes scheduled for June in two flights of Wing 1, so the following tabulation specifically applies to the motor inventory as it exists at the end of June 1975. The makeup of the population with regards to powder lots is given in Table 4-19. The weighted averages of the powder lot acceptance data are also given in the table.

TABLE 4-19

##### POWDER LOTS IN THE EXISTING MINUTEMAN II STAGE III MOTOR INVENTORY

Powder Lot	Number of Units
RAD 1-4-64	1
RAD 1-7-65	29
RAD 1-8-65	31
RAD 1-9-65	55
RAD 1-10-66	71
RAD 1-11-66	15
RAD 1-12-66	16
RAD 1-13-66	38
RAD 1-14-66	22
RAD 1-16-67	39
RAD 1-17-68	28
RAD 1-18-68	28
RAD 1-19-68	9
RAD 1-21-70	25
Weighted averages of lot acceptance values:	
Initial tangent modulus:	806 psi
Strain at rupture:	59.1 %
Maximum stress	310.4 psi

## 2. Calculation of Strain at Maximum Stress

The approach taken to calculate the mean strain at maximum stress at each strain rate is to multiply the correlation factors of Table 4-14 by the weighted average of the motor population. The upper statistical limit of the standard deviation is calculated as follows: (1) Calculate the coefficient of variation of the sample of Table 4-6 for each strain rate, (2) obtain the average coefficient of variation, (3) calculate the estimate of the standard deviation from the mean values of the sample of Table 4-6 and the average coefficient of variation found in step 2, and (4) calculate the upper limit of the standard deviation at the 95 percent

confidence level (the statistic  $\frac{(n-1)S^2}{\sigma^2}$  has a chi-squared distribution,

so the upper limit of the standard deviation is found by  $\sigma = S \sqrt{\frac{(n-1)}{X^2_{95, n-1}}}$ ).

The resulting standard deviation ( $\sigma$ ) is a limit value, which will be exceeded by the true value of the standard deviation only 5 percent of the time. All the information concerning the variability of strain is thus obtained from the data set of strain values. The propellant lot weighted average is used to adjust the average values and thus account for the possibility that the sample (Table 4-6) is not a truly random representation of the population of all motors. Table 4-20 presents the details of the calculations. Columns 6 and 8 of Table 4-20 are the calculated values of mean and standard deviation of strain at maximum stress at 77° F and are the final result of the parts of this report section concerned with strain. The calculation for service life of the motor is performed for a reference temperature of 70° F, so the strain versus strain rate of Table 4-20 is shown shifted to 70° F in Figure 4-18.

## 3. Calculation of Stress Relaxation Modulus

In the calculations concerning relaxation modulus, the data used to calculate variability and the average value of the population at 2.45 seconds are taken from the largest population available, which is presented in Table 4-6 and further developed in Table 4-18. However, this population does not extend into the relaxation time range of interest for the service life calculation. Therefore, the overall curve shape obtained from the stress relaxation data set (Table 4-4) is used to find the mean values by adjusting the curve vertically to pass through the average value at 2.45 seconds.

TABLE 4-20

CALCULATION OF STRAIN AT MAXIMUM STRESS FOR THE  
EXISTING POPULATION OF MOTORS

(1) Strain Rate in/in/min	(2) Average Sample Strain at Max Stress (Table 4-5) %	(3) Standard Deviation of Sample (Table 4-5) %	(4) Coefficient of Variation of Sample %	(5) Estimate of Standard Deviation(s) of Population %	(6) Upper Limit of Standard Deviation of Population %	(7) Correlation Factor (Table 4-14)	(8) Mean Value of Strain at Maximum Stress of Population %
10	48.71	3.12	6.41	2.73	3.90	.844	49.89
20	46.94	3.09	6.58	2.63	3.76	.814	48.12
40	44.74	2.84	6.35	2.51	3.59	.775	45.81
70	42.63	2.51	5.89	2.39	3.42	.740	43.74
100	41.19	2.27	5.51	2.31	3.30	.712	42.07
200	38.56	2.00	5.19	2.16	3.09	.668	39.49
400	35.79	1.61	4.50	2.00	2.86	.620	36.65
700	33.71	1.61	4.78	1.89	2.70	.583	34.46
1000	32.56	1.71	5.25	1.82	2.60	.564	33.34
Average			5.60				

(4) Coefficient of variation =  $\frac{\text{standard deviation (3)}}{\text{average strain (2)}}$

(5)  $S = (\text{Average coefficient of variation (4)}) \times (\text{average strain (2)})$

6  $\sigma = S \sqrt{\frac{n-1}{X^2}}_{95, n-1} = S \sqrt{\frac{15}{7.261}} = 1.43 S$

(8) Mean strain = (correlation factor (7)) x (weighted average lot value = 59.1)

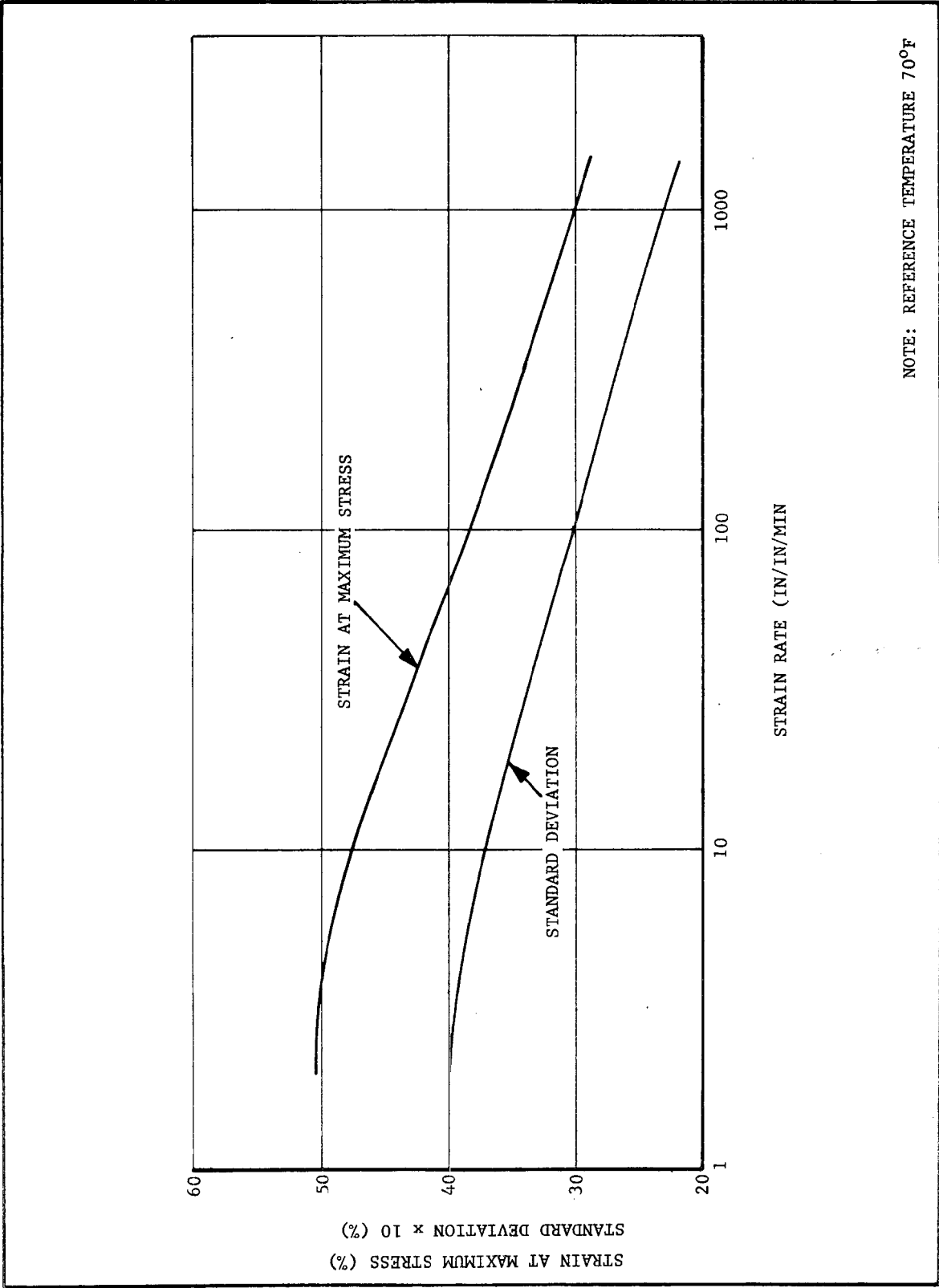


Figure 4-18. Strain at Maximum Stress for the Operational Motor Propulsion



The value of the average relaxation modulus at 2.45 seconds of the whole motor population is found as follows:

- (1) The weighted average of the powder lot acceptance value of initial tangent modulus of the population of all operational motors is 806 psi.
- (2) The equivalent relaxation modulus at 2.45 seconds of lot tangent modulus =  $806 \times 0.752 = 606.11$ .
- (3) Multiplying the lot relaxation modulus by the lot-to-unit correlation factor (Table 4-18) gives the average motor relaxation modulus at 2.45 seconds:  
 $606 \times 2.38 = 1442$  psi.

The average relaxation modulus at 2.45 seconds of the data set given in Table 4-4 is 1380 psi. These average values are presented in the second column of Table 4-21 which presents the calculations of the operational motor population mean and standard deviation. Each average value from the data set is multiplied by the constant  $1442/1380 = 1.04$ . This is equivalent to a vertical shift of the stress relaxation curve, when the curve is plotted on log-log scales. The resultant values of the mean of the stress relaxation modulus of the operational motor population are shown in column 3 of Table 4-21.

The estimate of the standard deviation is obtained by multiplying each relaxation modulus value of the motor population by the coefficient of variation obtained in Table 4-18. The upper limit of the standard deviation is obtained from the chi-squared statistic at the 95 percent confidence level as was done for strain. For the relaxation modulus calculation, the degrees of freedom of the chi-squared statistic are obtained from the population of 24 units given in Tables 4-6 and 4-18. Thus,  $\sigma = 1.29 S$ . Columns 3 and 5 of Table 4-21 are the calculated values of the mean and the standard deviation of stress relaxation modulus of the operational motor at 77° F, and are the final result of this report topic. The calculation of service life of the motor is performed at a reference temperature of 70° F, so the relaxation modulus versus time curve obtained in Table 4-21 is shown on Figure 4-19 shifted to a reference temperature of 70° F.

#### 4. Conclusions and Recommendations

The actual data set available for this task is not exactly ideal for illustrating the overttest concept. The most deficient feature is the lack of an aging trend of the propellant. Although the nonaging character of CYH propellant is very advantageous for the long term reliability of the Minuteman II Stage III rocket motor, it reduces the service life calculation to somewhat of an absurdity. That is, since nothing critical for failure of the motor is changing with time, the service life prediction is accomplished with one calculation that is independent of age.

TABLE 4-21

CALCULATION OF THE MEAN AND STANDARD DEVIATION OF THE  
STRESS RELAXATION MODULUS OF THE OPERATIONAL MOTOR POPULATION

Relaxation Time Sec	Average Relaxation Modulus of the Sample (Table 4-4) Psi	Average Relaxation Modulus of the Motor Population Psi	Estimate of the Standard Deviation Psi	Upper Limit of the Standard Deviation Psi
$10^{-6}$	41334	43176	6044	7792
$10^{-5}$	24285	25367	3551	4578
$10^{-4}$	13758	14371	2012	2593
$10^{-3}$	7447	7779	1089	1404
$10^{-2}$	3985	4163	583	751
$10^{-1}$	2321	2424	339	438
1	1586	1656	232	299
2.45	1381	1443	202	260
10	1166	1218	171	220

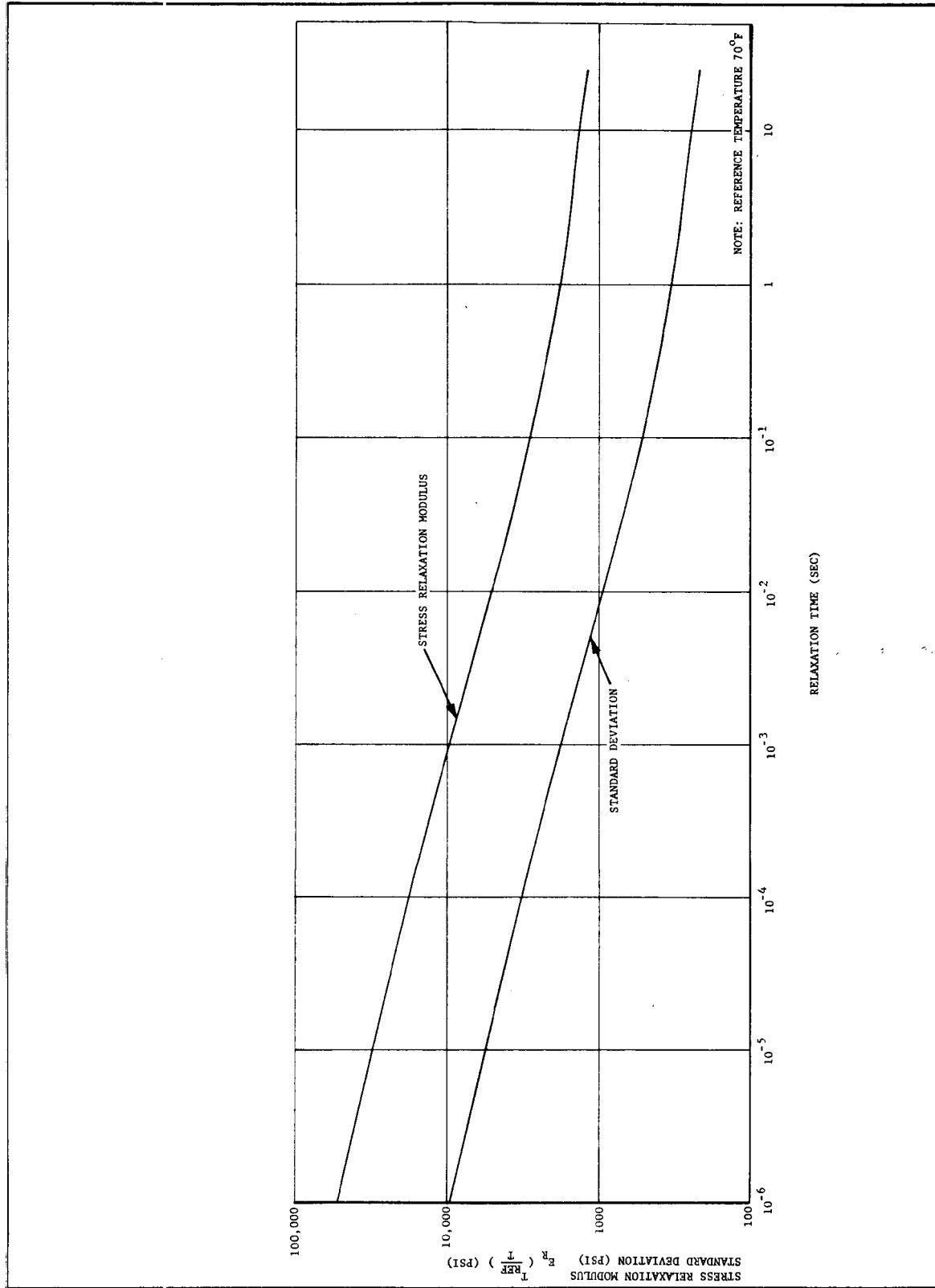


Figure 4-19. Stress Relaxation Modulus for the Operational Motor Propulsion

The manipulations of data necessary to transform the existing and ongoing data base from what it is to what was desired point up the necessity for the careful structuring of surveillance programs. Meaningful predictive surveillance is urgently needed. It seems widely recognized in the industry at this time that the methodology for predictive surveillance is not yet at a satisfactory level of excellence, and various activities and programs are underway to rectify this situation. It is also widely recognized that successful predictive surveillance can no longer be a simple and inexpensive effort added at the end of a motor manufacturing program, but must be started early in the motor development phase.

Since the data base for CYH propellant basically consists of what was previously tested, and therefore little can be done to improve it, only one recommendation is presented herein. The Dissected Motor Program at OALC is presently making periodic propellant tests on six Minuteman II Stage III motors: S/N 31064, 31134, 33174, 32434, Grain 131, and Grain 70. Three of these motors were manufactured from propellant lots that were never used for Minuteman II motor production. It is recommended that these three, S/N 31064, Grain 131, and Grain 70, not be further tested. Motor S/N 32831 has been tested twice in the Dissected Motor Program, and was made from a propellant lot still represented in the operational motor inventory. It is recommended that this motor be added to the five-motor composites. The other two motors should also be chosen from powder lots still in the missile inventory. It is further suggested that the usefulness of the Dissected Motor Program reports would be improved if all data from a Minuteman II motor previously obtained by OALC could be reported periodically for a few of the more critical physical properties tested in the Dissected Motor Program.

#### E. ACKNOWLEDGEMENTS

The writer wishes to thank the following individuals at OALC, who made information and data printouts available in a timely manner for use in preparation of this report section:

Elizabeth Dalabla  
Glen Groll  
Gene Lund  
Glen Ogilvie

F. BIBLIOGRAPHY

1. F. Beavers, "Stress Relaxation Modulus for CYH, EJC and DDP Propellants," Task 9, Minuteman Support Program, Library No. UR-63-103382, Hercules Incorporated, Magna, Utah, September 1963.
2. D. E. Richardson, "High Rate Uniaxial Failure Tests," Task 9, Minuteman Support Program, Library No. UR-63-103708, Hercules Incorporated, Magna, Utah, October 1963.
3. "Propellant Charge Stress-Strain-Time Relations in the M-57 Configuration," Task 9, Minuteman Support Program, Structural Mechanics Group, Hercules Incorporated, Magna, Utah, April 1964.
4. L. F. Myers, Material Property Tests on Propellant from Subscale and Full-Scale Motors, Library No. UR-64-101704, Hercules Incorporated, Magna, Utah, 24 June 1964.
5. L. F. Myers, The Effect of Aging on the Material Properties of CYH and DDP Propellants, Library No. UR-64-101836, Hercules Incorporated, Magna, Utah, 24 June 1964.
6. L. F. Myers, The Effect of Two Methods of Sample Preparation on the Propellant Material Properties, Library No. UR-64-201863, Hercules Incorporated, Magna, Utah, 24 June 1964.
7. S. R. Swanson, An Illustration of the Time-Temperature Super-Position Principle as Applied to Uniaxial Tensile Tests on Cast Modified Double-Base Propellants, Ref No. M051317/5/10-58, Hercules Incorporated, Magna, Utah, January 1965.
8. S. R. Swanson, A Method for Obtaining the Linear Tensile Relaxation Modulus from Constant Strain Rate Tests on Viscoelastic Materials, Ref No. MC51317/5/10-5y, Hercules Incorporated, Magna, Utah, January 1965.
9. F. R. Jensen and J. M. Anderson, Study on Revision of the CYH Propellant Acceptance Specification, Hercules Incorporated, Magna, Utah, no date.
10. W. R. Tucker, Effect of Humidity on the Physical Properties of HPC Composite Modified Double-Base Propellant, Ref No. MISC/5/5/371, Hercules Incorporated, Magna, Utah, 10 June 1965.
11. S. R. Swanson, Determination of a Failure Theory for a Double-Base Propellant Under Constant Strain Rate Loading, Ref No. -127/5/10-110, Hercules Incorporated, Magna, Utah, July 1965.
12. R. N. Chappell, OOAMA-Hercules Co-Operative Test Program, Ref. No. -127/5/10-141, Hercules Incorporated, Magna, Utah, 9 November 1965.

13. S. R. Swanson, "A Study of the Applicability of Time-Temperature Superposition to CYH and VBB Propellants," Task 2 - Propellant Structural Analysis, Ref No. -127/5/10-143, Hercules Incorporated, Magna, Utah, 2 December 1965.
14. Third Stage Minuteman Production Support Program Quarterly Progress Report, Tasks 2, 8 and 14, Hercules Incorporated, Magna, Utah, no date.
15. Third Stage Minuteman Production Support Program, Task 2, Report No. MTD-22-II, Hercules Incorporated, Magna, Utah, January 1966.
16. L. F. Myers, Series II Propellant Mechanical Property Results from a Minuteman Third Stage Surveillance Motor, Grain 336, Ref No. 544/5/10-194, Hercules Incorporated, 6 May 1966.
17. F. R. Jensen, "A Study on the Variation of the Margin of Safety as a Function of Propellant Age for the Third Stage Minuteman Propellant Grain," Minuteman Third Stage Surveillance Program, Hercules Incorporated, August 1966.
18. L. F. Myers, The Effect of Vibration and Constant Strain Environments on the Uniaxial Tensile Failure Properties of CYH Propellant, Ref No. 544/4/10-215, Hercules Incorporated, Magna, Utah, 30 September 1966.
19. S. R. Swanson and A. K. Phifer, Case Bond Failure Criteria Study, Ref No. 544/6/40-153, Hercules Incorporated, Magna, Utah, 31 October 1966.
20. R. N. Chappell, Propellant Grain Service Life Predictions, Ref No. -544/6/40-161, Hercules Incorporated, Magna, Utah, 28 December 1966.
21. Memo from R. N. Chappell, Propellant Grain Service Life Predictions, Ref No. -544/6/40-161, Hercules Incorporated, Magna, Utah, 18 January 1967.
22. S. R. Swanson, Subscale Motor Verification Program, Ref No. -544/6/40-168, Hercules Incorporated, Magna, Utah, 10 February 1967.
23. Minuteman Stage III Materials and Components Surveillance Studies, Weapon System 133A, Report No. MTO-1124-15, Hercules Incorporated, Magna, Utah, 20 July 1967.
24. Memo from L. F. Myers to J. C. Farber, Mechanical Property Results from CYH Propellant Cast with RAD-1-14-66 and RAD-1-15-67 Powder, Ref No. 17-10203/6/40-195, Hercules Incorporated, Magna, Utah, 15 August 1967.

25. L. F. Myers, Propellant Mechanical Property Results from the Second OOAMA-Hercules Cooperative Test Program, Ref No. F42600-42008/6/40-554, Hercules Incorporated, Magna, Utah, 15 September 1967.
26. R. D. Belnap and L. O. Murphy, Heat Transfer and Thermal Stress Analyses of Minuteman Stage III Motor Wings II-VI, Hercules Incorporated, Magna, Utah, February 1968.
27. "The Investigation of Pressure Oscillations During Firing of the Minuteman II Stage III Motor," Report No. MTO-1124-34, Vol. III, Task II - Analysis and Task III - Correlation and Categorization, Hercules Incorporated, Magna, Utah, January 1971.
28. Minuteman Service Life Study Program, Report No. MTO-1124-49-3, Hercules Incorporated, Magna, Utah, 1 November 1971.
29. Minuteman II Stage III Motor Categories and Service Life Studies, MTO-1124-60, Hercules Incorporated, Magna, Utah, 31 December 1971.
30. LGM-30 3rd Stage Dissected Motor Program Propellant Test Results, Report No. NR 272(73), MMEMP Project 2MP 105P, Department of the Air Force Headquarters, Ogden Air Materiel Area (AFLC), Hill Air Force Base, Utah, August 1973.
31. D. B. Gunn, Minuteman Stage III Process Control Charts, Acceptance Testing of Propellant Powder Lots, Hercules Incorporated, no date.
32. LGM-30 3rd Stage Dissected Motor Program Propellant Test Results, Report No. NR 243(72), MMEMP Project 763P and 768P, Department of the Air Force Headquarters, Ogden Air Materiel Area (AFLC), Hill Air Force Base, Utah, June 1972.
33. R. N. Chappell, Physical Properties Tests on Surveillance Grain 336, Ref No. -544/5/10-192, Hercules Incorporated, Magna, Utah, 12 May 1966.
34. L. F. Myers, Propellant Mechanical Property Results from a Minuteman Third Stage Surveillance Motor, Grain 336, Ref No. -544/6/40-162, Hercules Incorporated, Magna, Utah, 29 December 1966.
35. R. N. Chappell, Physical Properties Tests on Surveillance Grain 216, Ref No. -544/5/10-185, Hercules Incorporated, Magna, Utah, 9 April 1966.
36. L. F. Myers, Series II Propellant Mechanical Property Results from a Minuteman Third Stage Surveillance Motor, Grain 216, Ref No. 544/5/10-191, Hercules Incorporated, Magna, Utah, 20 April 1966.

37. L. F. Myers, Series I Propellant Mechanical Property Results from a Minuteman Third Stage Surveillance Motor, Grain 216, Ref No. 544/5/2/210, Hercules Incorporated, Magna, Utah, 30 August 1966.
38. R. N. Chappell, Physical Properties Tests on Surveillance Grain 131, Ref No. 544/4/10-193, Hercules Incorporated, Magna, Utah, 13 May 1966.
39. L. F. Myers, Series II Propellant Mechanical Property Results from a Minuteman Third Stage Surveillance Motor, Grain 131, Ref No. 544/5/10-195, Hercules Incorporated, Magna, Utah, 9 May 1966.
40. L. F. Myers, Propellant Mechanical Property Results from a Minuteman Third Stage Surveillance Motor, Grain 131, Ref No. 544/6/40-160, Hercules Incorporated, Magna, Utah, 28 December 1966.
41. L. F. Myers, Series I Propellant Mechanical Property Results from a Minuteman Third Stage Surveillance Motor, Grain 67, Ref No. 544/5/10-189, Hercules Incorporated, Magna, Utah, 25 March 1966.
42. L. F. Myers, Series II Propellant Mechanical Property Results from a Minuteman Third Stage Surveillance Motor, Grain 67, Ref No. 544/5/2-209, Hercules Incorporated, Magna, Utah, 30 August 1966.
43. L. F. Myers, Propellant Mechanical Property Results from a Minuteman Third Stage Surveillance Motor, Grain 67, Ref. No. 42008/6/40-411, Hercules Incorporated, Magna, Utah, 28 April 1967.
44. L. F. Myers, Propellant Mechanical Property Results from a Minuteman Third Stage Surveillance Motor, Grain 67, Ref No. 42008/6/40-194, Hercules Incorporated, Magna, Utah, 2 August 1967.
45. L. F. Myers, Propellant Mechanical Property Results from a Minuteman Stage III Surveillance Motor, Grain 70, Ref No. 0058/6/40-1166, Hercules Incorporated, Magna, Utah, 20 December 1968.
46. "Interconversion of Viscoelastic Material Properties for Minuteman Stage III Propellants," Task 9, Minuteman Support Program, Library No. UR-63-103299, Hercules Incorporated, Magna, Utah, September 1963.
47. "Development of an Improved Case Bond Tensile Specimen," Task 9, Minuteman Support Program, Library No. UR-63-103707, Hercules Incorporated, Magna, Utah, October 1963.
48. "Rapid Strain Rate to High Strain Tests," Task 9, Minuteman Support Program, Library No. UR-63-103400, Hercules Incorporated, Magna, Utah, October 1963.



49. "Long Term Constant Strain Tests," Task 9, Minuteman Support Program, Library No. UR-64-101279, Hercules Incorporated, Magna, Utah, March 1964.
50. The Investigation of Pressure Oscillations During Firing of the Minuteman II Stage III Motor, Vol. I, Program Summary, Report No. MTO-1124-34, Hercules Incorporated, Magna, Utah, January 1971.
51. The Investigation of Pressure Oscillations During Firing of the Minuteman II Stage III Motor, Vol. II, Task I - Ingredients and Process Investigation, Report No. MTO-1124-34, Hercules Incorporated, Magna, Utah, January 1971.
52. The Investigation of Pressure Oscillations During Firing of the Minuteman II Stage III Motor, Vol. IV, Task IV - Minimization of Effects, Report No. MTO-1124-34, Hercules Incorporated, Magna, Utah, January 1971.
53. LGM 3rd Stage Dissected Motor Program Propellant Test Results, MANCP Report NR 311(74), MMEMP Project 2MP 105P, Ogden Air Logistics, Hill Air Force Base, Utah, October 1974.
54. L. F. Myers, Physical Property Data Obtained from the Materials Taken from Minuteman Third Stage Motors for the Long Range Service Life Analysis Program, Ref No. LRSLA/6/40-4698, Hercules Incorporated, Magna, Utah, 29 January 1975.

## SECTION V

### M57A1 SERVICE LIFE ESTIMATES

#### A. INTRODUCTION

Motor service life estimates involved three techniques. First, theoretical analyses were performed using materials properties representative of the motors. In principle, properties as a function of age should be input to the analysis and service life determined by extrapolation of available data to future dates based on aging trends. In this case, however, no aging trends were evident and the repetitive analyses to represent various aging times were not required. Second, experimental overtest results from full-scale unit tests of motors of different ages were extrapolated to advanced ages. Third, and finally, analog units were tested to verify analytical techniques and to aid in further interpretation of results.

Results from the three approaches were evaluated collectively to produce a statistical prediction of service life.

Critical failure modes were previously determined<sup>1</sup> to be propellant cracking in the wing slot tip or aft centerport bond breakage, depending on motor configuration. An additional analysis of the aft centerport adhesive bond was performed using full-scale case properties adjusted to match case deflections obtained experimentally during chamber hydroproof acceptance testing. The revised analytical results indicated that bond failure was not the critical mode. This was verified by the full-scale overtest results. Therefore, propellant cracking in the wing slot tip is considered the critical failure mode limiting service life.<sup>2</sup>

Results of the analytical studies are presented first in the following discussion. Techniques used in modeling the motor and performing the requirement/capability analyses are then presented.

Next, analog test and full-scale overtest results are evaluated with regard to their applicability to service life estimates. Finally, results are combined to produce a statistical prediction of M-57 motor service life.

#### B. ANALYTICAL STUDIES

##### 1. Method

Analyses of the M57A1 Stage III motor for the critical loads and failure modes were performed in the evaluation of overtest approaches<sup>1</sup>. Those results are updated in this report to reflect more recent results and improved definitions of materials properties.

---

<sup>1</sup>References are shown at the end of the section

Theoretical analyses were performed by standard state-of-the-art analysis methods. Elastic solutions were obtained from axisymmetric finite element analyses modified to account for stress concentrations at slot tips. Unit step loadings were assumed over a range of moduli corresponding to relaxation moduli at various relaxation times on the ignition pressurization curve. Viscoelastic unit step loading solutions were determined by relating the elastic solutions to the stress relaxation time scale. Time-dependent solutions were obtained for the centerport and wing slot regions by superposition principles, (Duhammel integral).

The earlier analyses supported the selection of wing slot cracking and aft centerport bond failure as the most probable grain failure modes.

Input data to the analyses were treated statistically by a computerized probabilistic technique, designated the R/C analysis. By this method, the Monte Carlo Simulation technique is applied to all the analysis input that can be defined in probabilistic terms. For the M57A1 motor, this involved case and propellant mechanical properties and pressure-time curves for the ignition period of loading. The results thus obtained include the mean, standard deviation, and the three-sigma limits on the propellant failure index (damage factor).

The essential differences between results presented herein are the use of an improved case model in the analysis and a better definition of slot strain concentration factors which accounts for changes in slot geometry with loading.

The stress analysis method consisting of the viscoelastic response and cumulative damage portions of the R/C program was verified by the experimental results. The applicability of the strain at maximum stress-cumulative damage failure criterion was also confirmed. Material constitutive data and actual applied pressure from each full-scale overtest and analog pressurization test were input to the program. Predicted failure data were then compared to actual failure pressures.

## 2. Loads

Actual ignition pressure data are available for 169 M57 Stage III motors. These pressure data, corrected to 70° F, are presented in Table 5-1 and plotted in Figure 5-1, as a function of motor age at firing. To determine if aging produces a change in magnitude of the ignition pressure, a regression analysis was performed. The resultant equation is:

$$P = 276.808 - 0.0236A$$

where:

P = ignition pressure (psig)

A = motor age (months)

TABLE 5-1

## M-57 MOTOR IGNITION PRESSURES - CORRECTED TO 70° F

Motor No.	Age (mo)	P <sub>ignition</sub> (psig)	Motor No.	Age (mo)	P <sub>ignition</sub> (psig)	Motor No.	Age (mo)	P <sub>ignition</sub> (psig)	Motor No.	Age (mo)	P <sub>ignition</sub> (psig)	Motor No.	Age (mo)	P <sub>ignition</sub> (psig)
QA 31A	3.02	283.9	QA 44	2.33	266.6	QA 80	3.81	283.9	6-4-18	2.43	271.2	32064	85.51	274.5
QA 31B	3.29	279.1	QA 46	1.84	271.4	QA 81	2.43	280.7	32001	87.39	276.3	32071	112.14	277.0
QA 10	2.73	282.2	QA 47	2.56	276.3	QA 82	5.00	283.7	32003	70.82	282.5	32076	50.70	274.8
QA 11	2.79	286.4	QA 48	2.30	274.7	QA 83	2.63	281.1	32004	70.36	281.5	32085	87.12	277.1
QA 12	2.53	280.9	QA 49	3.02	284.3	QA 84	3.72	284.2	32005	65.42	276.5	32089	71.87	273.1
QA 13	2.66	276.6	QA 50	2.14	278.3	QA 1	1.48	286.4	32007	62.76	283.5	32096	63.58	272.8
QA 14	2.73	276.8	QA 51	4.18	281.6	QA 2	1.54	288.0	32008	71.64	277.8	32106	115.99	273.4
QA 15	2.00	280.7	QA 52	2.50	281.1	QA 3	1.97	289.6	32010	49.54	284.0	32145	76.86	278.0
QA 16	2.79	276.5	QA 53	4.70	276.6	QA 4	2.00	293.0	32011	104.45	278.7	32238	58.45	267.7
QA 17	2.83	278.7	QA 54	4.11	278.3	QA 5	2.14	289.0	32015	80.05	275.3	32262	56.94	272.3
QA 18	4.67	285.0	QA 55	3.55	273.4	QA 6	2.56	281.9	32018	112.54	275.1	32272	52.47	275.3
QA 19	2.93	279.5	QA 56	3.94	279.0	QA 7	3.65	284.8	32019	51.62	269.0	32335	43.86	252.6
QA 20	4.47	275.0	QA 57	2.99	273.3	QA 8	4.01	275.0	32022	43.59	276.1	32339	96.43	269.5
QA 21	2.76	276.1	QA 58	3.48	266.0	QA 9	3.32	282.5	32023	56.32	282.2	32344	60.20	270.1
QA 22	2.86	276.9	QA 59	2.43	276.3	2-5-1	25.68	282.8	32027	61.71	262.1	32348	75.75	271.2
QA 23	3.94	275.5	QA 60	3.68	281.7	2-5-2	37.61	279.9	32031	118.26	275.5	32350	96.66	272.3
QA 24	3.45	281.0	QA 61	2.79	284.8	6-4-1	3.16	273.1	32033	70.12	271.6	32818	51.98	270.8
QA 25	3.02	273.0	QA 62	3.52	280.7	6-4-2	3.19	256.8	32035	45.70	283.0	32918	66.80	264.3
QA 26	3.12	275.6	QA 64	5.23	274.1	6-4-3	1.61	270.2	32037	132.85	279.8	32934	88.64	261.0
QA 27	2.93	277.1	QA 65	4.40	280.1	6-4-4	2.10	269.0	32038	119.44	280.8	32935	67.96	263.9
QA 28	2.60	276.0	QA 66	3.35	273.7	6-4-5	2.76	269.6	32039	124.96	273.7	32948	84.36	267.6
QA 29	3.39	281.2	QA 67	3.52	277.8	6-4-6	2.30	266.5	32044	70.12	275.7	32949	89.36	266.4
QA 30	2.93	280.5	QA 68	3.32	278.8	6-4-7	2.63	262.0	32046	96.76	281.9	32958	67.99	268.0
QA 31	2.83	283.4	QA 69	3.81	280.9	6-4-8	2.83	267.8	32047	69.93	277.1	32966	63.09	257.2
QA 32	2.70	275.6	QA 70	4.24	276.2	6-4-9	2.30	266.5	32049	108.82	282.9	32968	79.30	261.5
QA 35	1.22	274.8	QA 71	3.81	278.5	6-5-1	37.54	270.0	32051	89.82	279.2	32971	63.94	269.6
QA 36	1.25	272.0	QA 72	3.48	280.2	6-5-2	65.06	266.1	32053	50.07	291.1	32978	76.04	268.0
QA 37	1.38	274.5	QA 73	4.54	279.1	6-4-10	2.50	268.5	32056	130.55	282.5	32989	89.79	272.5
QA 38	1.38	276.7	QA 74	5.03	275.7	6-4-11	2.53	269.0	32057	50.66	275.7	32992	72.06	277.6
QA 39	1.61	268.7	QA 75	3.68	281.7	6-4-12	2.50	268.3	32058	114.21	274.1	32993	77.52	275.1
QA 40	1.61	280.2	QA 76	2.89	281.6	6-4-14	2.56	272.3	32059	105.93	284.6	32996	69.30	281.3
QA 41	1.91	280.2	QA 77	1.54	288.6	6-4-15	2.27	267.5	32060	126.64	276.3	33004	90.61	275.0
QA 42	2.46	274.9	QA 78	4.37	281.0	6-4-16	2.00	268.0	32061	98.40	278.4	33063	91.17	280.3
QA 43	1.54	267.9	QA 79	3.98	279.5	6-4-17	2.56	270.3	32062	75.42	274.2			

P<sub>ignition</sub> = 276.004 psig σ<sub>P<sub>ignition</sub></sub> = 6.7519 psig

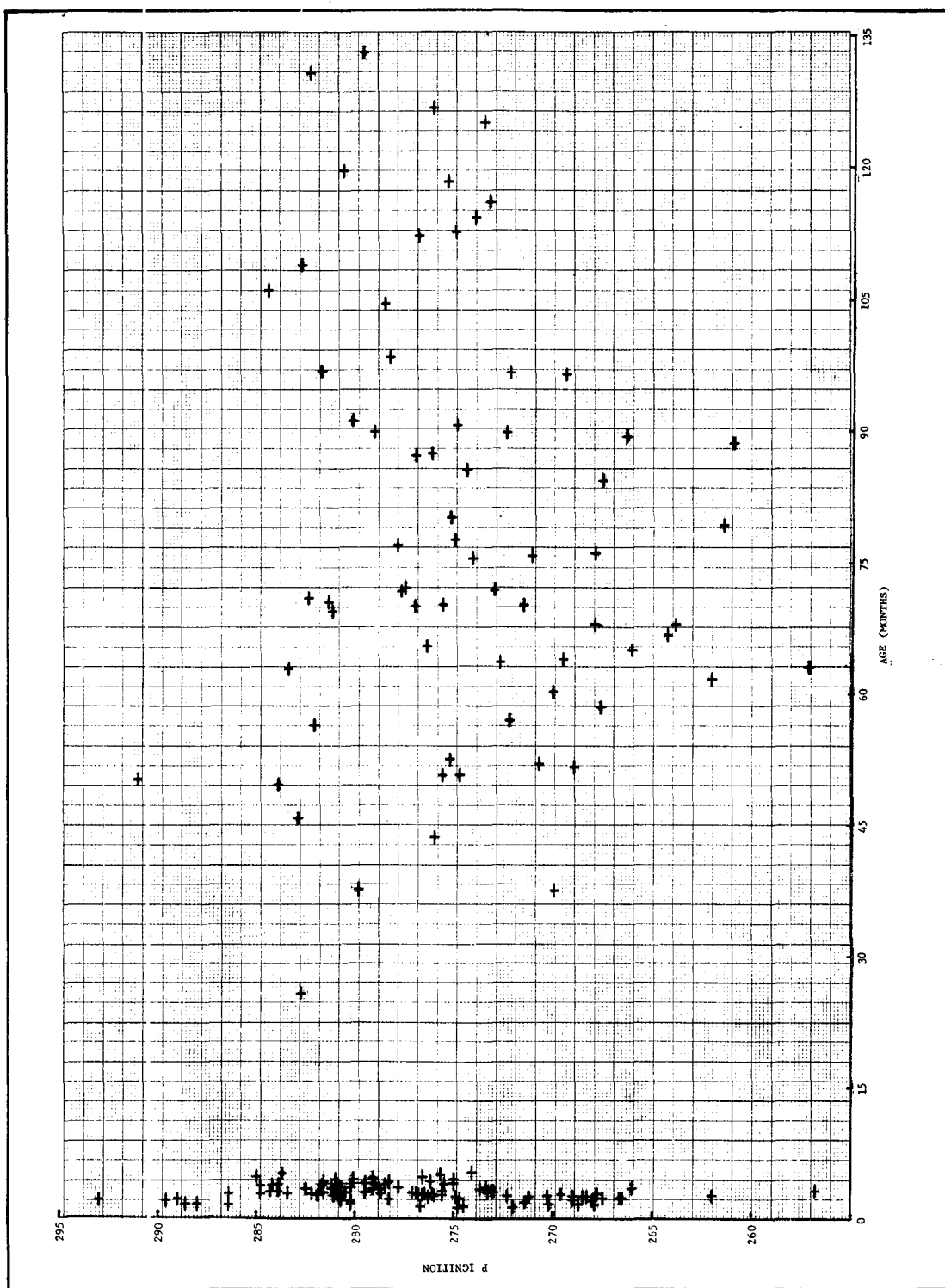


Figure 5-1. M-57 Motor Ignition Pressure as a Function of Motor Age  
from 169 Firings - Corrected to 70° F

The corresponding correlation coefficient ( $\gamma$ ) of pressure and motor age is only 0.14114. Thus, it can be assumed for purposes of service life predictions that any trend in ignition pressure with age is insignificant. A logical extension is that the complete ignition pressure transient is also independent of age since burn rate is a function of pressure. Any change in pressure level at times less than ignition time would affect burn rate throughout the remainder of the ignition transient and be reflected in ignition pressure data. Since cumulative damage is dependent upon strain rate, an additional test was required to verify that time to ignition is not a significant function of age. Complete ignition pressurization transient curves, including time to ignition, are available for 78 motors. A regression analysis showed a correlation coefficient for ignition time and motor age of only 0.055063. Therefore, ignition pressurization was considered to be independent of motor age for the analytical service life calculations.

Input to the R/C computer program was made in the form of 35 individual pressurization curves. The 35 pressurization curves were randomly selected from the 78 motor tests. To verify that a typical sampling was obtained, the mean and standard deviation of the ignition pressure of the 35 samples were compared to those of the total 169 motors. Mean ignition pressure was 276.951 psig compared to 276.004 psig for the 169 motors. Corresponding standard deviations were 7.0152 psig and 6.7519 psig, respectively. A complete tabulation of available ignition pressurization transient data is presented in Table 5-2 for the 78 motor tests.

### 3. Properties

To obtain propellant strain response to applied pressure at the critical wing slot region<sup>3</sup> as a function of propellant relaxation modulus, it was necessary to perform finite-element analyses for a range of propellant moduli. A finite-element analysis of the adhesive aft bond configuration was also required to verify that the adhesive aft bond was a significantly less critical region than the wing slot tip and could be disregarded in service life predictions. The properties shown in Table 5-3 were used in the finite-element analyses. The propellant property selection procedure and the resultant mean propellant relaxation modulus and allowable strain values (including standard deviations) used in the viscoelastic response and R/C analyses are presented in Section IV of this report.

Case deflections from 67 cases during hydroproofing were obtained from linear potentiometers and girth bands. Data are presented in Table 5-4 at 300 psig applied pressure. Calculated mean values and standard deviations are also shown. The resultant coefficients of variation are quite large. This was attributed to inherent variations in the instrumentation systems as well as the actual variation of the deflections. For this reason, the coefficient of variation of available chamber burst pressures was used to calculate the limits of expected case deflections. Burst pressures from 28 cases are presented in Table 5-5. A coefficient of variation of 0.08839 was calculated. Finite-element computer analyses were then performed with the motor case properties iterated to produce the desired mean and plus 3-sigma deflections at 300 psig applied internal pressure. These deflections are tabulated in Table 5-6.

TABLE 5-2

## M-57 MOTOR IGNITION PRESSURIZATION TRANSIENTS (70° F FIRINGS)

Motor	P <sub>1</sub> (psi)	t <sub>1</sub> (sec)	P <sub>2</sub> (psi)	t <sub>2</sub> (sec)	P <sub>3</sub> (psi)	t <sub>3</sub> (sec)	P <sub>4</sub> (psi)	t <sub>4</sub> (sec)	P <sub>5</sub> (psi)	t <sub>5</sub> (sec)	P <sub>6</sub> (psi)	t <sub>6</sub> (sec)	P <sub>ign</sub> (psi)	t <sub>ign</sub> (sec)
QA-1	56.25	0.052	214.72	0.062	242.5	0.062	249.0	0.062	279.7	0.117	283.3	0.137	286.4	0.151
QA-2	61.27	0.062	214.46	0.071	240.0	0.078	267.6	0.098	279.8	0.118	283.9	0.137	288.0	0.153
QA-3	65.26	0.057	208.02	0.067	234.9	0.078	276.3	0.098	282.4	0.118	285.5	0.137	289.6	0.149
QA-4	58.93	0.055	218.04	0.066	240.6	0.071	276.0	0.092	285.8	0.112	289.7	0.132	293.0	0.147
QA-5	51.06	0.054	224.67	0.066	253.3	0.078	272.7	0.098	279.8	0.118	283.9	0.137	289.0	0.143
QA-6	48.14	0.059	212.03	0.070	242.8	0.078	264.3	0.098	275.5	0.117	279.6	0.137	281.9	0.152
QA-7	56.84	0.052	223.32	0.064	249.7	0.074	263.9	0.086	271.0	0.098	278.1	0.123	284.8	0.150
QA-10	62.94	0.064	208.10	0.074	244.6	0.086	258.8	0.098	273.1	0.123	279.2	0.148	282.2	0.160
QA-11	69.24	0.054	210.76	0.065	240.3	0.074	257.6	0.086	271.8	0.098	280.0	0.123	286.4	0.145
QA-12	58.58	0.058	209.90	0.069	239.2	0.077	259.7	0.090	271.4	0.102	278.2	0.128	280.9	0.150
QA-13	40.79	0.056	205.98	0.071	220.2	0.074	261.0	0.098	270.2	0.123	275.3	0.147	276.6	0.153
QA-14	63.46	0.054	219.66	0.064	240.2	0.077	268.5	0.102	275.3	0.125	281.2	0.128	276.8	0.160
QA-15	45.96	0.057	194.03	0.069	219.6	0.073	245.1	0.086	259.4	0.098	271.6	0.122	280.7	0.149
QA-16	55.98	0.061	198.40	0.071	221.0	0.076	245.5	0.089	260.3	0.102	270.1	0.127	276.5	0.155
QA-17	61.09	0.054	210.76	0.066	239.3	0.074	254.5	0.086	264.7	0.098	272.9	0.123	278.7	0.147
QA-18	59.11	0.053	201.95	0.063	242.3	0.076	261.0	0.089	270.9	0.102	275.8	0.127	285.0	0.148
QA-19	81.94	0.059	204.86	0.066	239.7	0.073	266.3	0.098	271.4	0.122	276.6	0.146	279.5	0.160
QA-20	57.14	0.056	175.35	0.064	208.8	0.068	266.6	0.076	262.0	0.102	271.9	0.127	275.0	0.162
QA-21	51.37	0.057	200.34	0.071	217.8	0.073	252.7	0.097	267.1	0.122	272.2	0.146	276.1	0.160
QA-22	49.26	0.055	201.95	0.071	223.6	0.076	261.1	0.102	270.9	0.127	272.9	0.152	276.9	0.171
QA-23	54.45	0.057	215.75	0.073	242.4	0.085	256.8	0.097	264.0	0.122	267.1	0.146	275.5	0.164
QA-24	63.84	0.054	210.18	0.069	232.8	0.076	255.4	0.089	265.2	0.102	275.0	0.127	281.0	0.157
QA-25	56.34	0.059	194.62	0.070	240.7	0.085	253.0	0.098	266.3	0.122	271.4	0.146	273.0	0.160
QA-26	68.55	0.061	210.53	0.074	243.8	0.089	255.6	0.102	269.3	0.128	273.2	0.153	275.6	0.172
QA-27	61.37	0.061	206.60	0.073									277.1	0.164
QA-28	74.42	0.061	195.84	0.071	228.2	0.077	259.5	0.102	270.3	0.128	276.2	0.153	276.0	0.165
QA-29	65.36	0.059	209.35	0.069									281.2	0.168
QA-30	62.48	0.056	201.11	0.068	238.2	0.077	266.5	0.102	275.3	0.128	278.2	0.153	280.5	0.164
QA-31	56.17	0.054	200.16	0.066	232.8	0.073	264.5	0.098	271.6	0.122	280.8	0.147	283.4	0.159

TABLE 5-2 (Cont)

## M-57 MOTOR IGNITION PRESSURIZATION TRANSIENTS (70° F FIRINGS)

Motor	P <sub>1</sub> (psi)	t <sub>1</sub> (sec)	P <sub>2</sub> (psi)	t <sub>2</sub> (sec)	P <sub>3</sub> (psi)	t <sub>3</sub> (sec)	P <sub>4</sub> (psi)	t <sub>4</sub> (sec)	P <sub>5</sub> (psi)	t <sub>5</sub> (sec)	P <sub>6</sub> (psi)	t <sub>6</sub> (sec)	P <sub>ign</sub> (psi)	t <sub>ign</sub> (sec)
QA-31A	71.70	0.059	209.98	0.068	249.9	0.085	263.2	0.098	274.5	0.122	278.6	0.146	283.9	0.164
QA-31B	61.09	0.060	208.72	0.071	248.4	0.086	262.7	0.098	274.9	0.123	280.8	0.147	279.1	0.160
QA-32	62.67	0.061	188.01	0.071	219.3	0.076	257.5	0.102	268.3	0.128	272.2	0.153	275.6	0.166
QA-35	50.76	0.059	203.02	0.071	245.6	0.086	253.8	0.099	268.0	0.123	270.0	0.148	274.8	0.170
QA-36	54.02	0.051	209.20	0.066	235.7	0.076	256.3	0.102	264.2	0.127	269.1	0.153	272.0	0.165
QA-37	63.03	0.064	193.16	0.074	239.9	0.086	250.1	0.098	264.3	0.123	269.4	0.148	274.5	0.172
QA-38	58.67	0.056	209.24	0.069	229.8	0.077	262.0	0.102	270.8	0.128	271.8	0.153	276.7	0.164
QA-39	55.83	0.062	192.87	0.071	229.4	0.086	268.0	0.099	277.1	0.123	281.2	0.148	268.7	0.172
QA-40	68.55	0.061	207.59	0.071	233.0	0.076	263.4	0.102	270.3	0.128	274.2	0.153	280.2	0.173
QA-41	61.46	0.056	202.8	0.068	231.5	0.073	263.2	0.098	272.5	0.122	276.6	0.146	280.2	0.161
QA-42	54.18	0.061	193.1	0.073	220.7	0.076	256.1	0.102	266.0	0.127	270.9	0.152	274.9	0.165
QA-43	56.25	0.064	209.7	0.076	236.2	0.086	245.5	0.098	260.8	0.122	263.9	0.147	267.9	0.171
QA-44	59.11	0.063	206.9	0.076	229.5	0.089	248.2	0.102	261.0	0.127	267.0	0.152	266.6	0.175
QA-46	51.07	0.053	191.5	0.065	235.7	0.076	256.3	0.102	266.2	0.127	270.1	0.153	271.4	0.165
QA-50	59.12	0.061	197.1	0.074	246.4	0.089	260.1	0.101	272.0	0.127	276.9	0.152	278.3	0.156
QA-51	59.68	0.063	214.0	0.074	246.9	0.085	260.3	0.097	273.7	0.121	277.8	0.146	281.6	0.159
QA-52	49.34	0.063	192.4	0.073	240.8	0.089	252.6	0.101	271.4	0.127	276.3	0.152	281.1	0.170
QA-53	50.54	0.052	217.3	0.064	234.5	0.074	247.7	0.082	254.7	0.099			276.6	0.148
QA-54	60.89	0.064	215.1	0.074	251.7	0.086	264.9	0.099	274.0	0.123	274.0	0.148	278.3	0.150
QA-55	55.92	0.057	177.9	0.066	211.5	0.074	234.8	0.086	252.1	0.098	259.2	0.111	273.4	0.160
QA-56	54.74	0.065	214.0	0.078	243.8	0.088	260.7	0.100	276.7	0.126	279.6	0.151	279.0	0.165
QA-68	58.75	0.059	202.7	0.069	239.9	0.076	268.3	0.102	280.0	0.128	284.0	0.153	278.8	0.166
QA-72	60.89	0.056	193.5	0.066	235.7	0.076	269.1	0.102	279.9	0.127	284.8	0.153	280.2	0.165
QA-73					230.8	0.086	272.7	0.098	265.5	0.122	271.6	0.147	279.1	
QA-74	61.88	0.064	214.1	0.078	235.7	0.089	250.4	0.102	265.2	0.127	268.1	0.153	275.7	0.168
QA-76	44.20	0.056	201.3	0.071	229.8	0.076	256.3	0.102	268.1	0.127	273.0	0.153	281.6	0.160
QA-77	71.49	0.059	212.4	0.069	229.8	0.073	246.1	0.086	261.4	0.098	270.6	0.122	288.6	0.149
QA-78	49.58	0.058	203.3	0.071	228.1	0.076	247.9	0.088	262.8	0.101	272.7	0.126	281.0	0.154
QA-81	43.02	0.049	217.1	0.063	248.9	0.078	268.4	0.098	274.5	0.117	278.6	0.137	280.7	0.146



TABLE 5-2 (Cont)

M-57 MOTOR IGNITION PRESSURIZATION TRANSIENTS (70° F FIRINGS)

Motor	P <sub>1</sub> (psi)	t <sub>1</sub> (sec)	P <sub>2</sub> (psi)	t <sub>2</sub> (sec)	P <sub>3</sub> (psi)	t <sub>3</sub> (sec)	P <sub>4</sub> (psi)	t <sub>4</sub> (sec)	P <sub>5</sub> (psi)	t <sub>5</sub> (sec)	P <sub>6</sub> (psi)	t <sub>6</sub> (sec)	P <sub>ign</sub> (psi)	t <sub>ign</sub> (sec)
QA-83	41.05	0.058	226.8	0.073	260.6	0.088	275.0	0.107	282.2	0.127	287.3	0.146	281.1	0.156
2-5-1	50.76	0.059	207.1	0.071	248.7	0.086	264.9	0.099	274.1	0.123	274.1	0.148	282.8	0.160
2-5-2	56.17	0.054	204.2	0.066	240.0	0.073	265.5	0.098	272.7	0.122	275.7	0.147	279.9	0.159
6-4-1	53.18	0.061	199.4	0.071	240.3	0.086	250.6	0.098	265.9	0.122	268.0	0.147	273.1	0.172
6-4-2	55.83	0.057	152.3	0.069	199.0	0.074	225.4	0.099	238.6	0.123	253.8	0.148	256.8	0.177
6-4-3	50.98	0.054	198.8	0.064	229.4	0.074	254.9	0.098	263.1	0.122	267.2	0.147	270.2	0.165
6-4-4	50.76	0.052	203.0	0.062	236.5	0.074	254.8	0.099	261.9	0.123	266.0	0.148	269.0	0.162
6-4-5	56.17	0.061	199.1	0.071	234.9	0.086	246.1	0.098	261.4	0.122	266.5	0.147	269.6	0.172
6-4-6	53.70	0.054	190.4	0.064	228.4	0.077	253.8	0.102	259.7	0.128	264.6	0.154	266.5	0.172
6-4-7	53.37	0.054	186.3	0.064	224.2	0.077	248.4	0.103	257.2	0.129	261.0	0.154	262.0	0.165
6-4-8	57.02	0.059	188.4	0.069	224.0	0.074	250.5	0.098	262.7	0.123	264.7	0.147	267.8	0.169
6-4-9	50.77	0.054	185.5	0.064	219.7	0.077	249.0	0.102	263.6	0.128	272.4	0.154	266.5	0.172
6-4-10	52.72	0.051	185.5	0.059	232.4	0.077	249.0	0.102	259.7	0.128	262.6	0.154	268.5	0.164
6-4-11	50.76	0.052	182.7	0.062	225.4	0.074	249.7	0.098	260.9	0.123	269.0	0.148	269.0	0.165
6-4-12	48.96	0.054	190.9	0.064	230.1	0.077	248.7	0.102	257.5	0.128	260.5	0.153	268.3	0.167
6-4-14	50.98	0.049	193.7	0.059	229.4	0.074	262.1	0.098	283.5	0.122	289.6	0.147	272.3	0.161
6-4-15	48.81	0.054	195.3	0.067	226.5	0.077	249.9	0.102	258.7	0.128	263.6	0.154	267.5	0.168
6-4-16	50.76	0.059	197.9	0.071	226.4	0.077	244.6	0.099	255.8	0.123	260.9	0.148	268.0	0.169
6-4-17	48.96	0.050	200.7	0.061	227.2	0.077	249.7	0.089	267.3	0.102	284.0	0.128	270.3	0.163
6-4-18	53.86	0.056	195.8	0.066	230.1	0.077	255.6	0.102	263.4	0.128	267.3	0.153	271.2	0.163

TABLE 5-3

M-57 MATERIAL PROPERTIES USED IN  
FINITE ELEMENT STRESS ANALYSES

Material	Tensile Modulus (psi)	Bulk Modulus (psi)	Poisson's Ratio
Adhesive (C-7) Bond	80,000	88,889	0.35
Vulcanized Buna-S Rubber Bond	1,300	478,000	0.4995467
Buna-S Rubber Boot and Flap	1,300	478,000	0.4995467
Polyurethane Potting	1,300	478,000	0.4995467
CYH Propellant	325	700,000	0.4999226
	3,000	700,000	0.4992857
	5,500*	700,000	0.4986905
	10,000	700,000	0.4976191
*Used with adhesive bond analysis only			

TABLE 5-4

EXPERIMENTAL CASE DEFLECTION AT 300 PSIG FROM  
HYDROPROOFING OF M-57 MOTOR CHAMBERS

Case Number	Aft Dome Normal Deflection (in.)				Girth Growth (in.)**	
	R = 3.2 ± 0.2	R = 7.3*	R = 11.1*	R = 14.5*	37.5	6.5
600	0.200	0.237	0.107	0.070	0.920	0.377
610	0.185	0.201	0.097	0.055	0.815	0.375
627	0.204	0.245	0.109	0.070	0.912	0.370
637	0.200	0.235	0.110	0.066	0.914	0.364
641	0.203	0.239	0.125	0.074	0.992	0.516
647	0.162	0.146	0.083	0.053	0.780	0.360
652	0.204	0.221	0.142	0.072	--	--
660	0.191	0.209	0.100	0.056	0.732	0.328
661	0.171	0.213	0.127	0.063	0.796	0.313
664	0.183	0.193	0.117	0.066	1.012	0.368
676	0.206	0.214	0.135	0.073	0.802	0.313
682	0.194	0.225	0.121	0.062	--	--
687	0.151	0.194	0.109	0.065	0.830	0.263
688	0.184	0.187	0.085	0.059	--	0.352
690	0.171	0.204	0.109	0.065	0.874	0.310
693	0.177	0.213	0.123	0.072	--	--
698	0.189	--	0.134	0.082	--	--
699	0.178	0.219	0.124	0.077	0.881	0.354
700	0.200	0.239	0.124	0.069	--	--
705	0.189	0.238	0.122	0.074	--	--
706	0.180	0.217	0.140	0.076	0.833	0.306
708	0.176	0.179	0.119	0.058	0.752	0.400
709	0.190	0.223	0.125	0.077	0.680	--
710	0.183	0.215	0.120	0.073	--	--
712	0.186	0.216	0.146	0.082	0.820	0.454
716	0.171	0.174	0.083	--	0.700	0.316
Note: For legend see end of table						

TABLE 5-4 (Cont)

EXPERIMENTAL CASE DEFLECTION AT 300 PSIG FROM  
HYDROPROOFING OF M-57 MOTOR CHAMBERS

Case Number	Aft Dome Normal Deflection (in.)				Girth Growth (in.)**	
	R = 3.2 ± 0.2	R = 7.3*	R = 11.1*	R = 14.5*	37.5	6.5
720	0.238	0.261	0.168	0.075	1.102	0.425
722	0.178	--	0.089	0.055	0.792	0.320
729	0.179	0.231	0.117	0.061	0.825	0.279
734	0.186	0.224	0.141	0.076	0.860	0.459
736	0.183	0.206	0.143	0.097	0.833	0.380
741	0.156	0.170	0.075	0.040	0.712	0.340
744	0.176	--	0.079	0.050	0.820	0.436
747	0.204	0.204	0.101	0.061	0.836	0.345
751	0.192	0.219	0.116	--	0.816	0.437
754	0.233	0.214	0.105	0.049	0.880	0.420
759	0.186	0.193	0.109	0.067	0.866	0.353
761	0.195	0.209	0.114	0.053	0.790	0.320
769	0.209	--	--	0.072	0.968	--
785	0.190	0.207	0.093	0.045	0.760	0.390
789	0.186	0.207	0.151	0.063	0.840	0.348
792	0.215	0.228	0.117	0.052	0.770	0.360
811	0.245	0.263	0.138	0.061	0.810	0.400
824	0.198	0.148	0.064	--	0.720	0.320
843	0.197	0.243	0.178	0.074	0.923	0.411
848	0.193	0.204	0.106	0.072	1.320	--
892	0.215	0.220	0.184	--	0.999	0.306
901	0.210	0.230	0.155	0.072	0.917	0.453
909	0.210	0.243	0.186	0.083	0.872	0.403
918	0.152	0.161	0.089	0.057	0.778	0.313
922	0.181	0.196	0.142	0.081	0.838	0.344
927	0.160	0.167	0.081	0.051	0.675	0.552
Note: For legend see end of table						

TABLE 5-4 (Cont)

EXPERIMENTAL CASE DEFLECTION AT 300 PSIG FROM  
HYDROPROOFING OF M-57 MOTOR CHAMBERS

Case Number	Aft Dome Normal Deflection (in.)				Girth Growth (in.)**	
	R = 3.2 ± 0.2	R = 7.3*	R = 11.1*	R = 14.5*	37.5	6.5
931	0.173	--	0.138	0.077	0.903	0.307
973	0.187	0.187	0.107	0.063	0.754	0.348
981	0.198	0.224	0.113	0.066	1.100	0.705
1007	0.202	0.191	0.111	0.054	0.759	0.464
1013	0.200	0.202	0.107	0.061	0.647	0.330
1016	0.184	0.190	0.106	0.059	0.791	0.247
1028	0.211	0.195	--	0.058	0.765	--
1038	0.196	0.186	--	--	0.790	0.402
1049	0.196	0.193	--	--	0.686	0.343
1058	0.210	0.208	--	0.061	0.785	--
1066	0.189	0.206	0.093	0.059	0.695	0.350
1105	0.186	0.200	0.115	0.067	0.722	0.320
1118	0.197	--	0.115	0.070	0.966	0.419
1162	0.265	0.234	0.124	0.086	0.999	0.533
Mean	0.1923	0.2079	0.11722	0.06460	0.84016	0.37305
Sigma	0.0203	0.03575	0.033476	0.017944	0.119857	0.081462

\*Average of four measurements at 90° positions

\*\*From aft skirt R is the radial location of the measurement in inches

TABLE 5-5

## M-57 MOTOR CHAMBER EXPERIMENTAL BURST PRESSURES

Case Number	Burst Pressure (psi)
610	572
647	574
660	669
688	574
708	625
716	630
722	732
741	736
744	647
754	740
761	626
785	738
792	734
811	762
824	729
848	721
888	660
927	735
942	740
961	755
981	659
1013	628
1066	724
1105	685
1118	662
1162	770
1176	733
1202	737
Mean Burst Pressure	689.179
Standard Deviation	60.9168
Coefficient of Variation	0.08839

TABLE 5-6

M-57 MEAN AND PLUS 3-SIGMA CHAMBER DEFLECTIONS FOR 300 PSIG  
INTERNAL PRESSURE OBTAINED FROM FINITE ELEMENT ANALYSIS

Condition	Normal Aft Dome Deflections (in.) at Radii				Radial Growth 6.5 In. from Aft Skirt Tip (in.)	Radial Growth 37.5 In. from Aft Skirt Tip (in.)
	3.2 In.	7.3 In.	11.1 In.	14.5 In.		
Desired Mean Deflec- tions	0.1923	0.2079	0.1172	0.0646	0.0593	0.1340
Mean Deflections Obtained in Finite Element Analysis	0.2003	0.2679	0.1427	0.0633	0.0597	0.1340
Desired Plus 3-Sigma Deflections	0.2433	0.2619	0.1484	0.0817	0.0750	0.1695
Plus 3-Sigma Deflec- tions Obtained in Finite Element Analysis	0.2391	0.3242	0.1795	0.0809	0.0767	0.1695
Deflections from Original Finite Element Analysis	0.1548	0.2235	0.1882	0.0592	0.2336	0.1769

Short shear samples (Buna-S flap/C7/Buna-S boot) cut from the aft bond of motor S/N 0032570 were tested at 200 in./min crosshead speed.<sup>2</sup> The mean failure stress and mean time to failure of the four samples tested at 70° F with 600 psig superimposed pressure were 221 psi and 0.114 second, respectively. Considerable scatter was present in the failure data which was attributed to irregular sample cutting and possible damage to samples during motor sectioning and subsequent sample machining. It should be noted, also, that the experimental failure stresses were calculated on a nominal basis, by considering a uniform stress over the complete cross-sectional area of the sample; whereas, the corresponding analytical bond stresses were based on the plus 3-sigma flexible motor case and were computed for various propellant moduli at the radii where maximum values occurred.

Based on this evaluation of bond strength, the structural capability of the aft adhesive (C7) bond is estimated to be more than 94 percent greater than that of the wing slot tip with regard to motor ignition pressurization. The short shear sample is a poor analog of the stress state in the full-scale motor. However, the large margin of safety calculated, along with the fact that overtesting demonstrated the aft bond not to be the critical failure mode, appear to justify consideration of only wing slot cracking as the failure mode which limits service life.

#### 4. Slot Tip Concentration Effects

The number of Minuteman Stage III motors as of June 1975 remaining in the force inventory are 95 "B-1 Fix" (pre-OPRI) and 356 OPRI motors. The principal geometry changes affecting motor service life considerations incorporated in the OPRI configuration were the addition of wing slot fillets and the change in aft boot-to-flap bond from C7 adhesive to a vulcanized bond.

The OPRI slot tip configuration is shown compared to the pre-OPRI geometry in Figure 5-2. The strain concentration factor applicable to the B-1 Fix slot tip is 2.95, and that for the OPRI slot tip is 2.45. These apply at the critical slot tip radius of 3.7 inches.<sup>3</sup> The concentration factors are shown in Figure 5-3 as a function of radius from motor axis to slot tip.

A consideration for calculation of the strain at the slot tip is the change in slot tip shape with pressure and the corresponding change in strain concentration factor. A study was performed to determine the significance of this effect and whether it should be incorporated in the R/C analysis. This was analytically investigated in Reference 4. Finite-element techniques were applied to a cross-section of the M-57 motor at the location of the critical 3.7-inch slot tip radius. Incremental internal pressure loading of the plane-strain section (B-1 Fix configuration) resulted in a strain concentration factor relationship with pressure as follows:

$$K_{\epsilon} = 2.93 - 5.5 \times 10^{-4} P$$



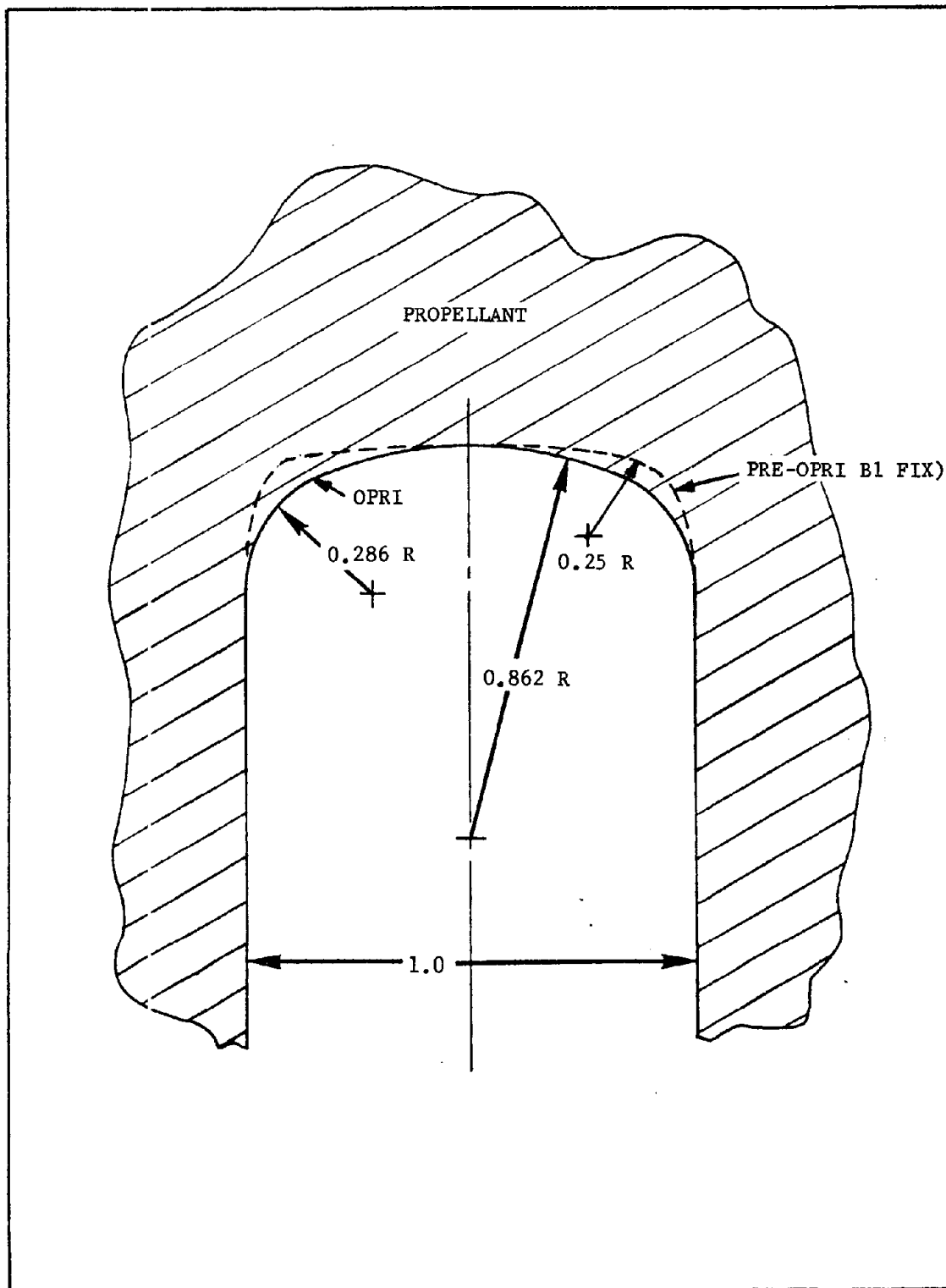


Figure 5-2. Comparison of OPRI and B1 Fix Wing Slot Tip Configurations

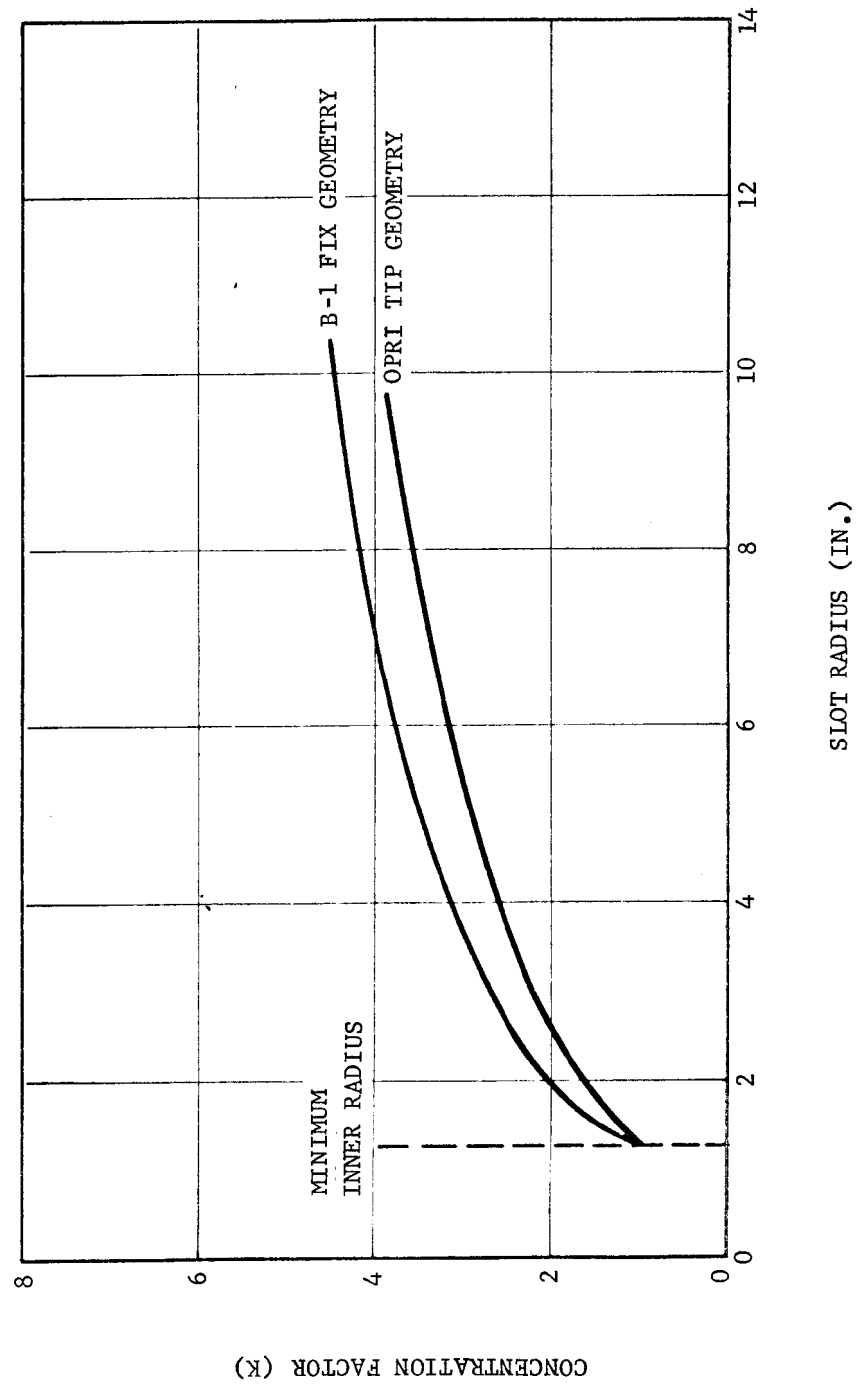


Figure 5-3. Concentration Factor as a Function of Slot Depth for Minuteman Stage III Rocket Motor

This result was based on a propellant tensile modulus of 4,400 psi, a propellant bulk modulus of 350,000 psi, and a case stiffness which resulted in a radial case deflection at its outer surface of 141  $\mu$ in. per psi applied internal pressure.

The change in slot tip strain concentration can also be related to the cylindrical hoop strain at the slot tip radius. The cylindrical hoop strain is directly proportional to slot geometry change, as was pressure for the constant case stiffness-propellant modulus analysis of Reference 4. The cylindrical hoop strain per unit applied pressure for the finite-element analysis of Reference 4 was 0.02333 percent.

Case deflections computed by axisymmetric finite-element analyses at the critical cross-section of the FSU for the actual mean and minus 3-sigma stiffness cases are presented in Table 5-7. The propellant bulk modulus was taken to be 700,000 psi for each run, while the propellant tensile modulus was varied from 325 to 10,000 psi. The percent of internal applied pressure carried by the propellant web for each condition is also included in Table 5-7.

Substituting the strain per unit pressure into the previous equation for K yields the following relationship between cylindrical hoop strain and strain concentration factor at the critical slot tip radius of 3.7 inches for the B-1 Fix geometry:

$$\begin{aligned} K_{\epsilon} &= 2.93 - \left( \frac{5.5 \times 10^{-4}}{0.02333} \right) \epsilon_{\theta}^C \\ &= 2.93 - 0.02357 \epsilon_{\theta} \end{aligned}$$

where  $\epsilon_{\theta}$  is the percent cylindrical hoop strain at 3.7 inches radius. This result makes it evident that  $K_{\epsilon}$ , being related to propellant hoop strain, is thus a time-dependent (viscoelastic) function of propellant relaxation modulus. The degree of dependence is reflected by the change in radial case deflection with propellant modulus shown in Table 5-7.

Incorporation of this effect into the viscoelastic response and cumulative damage program must be accomplished by first calculating the cylindrical hoop strain as a function of time with the convolution integral and then calculating the total strain by multiplying by the previous expression for strain concentration factor. The cumulative damage must then be calculated based on this total strain curve and the corresponding incremental strain rates.

TABLE 5-7  
COMPUTED RADIAL CASE DEFLECTIONS AND PERCENT OF INTERNAL PRESSURE  
LOAD CARRIED BY THE PROPELLANT AT THE CRITICAL SLOT TIP CROSS  
SECTION OF THE FSU

Case Stiffness	Propellant Tensile Modulus (psi)	Case Radial Deflection (micro-in./psi)	Propellant Load (%)
Mean	325	398.4	12.23
	3,000	233.5	53.21
	10,000	132.7	77.28
Minus 3-Sigma	325	492.9	14.47
	3,000	269.0	58.46
	5,500	201.6	71.35
	10,000	145.4	81.67

In Reference 4, it was shown from observation of parametric curves that the drop in strain concentration factor due to slot deformation (pressure) should be smaller for star grains with small  $a/b$  ratios, where "a" is the slot-tip radius and "b" is the outer radius of the grain. The consequence of this behavior, observing from Figure 5-4 that total slot tip strain is not a large function of slot tip radius, will be the shifting of the critical slot tip radius from 3.7 inches to some lesser radius. Thus, the instantaneous radius at which the maximum damage factor exists will shift during motor pressurization, and wing slot cracking will initiate at some slot tip radius less than the critical slot tip radius of 3.7 inches (which was calculated based on the undeformed slot tip geometry).

Figure 5-5 shows the effects of changing concentration factor with increased pressure. The difference from an assumed constant value was small; therefore, the remaining analyses were performed assuming a constant slot concentration.

## 5. Verification of Analysis

Subscale analog test results for the circular centerport and slotted configurations were presented in Section II of this report. Good agreement was obtained with failure predictions from the viscoelastic response computer program based on allowable strain and cumulative damage failure criteria.

Viscoelastic response analyses were also performed for the full-scale overtest motors 32570, 32743, 32765, and 33348. Relaxation modulus and allowable strain data used as input to the viscoelastic response analyses were obtained from material property testing of propellant sectioned from each motor. These data are presented in Tables 5-8 and 5-9, respectively; and are shown plotted in Figures 5-6 and 5-7, along with the mean values for all lots as determined in Section IV. The actual overtest pressurization transients input to the respective analyses are presented in Table 5-10.

Analytically predicted failure pressures and corresponding times are shown, along with the actual test results, in Table 5-11. Deviation of the predicted pressures, based upon mean case properties, from the actual failure pressures are tabulated in Table 5-12. Motor 33348 was of the OPRI configuration and a constant slot tip strain concentration factor of 2.45 was used. The remaining three motors were of the B-1 Fix configuration. A constant strain concentration factor of 2.95 was used in these analyses. The results presented in Tables 5-11 and 5-12 show good agreement between analytical and experimental data without use of strain dependence of the slot tip strain concentration factor in the analyses. The probable cause of this situation is compensating errors in the analyses. Inclusion of the decreased strain concentration factor with strain in the analyses would result in higher predicted failure pressures. A condition which would have the opposite effect of lowering the predicted failure pressures is non-axisymmetric radial deflection of the aft end of the motor case due to reinforcement from the four thrust termination ports.

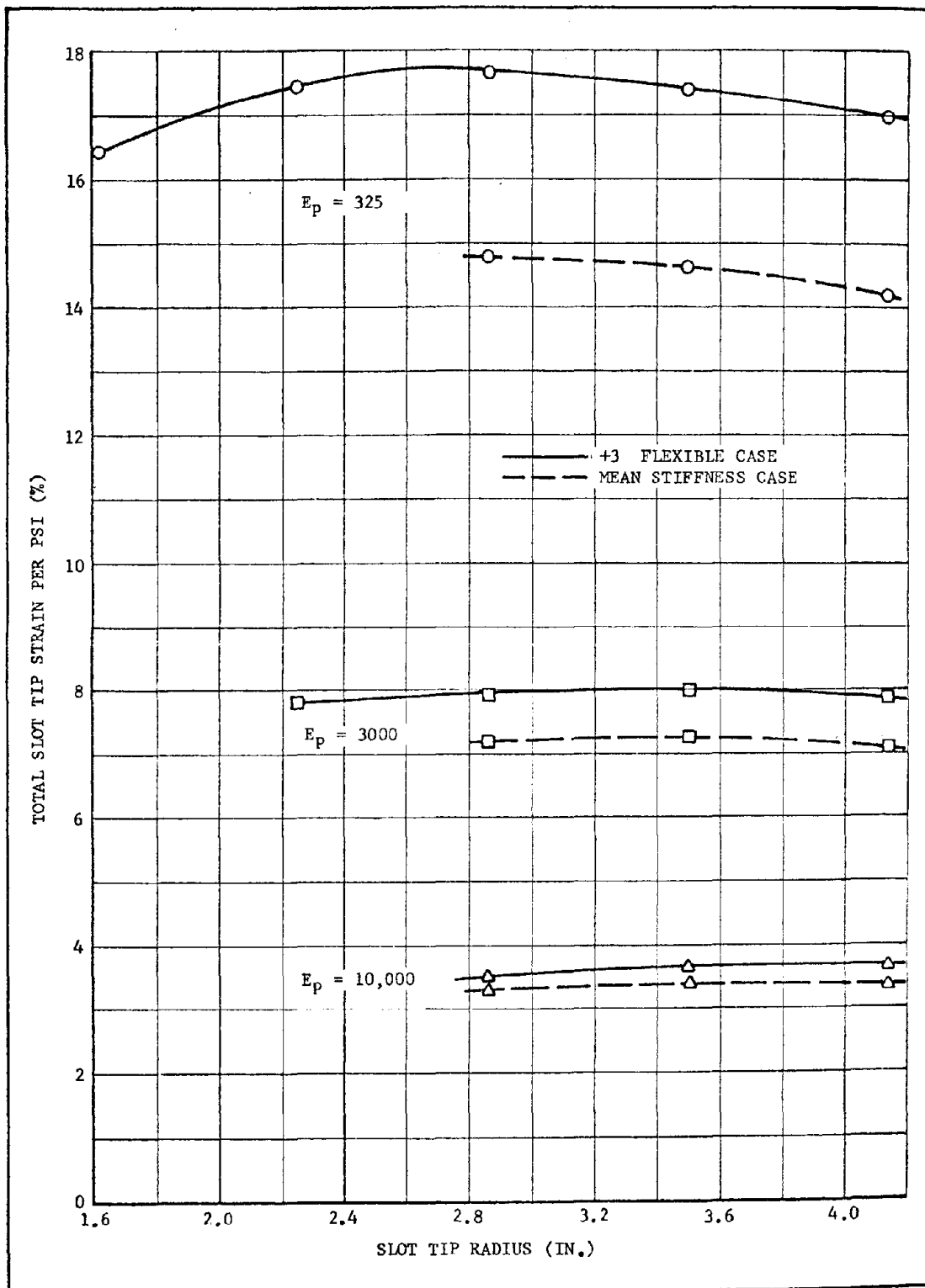


Figure 5-4. Total Slot Tip Strain ( $K_\epsilon * \epsilon_c$ ) as a Function of Slot Tip Radius for Various Propellant Tensile Moduli and Case Stiffness

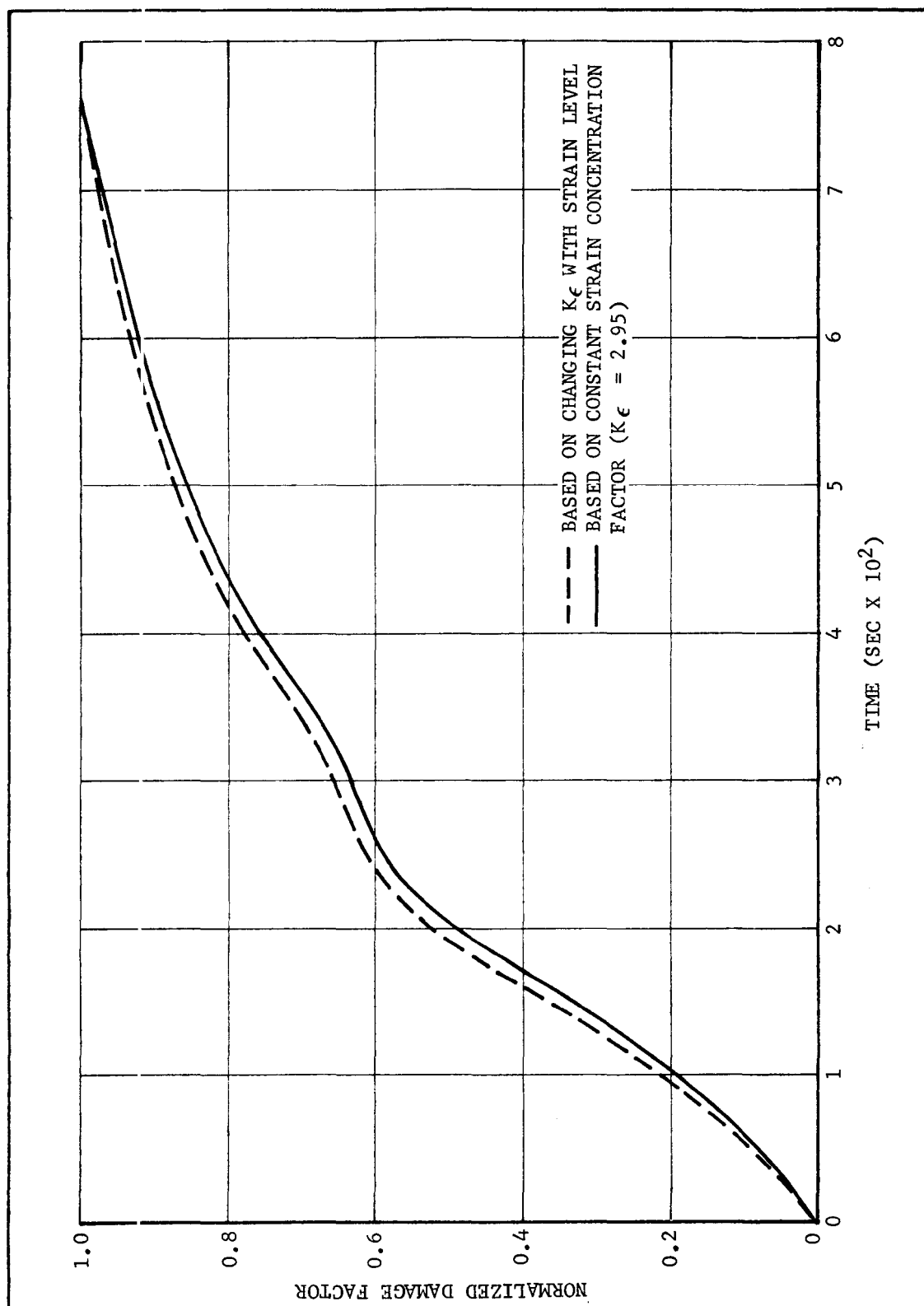


Figure 5-5. Normalized Damage Factors for Overtesting of Motor No. 32765  
Based on Strain Dependent and Constant Slot-Tip Strain  
Concentration Factors

TABLE 5-8

PROPELLANT STRESS RELAXATION MODULI (70° F)  
INPUT TO VISCOELASTIC RESPONSE ANALYSIS

Motor No. Time (sec)	Relaxation Modulus			
	32570	32743	32765	33348
1 x 10 <sup>-5</sup>	33,000	32,201	26,845	--
4 x 10 <sup>-5</sup>	22,600	22,772	18,232	19,000
1 x 10 <sup>-4</sup>	17,700	18,242	14,467	15,000
4 x 10 <sup>-4</sup>	12,000	12,863	10,129	11,000
1 x 10 <sup>-3</sup>	9,400	10,034	7,888	8,600
4 x 10 <sup>-3</sup>	6,410	6,772	5,496	6,000
1 x 10 <sup>-2</sup>	5,000	5,305	4,243	4,800
4 x 10 <sup>-2</sup>	3,490	3,369	3,035	3,400
1 x 10 <sup>-1</sup>	2,700	2,481	2,429	2,700
4 x 10 <sup>-1</sup>	2,300	1,550	--	1,920



TABLE 5-9

ALLOWABLE STRAIN VERSUS STRAIN RATE (70° F)  
INPUT TO VISCOELASTIC RESPONSE ANALYSIS

Motor No.	Strain Rate (in./in./min)	Allowable Strain (%)
32570	1	46.5
	2	47.2
	5	47.0
	10	46.1
	30	43.8
	60	41.5
	100	39.5
	200	37.0
	500	36.0
	1000	35.4
32743	1	50.5
	2	49.9
	5	47.9
	10	45.9
	30	42.0
	60	39.3
	100	38.0
	200	36.0
	500	34.3
	1000	33.9
32765	1	51.7
	3.5	50.4
	20	44.5
	250	35.0
	400	34.1
	1000	33.5
33348	1	50.5
	5	44.7
	20	40.9
	80	38.0
	130	37.1
	250	35.1
	500	32.2
	1000	28.8

TABLE 5-9 (Cont)

ALLOWABLE STRAIN VERSUS STRAIN RATE (70° F)  
 INPUT TO VISCOELASTIC RESPONSE ANALYSIS

	Strain Rate (in./in./min)	Allowable Strain (%)
Mean Data for all CYH Propel- lant Lots	2	50.4
	3.5	50.0
	6	49.0
	10	47.6
	16	45.9
	25	44.0
	40	42.1
	62	40.3
	100	37.4
	160	36.6
	250	34.9
	400	33.3
	620	32.0
	1000	30.2

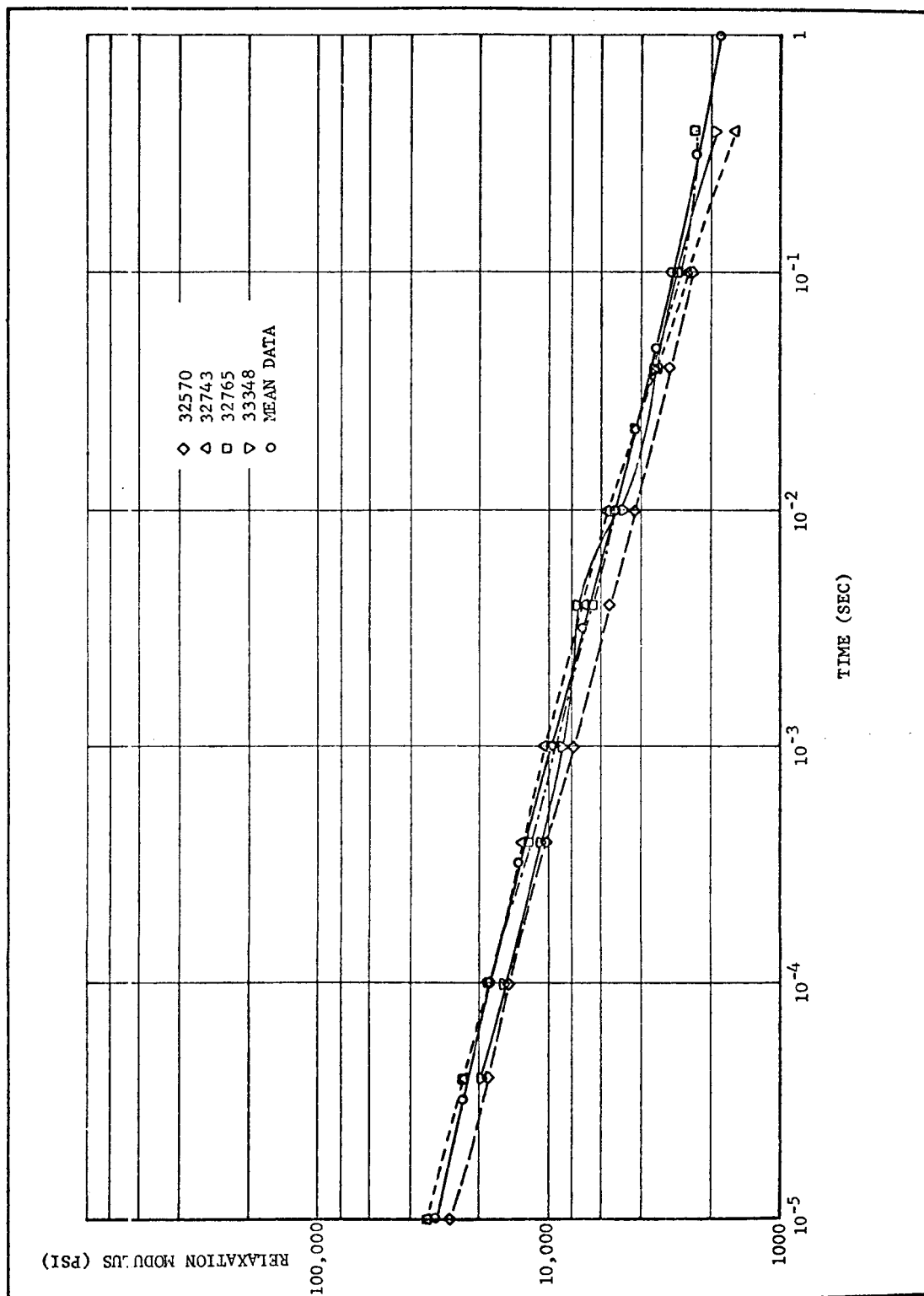


Figure 5-6. Stress Relaxation Moduli for Mean CYH Propellant Lot and for Overtested Motors

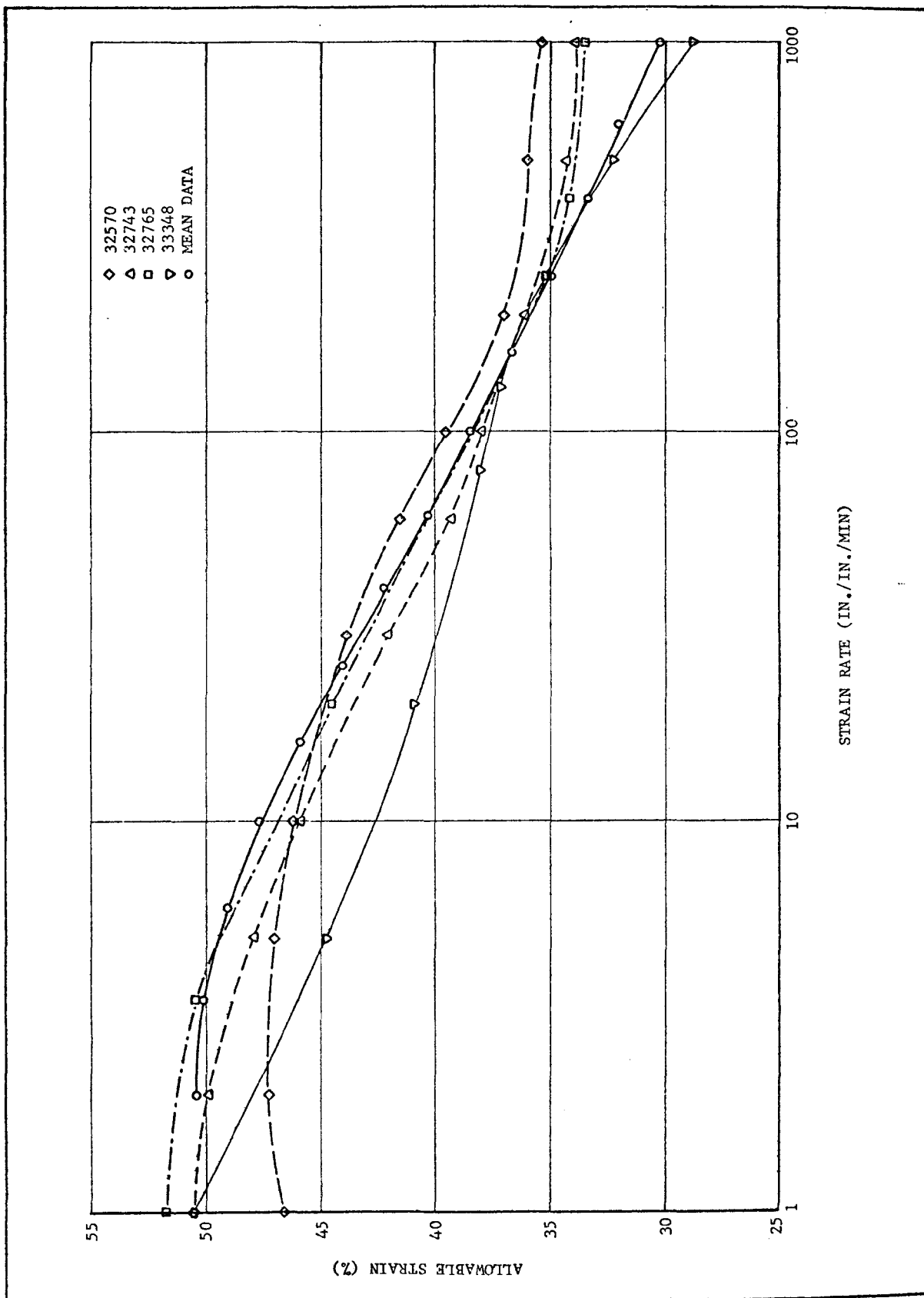


Figure 5-7. Allowable Strain Versus Strain Rate for Mean CYH Propellant Lot and for Overtested Motors

TABLE 5-10

## PRESSURIZATION TRANSIENT APPLIED DURING OVERTESTING

Motor No.	Time (sec)	Pressure (psi)
32570	0.016	275
	0.02	300
	0.026	300
	0.04	380
	0.072	465
	0.076	475
	0.086	500
	0.116	538
	0.124	547
32743	0.015	300
	0.022	369
	0.025	371
	0.03	390
	0.033	430
	0.04	450
	0.051	492
	0.055	500
	0.065	522
	0.085	552
	0.115	560
32755	0.012	167
	0.018	285
	0.021	321
	0.024	340
	0.029	344
	0.032	360
	0.038	400
	0.044	432
	0.052	459
	0.056	466
	0.064	478
	0.072	496
	0.076	502
	0.096	350

TABLE 5-10 (Cont)

## PRESSURIZATION TRANSIENT APPLIED DURING OVERTESTING

Motor No.	Time (sec)	Pressure (psi)
33348	0.004	83
	0.008	110
	0.01	157
	0.018	290
	0.0195	316
	0.0235	300
	0.03	333
	0.044	400
	0.064	470
	0.089	537
	0.106	566
	0.12	585
	0.1355	604
	0.154	620
	0.189	628
2-10-16	0.0375	25
	0.06	125
	0.0638	165
	0.0713	195
	0.08	305
	0.095	415
	0.1	415
	0.1125	470
	0.135	545
	0.1513	555
	0.16	550
	0.1713	510
	0.1913	393

TABLE 5-11

ANALYTICALLY PREDICTED OVERTEST FAILURE LEVELS OF FULL-SCALE MOTORS, CONSTANT  $K_e$ 

Analytical Configuration	Motor No.							
	32570		32743		32765		33348	
	Pressure (psi)	Time (sec)	Pressure (psi)	Time (sec)	Pressure (psi)	Time (sec)	Pressure (psi)	Time (sec)
Actual Test Results	475	0.076	525	0.066	500	0.075	575	0.106
Mean Case Stiffness	535	0.1136	525	0.066	490	0.0693	594	0.1288
3 $\sigma$ Flexible Case	500	0.086	491	0.0507	458	0.0517	551	0.0953
Mean Motor Population Propellant Properties:								
Mean Case Stiffness	514.9	0.0978	518.5	0.0634	*	*	615.7	0.1501
3 $\sigma$ Flexible Case	468.9	0.0736	479.4	0.0477	474.7	0.0618	570.5	0.1040
* Failure was not predicted in time span or applied pressure transient. A maximum constant of 0.964166 was obtained at 0.076 second (502 psi).								

TABLE 5-12

ERROR OF MEAN CASE CONFIGURATION PREDICTED PRESSURES FROM ACTUAL FAILURE PRESSURES

	Motor No.			
	32570	32743	32765	33348
Based on Individual Motor Propellant Properties	+ 60 psi + 12.6%	0 psi 0%	- 10 psi - 2%	+ 19 psi + 3.3%
Based on Mean Motor Population Propellant Properties	+ 39.9 psi + 8.4%	- 6.5 psi - 1.24%	+ 17.2 psi* + 3.44%	+ 40.7 psi + 7.08%
* Estimated, based on average calculated $3\sigma$ span from motors 32570 and 32743 (42.5 psi) added to lower $3\sigma$ case estimated failure pressure (474.7 psi)				



Wing slot tip damage factor as a function of time for motor 32765 based on the strain dependent and constant slot tip strain concentration factors was presented in Figure 5-5. The strain-dependent damage factors are shown normalized to their respective maximum values. The strain-dependent technique produces a greater portion of total damage at the small time (low pressure) portion of the overtest transient than does the constant slot tip strain concentration factor approach. Thus, the margin of safety predicted at lower pressures, using a constant concentration factor, will be slightly excessive.

Since this error is small and the propellant property data (Section IV) displayed no statistically discernible trends with age, the present analysis techniques were accepted. That is, if consideration of the statistical distribution of all parameters affecting motor serviceability results in a significantly positive margin of safety for the lower 3-sigma probability limit, no service life problems are predicted.

#### 6. Results and Interpretation of Results

Maximum calculated adhesive bond shear stress per unit applied pressure is shown in Figure 5-8 as a function of propellant modulus. These values were obtained from finite-element analyses using the plus 3-sigma flexible motor case.

A viscoelastic response computer analysis was performed to calculate maximum adhesive bond shear stress for the overtest pressurization of motor S/N 0032570. The pressure transient and propellant relaxation modulus data used are those presented previously in Tables 5-8 and 5-10. Maximum adhesive bond shear stress was calculated to be 114 psi occurring at 0.123 second. Based on a comparison with short shear sample results, the centerport bond failure mode was judged to be less critical than the centerport cracking.

Cylindrical hoop strains at various slot tip radii were obtained by extrapolating finite-element analysis results of the full-scale motor to the slot tip surface. These results were then multiplied by the corresponding strain concentration factor at each slot radius from Figure 5-3. These resultant curves, shown previously in Figure 5-4, reflect total slot tip strain per psi applied pressure as a function of radius to the slot tip.

Predicted propellant hoop strain at a radius of 3.7 inches, which corresponds to the critical wing slot tip location, is shown per unit applied pressure as a function of propellant modulus in Figure 5-9. Tabulated values used as input to the R/C analysis are presented in Table 5-13.

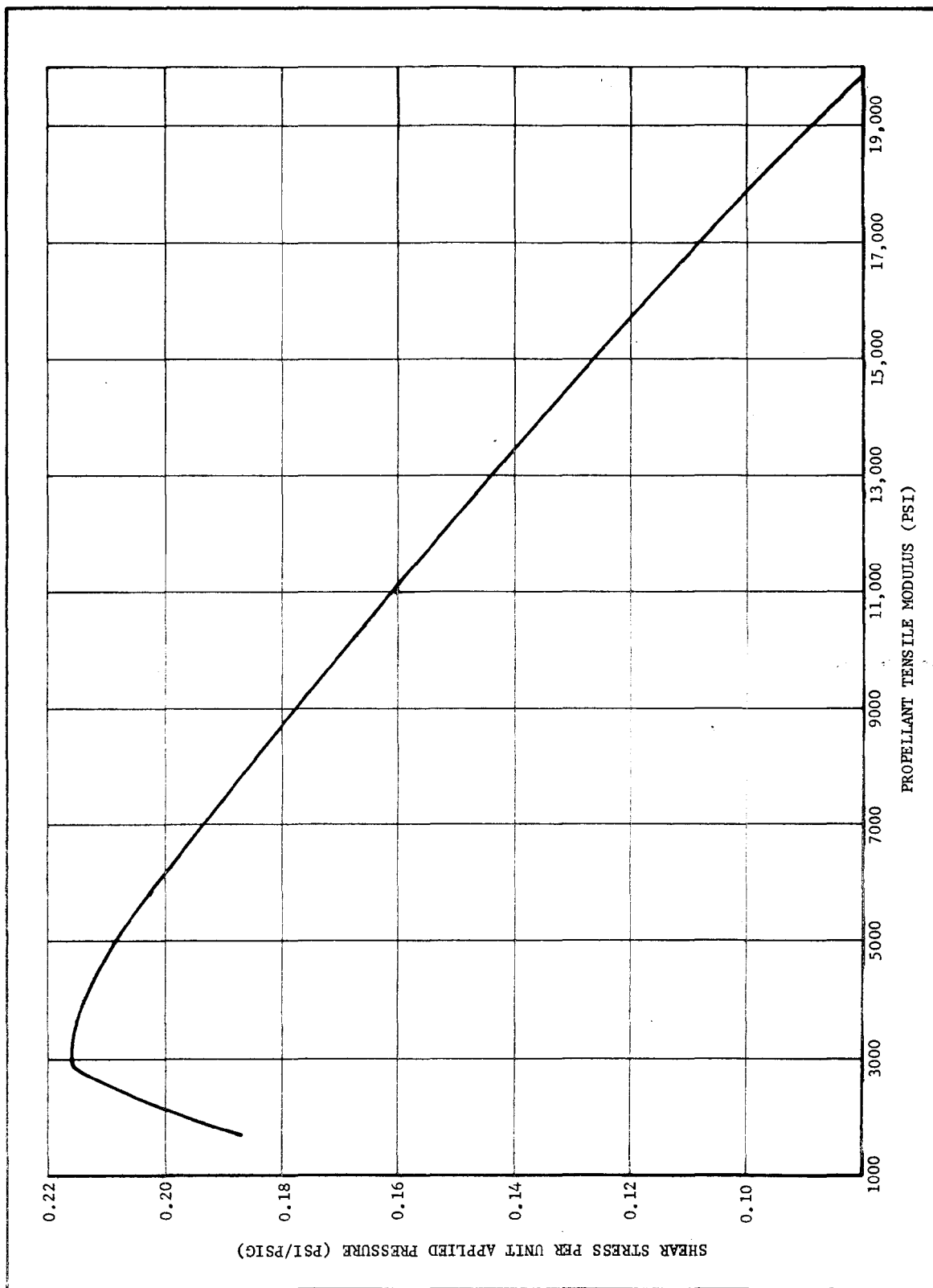


Figure 5-8. Calculated Maximum Adhesive Bond Shear Stress Per Unit Applied Pressure Versus Propellant Tensile Modulus

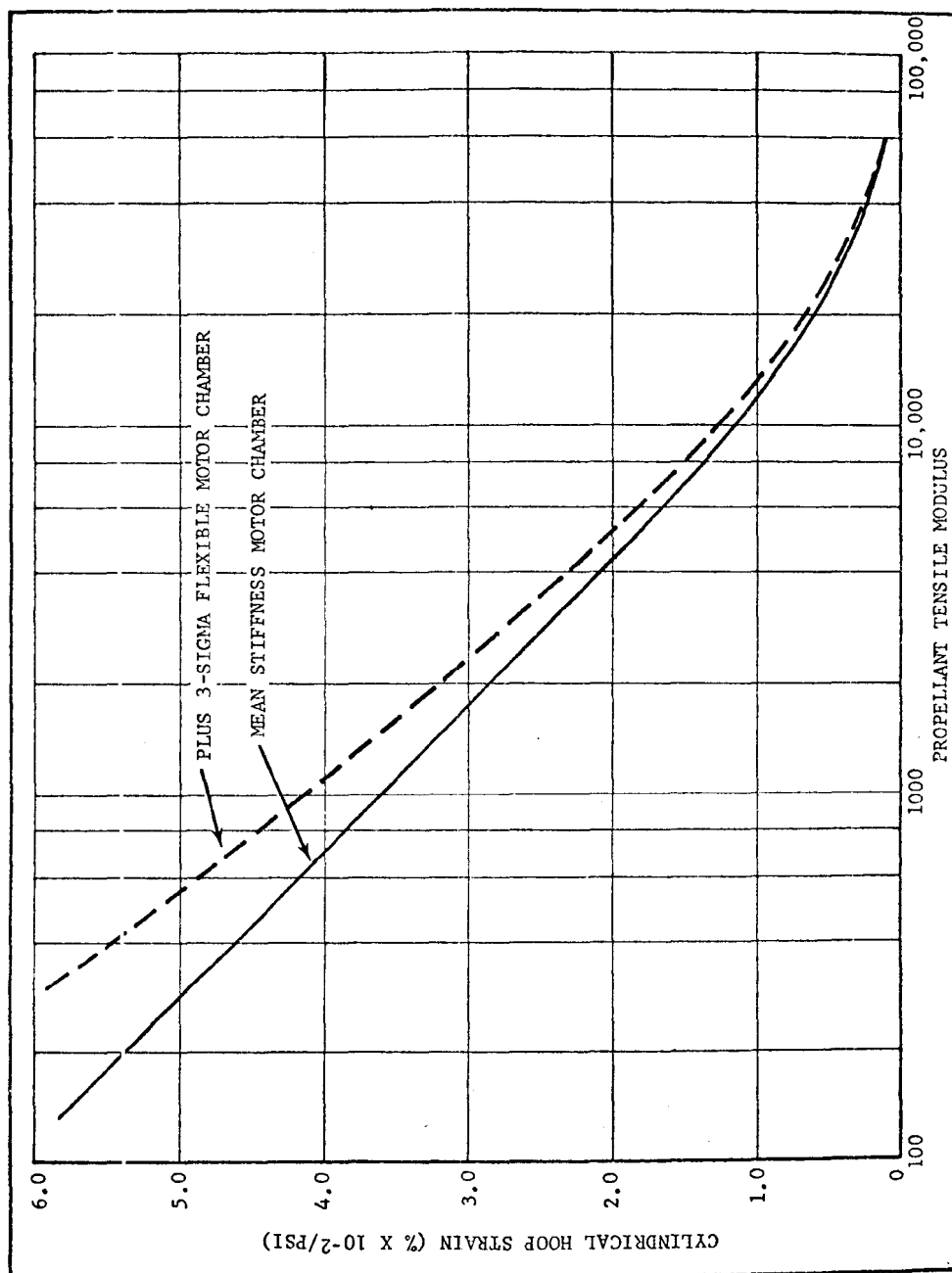


Figure 5-9. Predicted Cylindrical Hoop Strain at Critical 3.7 Inch Radius per Unit Applied Pressure Versus Propellant Tensile Modulus

TABLE 5-13

CYLINDRICAL HOOP STRAIN AT CRITICAL 3.7 INCH  
SLOT TIP RADIUS PER UNIT APPLIED PRESSURE AS A FUNCTION  
OF PROPELLANT MODULUS

Propellant Modulus (psi)	Mean Hoop Strain Per Unit Applied Pressure (%/psi)	Standard Deviation of Hoop Strain
325	$4.81 \times 10^{-2}$	$3.1 \times 10^{-3}$
3,000	$2.39 \times 10^{-2}$	$8.67 \times 10^{-4}$
10,000	$1.12 \times 10^{-2}$	$2.67 \times 10^{-4}$
21,000	$5.6 \times 10^{-3}$	$1.25 \times 10^{-4}$
52,000	$1.5 \times 10^{-3}$	$3.0 \times 10^{-5}$

Since analyses reported in the preceding section revealed that effects of changing slot-tip geometry are small, the R/C analysis was performed for the B-1 Fix wing slot tip geometry with a constant strain concentration factor of 2.95. Monte Carlo selection of applicable motor parameters was used to produce 105 statistical motor samples.

Results of the statistical analysis of these resultant samples show a mean damage factor of 0.53642 at ignition time with a standard deviation of 0.06941. Expressed in terms of the upper 3-sigma limit, only 0.135 percent of the motor population is predicted to have a damage factor greater than 0.74466.

Since the analytical service life predictions are based on propellant relaxation modulus and allowable strain data, a viscoelastic response analysis of motor 33348, subjected to the actual overtest pressure transient, was performed with the propellant relaxation modulus reduced by 10 percent. This change in modulus produced a 19 psi, or 3.2 percent, decrease in predicted failure pressure for the mean stiffness motor case and a 23 psi, or 4.17 percent, decrease for the 3-sigma flexible motor case. Therefore, these results demonstrate that, since only a portion of the pressure load is carried by the propellant web (dependent upon case stiffness), the percentage drop in predicted motor failure pressure will always be less than the percentage decrease in propellant modulus for constant allowable strains. However, analytically-predicted failure pressures will also be proportional to changes in propellant allowable strains and for the most critical propellant aging trend possible, that of concurrently decreasing relaxation modulus and allowable strains, a larger percentage drop could result in motor failure pressure than would occur in either propellant modulus or allowable strain. A statistical relationship does exist in propellant lot data between allowable strain and stress relaxation modulus. The higher modulus propellant tends to have low allowable strain capability and vice versa. The R/C analysis was performed with the two properties treated as independents and they were randomly selected. This produces a conservative capability estimate since the calculated coefficient of variation of damage factor will be larger than that of the actual experimental results.

For the M-57 motor, the predicted failure pressures are much larger than the actual ignition pressures and any detrimental propellant aging trends could be detected substantially before motor serviceability would be affected.

#### C. CONSIDERATION OF FULL-SCALE OVERTEST RESULTS

Full-scale overtest data were presented in Section III of this report. An attempt has been made to project the overtest failure data for the purpose of service life predictions. The ideal situation for overtest service life evaluation would be one in which several motors of various ages, each of which possess the same physical properties at zero age, are subjected to identical overtest pressurization transients (simulating actual ignition rates). The motors would also be conditioned at the same

relative humidity and temperature long enough to reach equilibrium before being tested. The motors should represent the mean physical property and dimensional characteristics for each component of the deployed motors. This would permit the determination of the mean margin of safety of the motors as a function of age with only age-related changes. Standard deviation, of overtest failure pressure would be evaluated through material property characterization and associated analysis for propellant from all motor lots. To obtain a reliable standard deviation by overtesting would require that a prohibitively large number of motors be tested at one age.

Eight full-scale motors have been high-rate pressure tested to failure (See Table 3-5, Section III). Five of those yielded results that are applicable to the ICBM Overtest Program (see below). In addition, motor 2-10-38 was tested to a pressure of 310 psi with no resulting failure.

<u>Motor No.</u>	<u>Configuration</u>	<u>Age at Overtest (months)</u>	<u>Failure Pressure (psi)</u>	<u>Failure Index<sup>a</sup></u>
2-10-16 <sup>b</sup>	Pre-B-1 Fix	2-1/2	500-530 <sup>c</sup>	1.67-1.79
33348	OPRI	69	575	1.71
32765	B-1 Fix	102	500	1.77
32743	B-1 Fix	108	492-525 <sup>c</sup>	1.71-1.88
32570	B-1 Fix	110	475	1.67

<sup>a</sup>Failure index is defined as ratio of cumulative damage factor at failure to factor at critical pressure following ignition. Recorded values reflect mean properties for case and propellant.

<sup>b</sup>Also subjected to modest thermal cycling test prior to hydrotest.

<sup>c</sup>Failure pressures not precisely determined.

In addition to age differences, the motors from which applicable data were obtained had design differences and normal variations to be expected in propellant and case properties. All of the motors except motor 2-10-16 are representative of motors in the force. Ideally, for proper interpretation, it is desirable to know to what extent a particular motor is representative of the mean of the motors it is supposed to represent. Since data were not available by which individual motors could be characterized completely with respect to the mean of the population, some arbitrary but conservative assumptions were made for interpretation.

Each of the motors was analyzed considering its particular loading program and known geometric features. Propellant and case properties were based on mean values for the total motor population. A cumulative damage factor was calculated for each motor based on these mean properties. The differences between a damage factor of unity and the calculated value indicates the degree to which the particular motor deviates from an average motor.

Hydroproof data are not available for the specific overtested motor cases. Therefore, a variation of approximately  $\pm 40$  psi in the overtest failure pressure data was considered due to possible case stiffness variability. This variation corresponds to that based on properties from cases for which hydroproof data are available.

Since the propellant behaves viscoelastically (allowable strain and tensile modulus are functions of time), the failure event is dependent on the exact applied pressure transient. For that reason it was necessary to neutralize the effects of variability in motor ignition pressure transients. This was accomplished by performing a viscoelastic response failure analysis using the actual pressure transients from each motor overtest. These analyses were made for the mean and minus 3-sigma stiffness motor cases using the propellant stress relaxation modulus and allowable strains previously calculated as the means for all propellant lots. Results from these analyses are presented in Figure 5-10 in terms of predicted damage factor at time of actual failure versus motor age at time of test. Each data point thus represents the capability (damage factor at failure for mean propellant properties) of the propellant in each overtested motor if the corresponding actual case were the mean or lower 3 sigma stiffness.

The spreads in damage factor shown for motors 2-10-16 and 32743 are the result of uncertainty of the exact failure pressures during overtest. Motor 2-10-16 was determined to have failed at between 500 and 530 psig internal pressure. Motor 32743 was previously reported to have failed at 525 psig. However, event gage E-2 in wing slot 2 (Reference 5) did show an indication of failure at 492 psig. This was previously discounted because of anomalies in response at lower pressures. Figure 5-10 also shows the resultant maximum damage factors from viscoelastic response analyses using both the mean stiffness and 3-sigma flexible motor cases in conjunction with the mean propellant properties determined for all motors and the mean motor ignition transient obtained from 78 actual motor firings. These damage factors represent the values to which predicted damage factor at overtest failure pressure, based on the same mean propellant property data as the previous data in Figure 5-10, could decrease before the chance of success declines to 50 percent for the mean and 3-sigma flexible cases, respectively.

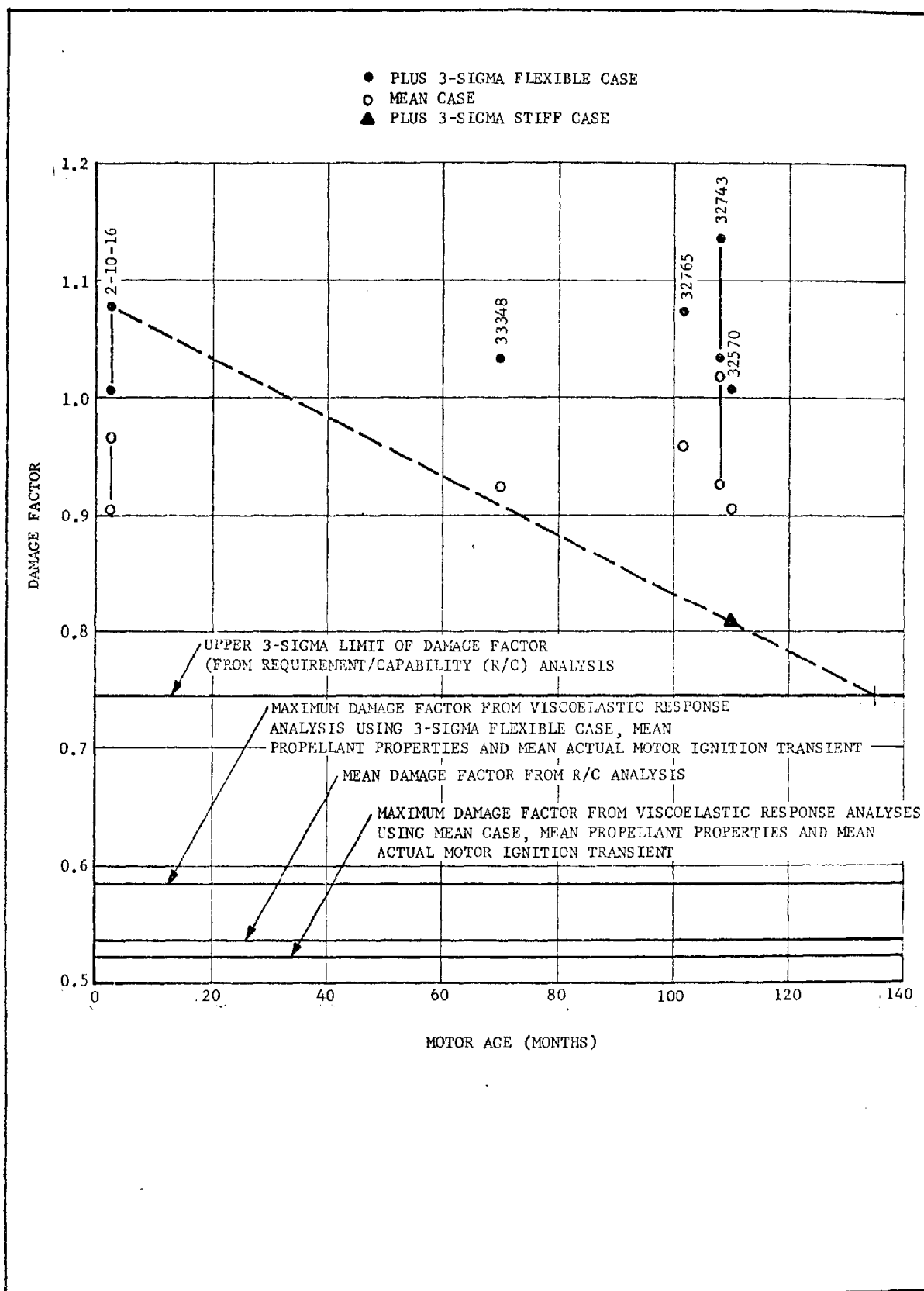


Figure 5-10. Analytically Calculated Damage Factors at Failure of Overtested Motors Based on Actual Pressure Transients and Mean Properties, All Motor Lots, Compared to Analytically Calculated Requirements



The worst possible condition relative to service life projection would be the situation in which the oldest motor overtested actually possessed a 3-sigma stiff case, and the youngest motor had a 3-sigma flexible case. The 3-sigma stiff case data point for motor 32570 is included in Figure 5-10 to illustrate this situation (see dashed projection line). This projection is related to possible variation due to case stiffnesses. A possible failure would be predicted at the 3-sigma level for the age indicated (134 + months), when this line intersects the upper 3-sigma limit of damage factor predicted by the R/C analysis. The age at which the mean motor is predicted to fail by this conservative technique is the point of intersection with the mean R/C damage factor; i.e., at 217 months or 18 years, 1 month.

A more logical approach is to treat the analytically-determined damage factors for the mean flexible motor case assumption as a random sampling of the motor population. The resultant mean and standard deviation of these damage factors, considering the lower failure pressures for motors 2-10-16 and 32743, were 0.918 and 0.025, respectively. Considering the maximum possible failure pressures for the two questionable data points, these statistics increased to 0.950 and 0.049, respectively.

This technique encompasses all sources of variability affecting motor service life except that of ignition pressurization. Comparison of the above statistical 3-sigma limits with the damage factors in Figure 5-10, corresponding to calculated 3-sigma variations in motor case stiffness, reveals that an excessive amount of case stiffness variability was probably used in the viscoelastic response and R/C analyses.

An estimate of service life was formulated from the calculated damage factors for mean case stiffness by performing a regression analysis. The upper limit of possible damage factor at failure was used for the 2-1/2 month motor and the lower value was used for the 108 month motor. These values yield the maximum negative slope for the linear regression of motor capability versus age. Figure 5-11 shows the resultant linear regression line and the 99 percent probability, 90 percent confidence lower limit. The R/C estimates of the upper 3-sigma and mean damage factors for the mean motor configuration subjected to actual ignition pressurization transients are also shown in Figure 5-11. The regression analysis curve represents motor capability as a function of age and the R/C mean and plus 3 sigma damage factor lines represent the motor requirements. The reliability of the system can be determined from the basic concept that a no-failure probability exists when the capability is not exceeded by the requirement. Based on normal distributions for both the capability and requirement, the reliability is determined by the difference density which is assumed to be normally distributed (Reference 6). The reliability R is expressed as follows:

$$R = \int_{-Z}^{\infty} e^{-(Z^2/2)} dZ,$$

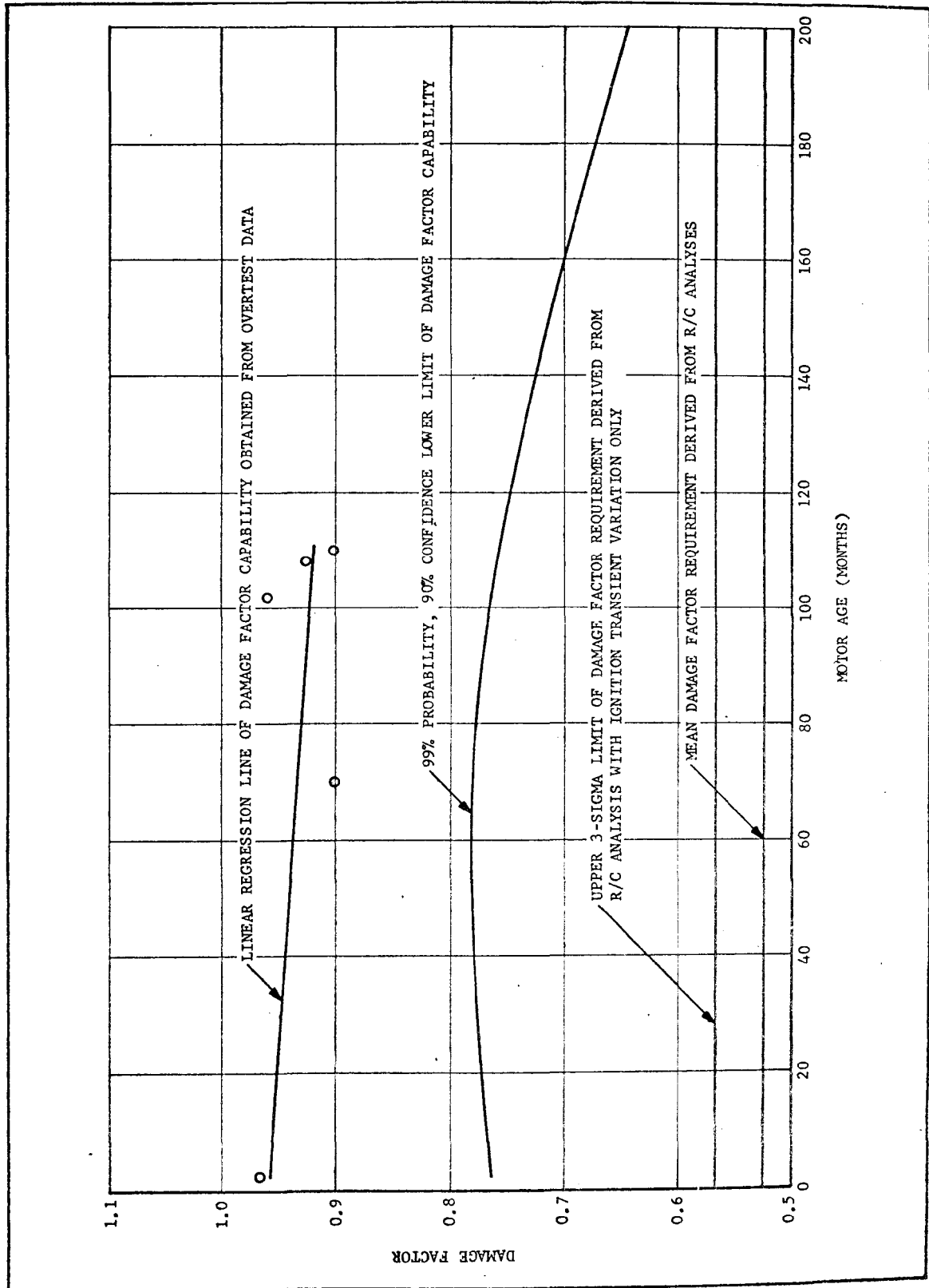


Figure 5-11. Graphic Comparison of Regression Curve of Damage Factor Capability with Required Damage Factor for Motor

where  $Z$  is the mean difference,  $\bar{\zeta}$ , divided by the standard deviation of the difference distribution,  $\sigma_{\zeta}$ .

$\bar{\zeta}$  is also equivalent to the absolute difference between the mean capability and the mean requirement and  $\sigma_{\zeta}$  is equivalent to the root sum squares (RSS) of the two standard deviations. The mean required damage factor was calculated by the R/C analyses to be 0.52538 with a standard deviation of 0.01429 due to expected variation of actual ignition pressurization transients. The linear regression line for capability was determined to be:

$$\bar{C} = 0.95793512 - 0.00034006 A$$

where  $\bar{C}$  is the calculated mean capability and  $A$  is the motor age in months.

The 99/90 lower limit of damage factor capability is equivalent to the lower 2.575-sigma level based on normal distribution. The standard deviation was then calculated at each motor age by dividing 2.757 into the difference between the regression line value and the lower confidence limit. This technique is the conservative approach since the standard deviation is predicted to increase with motor age. In actuality it would be expected that the standard deviation would remain constant or decrease as the mean capability decreased; i.e., the coefficient of variation remaining constant. However, the conservative approach was used to exhibit the worst aging trend. Calculated values for the lower 99/90 confidence limit of capability, along with corresponding mean values and corresponding standard deviations are presented in Table 5-14 for a range of advanced motor ages. Resultant probability of success is shown as a function of motor age in Figure 5-12.

No definite level of reliability has been specified to represent the limit of serviceability. However, a probability of success level of 0.9987, corresponding to the 3-sigma limit of a normal distribution, has been arbitrarily selected. Based on this criterion, the service life of the B-1 fix configuration M-57 motor is predicted to be 234 months, or 19 years, 6 months. The oldest motor of this configuration still deployed was cast on 24 August 1964.

The above technique for service life prediction was based on very conservative assumptions. For example, the selection of the upper failure pressure for motor 2-10-16 significantly decreased the slope of the regression line of damage factor capability in Figure 5-11. This effect was large because of the lack of other appropriate overtest data at the lower ages, and points out the importance to an overtest program of a reliable event gage technique to identify exact time of failure during overtest pressurization.

TABLE 5-14

## CAPABILITY STATISTICS AT ADVANCED M-57 MOTOR AGES

Age (mo)	Mean Damage Factor Capability	99/90 Lower Confidence Limit	2.575-sigma Value	1-sigma Value
160	0.903526	0.704856	0.198670	0.077153
180	0.896724	0.677203	0.219521	0.085251
200	0.889923	0.647408	0.242515	0.094181
250	0.872920	0.566811	0.306109	0.118877
300	0.855917	0.434411	0.421506	0.163692
350	0.838914	0.392619	0.446295	0.173318
400	0.821911	0.302473	0.519438	0.201723
450	0.804908	0.211351	0.593557	0.230508
500	0.787905	0.119546	0.668359	0.259557

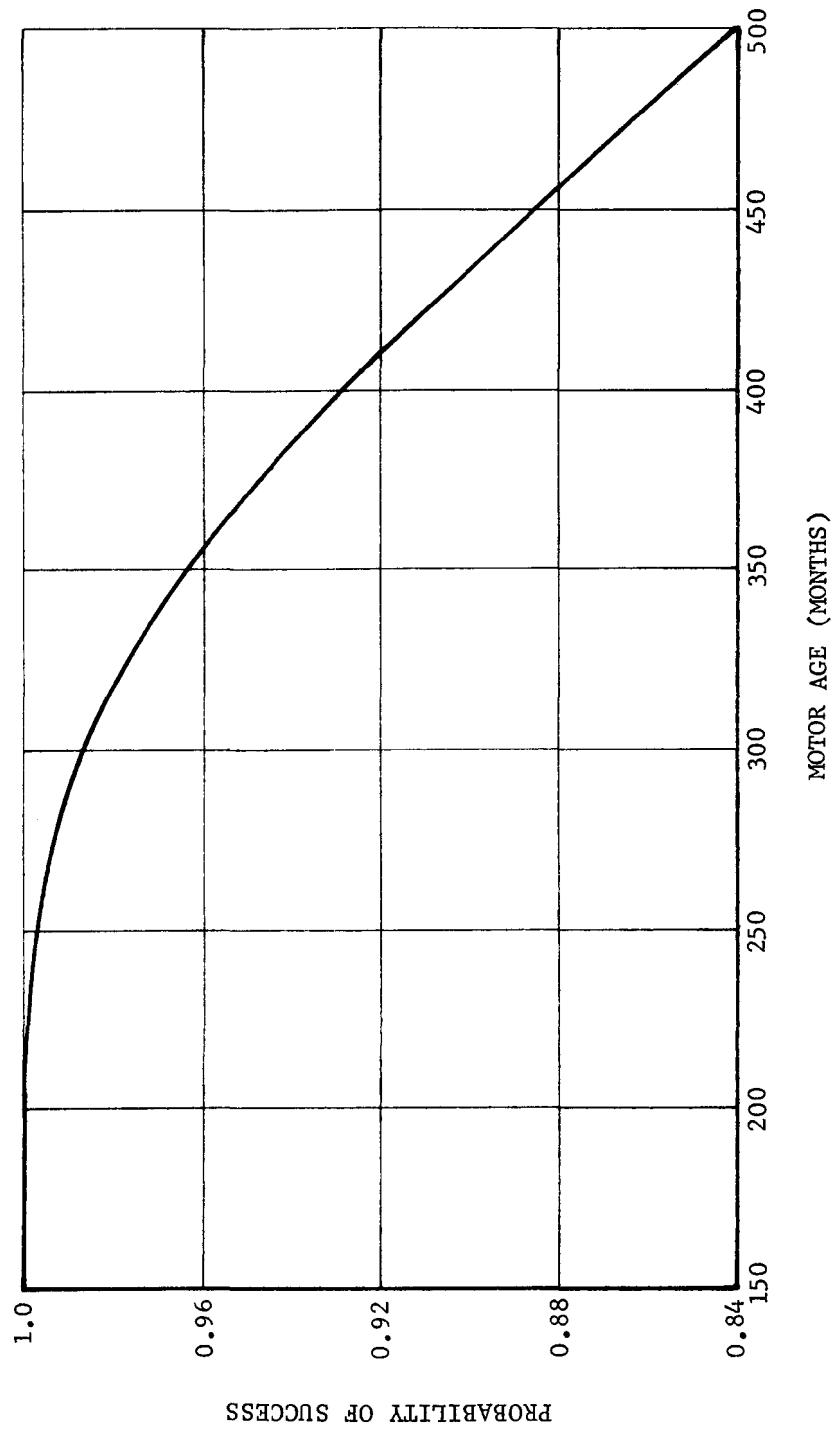


Figure 5-12. Probability of Successful Firing for M-57 Motor (B-1 Fix Configuration)  
Versus Motor Age-Extrapolated from Overtest Data

As mentioned previously, it would be desirable to manufacture all overtest motors from the same propellant lot with motor chambers of identical stiffness. This would aid in eliminating variability of components not direct functions of age. In the present analysis, no normalization of overtest data with respect to chamber variation could be performed since no proof test deflections were available for the individual motor cases. However, the problem appears to exist with an excessive coefficient of variation in available experimental case deflection data. There is the distinct possibility that errors in an attempted correction between units could produce an apparent variation larger than that which actually existed as a result of case variability.

A correction for lot-to-lot variation of zero age propellant properties was also tentatively considered. Examination of results from ranking tests (See Section IV) of relaxation modulus and allowable strain data at lot acceptance and later propellant ages revealed no definite correlation. Although there did appear to be a slight correlation of lots above and below the median property values, no appropriate quantitative correction could be accomplished.

#### D. CONCLUSIONS

Motor requirements as a function of age are dependent on magnitude and rate of the ignition pressurization transient. A regression analysis of ignition pressure data from 169 M57A1 motor firings indicated that ignition pressure can be considered to be independent of motor age.

Motor capability was analytically and experimentally determined to be primarily dependent upon the capability of the propellant in the region of the wing slot tip. Propellant cracking at the wing slot tip was found to be the primary M57A1 grain failure mode. It was concluded that no change in stress relaxation modulus and strain at maximum stress versus strain rate occurs with age in the CYH propellant; thus the motor grain capability was shown analytically to be independent of age.

Subscale analog tests provided no data on which to base service life predictions directly. However, the analog test results did verify analysis methods and failure criteria.

The full-scale overtest program successfully verified the failure mode and failure location for ignition pressurization of the M57A1 motor. No unusual failure modes were detected and the structural capability of the motor was found to be considerably greater than the operating pressure level.

Structural failure of the motor initiated in the forward trim area of the wing slots. This failure initiation site is near the wing slot section predicted by analysis to be the most critical for slot tip failure. Failure was predicted to occur at approximately 500 psi and 600 psi for B-1 Fix and OPRI configurations, respectively, which is reasonably close to the observed test failures.

The aft centerport boot-to-flap bond has a higher structural capability than does the wing slot tips. No boot-to-flap bond failures were induced by test pressures that were sufficient to fail the slot tips. That the boot-to-flap bonds were not broken was proven by the fact that bonded areas were removed from motors, made into shear specimens, and successfully tested.

The TT port area also has a higher structural capability than does the wing slot tip. Wing slot cracks did not propagate out to the TT ports, and there was no evidence of other structural failure in the TT ports.

LIST OF REFERENCES FOR SECTION V

1. A. S. Daniels, ICBM Overtest Technology, Task I, Failure Mode Selection; AFRPL-TR-72-123; Hercules Incorporated, Magna, Utah; November 1972.
2. A. S. Daniels, ICBM Overtest Technology, Motor Overtest and Posttest Examination, AFRPL-TR-75-27, Hercules Incorporated, Bacchus Works, Magna, Utah, February 1975.
3. "Propellant Charge Stress-Strain Time Relations in the M57 Configuration," Final Report - Structural Mechanics Group, Task 9, Minuteman Support Program; Prepared by Hercules Incorporated, Magna, Utah; April 1964.
4. A. S. Daniels and J. J. Rotter; ICBM Overtest Technology, Overtest Modeling (Task II) and Subscale Verification of The Model (Task III); AFRPL-TR-74-25; Hercules Incorporated, Magna, Utah; February 1974.
5. Summary Final Report for the Wing Slot Cracking and Aft Centerport Debonding Failure Mode During High Rate Pressurization Testing of Full-Scale Minuteman II, Stage III Rocket Motors for Long Range Service Life Analyses, MTO 1124-70, Hercules Incorporated, Magna, Utah, 1 May 1975, prepared for OALC-MMEM, Hill Air Force Base, Utah.
6. Haugen, E. B., Probabilistic Approaches to Design, John Wiley & Sons, New York, New York, 1968.



UNCLASSIFIED

SECURITY CLASSIFICATION OF THIS PAGE (When Data Entered)

REPORT DOCUMENTATION PAGE		READ INSTRUCTIONS BEFORE COMPLETING FORM								
1. REPORT NUMBER AFRPL TR-75-51	2. GOVT ACCESSION NO.	3. RECIPIENT'S CATALOG NUMBER								
4. TITLE (and Subtitle)  ICBM OVERTEST TECHNOLOGY Vol I		5. TYPE OF REPORT & PERIOD COVERED Final Report								
		6. PERFORMING ORG. REPORT NUMBER								
7. AUTHOR(s) A. S. Daniels S. C. Browning		8. CONTRACT OR GRANT NUMBER(s) F04611-73-C-0010								
9. PERFORMING ORGANIZATION NAME AND ADDRESS Hercules Incorporated Bacchus Works Magna, Utah 84044		10. PROGRAM ELEMENT, PROJECT, TASK AREA & WORK UNIT NUMBERS JON 305910LY								
11. CONTROLLING OFFICE NAME AND ADDRESS Air Force Rocket Propulsion Laboratory Edwards, CA 93523		12. REPORT DATE October 1975								
		13. NUMBER OF PAGES 256								
14. MONITORING AGENCY NAME & ADDRESS (if different from Controlling Office)		15. SECURITY CLASS. (of this report)  Unclassified								
		15a. DECLASSIFICATION/DOWNGRADING SCHEDULE N/A								
16. DISTRIBUTION STATEMENT (of this Report)  APPROVED FOR PUBLIC RELEASE; DISTRIBUTION UNLIMITED										
17. DISTRIBUTION STATEMENT (of the abstract entered in Block 20, if different from Report)										
18. SUPPLEMENTARY NOTES										
19. KEY WORDS (Continue on reverse side if necessary and identify by block number) <table border="0"> <tr> <td>Propellant</td> <td>Dissection</td> </tr> <tr> <td>Surveillance</td> <td>Failure gages</td> </tr> <tr> <td>Failure Modes</td> <td>Analog</td> </tr> <tr> <td>Aging Model</td> <td></td> </tr> </table>			Propellant	Dissection	Surveillance	Failure gages	Failure Modes	Analog	Aging Model	
Propellant	Dissection									
Surveillance	Failure gages									
Failure Modes	Analog									
Aging Model										
20. ABSTRACT (Continue on reverse side if necessary and identify by block number) <p>This is the final report on the ICBM Overtest Technology Program which was performed by Hercules Incorporated for the Air Force. The primary objective of the program was to develop overtest technology for the prediction of ICBM motor service life. An important secondary objective was to make predictions of the M57A1 motor life. The most critical failure modes were shown by analysis and verified by analog subscale and full-scale motor tests to be wing slot cracking and aft centerport debonding in response to the ignition transient. Event gages were developed for detecting time of failure and to verify gage response.</p>										

DD FORM 1473  
1 JAN 73

EDITION OF 1 NOV 65 IS OBSOLETE \*

UNCLASSIFIED

1. SECURITY CLASSIFICATION OF THIS PAGE (When Data Entered)

UNCLASSIFIED

SECURITY CLASSIFICATION OF THIS PAGE(When Data Entered)

Since no aging effects on the grain were determined, an indefinite service life was projected for the Minuteman II Stage III motor. A manual of recommended practice for incorporating overtest concepts in surveillance programs has been prepared.

ia

UNCLASSIFIED

SECURITY CLASSIFICATION OF THIS PAGE(When Data Entered)